

# **Influence of xenobiotic substance on hepatic co-cultures**

Inaugural-Dissertation

to obtain the academic degree

Doctor rerum naturalium (Dr. rer. nat.)

submitted to the Department of Biology, Chemistry, Pharmacy

of Freie Universität Berlin

by

Florian Padberg

2021

This thesis was carried out at the German Federal Institute for Risk Assessment (BfR) in Berlin from April 2016 to December 2020 under the supervision of Prof. Dr. Dr. Andreas Luch.

1st Reviewer: Prof. Dr. Dr. Andreas Luch

2nd Reviewer: Prof. Dr. Burkhard Kleuser

Date of defense: 28.09.2021

## Erklärung

Hiermit versichere ich, die vorliegende Arbeit mit dem Titel „Influence of xenobiotic substance on hepatic co-cultures“ ohne Benutzung anderer als der zugelassenen Hilfsmittel selbstständig angefertigt zu haben. Alle angeführten Zitate sind als solche kenntlich gemacht. Die vorliegende Arbeit wurde in keinem früheren Promotionsverfahren angenommen oder als ungenügend beurteilt.

Berlin, 2021

Florian Padberg

Die Dissertation wurde in englischer Sprache verfasst

## Danksagung

Beginnend möchte ich gerne Herrn Prof. Dr. Dr. Luch danken, nicht nur für die Möglichkeit meine Doktorarbeit in der Abteilung Chemikalien und Produktsicherheit am Bundesinstitut für Risikobewertung durchzuführen, sondern auch dafür, dass Herr Professor Luch mir sein Vertrauen gab meine Ideen umzusetzen und mir mit Rat und Tat zur Seite stand.

Herrn Prof. Dr. Kleuser danke ich für das Interesse an meinem Projekt und die Übernahme des Zweitgutachtens.

Im Besonderen gilt mein Dank Herrn PD Dr. Zellmer. Er hat das Projekt nicht nur initiiert, sondern war auch immer mit seiner Zeit, Expertise, seinem Weitblick und unerschütterlichem Optimismus für mich da.

Natürlich möchte ich auch Herrn Dr. Tarnow und Frau Dr. Kugler danken. Dabei waren neben den projektbezogenen auch die persönlichen Gespräche eine Bereicherung während der gesamten Promotionszeit.

So eine schöne Promotionszeit war natürlich auch durch die weiteren Kollegen des BfR möglich. Besonders möchte ich mich bei den Kollegen der Abteilung 7 bedanken. Gerade auch den Kollegen, die für die wunderbaren Stunden auch außerhalb des BfR verantwortlich waren. Besonders gilt mein Dank dem einzigartigen Großraumbüro, in dem es neben fachlichen Diskussionen auch unzählige unvergessliche Momente gab. Dabei sind auch lange Tage in diesem „Kinderspieleparadies“ viel zu schnell vergangen. Für die langen und dennoch schönen Labortage möchte ich allen Labormitarbeitern danken. Besonders möchte ich den „Genotox-Enthusiasten“ danken, bei denen nicht nur Protokolle erörtert wurden, sondern auch so mancher „schlechter“ Witz seinen Platz fand.

Neben diesen wunderbaren Kollegen gilt es auch den Personen außerhalb des BfR zu danken, wie zum Beispiel Frau Dr. Loßow, die sich durch das Korrekturlesen an dieser Arbeit beteiligt hat. Allen die mich mit Zuversicht und Freundschaft während dieser Zeit unterstützt haben, möchte ich meinen großen Dank aussprechen.

Abschließend möchte ich mich bei meinen Eltern, meiner Schwester und bei meinen Großeltern bedanken. Ohne Eure Geduld, Rückhalt und Verständnis wäre dieser Lebensabschnitt nicht möglich gewesen.

## Table of contents

<b>Zusammenfassung</b> .....	<b>1</b>
<b>Abstract</b> .....	<b>2</b>
<b>List of abbreviations</b> .....	<b>3</b>
<b>1. Introduction</b> .....	<b>5</b>
<b>1.1 The liver</b> .....	<b>5</b>
1.1.1 Xenobiotic metabolism .....	8
1.1.2 Inflammation .....	10
1.1.3 Drug-induced liver injury (DILI) .....	11
1.1.4 <i>In vitro</i> systems .....	12
<b>1.2 Bisphenols</b> .....	<b>14</b>
1.2.1 Use and consumer exposure .....	15
1.2.2 Risk assessment.....	15
1.2.3 Pharmacokinetic and metabolism.....	16
<b>2. Objectives</b> .....	<b>18</b>
<b>3. Results</b> .....	<b>19</b>
<b>3.1 Minor structural modifications of bisphenol A strongly affect physiological responses of HepG2 cells</b> .....	<b>19</b>
<b>3.2 Indirect co-cultivation of HepG2 with differentiated THP-1 cells induces AHR signaling and release of pro-inflammatory cytokines</b> .....	<b>45</b>
<b>3.3 Novel indirect co-culture of immortalised hepatocytes with monocyte derived macrophages is characterised by pro-inflammatory cytokine networks</b> .....	<b>71</b>
<b>4. Discussion</b> .....	<b>103</b>
<b>5. Conclusion &amp; Outlook</b> .....	<b>110</b>
<b>6. References</b> .....	<b>112</b>
<b>7. List of publications</b> .....	<b>122</b>
<b>7.1 Articles</b> .....	<b>122</b>
<b>7.2 Poster and Talks</b> .....	<b>122</b>
<b>Annex I</b> .....	<b>123</b>
<b>Annex II</b> .....	<b>126</b>
<b>Annex III</b> .....	<b>131</b>

## **Zusammenfassung**

In der Leber, als wichtiges metabolisierendes Organ des Menschen, laufen eine Vielzahl an komplexen Signalwegen oft gleichzeitig ab. An diesen Prozessen sind nicht nur Hepatozyten, sondern auch Kupffer-Zellen, als größte Population an leberständigen Makrophagen, involviert. In der vorliegenden Arbeit wurden – ausgehend von den spezifischen Effekten von Bisphenol A-Derivaten – bei der Hepatozyten-ähnlichen Zelllinie HepG2 strukturabhängige und molekularbiologische Reaktionsmuster untersucht. Diese chemikalieninduzierten Effekte wurden auch über eine indirekte Ko-Kultivierung von HepG2-Zellen mit der Makrophagen-ähnlichen differenzierten Zelllinie THP-1 detektiert. Dabei ist ein kausaler Zusammenhang zwischen strukturellen Änderungen des Bisphenol A-Moleküls und der mitochondrialen Membrandepolarisation mit anschließend eingeleiteter intrinsischer Apoptose gezeigt worden. Dieser spezifische zelluläre Effekt von zusätzlichen Methylgruppen des Moleküls konnte in der indirekten Ko-Kultur anhand einer erhöhten Sekretion des prognostischen Faktors TNF- $\alpha$  erklärt werden. Diese TNF- $\alpha$  Sekretion war zusätzlich auch ein Beleg für die erhöhte chemische Sensitivität der indirekten Ko-Kultur gegenüber der Einzelkultur von HepG2 Zellen. Diese Sensitivität ließ sich – entsprechend der Daten in dieser Arbeit – auf eine erhöhte Aktivität metabolisierender Enzyme (zum Beispiel der Cytochrom-P450-abhängigen Monooxygenase 1A1) und eine vermehrte  $\beta$ -Oxidation der intrazellulären Fettsäuren, was eine Reduzierung der intrazellulären Lipidtröpfchen nach sich zieht, zurückführen. All diese Änderungen sind begründet auf dem pro-inflammatorischen Einfluss der differenzierten THP-1 Zellen. Durch deren Sekretion von löslichen Faktoren (z.B. Zytokine) werden inflammatorische Signalwege in den Hepatozyten induziert. Die Korrelationsnetzwerke der Zytokinsekretion deuten dabei darauf hin, dass in der Ko-Kultur eine additive, sich gegenseitig ergänzende Reaktionslage der zwei verwendenden Zelllinien vorherrscht. Eine solche indirekte Ko-Kultivierung kann auch durch den Einsatz von primären, humanen, immortalisierten Hepatozyten (Fa2N-4) und Makrophagen aus primären humanen Monozyten (MDM) realisiert werden. Dabei wird im Korrelationsnetzwerk eine Zell-Zell-Kommunikation über die entsprechend sekretierten Zytokine detektierbar. Durch das Verhältnis der Zellzahl von MDM- zu Fa2N-4-Zellen kann der „inflammatorische Status“ des Systems beeinflusst werden. So ist die Erhöhung der MDM-Zellzahl an eine veränderte Expression von Genen (basierend auf Transkriptomdaten der Fa2N-4-Zellen) der akuten Phase-Reaktion gekoppelt. Das in dieser Arbeit verwendete Zellsystem reagiert auf die Behandlung durch potenziell Leberschäden induzierende Pharmazeutika wie Diclofenac und Adalimumab, sowie auf Lipopolysaccharide, mit einer Abweichung in der Zytokinsekretion. Dabei sind Parallelen zur *in vivo* Situation erkennbar.

## **Abstract**

In the liver, as an important metabolic organ, a large number of complex signaling pathways occur, often simultaneously. Not only hepatocytes are involved in these signaling pathways, also Kupffer cells, the largest population of liver macrophages, are part of these pathways. In this work, structure-dependent molecular cell responses were established based on the adverse effects of bisphenol A and its derivatives in the hepatocyte-like cell line HepG2 indirectly co-cultured with the differentiated macrophage-like cell line THP-1 cells. The causal relationship between the effects of two additional methyl groups in bisphenol A and the depolarisation of the mitochondrial membrane, along with subsequently induced intrinsic apoptosis, has been shown. This adverse effect of the additional methyl groups could be detected through the increased secretion of the prognostic factor TNF- $\alpha$  in the cell culture system. So, there is evidence that increases in TNF- $\alpha$  secretion mirrors a potentially increased chemical sensitivity in the indirect co-culture of the cells investigated. Based on the data of this work, this increased sensitivity is correlated with the increased expression and activity of metabolizing enzymes (e.g., cytochrome P450-dependent monooxygenase 1A1) and the accelerated  $\beta$ -oxidation of intracellular fatty acids, which results in the reduction of intracellular lipid droplets. All of these changes are due to the pro-inflammatory influence of the differentiated THP-1 cell line. Its secretion of soluble factors (e.g., cytokines) initiates certain signaling pathways. By looking into the correlation networks of these cytokines, an additive effect of the two cell lines used in this co-culture becomes obvious. However, when this indirect co-culture is replaced by using more primary cells, such as primary human immortalized hepatocytes (Fa2N-4) and primary human monocyte derived macrophages (MDM), cytokine-dependent cell-cell communication can be observed in the correlation network as well. The “inflammatory status” of the system can be influenced by the ratio of MDM to Fa2N-4 cells. For instance, an increase in the MDM cell number is associated with altered gene expression (based on transcriptome data of Fa2N-4 cells) related to an acute phase reaction. The cell system established in this work responds to the treatment with pharmaceuticals such as diclofenac and adalimumab, and to lipopolysaccharides, in terms of altered cytokine secretion. Parallels to the *in vivo* situation can be seen here. In conclusion, the present work provides evidence for an increased chemical sensitivity of HepG2 cells when growing in an indirect co-culture system along with THP-1 cells. Furthermore, it could be shown that indirect co-cultivation of Fa2N-4 cells and MDM would be advantageous in the detection of chemical-induced adversity in liver cells.

## List of abbreviations

AHR	aryl hydrocarbon receptor
AMB	Adalimumab
ARNT	AHR nuclear translocator
ATP	adenosine triphosphate
BPA	bisphenol A
BPA/C	bisphenol A/C
BPC	bisphenol C
BPF	bisphenol F
BPG	bisphenol G
BPS	bisphenol S
BW	body weight
CAR	constitutive androstane receptor
CC 15 %	physiological co-cultivation of Fa2N-4 and monocyte derived macrophages
CC 50 %	pro-inflammatory co-cultivation of Fa2N-4 and monocyte derived macrophages
CCL20	chemokine (C-C motif) ligand 20
CCL3	chemokine (C-C motif) ligand 3
CCL4	chemokine (C-C motif) ligand 4
CD	cluster of differentiation
CRP	c-reactive protein
CXCL1	chemokine (C-X-C motif) ligand 1
CXCL3	chemokine (C-X-C motif) ligand 3
CyC	cytochrome c
CYP	cytochrome P450-dependent monooxygenase
CYP1A1	cytochrome P450 1A1
CYP1A2	cytochrome P450 1A2
CYP1B1	cytochrome P450 1B1
CYP2C9	cytochrome P450 2C9
CYP3A4	cytochrome P450 3A4
DCN	diclofenac
DILI	drug induced liver injury
EC <sub>5</sub>	5 % of effective concentration
EC <sub>50</sub>	half-maximum effective concentration
EC <sub>50E</sub>	half maximal estrogenic activity
ECHA	European Chemical Agency
EFSA	European Food Safety Authority
FA	fatty acid
Fa2N-4/MDM	indirect co-cultivation consisting of Fa2N-4 cells and MDM
FAS	fatty acid synthase
FGF	fibroblast growth factor
GM-CSF	macrophage colony-stimulating factor
GST	glutathione S-transferases
HepG2/THP-1	indirect co-cultivation consisting of HepG2- and THP-1 cells
HGF	hepatocyte growth factor
HLA-B	human leukocyte antigen-B
IL-10	interleukin 10
IL-12	interleukin 12
IL-6	interleukin 6
IL-8	interleukin 8
KC	Kupffer cells



## List of abbreviations

KO	knock-out
LD	lipid droplets
logP <sub>ow</sub>	oil water distribution coefficient
LPS	lipopolysaccharides
LXR $\alpha$	liver X receptor $\alpha$
MCP-1	monocyte chemoattractant protein 1
MDM	monocyte derived macrophages
MTT	3-(4,5-dimethylthiazol-2-yl)-2,5-diphenyltetrazolium bromide
PMA	phorbol 12-myristate 13-acetate
PPAR	peroxisome proliferator-activated receptor
PXR	pregnane X receptor
S9	cellular fraction, containing cytosol and microsomes
ST	sulfotransferases
SV-40	simian virus 40
<i>TGFB1</i>	gene of transforming growth factor $\beta$ 1
TGF- $\beta$ 1	transforming growth factor $\beta$ 1
<i>TNF</i>	gene of tumor necrosis factor $\alpha$
TNF- $\alpha$	tumor necrosis factor $\alpha$
tTDI	temporary tolerable daily intake
UGT	UDP-glucuronosyltransferases
UGT1A9	UDP-glucuronosyltransferase 1A9
UGT2B1	UDP-glucuronosyltransferase 2B1
UGT2B7	UDP-glucuronosyltransferase 2B7
VLDL	very low-density lipoprotein particles
$\alpha$ IL-8	IL-8 neutralizing antibody
$\Delta\Psi_m$	mitochondrial membrane potential

## **1. Introduction**

### **1.1 The liver**

The liver is the largest organ with an average of 2 % to 3 % of body weight [1]. It's located in the right upper quadrant of the abdominal cavity beneath the right hemidiaphragm and is supplied with blood through the hepatic artery and the portal vein. The latter directly connects the liver with the intestinal tract, by carrying nutrient-rich blood from the intestinal tract [1]. The liver is the central metabolic organ, converting absorbed nutrients of the diet into usable substrates that are either stored or delivered to cells [2]. Furthermore, it converts potentially toxic substances into harmless substances, which can be released from the body either in urine or faeces [3]. Xenobiotic metabolites can be excreted directly through the urine by the kidneys, dependent on their structure or molecular weight (below 600 g/mol). In comparison, hepatic xenobiotic metabolites are excreted via the biliary route, returning in the small intestine. From there the metabolites can be eliminated from the body in the faeces or might be reabsorbed, entering the entero-hepatic circulation [3]. By that, metabolites subsequently return to the liver and might undergo further metabolism steps.

Histologically the liver is organized in so-called lobules (Figure 1 A), hexagonal units consisting of hepatocytes, sinusoidal endothelial cells, phagocytic Kupffer cells (KC), and stellate cells. Each lobule has on average three portal triad, consisting of portal vein, hepatic artery, and bile duct. Within these lobules, the hepatocytes are separated from the blood-carrying ducts (sinusoid) by the perisinusoidal space of Disse. This space of Disse is facing this sinusoidal lumen through a continuous (but fenestrated) line of endothelial cells. Inside the lumen, the KC are located. KC are adhesive to the endothelium and sometimes pass through the fenestration into the space of Disse, causing direct contact to the hepatocytes [4] (figure 1 A).

## Introduction

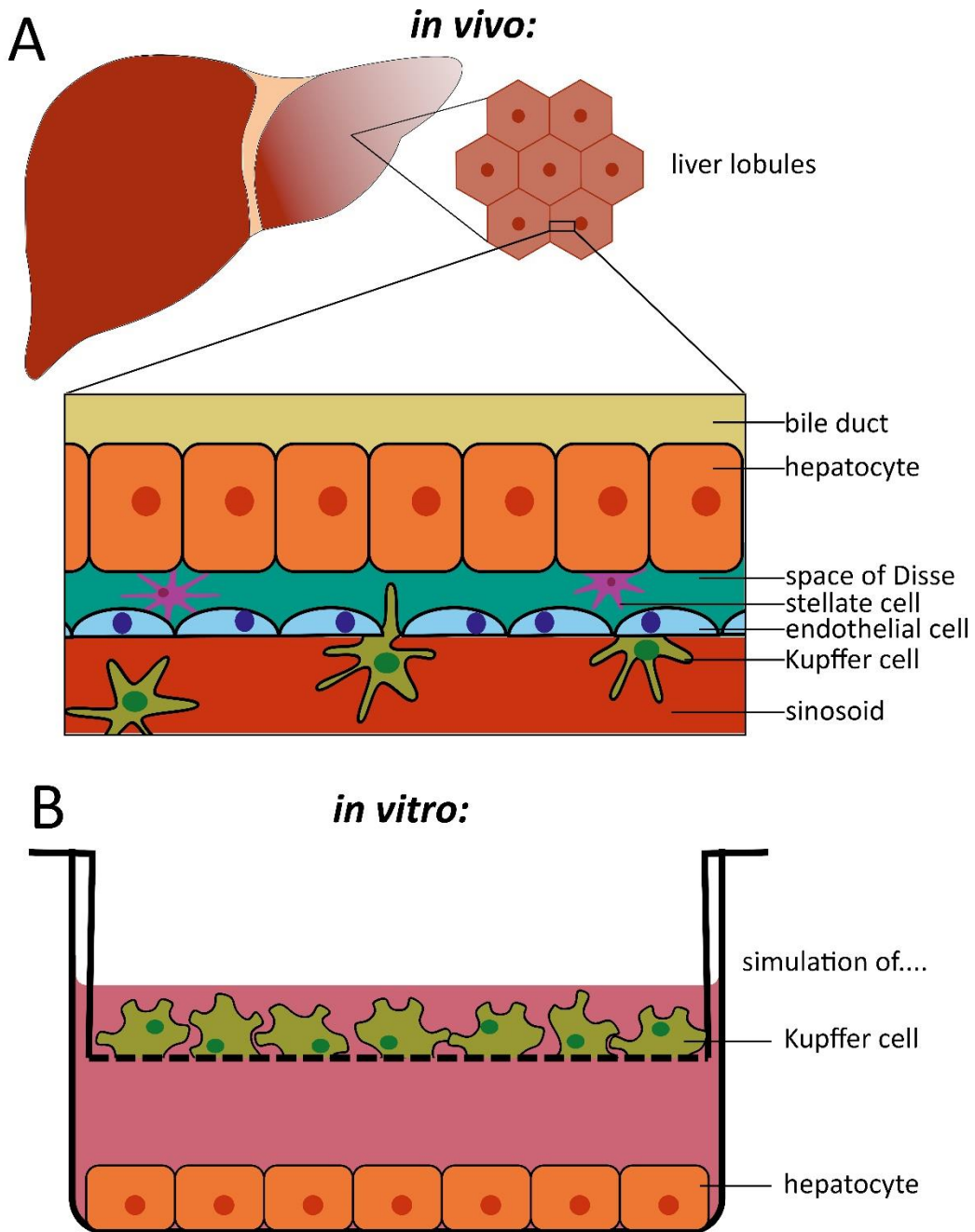


**Figure 1. Schematic overview of the liver physiology and *in vitro* model. (A)** The liver is histologically organized in liver lobules. The cellular composition of a liver lobule consists of hepatocytes, stellate cells, endothelial cells, and Kupffer cells. The hepatocytes are polarized cells which faced on the apical side the bile duct and on the basolateral side the space of Disse. The space of Disse (including the stellate cells) is demarcated to the sinusoid by a fenestrated line of endothelial cells. Within the sinusoid, the Kupffer cells are adhesive to the endothelium or sometimes pass through the fenestration into the space of Disse. **(B)** To simulate potential indirect communication of hepatocytes and Kupffer cells co-culture studies were performed *in vitro*. Therefore, hepatocytes are seeded on the bottom of the cell culture plate. The macrophage like cells (which are able to simulate Kupffer cells) are seeded in a second compartment (insert) and an exchange of messenger takes place through a semipermeable membrane.

## Introduction

All of these cell types have important functions in the liver, but on the basis of this work, the role of hepatocytes and KC are of particular interest and addressed below.

### Hepatocytes

The largest proportion of cells in the liver is represented by hepatocytes (up to 65 %) [5], which are exposed to absorbed substance of the intestine, whether nutritious or toxic. Hepatocytes are in general a polarized cell type. The apical (canalicular) and basolateral (sinusoidal) plasma membrane are characterized by distinct surface proteins, channels, and receptors. Based on that, an extensive endoplasmic reticulum and Golgi network in hepatocytes realize the secretion of many essential proteins into the circulation, including  $\alpha$ -fetoprotein, albumin, transferrin, plasminogen, and fibrinogen [2]. Additionally, hepatocytes participate in biotransformation processes [6] and are expressing a large number of biotransformation-associated enzymes, involved in systemic homeostasis. For example, dietary iron is absorbed and stored in the hepatocytes [2]. Also, worth mentioning is the central role of hepatocytes in lipid metabolism and storage [7]. Therefore, dietary lipids (chylomicron remnants) released from the intestine are taken up from the hepatocytes. In hepatocytes, very-low-density lipoprotein particles (VLDL) can be produced and secreted from these chylomicron remnants [8]. The circulating VLDL are converted in the peripheral tissues and in turn circulating as low- and high density lipoproteins. These lipoproteins can then be used by the hepatocytes to synthesize VLDL [8]. These VLDL structures primarily include cholesteryl esters and triacylglycerols enclosed in an apolipoprotein studded phospholipid monolayer [2]. This indicates that hepatocytes are an important component in the metabolism of triacylglycerols. Intracellular triacylglycerols are stored in intracellular lipid droplets (LD) if they are not directly used for VLDL synthesis [7]. Therefore, LD are responsible for the storage of triacylglycerols and fatty acids (FA). These FA can derived from the *de novo* FA synthesis. The *de novo* FA synthesis, starting from acetyl coenzyme A, is performed in the hepatocytes to store FA in the LD. The FA stored in this way can then be used after the  $\beta$ -oxidation to provide energy when needed (e.g., in a fasted state) [9]. Additionally, KC impact these FA metabolic activities by secretion of cytokines [10]. This confirms that KC also plays an important role in the physiological processes of hepatocytes and is therefore described in more detail below.

### Kupffer cells (KC)

The KC were first identified by Karl Wilhelm von Kupffer in 1876 [11]. They represent the largest population of tissue macrophages [12]. However, inter-individual variability in the ratio of KC (average =  $14.5 \pm 9.1$  %) to hepatocytes has been reported [13]. The origin and the renew capacity of KC are still

## Introduction

under discussion. Nguyen-Lefebvre (2015) summarized two possible theories about the renewal of KC [14]. First, KC are not able to self-renew and come from bone marrow-derived monocytes [14]. This theory is founded on the observation that labelled bone marrow-derived monocytes differentiate to macrophages and enters the liver followed by an inflammatory response. Accordingly, existing KC are not capable for cell division [15]. The second theory based on the hypothesis that KC is a self-renewing population and can proliferate as mature cells, or they come from local intrahepatic progenitors [14]. This theory is supported by the study of a murine irradiation and transplantation model [16]. In general, KC are completely (99%) replaced from a haematogenous origin within four weeks and immunohistology revealed distinct populations of bone marrow-derived and sessile KC [16]. Therefore, distinct renewing capacity of the KC is still under discussion. Besides the origin and renewing capacity, KC physiologically are one of the first cells with contact to substances absorbed from the intestine (e.g., bacterial lipopolysaccharides (LPS), toxins, pharmaceutical agents). In the role as immune cell, KC are able to recruit other immune cells (e.g., T cells or natural killer cells) [14]. Therefore, after metabolic or toxic damage of liver tissue, a massive infiltration of blood monocytes, which differentiate to macrophages, occurs [17]. In general, macrophages are derived from circulating monocytes. These monocytes can differentiate into M1 or M2 macrophages, depending on the surrounding cytokines. The M1 and M2 macrophage lineages have either pro- and anti-inflammatory properties [18]. In general, liver macrophages appear to express markers of both macrophage lineages simultaneously [19]. However, a specific surface marker for the identification of KC is missing and so far human KC can only be identified indirectly by their expression of cluster of differentiation (CD) 14, CD16, and CD68 [20]. Further, KC are capable to bind and endocytose proteins, foreign particles, bacteria, yeasts, and viruses [21]. Furthermore, murine peroxisome proliferator-activated receptor (PPAR)  $\delta$  knock-out (KO) experiments have shown that KC are also involved in oxidative metabolism and insulin resistance [22]. Additionally, Neyrinck *et al.* (1999) reported that KC participate on the xenobiotic metabolism. Therefore, reduction of KC number is associated with higher toxicity of paracetamol [23].

As mentioned before, the liver, especially hepatocytes but also KC, are important for the xenobiotic metabolism.

### **1.1.1 Xenobiotic metabolism**

The overall goal of the xenobiotic metabolism is the reduction of lipophilicity, followed by the enhanced excreatability of potentially toxic substances [6]. Classically, the xenobiotic metabolism can be divided into two phases.

## Introduction

### Phase I metabolism

During phase I metabolism, the cytochrome P450-dependent monooxygenases (CYP) play a central role. This enzyme family detoxify and/or bioactivate xenobiotic chemicals due to N- and O-dealkylation as well as aliphatic and aromatic hydroxylation [24]. In the human genome, 57 putative functional CYP genes are known. These genes can be grouped (according to their sequence similarity) into 18 families and 44 subfamilies. Among these, the 1-, 2-, and 3-CYP-families are known to be responsible for the metabolism of the majority of xenobiotics, due to the broad and overlapping substrate specificity [25].

### Phase II metabolism

The phase II metabolism includes a broader range of enzymes. Aim of this phase is the enhancement of hydrophilicity of the parent compound usually resulting in an increased excreatability. Reactions like glucuronidation, sulfation, methylation, acetylation, glutathione conjugation, and amino acid conjugation are of importance here. Among others, these additive reactions are catalysed by UDP-glucuronosyltransferases (UGT), sulfotransferases (ST), and glutathione S-transferases (GST) [24].

Furthermore, a third phase is discussed and should not remain unmentioned. Here active membrane transporters (e.g., solute carrier 22A organic ion transporter family members) are in the center of attention, due to their function of shuttling xenobiotics across cellular membranes [24].

In the following, phase I and II of the xenobiotic metabolism will be explained in more detail using the example substance diclofenac (DCN, Cas: 15307-86-5). DCN is a nonsteroidal anti-inflammatory, antipyretic, and analgesic drug [26]. Thus, in phase I DCN is hydroxylated by CYP2C9 and CYP3A4 to 4'-hydroxydiclofenac and 5-hydroxydiclofenac, respectively [27]. Within phase II metabolism UGT2B7 and UGT1A9 glucuronidate hydroxylated-DCN [28]. It is therefore not surprising that after oral administration of DCN the conjugated forms of 4'-hydroxydiclofenac and 5-hydroxydiclofenac can be detected in the urine [29].

Furthermore, it is possible that xenobiotics itself can be influence their corresponding metabolism cascade (phase I and phase II). Responsible for this are receptors (e.g., constitutive androstane receptor (CAR), pregnane X receptor (PXR), aryl hydrocarbon receptor (AHR), and PPAR) which can initiate the transcription of metabolizing enzymes upon their activation [24].

For example, the AHR receptor gets activated by ligands of the group of polycyclic aromatic hydrocarbons. Afterwards, the AHR dimerizes with AHR nuclear translocator (ARNT) and transfers to

## Introduction

the nucleus to trigger downstream gene transcription [30]. These downstream target genes are, among others, CYP1A1, CYP1A2, and CYP1B1 [31].

The xenobiotic metabolism in hepatocytes is generally well studied. However, in recent years the role of KC in hepatic metabolism reached the focus, indicating a possible involvement of KC in xenobiotic metabolism. To identify the role of KC in more detail a chemical blockage of KC via gadolinium chloride was realized. Pre-treatments of rats with gadolinium chloride blocked effects of LPS serum parameters and gene expression. This led to the conclusion, that KC mediate the LPS-induced effects [32]. The chemical blockade of KC is accompanied by a reduced CYP content and activity [33], as reported for the metabolism of ethanol. Here, a significant reduction of the ethanol-induced acetaldehyde and malondialdehyde formation was measurable, after chemical blockade of KC activation [34]. In addition to this classical metabolism by CYP enzymes in hepatocytes, KC can participate directly in the metabolism/degradation of substances. The approved medical drug adalimumab (AMB) is a monoclonal human immunoglobulin G antibody, applied to neutralize the soluble and transmembrane tumor necrosis factor  $\alpha$  (TNF- $\alpha$ ). AMB has a half-life of 10-20 days and is approved for the treatment of rheumatoid arthritis [35]. The degradation of AMB is assumed to rely on receptor-mediated endocytosis and subsequent degradation [36], partially mediated by KC [17], by that contributing to the elimination of AMB.

### **1.1.2 Inflammation**

The fact that the liver harbors the largest population of tissue-specific macrophages [12] indicates that inflammatory processes in liver are of great importance. Hepatic inflammation can be triggered by liver disease and hepatic tissue damage. These tissue damage can be caused by chronic infections, bile duct damage or the progression of non-alcoholic fatty liver disease. This impairment of hepatic tissue can lead to severe fibrogenesis and finally to hepatocellular carcinoma [37]. All these mentioned diseases starting with hepatic inflammation. This process is initiated by metabolic and/or toxic stress [38]. In general, the liver is constantly exposed to substances that have a high inflammatory potential (e.g., intestinal derived microbial components like LPS). This persistent exposure requires a tightly regulated inflammatory homeostasis and may lead to an intensified reaction to get rid of hepatotropic pathogens, malignant cells or toxic products of metabolic activity [39]. Besides the intrahepatic regulation of inflammatory processes, the liver is also involved in extrahepatic inflammatory processes. Thus, cytokines that are secreted outside the liver can cause production of acute-phase response proteins and interleukin (IL)-6 by hepatocytes, by that contributing to systemic inflammation [39].

## Introduction

Based on hepatic inflammatory reactions, KC are activated and secrete cytokines and chemokines such as IL-1, IL-6, TNF- $\alpha$  [39], IL-8, chemokine (C-X-C motif) ligand 1 (CXCL1), chemokine (C-X-C motif) ligand 2 (CXCL2), chemokine (C-X-C motif) ligand 3 (CXCL3), monocyte chemoattractant protein 1 (MCP-1), chemokine (C-C motif) ligand 3 (CCL3), and chemokine (C-C motif) ligand 4 (CCL4) [40]. In acute liver inflammation, KC are able to recruit and activate other immune cells [39], like neutrophils, monocytes, and/or macrophages, depending on cytokine secretion [40].

In human KC, it has been shown that stimulation with LPS leads to secretion of IL-10. In turn, IL-10 leads to a reduction of IL-6 and TNF- $\alpha$  secretion, which implies an anti-inflammatory immune-modulating effect in response to LPS [41].

In addition to these KC-driven effects, hepatocytes also actively participate in immune responses [42]. It has long been known that human hepatocytes induce the synthesis of the “classic” acute-phase response proteins (e.g., serum amyloid A, C-reactive protein (CRP), haptoglobin,  $\alpha$ 1-antichymotrypsin, and fibrinogen) in response to IL-6, whereas the synthesis of “systemic” serum proteins (e.g., albumin, transferrin, and fibronectin) is reduced [43]. Immune responses of hepatocytes and KC can vary after stimulation with cytokines. For example, it was shown that rodent macrophages stimulated with hepatocyte growth factor (HGF) reduced the production of IL-6, whereas rodent hepatocytes showed the opposite [44].

In general, the inflammatory response of the liver is very complex which, if it becomes chronic, can lead to severe liver disease. For example, inflammation of chronic hepatitis C virus infection, alcohol abuse, and/or non-alcoholic steatohepatitis can lead to an accumulation of extracellular matrix and thus to liver fibrosis [45]. In principle, liver fibrosis can be described as a passive, irreversible process in which the hepatic parenchyma is replaced by extracellular matrix, mainly collagen. However, if hepatic damage persists, regeneration may fail and hepatocytes are replaced by an abundant extracellular matrix produced by stellate cells [45], resulting in the restructure of the liver and its involved cell types, accompanied by liver dysfunctions [46].

### **1.1.3 Drug-induced liver injury (DILI)**

Hepatic damage could also be a consequence of drug administration, based on the toxicity itself or immune-mediated mechanisms, called drug induced liver injury (DILI) [47].

DILI can be classified as intrinsic and idiosyncratic. The intrinsic DILI underlies a distinct dose-response relationship and has a predictable toxic effect. In comparison, idiosyncratic DILI shows no dose-response correlation. Accordingly, the toxic effect is unpredictable due to adverse reactions [48]. This



## Introduction

idiosyncratic DILI can be a problem for clinicians, drug developers, and regulatory agencies, as some patients will develop DILI after drug administration whereas others do not [49]. Evidence that DILI is immune-mediated is based on studies regarding the human leukocyte antigen (HLA) genotype [50]. According to these studies, patients with a HLA-B\*5701 genotype have a 0.2 % higher risk to develop DILI after administration of the  $\beta$ -lactam antibiotic flucloxacillin [51]. It is assumed that the reactive metabolite of the drug binds to proteins and can thus be presented via the corresponding HLA molecules [49]. However, the effect via the HLA not only rely on the DILI mechanism. Large variations in latency of DILI diagnosed patients (up to 12 months) [52] indicate that additionally the adaptive immune system might be involved as the extended time windows could be relevant for activation and proliferation of sufficient lymphocytes. Therefore, DILI recurs if the patient is rechallenged with the offending drug, due to the required time for antigen-specific lymphocytes to be activated and proliferate to sufficient numbers [53]. Consequently, this effect is an immune-mediated DILI that includes an early and late phase.

An example for a partly immune-mediated idiosyncratic DILI substance is DCN [54]. Therefore, DCN is listed on the 12<sup>th</sup> place in a ranking of over 3300 DILI case reports [55]. Two possible routes for a DCN-mediated DILI are discussed. First, the hepatic metabolism of DCN lead via reactive intermediates to protein adducts, thereby causing mitochondrial dysfunction and finally result in apoptosis or necrosis of hepatocytes. Second, clinical-pathological evidence suggest a type of hypersensitivity, i.e., an immune-mediated toxic effect [54], as reported in a mouse model [56]. Here transcriptome analyses indicated that DCN-mediated DILI involves pro-inflammatory cytokine and acute phase responses [56].

### **1.1.4 *In vitro* systems**

*In vitro* models are developed and discussed for drug development and toxicological research [57-59]. The "gold-standard" for hepatic *in vitro* investigations are primary human hepatocytes [57, 58]. However, this "gold standard" is not free of limitations, as large inter-individual differences and the reduction of functionality within days influence the outcomes [58]. The origin of these primary human hepatocytes cannot be neglected either, since signaling pathways and enzyme activity can be influenced by individualized drug treatment and lifestyle of the donor [60].

Another option of *in vitro* studies based on hepatic cell lines (e.g., HepG2, Huh7). Although the reproducibility of the results is increased, there are limitations with regard to the enzyme activity compared to primary hepatocytes [61, 62]. Like many other cell lines, the HepG2 cell line, which was established by Aden *et al.* (1979), derived from a intravital tumor environment [63]. Thereby, some essential characteristics of hepatocytes have also been demonstrated in the cultured HepG2 cells, such

## Introduction

as synthesis and secretion of bile acids, synthesis of cholesterol, and internalization of VDL [64]. However, the absolute number of most CYP-transcripts in primary hepatocytes is several times higher (between 14- and 5028-fold) than in HepG2 cells. In comparison, benzo[*a*]pyrene treatment, a known promutagenic contaminant (e.g., of food and cigarette smoke) revealed a comparable gene induction of relevant metabolizing enzymes between primary hepatocytes and HepG2 cells [65].

To stay with the already mentioned example (DCN metabolism, *cf.* 1.1.1), the activity of the phase I metabolizing enzyme CYP2C9 is negligible in HepG2 cells [66]. Thus, a human *in vivo* relevant xenobiotic metabolism of DCN in HepG2 cells alone can be excluded. However, transcriptome data show that cell lines from an intravital tumor environment, like HepG2 cells, still share many similarities with primary human tumor cells [67]. This example shows the limitations of HepG2 cells. Thus, the altered metabolism of the HepG2 cells must be considered in studies involving the metabolism of a substance.

To overcome this issue, cell lines have been developed that come from healthy donors and have been immortalized. One example is the Fa2N-4 cell line. This cell line is developed by MultiCell Technologies (Warwick, RI) as a primary human simian virus 40 (SV-40) immortalized hepatic cell line [68]. Due to the Fa2N-4 cells, the xenobiotic metabolism-associated enzymes can also be examined more reliably. Hariparsad et al. (2008) compared the transcription of different metabolically involved proteins in Fa2N-4 cells with four different batches of cryopreserved primary human hepatocytes. Here the expression of UGT2B7 and CYP2C9 was comparable with two and three batches of primary human hepatocytes, respectively [69]. Furthermore, the transcription of CYP2C9, CYP3A4, and UGT1A could be induced in the Fa2N-4 cells in response to corresponding inducers and the activity of CYP2C9 enzyme has been confirmed due to the hydroxylation of DCN [68].

In addition to individual cell cultivation, in recent years it has been stated that *in vitro* co-cultivation probably reflects the *in vivo* situation more appropriate. Mitaka *et al.* (1999) demonstrated that primary rat hepatocytes maintained proliferation in an artificial 3-dimensional setting due to the presence of non-parenchymal cells. In contrast, single cultured primary rat hepatocytes de-differentiate within three days [70]. Concerning human primary hepatocytes, co-cultivation with supportive 3T3 fibroblasts shows that functionality is maintained for six weeks [71]. However, different cell lines can lead to different results in a co-cultivation compared to the corresponding individual cultivation. Thus, co-cultivation of the hepatocyte and monocyte cell line (Huh7 and THP-1 cells), respectively, showed an improved chemical sensitivity and represent a pro-inflammatory *in vitro* model [72]. THP-1 cells can be differentiated by phorbol 12-myristate 13-acetate (PMA) and reveal a

## Introduction

macrophage-like phenotype [73]. Indirect co-cultivation (figure 1 B) of HepG2 and PMA-differentiated THP-1 cells, established by Wewering *et al.* (2017), results in a pro-inflammatory system, as indicated by the secretion of IL-8, granulocyte macrophage colony-stimulating factor (GM-CSF), and macrophage migration inhibitory factor [74]. Granitzny *et al.* (2017) investigated the suitability of this co-cultivation system for the identification of drugs that induce DILI [75] coming to the conclusion, that positive as well as negative reference substances were correctly identified by the metabolic activity of water soluble tetrazolium-1 assays. In addition, TNF- $\alpha$  is identified as a prognostic factor for DILI development *in vitro* [75].

### 1.2 Bisphenols

The simplest form a of phenolic substances (figure 2) is phenol (hydroxybenzene), consisting of a hydroxyl group attached to an aromatic ring [76]. When two of these phenols are joined with a hydrocarbon bridge supplemented by two methyl groups, the structure of bisphenol A (BPA) results [77]. Further common bisphenols with slightly varying residues are bisphenol C (BPC), bisphenol F (BPF) and bisphenol S (BPS), as shown in Figure 2.

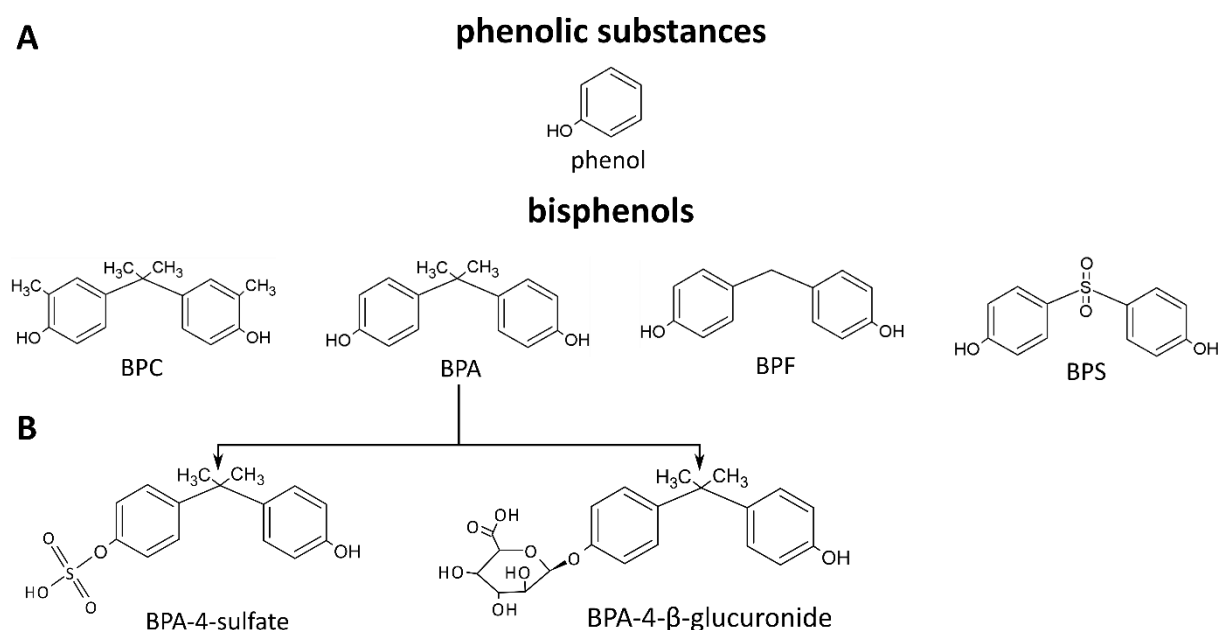


**Figure 2. Chemical structure of selected bisphenols. (A)** Shown are the chemical structures of phenol, bisphenol A (BPA), bisphenol C (BPC), bisphenol F (BPF), and bisphenol S (BPS). **(B)** The major metabolism (after phase I and phase II) of BPA to BPA-4-sulfate and BPA-4- $\beta$ -glucuronide occurs in the liver.

## Introduction

### **1.2.1 Use and consumer exposure**

BPA is an important industrial basic chemical due to its usage in epoxy resins since 1945. Furthermore, the most common thermoplastic polymer (i.e. polycarbonate) is based on BPA [77]. These polycarbonates are one among the sources of exposure of humans to BPA. Therefore, the amount of BPA is reported to be elevated in the urine of humans who are using BPA-containing drinking vessels [78]. Unused newly purchased BPA-containing polycarbonate bottles exhibit migration levels below 1 µg BPA/L (water extraction, 100°C, 1 h). However, after normal usage (dishwashing, boiling, brushing) the migration level increases (up to 15 µg/L) due to polymer degradation [79]. In addition to oral exposure, dermal exposure was identified since color developers of thermographic paper can be made of BPA or BPS. For this reason, it is not surprising that BPA and BPS could be detected in the urine of cashiers, depending on the extent of thermal paper usage/exposure [80]. Meanwhile, manufacturers and consumers are striving to replace BPA with related bisphenols [81], as a large body of evidence (over 300 published studies) links BPA to adverse health effects [82]. Also, BPC (like BPA) has been detected in bottled carbonated beverages [83]. On the other hand, BPS and BPF are being detectable in various personal care products, such as body wash, hair care products, makeup, lotions, and toothpaste [84]. Additionally, BPS was also detected in airplane luggage tags and boarding passes as well as food contact paper. The calculated dermal exposures from these sources reached levels of up to 789 ng/day [85].

The bisphenols mentioned here were also tested by Kitamura *et al.* (2005) for their estrogenic activity, since BPA is known for the endocrine-disrupting effects *in vivo*. In *in vitro* experiments concentrations were determined at which the estrogen receptor binding activity exhibits the half-maximum level ( $EC_{50}$ ). These results show that BPC binds to the estrogen receptor significantly stronger ( $EC_{50}$ = 0.42 µM) than BPA ( $EC_{50}$ = 0.63 µM), BPF ( $EC_{50}$ = 1 µM), and BPS ( $EC_{50}$ = 1.1 µM) [86]. These results show that the estrogenic activity of bisphenols varies depending on their structural features.

### **1.2.2 Risk assessment**

Risk assessment is of crucial importance to assess the estimates of exposure concentrations. The EFSA has estimated an increased dietary exposure of more than 30 µg BPA per kg canned food [87]. Besides dietary exposure, additional sources such as cosmetics and thermal paper account for BPA levels of up to 31 µg and 863 ng/kg BW/day, respectively [87]. Such BPA exposures result in blood serum concentrations of 0.002 µM [88] up to 0.004 µM (1 µg/L) [87]. As the exposure of consumers to BPA is non-negligible, the European Chemicals Agency (ECHA) has listed BPA as a substance of very high concern (EU Nr. 1272/2008). In this context, the European Commission adopted a regulation (EU Nr.

## Introduction

2016/2235) in 2016 that has set the maximum usage of BPA in thermal papers (such as receipts) at a level of 0.02 % (by weight). This European regulation came into force on January 2, 2020.

In general, BPA has been classified as reprotoxic (Repr. 1B) [89], as potential skin sensitizer (Skin Sens. 1), as well as a respiratory (STOT SE 3) and potential eye (Eye Dam. 1) irritant [90]. The Member State Committee of ECHA agreed to classify BPA also as an endocrine disruptor [89]. The EFSA was also able to identify possible BPA target organs such as liver, kidney, and mammary glands (proliferation) [87]. Based on this data, a temporary tolerable daily intake (tTDI) level of 4 µg/kg BW/day was derived. The toxicological data basis of BPC is by far not as detailed as for BPA. BPC is currently labelled as skin irritant (Skin Irrit. 1) and as severe eye-damaging (Eye Irrit. 2) substance. However, up to now there is no harmonized classification of BPC. Similarly, BPS has so far only been classified by the industrial registrants and a harmonized classification is still pending. The ECHA has concluded that BPS could be classified as reprotoxic (Repr. 1B) and skin irritant (Skin Irrit. 2) [91].

The bisphenols examined here display a high degree of structural similarity (*cf.* chapter 1.2 figure 2). BPC differs from BPA only by two additional methyl groups each of which being attached to the phenolic ring (figure 2 A). BPS is also structurally comparable since one dimethyl methylene group (-CH(CH<sub>3</sub>)<sub>2</sub>) is replaced by a sulfonyl group (-SO<sub>2</sub>-). These supposedly small structural differences make these bisphenols ideal candidates for the investigation of structure-dependent cell toxicity and a possible read-across approach. The read-across approach is an accepted method for risk assessment, suitable to substitute data gaps of a certain target substance by using information from analogous substances [92]. Using bisphenols as an example, BPA might be a candidate to fill the data gaps of the potential target substance BPC.

### **1.2.3 Pharmacokinetics and metabolism**

A large number of studies (> 300 publications) focus on the effects of BPA [82], including the pharmacokinetic properties. Accordingly, BPA has a half-life of 53 min and is taken up and eliminated from the central compartment (plasma) within 17 min [93]. These analyses can also be used to determine pharmacokinetic parameters. BPA has a clearance rate from plasma of 0.13 L/min and a volume of distribution related to the terminal kinetic phase of 37 L [93].

BPA is subject of xenobiotic metabolism. Studies in primary human, rat, and mouse hepatocytes confirmed that BPA undergoes glucuronidation or sulfatation [94]. Figure 2 B displays the structures of the resulting BPA-glucuronide and BPA-sulfate, respectively. Studies that applied liver microsomes from rats confirmed glucuronidation catalyzed by the enzyme UGT2B1 [95]. In humans, a recombinant variant of UGT2B15 was found to be involved in BPA glucuronidation [96]. The BPA-glucuronide loses

## Introduction

any binding capacity to the estrogen receptor [97]. Sulfation of BPA also leads to a lower estrogen receptor binding activity. However, in human metabolism conjugation of BPA to sulfate occurs only to a minor extent [98].

To some extent, metabolic conversion of all other bisphenols (BPS, BPF, BPC) considered in this work goes beyond sulfation and glucuronidation. However, human primary hepatocytes and human liver enzymes (S9 fraction) predominantly catalyse glucuronidation and sulfatation of BPS and BPF [99, 100]. For BPC, studies with human liver microsomes could also confirm glucuronidation [101]. These results show that all of these BPA derivatives, like BPA itself, are mainly converted into glucuronides and sulfates. EFSA summarized that human excretion of bisphenols, such as BPA, occurs via urine within 24 h almost completely in its metabolized (conjugated) form [102].

## 2. Objectives

Substances such as BPA can initiate adverse toxic effects in the liver and other organs. One way of predicting such adverse effects takes advantage of the so-called read across approach. The first part of this thesis will address this approach. It will be investigated whether or not it would be possible to foresee the adverse effects of BPC based on the toxicological data of BPA.

Pro-inflammatory systems are very sensitive to study certain substance effects. It has been proven that even bounded cellular and tissue inflammation can lower the threshold of the onset of a substance specific adverse effect [103]. Such modest inflammation can be induced in an animal model by performing pre- or co-treatment with low doses of LPS [104-106]. In this context, it is not fully understood whether LPS itself may trigger any additional effects in the cells besides pro-inflammatory signaling pathways. It is known that LPS can be modified *in vivo* by KC and then degraded by hepatocytes [107], the role of this metabolic conversion for the initiation of substance-specific adverse effects remains open though.

Accordingly, a reliable hepatic pro-inflammatory system becomes desirable, especially for the identification of adverse substance effects, which at best does not require the co-stimulus of LPS.

For this reason, the second part of the thesis will focus on the characterization of an already established co-culture model consisting of HepG2 and THP-1 cells. It will be examined whether the already postulated prognostic factor TNF- $\alpha$  [75] is able to indicate bisphenol-related adverse effects and which physiological processes of the cells are being altered in the co-culture. The investigated physiological processes include xenobiotic metabolism, cholesterol biosynthesis, lipid metabolism, and characteristics of inflammation (e.g., interactions of cytokines).

In a second step it will be clarified whether reproducible primary SV-40 immortalized hepatocytes (Fa2N-4) are also able to form a pro-inflammatory system without the need for LPS co-stimulation. For this reason, the Fa2N-4 cells will be indirectly co-cultivated with monocyte derived macrophages (MDM). Indirect co-cultivation is assumed to reflect the physiological topology in the liver in a more appropriate way. With this new co-culture system, pro inflammatory signaling pathways will be investigated, potential interactions of cytokines will be uncovered, and interactions will be evaluated by applying specific cytokine-neutralizing antibodies. Finally, these interactions will be compared with the previously established liver cell co-culture model (HepG2/THP-1).

### **3. Results**

#### **3.1 Minor structural modifications of bisphenol A strongly affect physiological responses of HepG2 cells**

Florian Padberg, Patrick Tarnow, Andreas Luch, and Sebastian Zellmer

*Archives of Toxicology* volume 93, pages1529–1541(2019)

Published online: 4 May 2019

DOI: 10.1007/s00204-019-02457-y

Link: <https://doi.org/10.1007/s00204-019-02457-y>

Involvement of the author within this publication: project planning: 70 %, project execution: 95 %, data analysis: 95 %, writing the manuscript: 70 %

The supplementary material to the publication embedded on the following pages is contained in Annex I.



## Abstract

Bisphenols represent a large group of structurally similar compounds. In contrast to bisphenol A (BPA) and bisphenol S (BPS), however, toxicological data are usually scarce, thus making bisphenols an ideal candidate for read-across assessments. BPA, bisphenol C (BPC) and a newly synthesized bisphenol A/C (BPA/C) differ only by one methyl group attached to the phenolic ring. Their  $EC_{50}$  values for cytotoxicity and  $\log P_{OW}$  values are comparable. However, the estrogenic activities of these bisphenols are not comparable and among this group only BPC leads to a decrease of the mitochondrial membrane potential and ATP concentration in HepG2 cells. Conversely, the cell division rate was decreased by BPS, BPA, BPC and BPA/C at 10 % toxicity ( $EC_{10}$ ). At lower concentrations, only BPC significantly affected proliferation. The pro-inflammatory cytokines *TGFB1* and *TNF* were significantly upregulated by BPC only, while *SPP1* was upregulated by BPA, BPA/C and BPS. BPC led to the release of cytochrome c from mitochondria, indicating that this compound is capable of inducing apoptosis. In conclusion, the read-across approach revealed non-applicable in the case of the various structurally and physicochemically comparable bisphenols tested in this study, as the presence of one or two additional methyl group(s) attached at the phenol ring profoundly affected cellular physiology.

Keywords: 2,2-bis(4-hydroxyphenyl) propane, 2,2-bis(4-hydroxy-3-methylphenyl) propane, 4,4'-sulfonyl-diphenol, mitochondria, intrinsic apoptosis, HepG2 cells

## Introduction

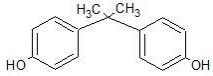
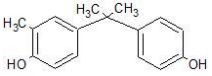
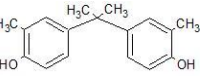
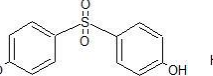
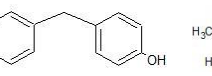
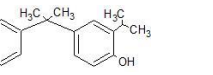
Bisphenol A (BPA, see table 1) is used in different consumer products. At high nanomolar concentrations it exhibits estrogenic activity, as well as liver and kidney toxicity (EFSA 2017). Therefore, BPA is often replaced by bisphenol S (BPS) in its manufacture (Rochester and Bolden 2015). The presence of BPS has been reported in thermal paper, advertised as “BPA-free” (Liao et al. 2012). The presence of bisphenol C (BPC) has been detected in bottled carbonated beverages (Mandrah et al. 2017) as well as in waste water (Cesen et al. 2018). In MCF7 cells BPS and BPA showed a lower estrogenic activity compared to BPC (Kitamura et al. 2005). The human serum levels of BPA are 0.002  $\mu$ M (Kuroda et al. 2003) and the European Food Safety Authority (EFSA) published a concentration level of up to 1  $\mu$ g/l (0.004  $\mu$ M) (EFSA 2015). Interestingly, in the urine of cashiers a two-fold increase of BPA (up to 2.76  $\mu$ g/g creatinine) and a slight increase of BPS (up to 0.54  $\mu$ g/g creatinine) compared to non-cashiers has been determined, dependent upon the use of thermal paper (Thayer et al. 2016). So far there are no exposure data available for BPC. To close this gap, a European human biomonitoring program has been initiated (<https://www.hbm4eu.eu/>). The presence of different bisphenols in consumer products underlines the need for further risk characterization. The European

### Minor structural modifications of bisphenol A strongly affect physiological responses of HepG2 cells

Chemical Agency (ECHA) has evaluated BPA as substance of very high concern (SVHC) (EU (Nr. 1272/2008) due to its reprotoxic properties (Repr. 1B) and in June 2017 the Member State Committee of ECHA agreed to classify BPA as an endocrine disruptor (ECHA 2018b). Furthermore, it is classified as potential skin sensitizer (Skin Sens. 1), as well as a respiratory (STOT SE 3) and potential eye (Eye Dam. 1) irritant (ECHA 2017c). The EFSA identified several 'likely' target tissues of BPA toxicity, being liver as well as kidney and mammary glands (proliferation). Effects on these organs were used for risk characterisation (EFSA 2015). Based on the 'likeness' of effects the EFSA has derived a temporary tolerable daily intake (tTDI) of 4 µg/kg BW/day. The general toxicity of BPA to liver and kidney as well as reproductive, developmental, neurological, immune metabolic and cardiovascular toxicity, mammary gland changes, carcinogenicity and genotoxicity are currently re-evaluated (EFSA 2017).

Minor structural modifications of bisphenol A strongly affect physiological responses of HepG2 cells

**Table 1** Structure, IUPAC name, molecular weight (MW), CAS number, distribution coefficient (logP<sub>ow</sub>), 50% (EC<sub>50</sub>) and 10% (EC<sub>10</sub>) of the effective concentration of the bisphenol A (BPA), bisphenol A/C (BPA/C), bisphenol C (BPC), bisphenol S (BPS), bisphenol F (BPF) and bisphenol G (BPG).

Structure	BPA	BPA/C	BPC	BPS	BPF	BPG	
							
IUPAC name	2,2- <i>bis</i> (4-hydroxyphenyl)propane	2-(4-hydroxy-3-methylphenyl)-2-(4'-hydroxyphenyl)propane	2,2- <i>bis</i> (4-hydroxy-3-methylphenyl)propane	4,4'-Sulfonyldiphenol	4,4'-Methylene-diphenol	2,2- <i>bis</i> (4-hydroxy-3-isopropylphenyl)propane	
CAS	80-05-7	14151-63-4	79-97-0	80-09-1	620-92-8	127-54-8	
logP <sub>ow</sub>	[-]	3.64	4.06	4.46	1.66	2.89	6.00
MW	[g/mol]	228.29	242.31	256.34	250.27	200.23	312.45
EC <sub>50</sub>	μM	261	153	196	2061	735	59
EC <sub>10</sub>	μM	131	60	117	284	224	21

## Minor structural modifications of bisphenol A strongly affect physiological responses of HepG2 cells

BPC has been registered under REACH, resulting in labels for skin irritation (Skin Irrit. 2), serious eye damage (Eye Irrit. 2) and respiratory irritancy (STOT SE 3) (ECHA 2018d). In contrast, BPS has been fully registered at ECHA, is listed on the Community Rolling Action Plan (CORAP), and has a self-classification for harmfulness against aquatic life with long lasting effects (Aquatic Chronic 3), as well as for serious eye irritancy (Eye Irrit. 2) (ECHA 2018a). Structurally, these bisphenols are quite similar: BPC differs from BPA only by two additional methyl groups on either phenolic ring. BPS is a close analog of BPA as well, in which the dimethyl methylene group ( $C(CH_3)_2$ ) is replaced by a sulfonyl functional group ( $SO_2$ ).

One accepted method to validate the potential risk, is the read-across assumption, which can be used to substitute for data gaps of a certain target substance using information from analogous substances (ECHA 2017b). Choosing an appropriate model for the route of metabolism is essential in order to fill these data gaps. The first evidence that described the route of metabolism demonstrated the involvement of the enterohepatic cycle in the metabolism of BPA in rats (Doerge et al. 2010). The enterohepatic cycle is responsible that the same molecule of a potentially toxic substance is metabolized several times in the liver (Malik et al. 2016). Due to this repeated tissue exposure, hepatocytes may be strongly affected by BPA. According to EFSA, liver is one of the main target organs of BPA toxicity (EFSA 2015). Hepatic cell lines are a suitable model for the investigation of potentially adverse effects. Based on a dose-dependent increase of DNA strand breaks observed in hepatoblastoma HepG2 cells, a recent study claimed that BPA and BPS, but not BPC, were genotoxic (Fic et al. 2013). Yet, it is still generally accepted that BPA is not genotoxic (EFSA 2015). One reason might be that different bisphenols can have different effects on various hepatic cell lines.

The aim of this study was to apply a read-across approach using BPA as source substance and the structurally related BPC and BPA/C as target substances. The outcome has been compared with the results obtained *in vitro* by exposing HepG2 cells to the respective compounds. Mechanistic investigations were performed in order to evaluate whether a read-across approach is suitable in this case, or not.

### **Materials and methods**

#### Chemicals and antibodies

All chemicals were purchased from Sigma-Aldrich (Taufkirchen, Germany) unless stated otherwise. Furthermore, Dulbecco's phosphate-buffered saline (DPBS) (PAN-Biotech, Aidenbach, Germany) and Bisphenol A/C (BPA/C) (Angene, London, UK) was used. The following antibodies were used:  $\beta$ -actin

## Minor structural modifications of bisphenol A strongly affect physiological responses of HepG2 cells

(AC-15),  $\alpha$ -tubulin, cytochrome C (EPR1327), mitofilin (2E4AD5) (all from Abcam, Cambridge, UK) and ER $\alpha$  (F-10) (Santa Cruz Biotechnology, Heidelberg, Germany).

### Cell culture

All single-use plastics were purchased from TPP (Trasadingen, Switzerland) and all cell lines were purchased from DSMZ (Braunschweig, Germany). HepG2 cells were grown in RPMI 1640 (PAN-Biotech, Aidenbach, Germany) containing 10% (v/v) FCS (PAN-Biotech, Aidenbach, Germany), 100 U/ml penicillin, 100 mg/ml streptomycin, 2 mM L-glutamine at 37 °C and 5% CO<sub>2</sub>. THP-1 cells were differentiated under the influence of 100 nM phorbol-12-myristate-13-acetate (PMA) for 24 h. THP-1 cultivation and the co-culture were done according to Wewering et al. (2017). When THP-1 and HepG2 cells were combined, the bisphenol treatment started immediately. MCF7 cells were purchased from American Type culture collection (Manassass, VA, USA) and were grown in DMEM (PAN-Biotech, Aidenbach, Germany) containing 100 U/ml penicillin, 100 mg/ml streptomycin, 2 mM L-glutamine at 37 °C and 5% CO<sub>2</sub>. Hela9903 cells were purchased from JCRB cell bank (JCRB-No. 1318) (Tokio, Japan) and were cultivated according to Tarnow *et al.* (2013).

### Cytotoxicity testing

The MTT Assay was performed with minor modifications according to Mosmann (1983). All values were corrected for the DMSO solvent controls. All substances were tested in a concentration range using log<sub>2</sub> serial dilutions [BPA (1.75 mM–0.22  $\mu$ M), BPA/C (1.6 mM–54.75  $\mu$ M), BPC (1.56 mM–0.22  $\mu$ M), BPS (6.39 mM–0.88  $\mu$ M), BPF (1.99 mM–0.44  $\mu$ M), BPG (1.28 mM–0.22  $\mu$ M)].

### Mitochondrial membrane potential

Cells were seeded at a density of  $1.3 \times 10^6$  cells per cm<sup>2</sup>. After treatment for 24 h, cells were detached using trypsin/EDTA (PAN-Biotech, Aidenbach, Germany). Before staining the cells were incubated for 2 h at 37 °C and 5% CO<sub>2</sub> with 100  $\mu$ M of the decoupling agent carbonyl cyanide 3-chlorophenylhydrazone (CCCP). The mitochondrial membrane potential ( $\Delta\Psi$ ) was determined via incubation with 30  $\mu$ M JC-10 (Adipogen, Liestal, Switzerland) for 30 min at 37 °C. Fluorescence intensities were measured with the FACS Aira III (PE channel settings: 585/42 nm, FITC channel settings: 530/30) (BD Biosciences, Heidelberg, Germany) and the cells were analyzed with the software FlowJo v 10 (FlowJo LLC, Ashland, OR, USA).

## Minor structural modifications of bisphenol A strongly affect physiological responses of HepG2 cells

### ATP measurements

Cells were seeded at a density of  $1.3 \times 10^6$  cells per  $\text{cm}^2$ . After treatment for 24 h, the ATP concentration was determined using the Bioluminescence Assay Kit HS II (Roche, Basel, Switzerland) according to the manufacturer's protocol.

### Cell division analysis

Cells were seeded at a density of  $0.75 \times 10^5$  cells per  $\text{cm}^2$ . After 48 h the cells were stained for 30 min at room temperature with 5(6)-carboxyfluorescein *N*-hydroxysuccinimidyl ester (CFSE) (Cayman, Hamburg, Germany). Staining was terminated with 10% FCS in phosphate-buffered saline (PBS) followed by washing with DPBS. Fluorescence was measured with the FACS Aria III (FITC channel settings: 530/30) (BD Biosciences, Heidelberg, Germany) and analyzed with the FlowJo v 10 (FlowJo LLC, Ashland, OR, USA).

### PCR analysis

RNA was isolated using the NucleoSpin RNA Kit (Machery-Nagel, Düren, Germany) and the reverse transcriptions were performed with the high-capacity cDNA Reverse Transcription Kit (Applied Biosystems, Foster City, CA, USA) according to the manufacturer's protocol. Quantitative PCR (qPCR) was performed with 7500 Fast Real-Time PCR Instrument using Fast SYBR Green Master Mix (Applied Biosystems, Foster City, CA, USA) according to the manufacturer's protocol. The primer sequences are listed in Table 2. The  $\Delta\Delta\text{CT}\Delta\Delta\text{CT}$ -value was calculated according to Livak and Schmittgen (2001) and normalized to the expression of hypoxanthine–guanine phosphoribosyltransferase (*HPRT*) in control (DMSO treated) cells.

## Minor structural modifications of bisphenol A strongly affect physiological responses of HepG2 cells

**Table 2** Primer sequences used. The gene symbol, the sequence of the forward and reverse primers and the product size in base pairs (bp) is given.

gene	forward primer	reverse primer	product
<i>HPRT</i>	gttctgtggccatctgcttag	gcccaaagggaactgatagtc	144 bp
<i>BCL2</i>	gaggattgtggccttctttg	acagttccacaaaggcatcc	170 bp
<i>TGFB1</i>	gtggaaaccacacacgaaat	cacgtgctgctccacttta	165 bp
<i>SPP1</i>	gccgaggtgatagtgtggtt	ctcctcgctttccatgtgtg	119 bp
<i>TNF</i>	cttctgcctgctgcactttggag	ggctacaggcttgcactcgg	130 bp

### Elisa

HepG2 cells and THP-1 cells were seeded at densities of  $1.3 \times 10^6$  cells per  $\text{cm}^2$  and of  $0.65 \times 10^6$  cells per  $\text{cm}^2$ , respectively. TNF- $\alpha$  in the supernatant of cell culture was measured using the DuoSet<sup>®</sup> ELISA Human TNF- $\alpha$  (R&D Systems, Abingdon, UK) according to the manufacturer's protocol.

### Western-blot

Cells were lysed at 4 °C with RIPA buffer (50 mM Tris/HCl (pH 7.4), 159 mM NaCl, 1 mM EDTA, 1% Igepal<sup>®</sup>, 0.25% sodium deoxycholate, and protease inhibitor cocktail). Mitochondrial isolation (Clayton and Shadel 2014a) and purification was performed according to Clayton and Shadel (2014b) including lysis with tight fit douncer, ultracentrifugation using a sucrose step density gradient. The enrichment of the mitochondrial fraction was validated in pooled samples (Figure S1). Protein concentration was measured with the Pierce<sup>™</sup> BCA Protein Assay Kit (Thermo Scientific, Waltham, MA, USA) and equal amounts of protein were applied to SDS-PAGE transferred onto nitrocellulose membranes according to the manufacturer's instructions. Primary anti-bodies were labelled with the corresponding horseradish peroxidase coupled secondary antibody and visualized with Pierce ECL Substrate (Thermo Fisher Scientific, Waltham, MA, USA).

### Estrogen activity

Estrogenic activity was measured according to TG 455 (OECD 2016).

## Statistics

All shown data contain at least three independent biological replicates. Means, standard deviations and the  $p$  values of the ANOVA followed by Bonferroni correction were calculated with GraphPad Prism 6 (Statcon, Witzenhausen, Germany). The effective concentrations ( $EC_{50}$ ,  $EC_{10}$  and  $EC_{50E}$ ) were calculated under the programming environment R (R Core Team 2018) according to Wewering *et al.* (2017). The distribution coefficient ( $\log P_{ow}$ ) was calculated with Gastro Plus™ version 9.5 (Simulations Plus, Lancaster, CA, USA).

## **Results**

### Physicochemical properties and toxicity of bisphenols in HepG2 cell cultures

BPA/C, BPC and BPS are of comparable molecular weights (MW), that is, between 242.31 g/mol and 256.34 g/mol (Table 1). In contrast, BPA and BPF are of lower MW, being 228.29 g/mol and 200.23 g/mol, respectively. In this series of compounds, only the MW of BPG is greater than 300 g/mol. The oil/water distribution coefficients ( $\log P_{ow}$ ) of BPA, BPA/C and BPC are in the range of 3.64–4.46 (Table 1). BPS and BPF exhibit lower  $\log P_{ow}$  values of only 1.66 and 2.89, respectively, while BPG had the highest  $\log P_{ow}$  value of 6.0. In summary BPA, BPA/C, BPC have similar molecular structures, similar molecular weights and comparable  $\log P_{ow}$  values. A closer look shows that the  $\log P_{ow}$  of these three bisphenols increases with increasing numbers of methyl groups (BPA < BPA/C < BPC), making these bisphenols ideal candidates for a read-across approach.

To support the read-across approach further, the cytotoxicity of bisphenols was studied *in vitro*. HepG2 cells were incubated with different concentrations of BPA, BPA/C, BPC, BPG, BPF and BPS and half maximal effective concentrations ( $EC_{50}$ ) were determined (Fig. 1). BPA and BPC showed  $EC_{50}$  values of  $261 \pm 27 \mu\text{M}$  and  $196 \pm 53 \mu\text{M}$ , respectively. BPA/C was characterized by an  $EC_{50}$  value of  $153 \pm 8 \mu\text{M}$ , BPS was found about tenfold less toxic compared to BPC with an  $EC_{50}$  value of  $2061 \pm 1580 \mu\text{M}$ . The cytotoxicity of BPF was between BPA and BPS with an  $EC_{50}$  of  $735 \pm 412 \mu\text{M}$ . The most toxic bisphenol investigated in our study was BPG with an  $EC_{50}$  of  $59 \pm 22 \mu\text{M}$ . In summary, the  $EC_{50}$  values of the six bisphenols investigated correlated roughly with the respective  $\log P_{ow}$  values. Significant differences ( $p \leq 0.01$ ) were detectable between  $EC_{50}$  values of BPA and BPA/C but not for BPA and BPC or BPA/C and BPC. The four compounds BPA, BPA/C, BPC, BPS were selected for further investigation, either based on their relevance as contaminant of food contact materials (BPA, BPS, BPC) or based on their structural and physicochemical similarities (BPA/C). For further experimental studies, the  $EC_{10}$  values were calculated, based on the experimental data (Figure S2, Table 1).



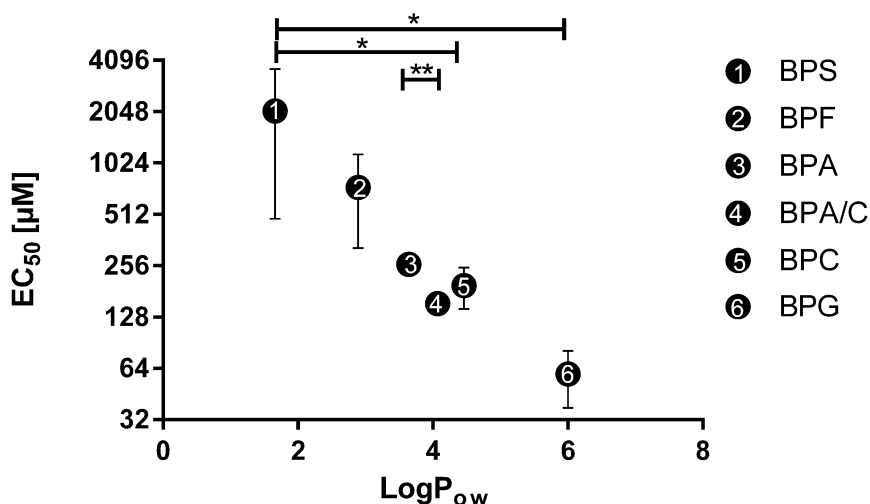


**Fig. 1** Correlation between the  $\log P_{ow}$  and the  $EC_{50}$ . HepG2 cells were treated with bisphenol S (BPS), bisphenol F (BPF), bisphenol A (BPA), bisphenol A/C (BPA/C), bisphenol C (BPC) and bisphenol G (BPG) for 24 h ( $n = 3$ ). The mean and the SD of the half maximal effective concentration ( $EC_{50}$ ) were calculated under the program environment R and the oil/water distribution coefficient ( $\log P_{ow}$ ) with Gastro Plus™ version 9.5. \* $p < 0.05$ , \*\* $p < 0.01$

#### Bisphenol treatment decreases cell division rate

BPA affects the cell division rate in vitro, depending on substance concentration and the cell line. Previously, a BPA-mediated increase of cell proliferation has been observed in MCF7 cells due to estrogen receptor (ER) activation (Potratz et al. 2017). Conversely a BPA-mediated decrease in cell proliferation was observed in murine osteosarcoma cells (Kidani et al. 2017). In our study, we looked into the effects of bisphenols on HepG2 cell division rates. Low, non-toxic concentrations ( $EC_{10}$ ) were used for cell treatments (see Table 1). At  $EC_{10}$  the cell division rates were significantly ( $p \leq 0.01$ ) reduced by 0.37-, 0.63- and 0.41-fold for BPA, BPA/C and BPC, respectively (Fig. 2b). In contrast, BPS did not change the cell division rate of HepG2 cells. At the dose of one-third of the  $EC_{10}$ , that is, 44 µM of BPA, 19 µM of BPA/C, 39 µM of BPC, and 95 µM of BPS, only BPC decreased the cell division rate significantly ( $p \leq 0.01$ ) 0.65-fold, compared to the vehicle control (Fig. 2a).

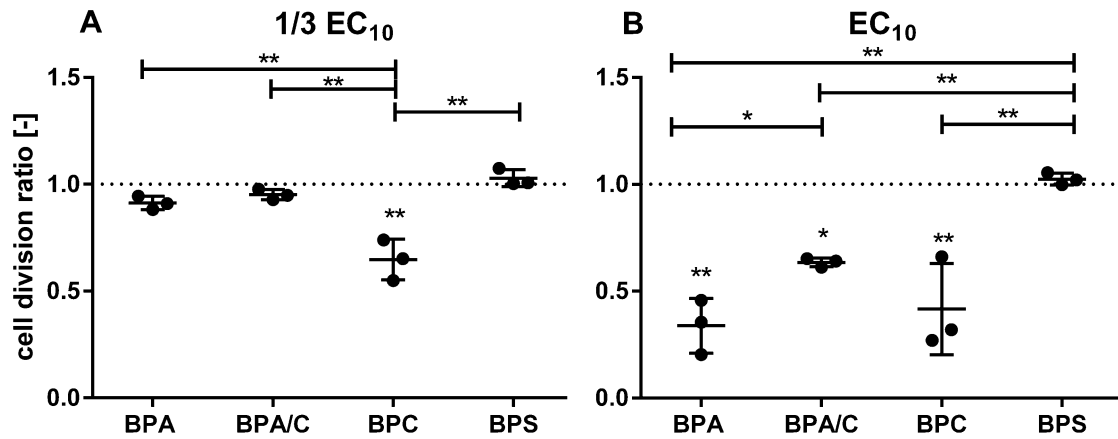


**Fig. 2** Cell division rate is affected by bisphenols. Effects of different bisphenols on the cell division rate of HepG2 cells after 48 h. HepG2 cells were treated with bisphenol A (BPA), bisphenol A/C (BPA/C), bisphenol C (BPC) and bisphenol S (BPS) for 48 h ( $n = 3$ ). Measurements ( $\bullet$ ), mean ( $-$ ) and SD ( $-$ ) of the cell division related to solvent control ( $\cdots$ ) are shown. Treatment concentrations: **a** 1/3 of 10% of the effective concentration ( $EC_{10}$ ) and **b** the  $EC_{10}$ . \* $p < 0.05$ , \*\* $p < 0.01$

#### Bisphenol C decouples the mitochondrial membrane potential $\Delta\psi_m$

There is evidence that the mitochondrial membrane potential and the oxygen consumption changes in different cell types (Jurkat, HeLa and HEK-293T) during early and late phase of the cell cycle (Schieke et al. 2008). Therefore, we were interested to determine whether changes in the cell division rate were linked to the mitochondrial membrane potential ( $\Delta\psi_m$ ) in HepG2 cells. The  $EC_{10}$  and one-third of  $EC_{10}$  were used to study the effect on the  $\Delta\psi_m$ . Only the BPC-treated cells showed a significant decrease in  $\Delta\psi_m$  (Fig. 3a). This decrease of  $\Delta\psi_m$  was dependent on the BPC concentration applied. The  $\Delta\psi_m$  value at the  $EC_{10}$  of BPC significantly decreased to  $46 \pm 37\%$  ( $p \leq 0.05$ ) in HepG2 cells when compared to the treatment with one-third of  $EC_{10}$  (Fig. 3b). In summary, BPA, BPA/C and BPS did not reduce the  $\Delta\psi_m$ , while BPC had a strong effect on this cellular parameter.

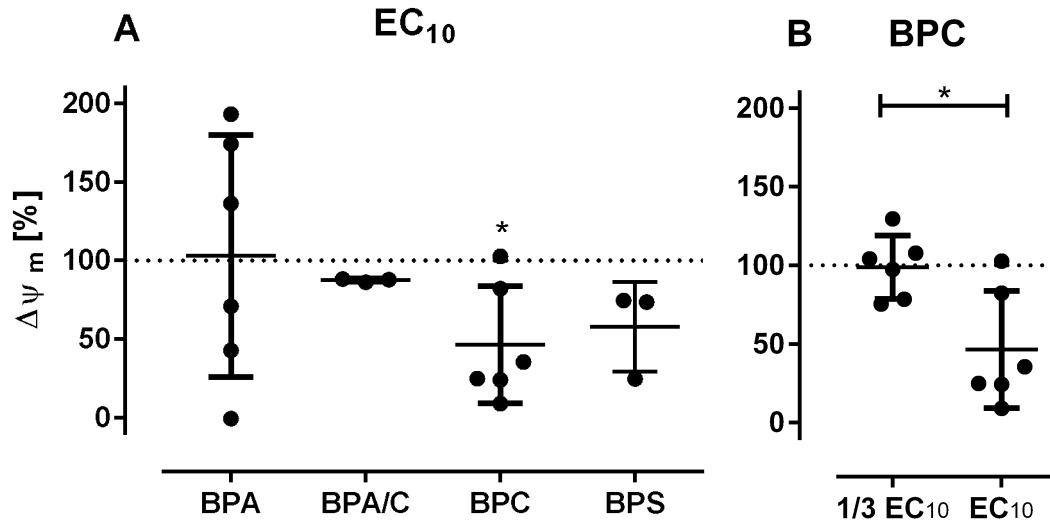


**Fig. 3** Effects of different bisphenols on mitochondrial membrane potential  $\Delta\psi_m$ . HepG2 cells were treated with bisphenol A (BPA), bisphenol A/C (BPA/C), bisphenol C (BPC) and bisphenol S (BPS) for 24 h ( $n = 3$ ). Measurements ( $\bullet$ ), mean ( $-$ ) and SD ( $-$ ) of the mitochondrial membrane potential ( $\Delta\psi_m$ ) related to solvent control ( $\cdots$ ) and based to the positive control (carbonyl cyanide 3-chlorophenylhydrazone, CCCP) are shown. **a** Shown are the 10% of effective concentration ( $EC_{10}$ ) and **b** one-third of  $EC_{10}$  and the  $EC_{10}$  of BPC.  $*p < 0.05$

#### BPC reduces the intracellular ATP concentration

The  $\Delta\psi_m$  is used for the generation of ATP. Therefore, we asked whether changes in  $\Delta\psi_m$  would affect the ATP levels in the cells. Neither BPA, BPA/C nor BPS treatment led to a significant reduction of the intracellular ATP concentration compared to the solvent control (DMSO). In contrast a significant 5-fold ( $p \leq 0.01$ ) reduction occurred after treatment with BPC at  $EC_{10}$  after 24 h (Fig. 4).

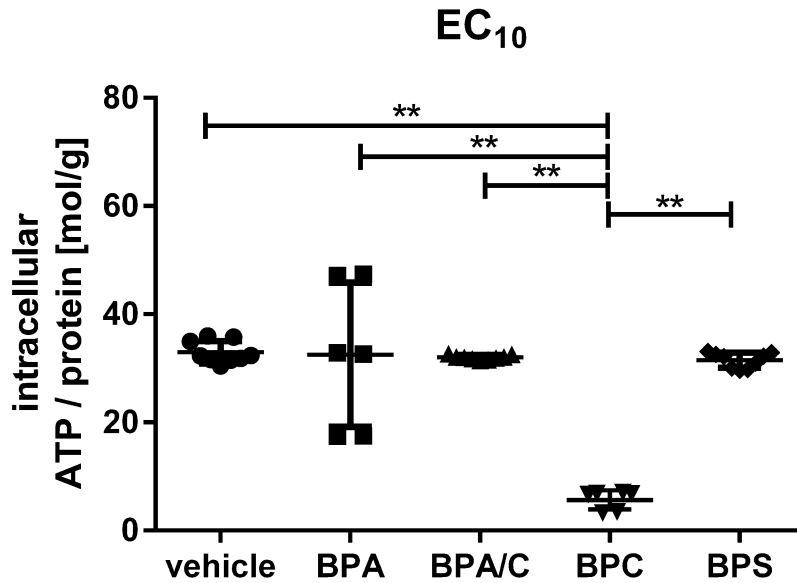


**Fig. 4** Effects of bisphenols on intracellular ATP levels, normalized to the total protein. HepG2 cells were treated with 10% of the effective concentration ( $EC_{10}$ ) of bisphenol A (BPA), bisphenol A/C (BPA/C), bisphenol C (BPC), bisphenol S (BPS) and dimethyl sulfoxid (vehicle control) for 24 h ( $n = 3$ ). Measurements ( $\bullet$ ), mean ( $-$ ) and SD ( $-$ ) of the ATP concentration per g total protein are shown from 3 biological replicates.  $**p < 0.01$

#### Cytokine gene expression differs after exposure to different bisphenols

The intracellular ATP concentration might be associated with inflammation. It has already been shown that treatment of neutrophils with nonsteroidal anti-inflammatory drugs, like flufenamic acid, reduces the intracellular ATP levels (Manica et al. 2018). Therefore, the expression profiles of the cytokines *TNF*, *TGFB1* and *SPP1* (osteopontin) were investigated to study the pro- or anti-inflammatory effects of the bisphenols in focus. The pro-inflammatory cytokine osteopontin participates in several adaptive and innate immune responses, including the migration of macrophages and T-helper (Th) cells and the proliferation and survival of Th cells (Clemente et al. 2016). TGF- $\beta$  (*TGFB1*) represents a cytokine with both pro- and anti-inflammatory effects depending on the physiological conditions (Worthington et al. 2012). HepG2 cells were treated at the  $EC_{10}$  of bisphenols and the gene expression was quantified 24 h later (Fig. 5). The *TGFB1* expression of HepG2 cells exposed to BPA, BPC and BPS was significantly ( $p \leq 0.01$ ) upregulated (between 1.4- and 6-fold) compared to the vehicle control. By contrast, treatment with BPA/C did not affect the expression of *TGFB1* compared to solvent control (Fig. 5a). In addition, treatment of HepG2 cells with BPA, BPA/C or BPS resulted in a comparable up-regulation of *SPP1* (two and threefold), while BPC had no effect

(Fig. 5b). Interestingly, BPC caused a significant ( $p \leq 0.01$ ) threefold up-regulation of *TNF*, the gene encoding for TNF- $\alpha$ . In contrast, BPA, BPA/C and BPS had no significant effect (Fig. 5c).

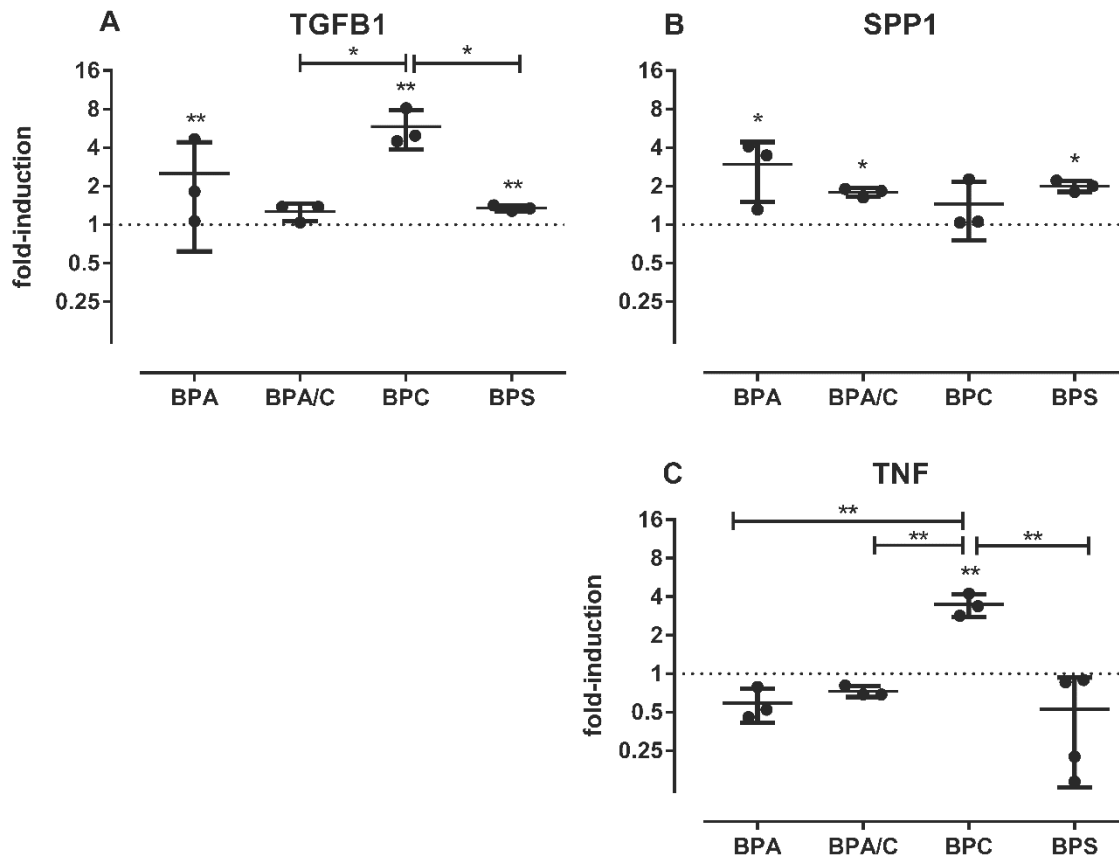


**Fig. 5** Expression of cytokines in HepG2 under the influence of bisphenols. HepG2 cells were treated with 10% of the effective concentration of bisphenol A (BPA), bisphenol A/C (BPA/C), bisphenol C (BPC) and bisphenol S (BPS) for 24 h ( $n = 3$ ). Measurements ( $\bullet$ ), mean ( $-$ ) and SD ( $-$ ) of the expression of **a** the transforming growth factor  $\beta$  1 (*TGFB1*), **b** osteopontin (*SPP1*) and **c** tumor necrosis factor (*TNF*)  $\alpha$  related to solvent-control ( $\cdots$ ) and *HPRT* ( $\Delta\Delta C_T$ ) are shown. \* $p < 0.05$ , \*\* $p < 0.01$

At pro-inflammatory cellular conditions bisphenols alter the expression of BCL2

Under single cell culture conditions treatment of HepG2 cells with bisphenols changed the expression of selected cytokines (Fig. 5). Here, we wanted to investigate cytokine expression in a co-culture system under pro-inflammatory conditions. It has been shown before, that this co-cultivation resulted in the release of chemokines and cytokines such as CCL3, IL-1 $\alpha$ , and CXCL8 (Wewering et al. 2017).

The protein BCL-2 (*BCL2*) is commonly known as inhibitor of the intrinsic apoptotic pathway (Czabotar et al. 2014). The expression levels of *BCL2* in single cell cultures of HepG2 cells were not affected by

any of the bisphenols applied (data not shown). However, this expression profile changed when cells were cultivated in a pro-inflammatory environment (Fig. 6a). BPA ( $EC_{10}$ ) led to a significant ( $p \leq 0.05$ ) up-regulation (1.8-fold) of *BCL2* in co-cultivated HepG2 cells compared to the solvent control (Fig. 6a). BPS and BPA/C showed no effect on the expression of *BCL2* compared to cells treated with the vehicle, while HepG2 cells treated with BPC ( $EC_{10}$ ) showed a fourfold down-regulation of *BCL2*. In summary, an inflammatory environment in combination with bisphenol treatment seems to affect the up- or down-regulation of key genes of the intrinsic apoptotic pathway.

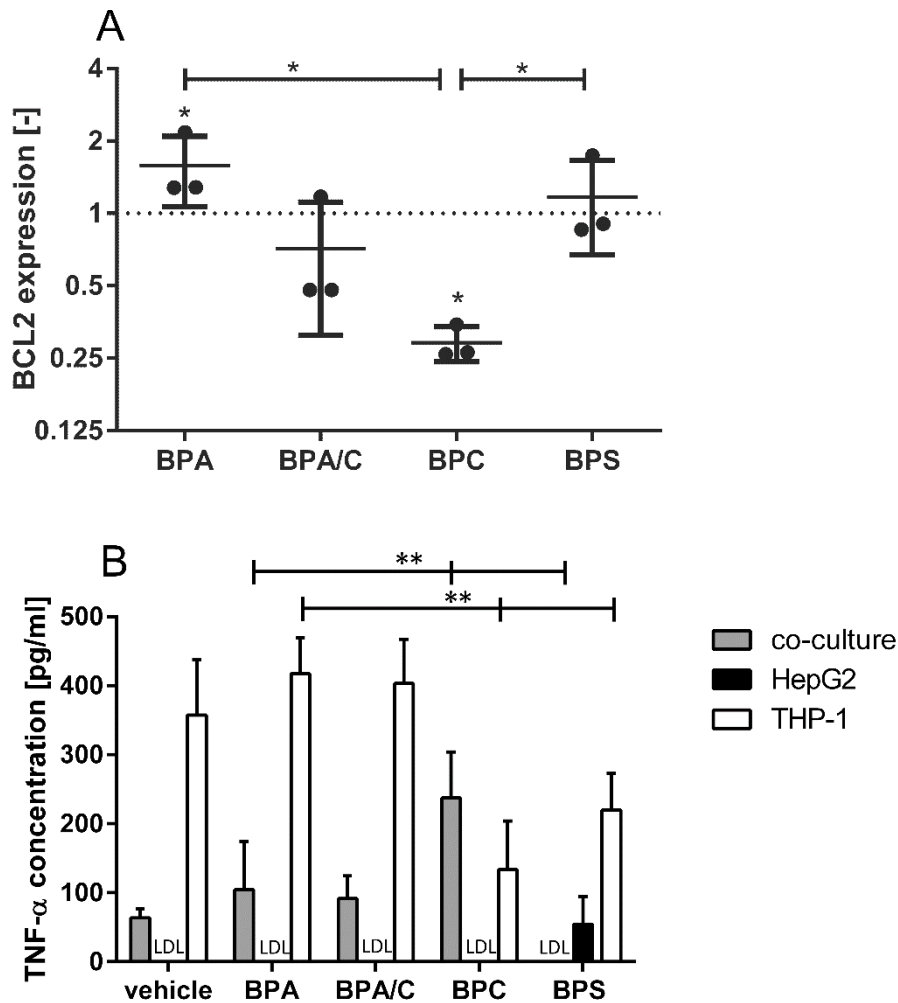


**Fig. 6** Pro-inflammation model under influence of bisphenols. HepG2 cells were co-cultivated with PMA-activated THP-1 cells and treated with the  $EC_{10}$  of bisphenol A (BPA), bisphenol A/C (BPA/C), bisphenol C (BPC) and bisphenol S (BPS) for 24 h. **a** Measurements ( $\bullet$ ), mean ( $—$ ) and SD ( $-$ ) of the expression of the B-cell lymphoma 2 (*BCL2*) related to solvent-control ( $\cdots$ ) and *HPRT* ( $\Delta\Delta CT$ ) are shown ( $n = 3$ ). **b** Concentration of tumor necrosis factor  $\alpha$  (TNF- $\alpha$ ) in the supernatant of single- and co-cultivated HepG2 and PMA differentiated THP-1 cells ( $n = 4$ ). LDL indicates values below the limit of detection of 7.8 pg/ml. \* $p < 0.05$ , \*\* $p < 0.01$

TNF- $\alpha$  secretion is affected by bisphenols

While BCL2 is a known inhibitor of the intrinsic apoptotic pathway, the cytokine TNF- $\alpha$  is known as pro-apoptotic (van Horssen et al. 2006) and essential pro-inflammatory mediator (Sedger and McDermott 2014). Consequently, the TNF- $\alpha$  secretion of bisphenol-treated HepG2 and PMA-differentiated THP-1 kept in co- and single-culture (Fig. 6b) was determined. To exclude combinatory effects of bisphenols and cytokines already secreted due to the co-culture conditions, the bisphenols were added at the onset of co-cultivation conditions. PMA-differentiated THP-1 cells secrete  $404 \pm 59$  pg/ml TNF- $\alpha$ . After BPC or BPS treatment the secretion is significantly ( $p < 0.01$ ) reduced to  $133 \pm 70$  pg/ml and  $220 \pm 53$  pg/ml, respectively. In contrast, no TNF- $\alpha$  was detectable in the single culture of HepG2 cells, except for BPS treatment (TNF- $\alpha$ :  $54 \pm 40$  pg/ml). In general, TNF- $\alpha$  secretion at co-cultivation conditions was higher  $64 \pm 13$  pg/ml to  $237 \pm 67$  pg/ml when compared to the single cultivation conditions of HepG2 and lower as in the single cultivation of PMA-differentiated THP-1. However, under the influence of BPC, the concentration of TNF- $\alpha$  in co-cultivation are comparable to PMA-differentiated THP-1 cells alone ( $237 \pm 67$  pg/ml and  $133 \pm 70$  pg/ml). TNF- $\alpha$  levels in the supernatant of co-cultures was not detectable after treatment with BPS (Fig. 6b). In brief, the TNF- $\alpha$  amount is thus dependent on the cultivation conditions and on the kind of bisphenol treatment. BPC increases the secretion of the pro-apoptotic TNF- $\alpha$  in co-cultivated HepG2 cells thereby promoting apoptosis. This coincides with the concomitant decrease in the expression level of the anti-apoptotic BCL2 protein.

Bisphenol C changes intracellular cytochrome c localisation

The activation of the intrinsic apoptotic pathway can result in a cytochrome c (CyC) release from mitochondria (Ichim and Tait 2016). This results in a decreased mitochondrial CyC concentration, while the total cellular amount of CyC remains constant. An activation of the intrinsic apoptotic pathway was studied by comparison of the CyC concentration in the mitochondrial fraction (Figure S1) and the total cell lysate (Fig. 7a). Only BPC treatment resulted in a decrease of the CyC concentration, while BPA, BPA/C and BPS had no effect. Therefore, these data support the results of the cytokine determinations and it can be concluded that only BPC activates the intrinsic apoptotic pathway, which resulted in a release of CyC.

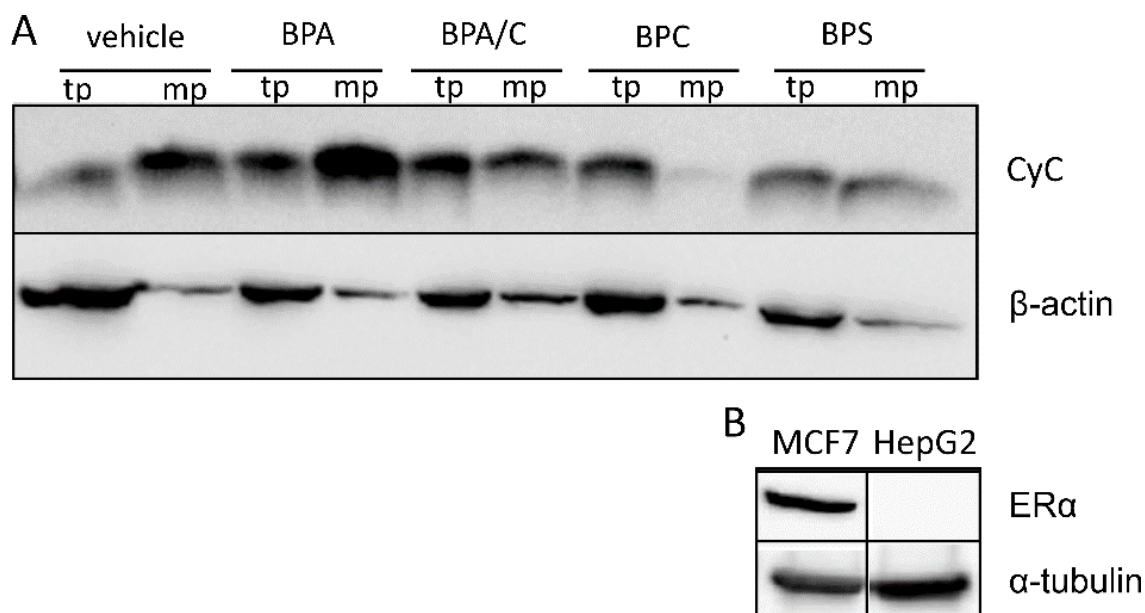


**Fig. 7** Qualitative analysis of the estrogen receptor (ER) and intracellular distribution of the protein cytochrome C. **a** HepG2 were treated with the EC<sub>10</sub> of bisphenol A (BPA), bisphenol A/C (BPA/C), bisphenol C (BPC) and bisphenol S (BPS) for 24 h. The total protein (tp) and the mitochondrial protein fraction (mp) were analyzed for cytochrome C (CyC) content, with β-actin as loading control. **b** Determination of the expression of ERα in HepG2 and MCF7 cells. The loading control α-tubulin was used

The estrogen receptor is not detectable in HepG2 cells

BPA is a known xenoestrogen (Kitamura et al. 2005). Since MCF7 cells undergo apoptosis after long-term estrogen deprivation and subsequent estrogen treatment (Song et al. 2001), we determined the total estrogen receptor α (ERα) levels in HepG2 cells to clarify whether estrogenic activity plays a crucial role for the cellular endpoints investigated in our study. Yet, Fig. 7b shows that HepG2 cells do not express any detectable levels of the ERα protein. Therefore, the described effects of bisphenols in HepG2 cells are likely independent from any estrogen receptor signaling pathways.

To validate this conclusion, the activation of the ERα signalling by the different bisphenols was investigated according to TG 455 (OECD 2016). The half maximal effective concentration for estrogen activity (EC<sub>50E</sub>) was  $0.7 \pm 0.2 \mu\text{M}$ ,  $1.2 \pm 0.2 \mu\text{M}$  and  $0.2 \pm 0.02 \mu\text{M}$  for BPA, BPA/C and BPC, respectively (Fig. 8). BPS and BPF had an EC<sub>50E</sub> of  $1.5 \pm 0.4 \mu\text{M}$  and  $1.1 \pm 0.3 \mu\text{M}$ . The highly toxic BPG had an EC<sub>50E</sub> of  $0.89 \pm 0.23 \mu\text{M}$ , similar to BPA. This shows that the increase in the number of methyl groups (BPA → BPA/C → BPC) has no comparable linear effect on the ERα activation. The EC<sub>50E</sub> of the ERα activation does not follow the same sequence, since BPC has the lowest and BPA/C the highest EC<sub>50E</sub> (Fig. 8).



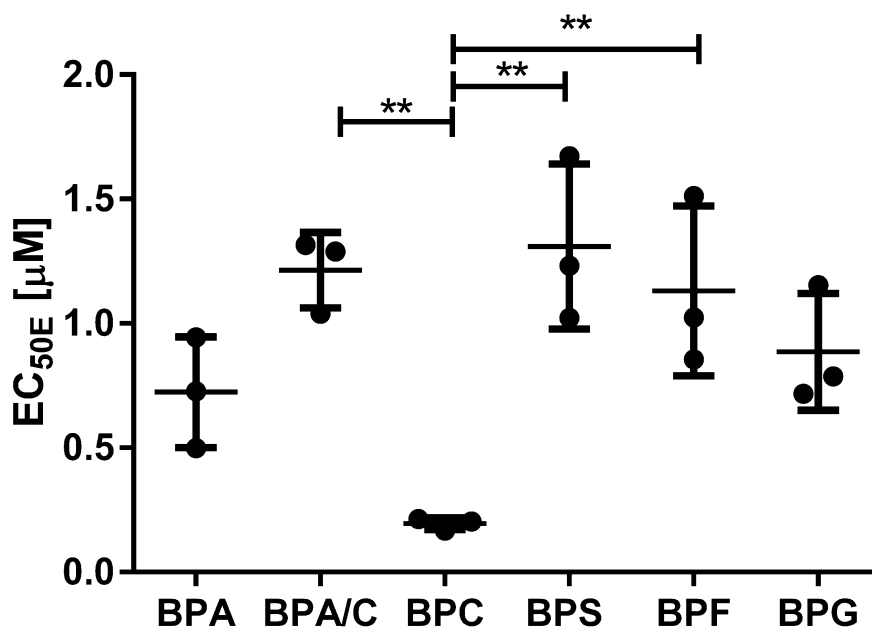


**Fig. 8** Concentration of half maximal estrogen receptor activation ( $EC_{50E}$ ). HeLa9903 cells were treated with bisphenol A (BPA), bisphenol A/C (BPA/C), bisphenol C (BPC), bisphenol S (BPS), bisphenol F (BPF) and bisphenol G (BPG) or dimethyl sulfoxide (vehicle control) and 2 nM Estrogen (positive control) for 24 h ( $n = 3$ ). The  $EC_{50E}$  were calculated under the program environment R (•) and shown are mean (—) and SD (–). \*\* $p < 0.01$

ER $\alpha$  is expressed in healthy liver tissue. Therefore, we asked, whether the results of the presented work might be affected by the absence of estrogen receptor signalling in HepG2 cells. The ER $\alpha$  signalling was activated by BPA, BPC and BPF at 10  $\mu$ M, 3.16  $\mu$ M and 10  $\mu$ M, respectively. BPA/C activated the ER $\alpha$  to  $73.4 \pm 8.8\%$  at 10  $\mu$ M. This result clearly demonstrates that the  $EC_{50}$  and  $EC_{10}$  concentrations used in the present study are sufficient to activate ER $\alpha$  in healthy liver.

## Discussion

The read-across approach allows the prediction of missing toxicological data for a target substance, based on data from similar substances (source substance). The starting point of the read-across approach could be the grouping of several source substances. This grouping is based on common functional groups, precursors, and a reportedly consistent pattern in terms of the changes in physicochemical and/or biological properties (ECHA 2017a). Based on this, BPA and BPA/C (source substance) were grouped to predict the toxicological properties of BPC (target substance). These three bisphenols had comparable  $EC_{50}$ ,  $EC_{10}$  and  $\log P_{ow}$  values (Table 1). Structurally, the BPA, BPA/C and

BPC differed only with respect to the number of additional methyl groups (Table 1). Experimental data were generated to validate the predictions for BPC and will be discussed in the following section.

We showed that the *in vitro* toxicity ( $EC_{50}$ ) correlates well with the  $\log P_{ow}$  (Fig. 1); the latter represents the distribution of a substance between water and the lipophilic solvent octanol (Sangster 1989). Our data showed that the toxicity increased with decreasing water solubility (Fig. 1).

Bisphenols with a higher hydrophobicity had previously been shown to be located in the hydrophobic layer of the cell membrane thereby disturbing the membrane fluidity (Macczak et al. 2017). Recent computer-based simulations underlined that BPA accumulates in the membrane, causes potential cluster generation and increased numbers of membrane pores, and leads to an enhanced water influx into the cell (Chen et al. 2016). Based on this computer-based simulation, it is likely that the cell membrane of HepG2 cells becomes disturbed by BPA, which might result in the generation of membrane pores.

BPA/C produced a significant increase of the cell division rate at the  $EC_{10}$  (compared to BPA) in concert with an increase in one methyl group. Therefore, one would predict that BPC with two additional methyl groups would show a further increase in the cell division rate. However, experimental data using BPC showed that a decrease in cell division was detectable (Fig. 2b). At a lower dose of  $1/3 EC_{10}$  there was no change in the cell division rate between BPA, BPA/C and BPS, despite differences in the  $\log P_{ow}$ . Even at this  $1/3 EC_{10}$  concentration, BPC resulted in a significantly lower number of cell divisions (Fig. 2a).

Using a read-across approach one would predict different effects of BPC on the cell division rate: at the  $EC_{10}$  the cell division rate of BPC-treated cells should be above the rate found in cells treated with BPA or BPA/C, since BPA and BPA/C induced increasing cell division ratios corresponding to the increasing number of additional methyl groups (Fig. 2b). In summary, an application of read-across in terms of cell division rates is not possible for BPA, BPA/C and BPC.

In general, the initiation of cell division depends not only on cyclins and the corresponding kinases but also on factors like ATP and oxygen (Gelfant 1960). Therefore, the effect of the bisphenols on the mitochondrial membrane potential  $\Delta\psi_m$  was studied (Fig. 3). Uncoupling of  $\Delta\psi_m$  led to an opening of the mitochondrial permeability transition pores (Petronilli et al. 1993). In contrast to BPA, BPA/C and BPS, only BPC decreased  $\Delta\psi_m$  significantly at  $EC_{10}$  concentrations (Fig. 3a). At lower concentrations ( $1/3 EC_{10}$ ), no effect was detectable. Therefore, a read across from BPA and BPA/C to BPC is not possible.

A recent study has shown that the intracellular ATP concentration is a sensitive endpoint for mitotoxicity (i.e., mitosis toxicity) in the absence of cell death (Kamalian et al. 2015). In our study, the determination of the intracellular ATP concentration clearly showed that only BPC had an effect. The other investigated bisphenols (BPA, BPA/C, and BPS) had no mitotoxic effects, regardless of the chemical structure. Macczak *et al.* (2017) showed that derivatives of BPA exerted different effects on erythrocyte membranes, depending on its hydrophobicity; this also suggests the potential for mitochondrial membrane disturbance. It has been reported that 1000-fold lower concentrations of BPA can induce a reduction in the  $\Delta\Psi_m$  in HepG2 cells after 12 h of incubation (Moon et al. 2012), indicating a short-term effect (12 h) of BPA. In the present study, no change in  $\Delta\Psi_m$  was detected after 24 h, except for BPC, for which a decreased  $\Delta\Psi_m$  was detectable after 24 h (Fig. 3). The only structural differences between BPA and BPC are the two additional methyl groups attached to the phenol rings, which might be essential for the decoupling effect. To validate a potential structure–activity relationship (SAR), the effects of an intermediate structure, BPA/C, were investigated (Table 1). Ultimately, BPA/C was shown to lack any effect on  $\Delta\Psi_m$  (Fig. 3). Therefore, it can be concluded that the membrane potential related effects of BPC are dependent on the presence of both methyl groups. Interestingly, the effect of  $\Delta\Psi_m$  seemed to be a reliable indicator for the intracellular ATP concentration. In summary, the decrease of the intracellular ATP concentration is supported by the  $\Delta\Psi_m$  determinations. Yet, a prediction of the effects of BPC, based on data from BPA and BPA/C, seemed to be limited.

The effects of BPC on HepG2 cells differ, when compared to BPA, BPA/C and BPS. The differences are based not only on the cell division rate but also on  $\Delta\Psi_m$  (Fig. 3) and the cellular ATP concentration (Fig. 4). It has been reported that decoupling of  $\Delta\Psi_m$  can result in the mitochondrial release of CyC (Li et al. 2010). CyC is part of the mitochondrial electron transport chain. A release of CyC into the cytosol subsequently results in an activation of apoptosis-related caspases, which then may trigger the intrinsic apoptosis pathway (Tait and Green 2010). Since only BPC-treated cells revealed a reduced amount of CyC in the mitochondrial fraction (Fig. 7a), it was assumed that only BPC might be capable to activate the intrinsic apoptotic pathway by mitochondrial depolarisation and translocation of CyC into the cytosol. The activation of this apoptotic pathway could be enhanced by the recently established co-cultivation system (Wewering et al. 2017), reflecting a pro-inflammatory cell state. BCL-2 is an inhibitor of apoptosis pathway (Kluck et al. 1997). It was significantly down-regulated by BPC during conditions of pro-inflammation in HepG2 and PMA-activated THP-1 cells while growing in co-culture (Fig. 6a). Especially the increased secretion of TNF- $\alpha$  during co-cultivation enhanced the effect

on BPC treated cells (Fig. 6b). It has been already shown, that intracellular TNF- $\alpha$  occurs in HepG2-cells (Zhang et al. 2013) and we could show that BPS treatment led to secretion of TNF- $\alpha$  (Fig. 6b).

In general, HepG2 cells were also capable of expressing pro-inflammatory cytokines under the influence of external stimuli (Gutierrez-Ruiz et al. 1999). The investigated bisphenols were known to carry intrinsic estrogenic activity (Kitamura et al. 2005). It has been shown that pro-inflammatory cytokines, like TNF- $\alpha$ , were upregulated in liver after treatment with estrogens (Colantoni et al. 2003). Due to the lack of ER $\alpha$  protein in HepG2 cells, all effects on cytokine expression were independent from the estrogenic properties of the investigated bisphenols though (Fig. 7b). However, one has to keep in mind that the ER $\alpha$  is expressed in normal liver tissue (Zhao and Li 2015) and that differences in the activation of ER $\alpha$  by bisphenols might alter the reported effects. BPA and BPC activated the ER $\alpha$  signaling completely and BPA/C up to  $73.8 \pm 8.8$  % at concentrations lower than the ones used in the present study (Figure S3). Furthermore, the EC<sub>50E</sub> of ER $\alpha$  activation differs between BPA, BPA/C and BPC, and no correlation between the number of methyl-groups and the EC<sub>50E</sub> was detected (Fig. 8). The EC<sub>50E</sub> values of BPA, BPC, BPS and BPF were similar to the values reported by Kitamura *et al.* (2005). Moreover, the data support the scheme proposed by the authors only partly. It remains to be elucidated why the single methyl group of BPA/C reveals with highest EC<sub>50E</sub> of ER $\alpha$  activation, while one less (BPA) or an additional methyl group (BPC) lowers this value.

These results show that there is no constant increase in ER $\alpha$  activation by the addition of single methyl groups. Therefore, a read across from BPA and BPA/C to BPC is not possible. In addition, the data show that ER $\alpha$  is already activated at concentrations below the ones used in the present study. It is likely that this situation occurs in healthy liver. Effects based on differences in the activation are unlikely.

The read-across approach was used to predict the expression of cytokines in treated HepG2 cell culture. BPA, BPA/C were used as source substances and BPC as target substance. The expression of the pro-inflammatory cytokine TGF- $\beta$  (Worthington et al. 2012) was significantly up-regulated in the presence of BPC and BPA (Fig. 5a) but not by BPA/C. Since both former substances differed only by the number of methyl-groups and its log $P_{ow}$  values, it should be expected that the addition of a single methyl group to BPA/C would result in the down-regulation or at least in the lack of any expression changes of this pro-inflammatory cytokine. However, our experimental data show that BPC increases *TGFB1* expression even more than BPA. Therefore, it seems that BPA and BPA/C cannot be used as reliable source substances to predict the expression of BPC. To summarize, the prediction of the read-across approach was not found to be reliable for the set of bisphenols investigated in our

study due to the fact that the expression of *TGFB1* was significantly up-regulated compared to the expression produced by a structurally similar BPA/C.

We next studied additional pro-inflammatory cytokines. The expression profiles of *SPP1* and *TNF* differed between BPC-treated HepG2 cells when compared to the other bisphenol treatments. The treatment with BPA, BPA/C and BPS led to an up-regulation of *SPP1*, but not of *TNF*. BPC did not change the expression of *SPP1*, but up-regulated the expression of *TNF* (Fig. 5b, c). Actually, applying the read-across approach one would expect an up-regulated *SPP1* expression, similar to BPA and BPA/C, and an unchanged expression of this cytokine in BPC-treated cells. However, the strong up-regulation of *TNF* contradicted this prediction.

Generally TNF- $\alpha$  secretion can be also used for the read-across approach. One would expect that the TNF- $\alpha$  secretion levels in co-cultures treated with BPA and BPA/C (Fig. 6b) would be comparable to the BPC-treated co-culture, based on the structural similarities. But our data clearly show that only BPC significantly enhances the TNF- $\alpha$  secretion in co-culture (Fig. 6b). However, no TNF- $\alpha$  was secreted in BPS-treated co-culture (Fig. 6b). In brief, the read-across approach could be not applied to the current set of substances.

In theory, a read-across approach for the prediction of the effects of BPC seemed feasible using data from BPA- and BPA/C-treated HepG2 cells. The more so as these bisphenols differed only by one or two methyl groups. Yet our data clearly showed that the application of read-across was impossible within this group, despite the high structural similarity. At non-toxic concentrations ( $EC_{10}$ ), different biochemical effects of BPA, BPA/C, BPC and BPS became obvious in HepG2 cell cultures.

The *in vitro* data on bisphenol derivatives indicate that a single methyl group can have a profound effect on cellular toxicity. Similar effects have been shown with other chemicals as well, such as, 1-amino-2-propanol (CAS 78-96-6) and 2-aminoethanol (CAS 141-43-5). Both chemicals differ only in a single methyl group. Here, this small structural change caused significantly different *in vivo* toxicity in rats, with 1-amino-2-propanol resulting in an increased liver weight, generally, and an increased thymus weight in females only (ECHA 2018c). In contrast, oral exposure to 1-aminoethanol resulted in decreased weights of prostate, as well as corpus and cauda epididymis (ECHA 2016). Our study adds to these observations and prompts us to suggest caution in cases where the read-across approach is thought to be applicable due to small structural alterations of the compounds under investigation, such as the adding or loss of a single methyl side chain.

## Conclusion

In this study, we showed that the cytotoxicity of a selected set of bisphenols depended largely on the respective  $\log P_{ow}$  values. Furthermore, methylation of both phenolic moieties is required to trigger the intrinsic apoptotic pathway in HepG2 cells. This is mediated by the compound's decoupling effect on the mitochondrial membrane or the activation of the TNF pathway. BPS, used as an alternative for BPA in consumer products, revealed with a similar expression pattern for *TGFB1*, *SPP1* and *TNF*. BPS was able to evoke the expression of similar cytokines (*SPP1* and *TGFB1*) as BPA suppressed TNF- $\alpha$  secretion in a pro-inflammatory co-culture system without affecting cell division rates. In conclusion, the read-across method should be used carefully with regard to bisphenols, since the addition of a single methyl group can trigger large differences in terms of potentially adverse biological effects.

## References

- Cesen M, Lenarcic K, Mislej V et al (2018) The occurrence and source identification of bisphenol compounds in wastewaters. *Sci Total Environ* 616–617:744–752. <https://doi.org/10.1016/j.scitotenv.2017.10.252>
- Chen L, Chen J, Zhou G, Wang Y, Xu C, Wang X (2016) Molecular dynamics simulations of the permeation of bisphenol A and pore formation in a lipid membrane. *Sci Rep* 6:33399. <https://doi.org/10.1038/srep33399>
- Clayton DA, Shadel GS (2014a) Isolation of mitochondria from tissue culture cells. *Cold Spring Harb Protoc* 20(10):pdb.prot080002. <https://doi.org/10.1101/pdb.prot080002>
- Clayton DA, Shadel GS (2014b) Purification of mitochondria by sucrose step density gradient centrifugation. *Cold Spring Harb Protoc* 10:pdb.prot080028. <https://doi.org/10.1101/pdb.prot080028>
- Clemente N, Raineri D, Cappellano G et al (2016) Osteopontin bridging innate and adaptive immunity in autoimmune diseases. *J Immunol Res* 2016:7675437. <https://doi.org/10.1155/2016/7675437>
- Colantoni A, Idilman R, De Maria N et al (2003) Hepatic apoptosis and proliferation in male and female rats fed alcohol: role of cytokines. *Alcohol Clin Exp Res* 27(7):1184–1189. <https://doi.org/10.1097/01.ALC.0000075834.52279.F9>
- Czabotar PE, Lessene G, Strasser A, Adams JM (2014) Control of apoptosis by the BCL-2 protein family: implications for physiology and therapy. *Nat Rev Mol Cell Biol* 15(1):49–63. <https://doi.org/10.1038/nrm3722>
- Doerge DR, Twaddle NC, Vanlandingham M, Fisher JW (2010) Pharmacokinetics of bisphenol A in neonatal and adult SpragueDawley rats. *Toxicol Appl Pharmacol* 247(2):158–165. <https://doi.org/10.1016/j.taap.2010.06.008>
- ECHA (2016) Substance evaluation report for 2-aminoethanol EC No 205-483-3 CAS No 141-43-5. <http://echa.europa.eu/web/guest/information-on-chemicals/registered-substances>
- ECHA (2017a) Read-across assessment framework (RAAF). <https://doi.org/10.2823/619212>

Minor structural modifications of bisphenol A strongly affect physiological responses of HepG2 cells

- ECHA (2017b) Read-across assessment framework (RAAF)—considerations on multi-constituent substances and UVCBs. <https://doi.org/10.2823/794394>
- ECHA (2017c) Substance evaluation conclusion as required by reach Article 48 and evaluation report for 4,4'-Isopropylidenediphenol EC No 201-245-8 CAS No 80-05-7. <https://echa.europa.eu/documents/10162/7971ab80-03c9-4d87-e117-e4dbc9cc54d2>
- ECHA (2018a) Decision on substance evaluation pursuant to article 46(1) of regulation (EC) No. 1907/2006 for 4,4'-sulfonyldiphenol, CAS No 80-09-1 (EC No201-250-5). <https://echa.europa.eu/documents/10162/776a7a2e-1526-430a-8630-70163473df c0>
- ECHA (2018b) Annex XV report – proposal for identification of a substance of very high concern on the basis of the criteria set out in reach article 57, Substance Name(s): 4,4'-isopropylidenediphenol (Bisphenol A). <https://echa.europa.eu/docum ents/10162/f19ec5b1-dfae-107a-44d2-6e74979d68f1>
- ECHA (2018c) Registration dossier (Regulation (EC) No 1907/2006) of 1-aminopropan-2-ol. <https://echa.europa.eu/registration-dossier/-/registered-dossier/13935/7/6/2>
- ECHA (2018d) Registration dossier (Regulation (EC) No 1907/2006) of 4,4'-isopropylidenedi-o-cresol. <https://echa.europa.eu/registration-dossier/-/registered-dossier/24781>
- EFSA (2015) Scientific Opinion on the risks to public health related to the presence of bisphenol A (BPA) in foodstufs. EFSA J 13(1):3978. <https://doi.org/10.2903/j.efsa.2015.3978>
- EFSA, Gundert-Remy U, Bodin J, Bosetti C, FitzGerald RE, Hanberg A, Hass U, Hooijmans C, Rooney AA, Rousselle C, van Loveren H, Wölfe D, Barizzone F, Croera C, Putzu C, Castoldi AF (2017) Bisphenol A (BPA) hazard assessment protocol. EFSA Support Publ 14(12):EN-1354. <https://doi.org/10.2903/ sp.efsa.2017.en-1354>
- Fic A, Žegura B, Sollner Dolenc M, Filipič M, Peterlin Mašič L (2013) Mutagenicity and DNA damage of bisphenol A and its structural analogues in HepG2 cells. Arch Ind Hyg Toxicol 64(2):189–200. <https://doi.org/10.2478/10004 -1254-64-2013-2319>
- Gelfant S (1960) The energy requirements for mitosis. Ann N Y Acad Sci 90(2):536–549. <https://doi.org/10.1111/j.1749-6632.1960.tb23271.x>
- Gutierrez-Ruiz MC, Quiroz SC, Souza V et al (1999) Cytokines, growth factors, and oxidative stress in HepG2 cells treated with ethanol, acetaldehyde, and LPS. Toxicology 134(2–3):197–207
- Ichim G, Tait SW (2016) A fate worse than death: apoptosis as an oncogenic process. Nat Rev Cancer 16(8):539–548. <https://doi.org/10.1038/nrc.2016.58>
- Kamalian L, Chadwick AE, Bayliss M et al (2015) The utility of HepG2 cells to identify direct mitochondrial dysfunction in the absence of cell death. Toxicol In Vitro 29(4):732–740. <https://doi.org/10.1016/j.tiv.2015.02.011>
- Kidani T, Yasuda R, Miyawaki J, Oshima Y, Miura H, Masuno H (2017) Bisphenol A inhibits cell proliferation and reduces the motile potential of murine LM8 osteosarcoma cells. Anticancer Res 37(4):1711–1722. <https://doi.org/10.21873/anticanres.11503>
- Kitamura S, Suzuki T, Sanoh S et al (2005) Comparative study of the endocrine-disrupting activity of bisphenol A and 19 related compounds. Toxicol Sci 84(2):249–259. <https://doi.org/10.1093/toxsci/kf074>

Minor structural modifications of bisphenol A strongly affect physiological responses of HepG2 cells

- Kluck RM, Bossy-Wetzell E, Green DR, Newmeyer DD (1997) The release of cytochrome c from mitochondria: a primary site for Bcl-2 regulation of apoptosis. *Science* 275(5303):1132–1136
- Kuroda N, Kinoshita Y, Sun Y et al (2003) Measurement of bisphenol A levels in human blood serum and ascitic fluid by HPLC using a fluorescent labeling reagent. *J Pharm Biomed Anal* 30(6):1743–1749. [https://doi.org/10.1016/s0731-7085\(02\)00516-2](https://doi.org/10.1016/s0731-7085(02)00516-2)
- Li T, Brustovetsky T, Antonsson B, Brustovetsky N (2010) Dissimilar mechanisms of cytochrome c release induced by octyl glucoside-activated BAX and by BAX activated with truncated BID. *Biochem Biophys Acta* 1797(1):52–62. <https://doi.org/10.1016/j.bbabi.2009.07.012>
- Liao CY, Liu F, Kannan K, Bisphenol S (2012) A new bisphenol analogue, in paper products and currency bills and its association with bisphenol A residues. *Environ Sci Technol* 46(12):6515–6522. <https://doi.org/10.1021/es300876n>
- Livak KJ, Schmittgen TD (2001) Analysis of relative gene expression data using real-time quantitative PCR and the  $2^{-\Delta\Delta C_T}$  method. *Methods* 25(4):402–408. <https://doi.org/10.1006/meth.2001.1262>
- Macczak A, Duchnowicz P, Sicinska P, Koter-Michalak M, Bukowska B, Michalowicz J (2017) The in vitro comparative study of the effect of BPA, BPS, BPF and BPAF on human erythrocyte membrane; perturbations in membrane fluidity, alterations in conformational state and damage to proteins, changes in ATP level and Na(+)/K(+) ATPase and AChE activities. *Food Chem Toxicol* 110:351–359. <https://doi.org/10.1016/j.fct.2017.10.028>
- Malik MY, Jaiswal S, Sharma A, Shukla M, Lal J (2016) Role of enterohepatic recirculation in drug disposition: cooperation and complications. *Drug Metab Rev* 48(2):281–327. <https://doi.org/10.3109/03602532.2016.1157600>
- Mandrah K, Satyanarayana GNV, Roy SK (2017) A dispersive liquid-liquid microextraction based on solidification of floating organic droplet followed by injector port silylation coupled with gas chromatography-tandem mass spectrometry for the determination of nine bisphenols in bottled carbonated beverages. *J Chromatogr A* 1528:10–17. <https://doi.org/10.1016/j.chroma.2017.10.071>
- Manica A, Da Silva AM, Cardoso AM et al (2018) High levels of extracellular ATP lead to chronic inflammatory response in melanoma patients. *J Cell Biochem* 119(5):3980–3988. <https://doi.org/10.1002/jcb.26551>
- Moon MK, Kim MJ, Jung IK et al (2012) Bisphenol A impairs mitochondrial function in the liver at doses below the no observed adverse effect level. *J Korean Med Sci* 27(6):644–652. <https://doi.org/10.3346/jkms.2012.27.6.644>
- Mosmann T (1983) Rapid colorimetric assay for cellular growth and survival: application to proliferation and cytotoxicity assays. *J Immunol Methods* 65(1–2):55–63
- OECD (2016) Test No. 455: performance-based test guideline for stably transfected transactivation in vitro assays to detect estrogen receptor agonists and antagonists
- Petronilli V, Cola C, Massari S, Colonna R, Bernardi P (1993) Physiological effectors modify voltage sensing by the cyclosporin A-sensitive permeability transition pore of mitochondria. *J Biol Chem* 268(29):21939–21945



Minor structural modifications of bisphenol A strongly affect physiological responses of HepG2 cells

- Potratz S, Tarnow P, Jungnickel H et al (2017) Combination of metabolomics with cellular assays reveals new biomarkers and mechanistic insights on xenoestrogenic exposures in MCF-7 cells. *Chem Res Toxicol* 30(4):883–892. <https://doi.org/10.1021/acs.chemrestox.6b00106>
- Rochester JR, Bolden AL (2015) Bisphenol S and F: a systematic review and comparison of the hormonal activity of bisphenol A substitutes. *Environ Health Perspect* 123(7):643–650. <https://doi.org/10.1289/ehp.1408989>
- Sangster J (1989) Octanol-water partition-coefficients of simple organic-compounds. *J Phys Chem Ref Data* 18(3):1111–1229. <https://doi.org/10.1063/1.555833>
- Schieke SM, McCoy JP, Finkel T (2008) Coordination of mitochondrial bioenergetics with G(1) phase cell cycle progression. *Cell Cycle* 7(12):1782–1787
- Sedger LM, McDermott MF (2014) TNF and TNF-receptors: from mediators of cell death and infammation to therapeutic giants— past, present and future. *Cytokine Growth Factor Rev* 25(4):453– 472. <https://doi.org/10.1016/j.cytogfr.2014.07.016>
- Song RX, Mor G, Naftolin F et al (2001) Effect of long-term estrogen deprivation on apoptotic responses of breast cancer cells to 17beta-estradiol. *J Natl Cancer Inst* 93(22):1714–1723
- Tait SW, Green DR (2010) Mitochondria and cell death: outer membrane permeabilization and beyond. *Nat Rev Mol Cell Biol* 11(9):621–632. <https://doi.org/10.1038/nrm2952>
- Tarnow P, Tralau T, Hunecke D, Luch A (2013) Effects of triclocarban on the transcription of estrogen, androgen and aryl hydrocarbon receptor responsive genes in human breast cancer cells. *Toxicol In Vitro* 27(5):1467–1475. <https://doi.org/10.1016/j.tiv.2013.03.003>
- R Core Team (2018) R: a language and environment for statistical computing. <https://www.R-project.org/>, Vienna, Austria. R Foundation for Statistical Computing
- Thayer KA, Taylor KW, Garantziotis S et al (2016) Bisphenol A, bisphenol S, and 4-hydroxyphenyl 4-isopropoxyphenylsulfone (BPSIP) in urine and blood of cashiers. *Environ Health Perspect* 124(4):437–444. <https://doi.org/10.1289/ehp.1409427>
- van Horssen R, Ten Hagen TL, Eggermont AM (2006) TNF-alpha in cancer treatment: molecular insights, antitumor effects, and clinical utility. *Oncologist* 11(4):397–408. <https://doi.org/10.1634/theoncologist.11-4-397>
- Wewering F, Jouy F, Wissenbach DK et al (2017) Characterization of chemical-induced sterile infammation in vitro: application of the model compound ketoconazole in a human hepatic co-culture system. *Arch Toxicol* 91(2):799–810. <https://doi.org/10.1007/s00204-016-1686-y>
- Worthington JJ, Fenton TM, Czajkowska BI, Klementowicz JE, Travis MA (2012) Regulation of TGFβ in the immune system: an emerging role for integrins and dendritic cells. *Immunobiology* 217(12):1259–1265. <https://doi.org/10.1016/j.imbio.2012.06.009>
- Zhang C, Wang C, Tang S et al (2013) TNFR1/TNF-alpha and mitochondria interrelated signaling pathway mediates quinocetoneinduced apoptosis in HepG2 cells. *Food Chem Toxicol* 62:825–838. <https://doi.org/10.1016/j.fct.2013.10.022>
- Zhao Y, Li Z (2015) Interplay of estrogen receptors and FOXA factors in the liver cancer. *Mol Cell Endocrinol* 418(Pt 3):334–339. <https://doi.org/10.1016/j.mce.2015.01.043>

Indirect co-cultivation of HepG2 with differentiated THP-1 cells induces AHR signaling and release of pro-inflammatory cytokines.

### **3.2 Indirect co-cultivation of HepG2 with differentiated THP-1 cells induces AHR signaling and release of pro-inflammatory cytokines.**

Florian Padberg, Henrik Hering, Andreas Luch, and Sebastian Zellmer

*Toxicology in Vitro* volume 68, 104957 (2020)

Published online: 30 July 2020

DOI: 10.1016/j.tiv.2020.104957

Link: <https://doi.org/10.1016/j.tiv.2020.104957>

Involvement of the author within this publication: project planning: 80 %, project execution: 90 %, data analysis: 90 %, writing the manuscript: 70 %

The supplementary material to the publication embedded on the following pages is contained in Annex II.

Indirect co-cultivation of HepG2 with differentiated THP-1 cells induces AHR signaling and release of pro-inflammatory cytokines.

**Abstract**

HepG2 and THP-1 cells, the latter differentiated by phorbol 12-myristate 13-acetate (PMA), were co-cultured and characterized for typical liver-specific functions, such as xenobiotic detoxification, lipid and cholesterol metabolism. Furthermore, liver injury-associated pathways, such as inflammation, were studied. In general, the co-cultivation of these cells produced a pro-inflammatory system, as indicated by increased levels of cytokines (IL-8, TGF- $\alpha$ , IL-6, GM-CSF, G-CSF, TGF- $\beta$ , and hFGF) in the respective supernatant. Increased expression levels of target genes of the aryl hydrocarbon receptor (AHR), *e.g.*, *CYP1A1*, *CYP1A2* and *CYP1B1*, were detected, accompanied by the increased enzyme activity of CYP1A1. Moreover, transcriptome analyses indicated a significant upregulation of cholesterol biosynthesis, which could be reduced to baseline levels by lovastatin. In contrast, total *de novo* lipid synthesis was reduced in co-cultured HepG2 cells. Key events of the adverse outcome pathway (AOP) for fibrosis were activated by the co-cultivation, however, no increase in the concentration of extracellular collagen was detected. This indicates, that AOP should be used with care. In summary, the indirect co-culture of HepG2/THP-1 cells results in an increased release of pro-inflammatory cytokines, an activation of the AHR pathway and an increased enzymatic CYP1A activity.

Keywords: HepG2; THP-1; Co-culture; Lipids; Cholesterol; Cytokines; Inflammation; Metabolism; Adverse outcome pathway

**1. Introduction**

The liver is the main organ of intermediary metabolism. When taken up orally, nutrients, noxious and/or pharmacologically active compounds reach the liver through the portal vein. Consequently, appropriate *in vitro* liver models are widely discussed and developed for toxicological and pharmacological studies (Zeilinger et al., 2016; Soldatow et al., 2013; Toyoda et al., 2017; Zhou et al., 2019). Primary human liver cells are thus far the “gold standard” for these *in vitro* investigations (Zeilinger et al., 2016; Soldatow et al., 2013). However, one should be aware of the short comings of this “gold standard”, for instance, large inter-individual differences, reduction in functionality within days (Soldatow et al., 2013) and induction of signalling pathways and changes in enzyme activity due to disease-related patient treatment. On the other hand, hepatic cell lines (*e.g.*, HepG2, Huh7) also have limitations, since the metabolic enzyme activity of these cells is often much lower or absent than that of primary cell cultures (Hewitt and Hewitt, 2004; Lin et al., 2012). However, availability is almost unlimited, since these cells can be easily expanded in the laboratory.

Indirect co-cultivation of HepG2 with differentiated THP-1 cells induces AHR signaling and release of pro-inflammatory cytokines.

Differences between primary human hepatocytes and HepG2 cells in the response to pharmacologically active substances were investigated recently (Albrecht et al., 2019). Primary hepatocytes were more suitable for the detection of toxic effects, compared to HepG2 cells. In addition, it was shown that the read out was of crucial importance. The authors concluded that HepG2 cells represent a suitable screening tool to study most of these substances (Albrecht et al., 2019). Besides the single cultivation of HepG2 cells, co-culturing of HepG2 cells (e.g. with THP-1 cells) could also lead to more sensitive cell culture model. However, much more complex 3D co-cultures have generated promising pro-fibrotic hepatic *in vitro* systems (Prestigiacomo et al., 2017). In this system, essential interactions between hepatocytes, Kupffer cells and stellate cells (by HepaRG, THP-1, hTERT-HSC) were successfully simulated *in vitro*. This study showed that co-cultivation systems could have a higher validity compared to single cultures and that THP-1 cells can be a possible surrogate for human Kupffer cells. (Prestigiacomo et al., 2017). THP-1 cells, differentiated by phorbol 12-myristate 13-acetate (PMA), convert into a macrophage-like phenotype (Schwende et al., 1996). Wewering and co-workers (Wewering et al., 2017a) established an indirect co-cultivation system with HepG2 and PMA-differentiated THP-1 cells. This co-cultivation resulted in a pro-inflammatory system, as indicated by the secretion of C-X-C-motif ligand 8 (CXCL8 or IL-8), granulocyte macrophage colony-stimulating factor (GM-CSF) and macrophage migration inhibitory factor. Granitzny and co-workers (Granitzny et al., 2017) investigated the suitability of this co-cultivation system for the identification of drugs that induce liver injury (DILI). Positive reference substances for DILI like troglitazone, trovafloxacin, diclofenac and ketoconazole as well as negative reference substances like rosiglitazone, levofloxacin, acetylsalicylic acid, fluconazole were correctly identified and proved the functionality of the system. In addition, tumour necrosis factor  $\alpha$  (TNF- $\alpha$ ) was identified as a prognostic factor for DILI development *in vitro* (Granitzny et al., 2017). These findings support the hypothesis that pro-inflammatory conditions might lower the hepatotoxic thresholds of xenobiotics or drugs and can lead to DILI (Roth et al., 2003).

The main focus of the present paper are changes at the cellular level that were induced by the indirect co-cultivation of HepG2 and PMA-differentiated THP-1 cells. Therefore, gene expression profiles were determined by transcriptome analyses. The predictions were then validated by measuring cytokine secretion, CYP enzyme expression and specific enzyme activities, collagen accumulation and changes in the amount of total lipids. Finally, crucial hepatic pathways that were changed due to the co-cultivation conditions were identified, which allows a deeper understanding of the co-cultivation system.

## Indirect co-cultivation of HepG2 with differentiated THP-1 cells induces AHR signaling and release of pro-inflammatory cytokines.

### **2. Methods**

All methods were carried out according to the manufacturer's protocol. Only the modifications are given below.

#### **2.1. Chemicals and antibodies**

All chemicals were purchased from Sigma-Aldrich (Taufkirchen, Germany) unless stated otherwise. In general, Dulbecco's phosphate-buffered saline (DPBS, PAN-Biotech, Aidenbach, Germany) was used. A list of the antibodies used is provided in supplementary table S1.

#### **2.2. Cell culture**

All single use consumables were purchased from TPP (Trasadingen, Switzerland). Cell lines were purchased from DSMZ (Braunschweig, Germany). HepG2 cells were grown in RPMI 1640 (PAN-Biotech, Aidenbach, Germany) contained 10% (v/v) FCS, 100 U/ml penicillin, 100 mg/ml streptomycin, 2 mM l-glutamine at 37 °C and 5% CO<sub>2</sub> as described previously. THP-1 cells were grown in RPMI 1640 (PAN-Biotech, Aidenbach, Germany) contained 10% (v/v) FCS, 100 U/ml penicillin, 100 mg/ml streptomycin, 2 mM l-glutamine, 1 mM sodium pyruvate, 10 mM HEPES and the co-culture were performed using Falcon® cell culture inserts (VWR, Darmstadt, Germany) according to Wewering and co-workers (Wewering et al., 2017a). HepG2 cells were seeded at a density of  $1.3 \times 10^5$  cells per cm<sup>2</sup>. THP-1 cells were seeded at a density of  $0.65 \times 10^5$  cells per cm<sup>2</sup> and differentiated using 100 nM phorbol-12-myristat-13-acetat (PMA) for 24 h. Immediately after differentiation the co-cultivation with the HepG2 cells was started. Previously it has been shown that PMA in the concentration range of 8–200 nM can be used for a successful differentiation and adherence of the cells to the culture vessel within 24 h (Lund et al., 2016). However, during a subsequent PMA free cultivation phase the adherence decreased with a decreasing PMA concentration. THP-1 cells, that were differentiated with 100 nM PMA showed the highest adherence 24 h after cultivation in the absence of PMA. Secondly, the concentration of PMA as well as incubation and resting phase seems to affect the toxicity of drugs. Granitzny and co-workers (Granitzny et al., 2017) studied the effect of ketoconazole on THP-1 cells, differentiated for 72 h in the presence of 50 nM PMA, followed by a resting phase in PMA-free growth medium for another 24 h. In co-culture, ketoconazole had a much higher toxicity to THP-1 cells, compared to the HepG2 cells (Granitzny et al., 2017). In contrast, the differentiation with 100 nM PMA for 24 h without a resting phase decreased the toxicity of ketoconazole (Wewering et al., 2017a). In order to warrant a high adherence of the THP-1 cells and a similar toxicity of drugs to THP-1 cells and HepG2 cells, 100 nM PMA was used for differentiation.

Indirect co-cultivation of HepG2 with differentiated THP-1 cells induces AHR signaling and release of pro-inflammatory cytokines.

In Fig. 1 the set-up of a co-cultivation can be seen. In order to further investigate the differentiation protocol used, the basic property of phagocytosis of PMA differentiated THP-1 cells (Kurycina et al., 2018) was confirmed (Fig. 1B). The THP-1 cells were capable of active phagocytosis from the beginning of co-cultivation to the end. Therefore, all cultures were incubated for 24 h and culture medium with 0.1% DMSO was used as control.

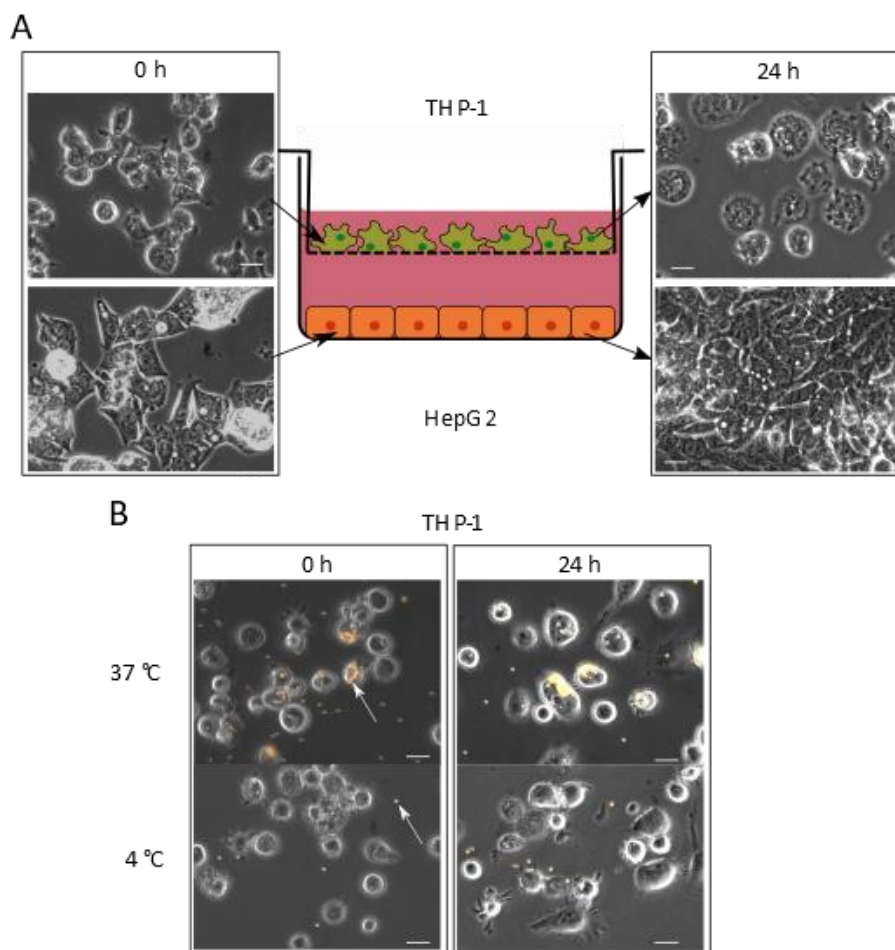


**Fig. 1.** Set-up of the co-cultivation and phagocytic capacity of THP-1 cells. THP-1 cells were differentiated using 100 nM phorbol-12 myristat-13 acetat (PMA) for 24 h and the co-cultivation with HepG2 starts without a resting phase. (A) Shown are set-up und photomicrographic images at the beginning ( $t = 0$ ) and the end ( $t = 24$  h) of the co-cultivation. (B) Phagocytosis is a characteristic of PMA differentiated THP-1 cells. The internalisation of latex beads ( $2 \mu\text{m}$ ,  $5 \mu\text{l/ml}$  culture medium) after 2 h incubation is temperature dependent ( $4 \text{ }^\circ\text{C}$  or  $37 \text{ }^\circ\text{C}$ ). The white arrow indicates exemplarily the latex beads. The scale bar denotes  $20 \mu\text{m}$ .

### 2.3. Cell viability testing

The MTT Assay was performed according to Mosmann (Mosmann, 1983). All values were corrected for the solvent control DMSO.

Indirect co-cultivation of HepG2 with differentiated THP-1 cells induces AHR signaling and release of pro-inflammatory cytokines.

#### **2.4. RNA isolation**

RNA was isolated using the NucleoSpin® RNA Kit (Machery-Nagel, Düren, Germany).

#### **2.5. Microarray analyses**

All samples (RNA integrity number (RIN) >8.5) were analysed using a Human Clariom™ S Assay (Applied Biosystems, Foster City, CA, USA). Microarray data have been deposited in the Gene Expression Omnibus (GEO) database, [www.ncbi.nlm.nih.gov/geo](http://www.ncbi.nlm.nih.gov/geo) (accession no. GSE140141). To analyse microarray data, the exclusion criterion of  $p \leq 0.05$  was used. Detailed information is provided in the supplementary material.

#### **2.6. Cytokines**

Cytokines in the supernatant were measured using the Cytokine LEGENDplex™ including Anti-Virus Response Panel (IL-8, IL-6, human fibroblast growth factor (hFGF)), Cytokine Panel 2 (interleukin 1 $\alpha$  (IL-1 $\alpha$ )) and Growth Factor Panel (TGF- $\alpha$ , GM-CSF, granulocyte colony-stimulating factor (G-CSF)) (Biolegend, San Diego, CA, USA). The results were analysed using LEGENDplex™ 8.0 software (Biolegend, San Diego, CA, USA). TGF- $\beta$  was quantified using the BD™ Cytometric Bead Array (CBA) with the Human TGF- $\beta$ 1 Single Plex Flex Set (BD Biosciences, Heidelberg, Germany) and analysed with FCAP Array v1.0.1 software (BD Biosciences, Heidelberg, Germany).

#### **2.7. PCR analyses**

Reverse transcription was performed with the High-Capacity cDNA Reverse Transcription Kit (Applied Biosystems, Foster City, CA, USA). Quantitative PCR (qPCR) was performed with a 7500 Fast Real-Time PCR Instrument using Fast SYBR Green Master Mix (Applied Biosystems, Foster City, CA, USA). The primer sequences are listed in table S2. The  $\Delta\Delta$ CT-value was calculated according to Livak and Schmittgen (Livak and Schmittgen, 2001) and normalized to the expression of hypoxanthine-guanine phosphoribosyl transferase (HPRT) and to the corresponding control sample. Positive controls were generated by the treatment with 10 nM 2,3,7,8-tetrachlorodibenzo-*p*-dioxin (TCDD) (LGC Standards, Wesel, Germany) or 1  $\mu$ M lovastatin before RNA isolation.

#### **2.8. Western blots**

Cells were lysed at 4 °C in RIPA buffer (50 mM Tris/HCl (pH 7.4), 159 mM NaCl, 1 mM EDTA, 1% Igepal®, 0.25% sodium deoxycholate) supplemented with a protease inhibitor cocktail (Merck, Darmstadt,

Indirect co-cultivation of HepG2 with differentiated THP-1 cells induces AHR signaling and release of pro-inflammatory cytokines.

Germany). Protein concentrations were determined with the Pierce™ BCA Protein Assay Kit (Thermo Scientific, Waltham, MA, USA), and equal amounts of protein were applied to SDS-PAGE and transferred onto nitrocellulose membranes. After binding of primary antibodies (24 h at 4 °C), the secondary antibody (horseradish peroxidase labelled) was added, and visualized with Pierce ECL Substrate (Thermo Fisher Scientific, Waltham, MA, USA) using a ChemiDoc XRS (Bio-Rad, Munich, Germany).

### **2.9. CYP1A1 activation**

CYP1A1 activation was measured using the P450-Glo™ CYP1A1 Assay System (Promega Corporation, Madison, WI, USA).

### **2.10. Cholesterol measurements**

The cholesterol concentration was quantified using the Amplex™ Red Cholesterol Assay Kit (Thermo Fisher Scientific, Waltham, MA, USA).

### **2.11. Lipid staining**

The cellular layer was fixed with Roti®-Histofix 4% (Roth, Karls-ruhe, Germany) for 10 min, and cells were permeabilized with 0.2% TRITON™X-100 for 10 min. Lipids were stained using a freshly prepared 6 mM Sudan Red 7 B solution in 60% 2-propanol for 10 min. After carefully removing excess staining solution, nuclear staining was performed with 1 µg/ml Hoechst33342. Images were repeatedly taken using an Olympus BX51 microscope (U Plan FLN 20×/0.50) connected to a ColorView III camera (Olympus, Hamburg, Germany). Finally, the number of nuclei and the areas of stained droplets were calculated using CellProfiler® 3.1.5 software (Carpenter et al., 2006) An example of the evaluation and its calculation is given in fig. S1.

### **2.12. ATP measurements**

The ATP concentration was determined using a Bioluminescence Assay Kit HS II (Roche, Basel, Switzerland).

### **2.13. Collagen staining**

The Sirius Red/Fast green collagen staining kit (AMS Biotechnology, Abingdon, UK) was used.



Indirect co-cultivation of HepG2 with differentiated THP-1 cells induces AHR signaling and release of pro-inflammatory cytokines.

## **2.14. Statistics**

Detailed information on the exploratory grouping analysis is provided in the supplementary section. All data shown contain at least three independent biological replicates. Means, standard deviations and ANOVA  $p$ -values followed by Bonferroni correction were calculated with GraphPad Prism 6 (Statcon, Witzenhausen, Germany). Analysed gene lists were selected due to the pathway relevance and the significance ( $p < 0.05$ ) using Ingenuity® Pathway Analysis (Qiagen, Aarhus, Denmark). The Z-score and the hierarchical clustering were calculated with Perseus Software (Tyanova et al., 2016). Three-dimensional figures were generated using Plotly (<https://plot.ly>) (Plotly Technologies Inc, 2015).

## **3. Results**

### **3.1. Toxicity of selected substances on 100 nM PMA differentiated THP-1 cells**

The toxicity of drugs, used in co-cultivation experiments should have similar half effective concentrations for all cell lines. PMA differentiated THP-1 cells are very sensitive against drugs (Granitzny et al., 2017). Therefore, in a first step, we tested the effect of three different drugs on the cell viability of PMA differentiated THP-1 cells, after single and co-culture. The selected PMA concentration was 100 nM (*cf.* 2.2).

The loss of cell viability induced by primaquine, flutamide and amiodarone (Fig. 2) was almost lower or equal (Fig. 2) for co-cultivated THP 1 cells compare to the corresponding single cultivation. Therefore, THP-1 differentiation with 100 nM PMA for 24 h without a resting phase was chosen for all experiments, in order to obtain high adherence and low loss of viability of the THP-1 cells.

Indirect co-cultivation of HepG2 with differentiated THP-1 cells induces AHR signaling and release of pro-inflammatory cytokines.

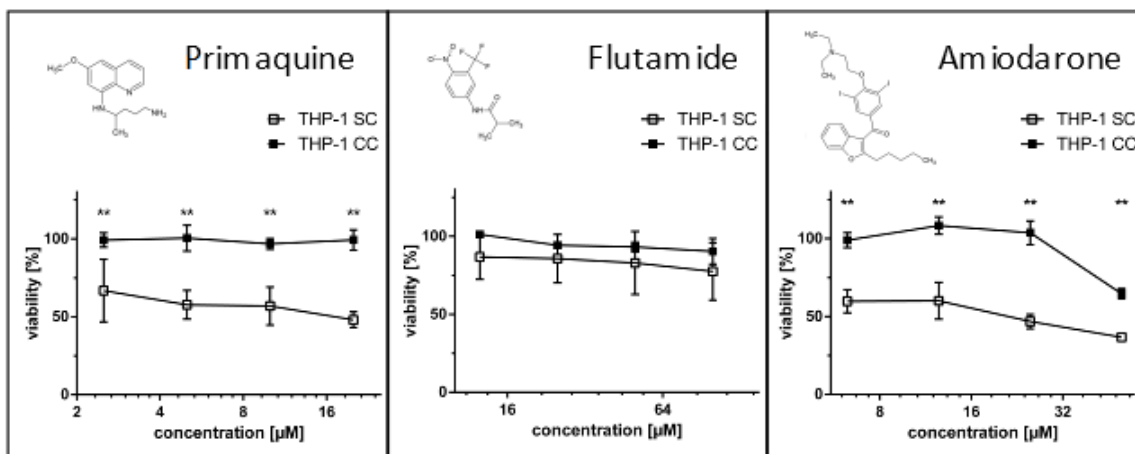


**Fig. 2.** Dose dependent loss of cell viability on co- and single-cultivated THP-1 cells. THP-1 cells were exposed to increasing concentration of primaquine, flutamide, or amiodarone for 24 h in co- (CC) or single- (SC) cultivation condition. Viability was determined using a MTT assay. All values were corrected to % of the corresponding DMSO solvent controls.  $n = 3$ ,  $**p < 0.01$ .

### 3.2. Exploratory grouping analysis highlights differences between single- and co-cultivated HepG2 cells

Outlier and batch effects can occur if there are any differences in batch-to-batch cultivation conditions or in the handling and preparation of samples. These outliers can be identified, for example, by exploratory grouping analysis (Bro and Smilde, 2014). We compared the cultivation conditions (single- and co-cultivation) of HepG2 cells and PMA-differentiated THP-1 cells (Fig. 3). The distances of the individual samples in terms of expression profiles indicate that the variation in the data is mainly affected by culture conditions (single- vs. co-cultivation) and the kind of cell type (HepG2 or THP-1), but not by batch-to-batch variations between individual samples. Therefore, the presence of outliers and a batch-to-batch variation was excluded and all samples were included in the subsequent analyses.

Indirect co-cultivation of HepG2 with differentiated THP-1 cells induces AHR signaling and release of pro-inflammatory cytokines.

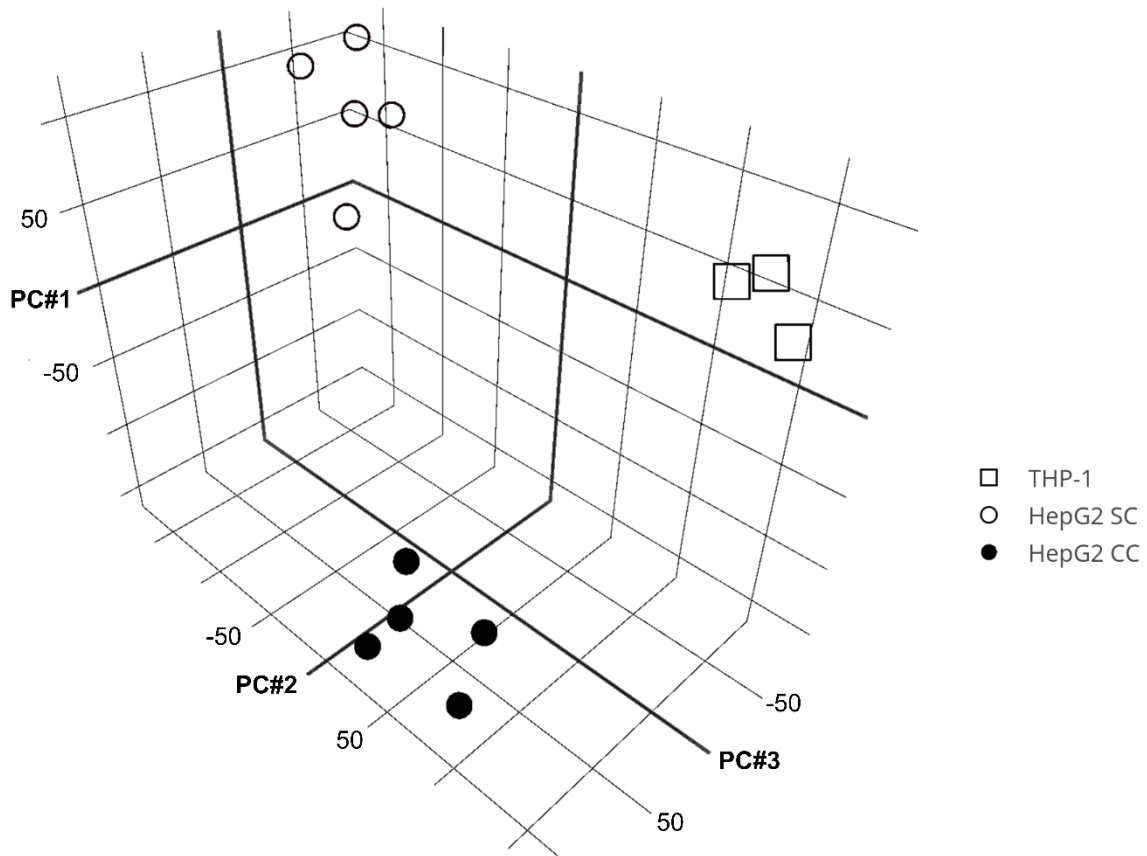


**Fig. 3.** Exploratory grouping analysis shows that the cultivation conditions affect gene expression profiles to a larger extent than the factor of sample-to-sample variability within the same group. HepG2 cells were cultivated with PMA-differentiated THP-1 cells in co-culture (●, HepG2 CC,  $n = 5$ ) and compared to single cultivated HepG2 (○, HepG2 SC,  $n = 5$ ) or PMA-differentiated THP-1 (single cell) cultures (□, THP-1,  $n = 3$ ) for 24 h.

### 3.3. Genes associated with liver inflammation are upregulated

The analysis of the transcriptomes identified differentially expressed cytokines and cytokine receptors. A total of 73.9% of the significantly upregulated genes ( $p < 0.05$ ) were associated with liver inflammation (Fig. 4A). Based on these microarray data, we quantified a selection of secreted cytokines in the cell culture supernatants (Fig. 4B). To identify the cell type responsible for the secretion (HepG2 or THP-1), we also quantified cytokine concentrations in pure THP-1 and HepG2 (single cell) cultures. Among the set of cytokines investigated, hFGF, TGF- $\alpha$ , and G-CSF were only detectable under co-cultivation conditions (Fig. 4B), whereas HepG2 cells alone also secreted GM-CSF and IL-6. However, the levels of these two biomarkers were still further and significantly ( $p < 0.01$ ) upregulated under the condition of co-cultivation with THP-1 cells. Conversely, PMA-differentiated THP-1 cells alone secreted

## Indirect co-cultivation of HepG2 with differentiated THP-1 cells induces AHR signaling and release of pro-inflammatory cytokines.

IL-8 to a much higher extent than did HepG2 cells alone. IL-8 levels under co-cultivation conditions were again in the same range as observed for THP-1 cells in the absence of HepG2 cells. In contrast, TGF- $\beta$  concentrations in the supernatant were 2-fold higher (non-significantly) under co-cultivation than in individual cell cultures but represented approximately the sum of levels that were measured in the latter. Interestingly, the cytokine IL-1 $\alpha$  was only detectable when THP-1 cells were cultured alone but absent in HepG2 cell cultures or co-cultures of THP-1 and HepG2 cells.

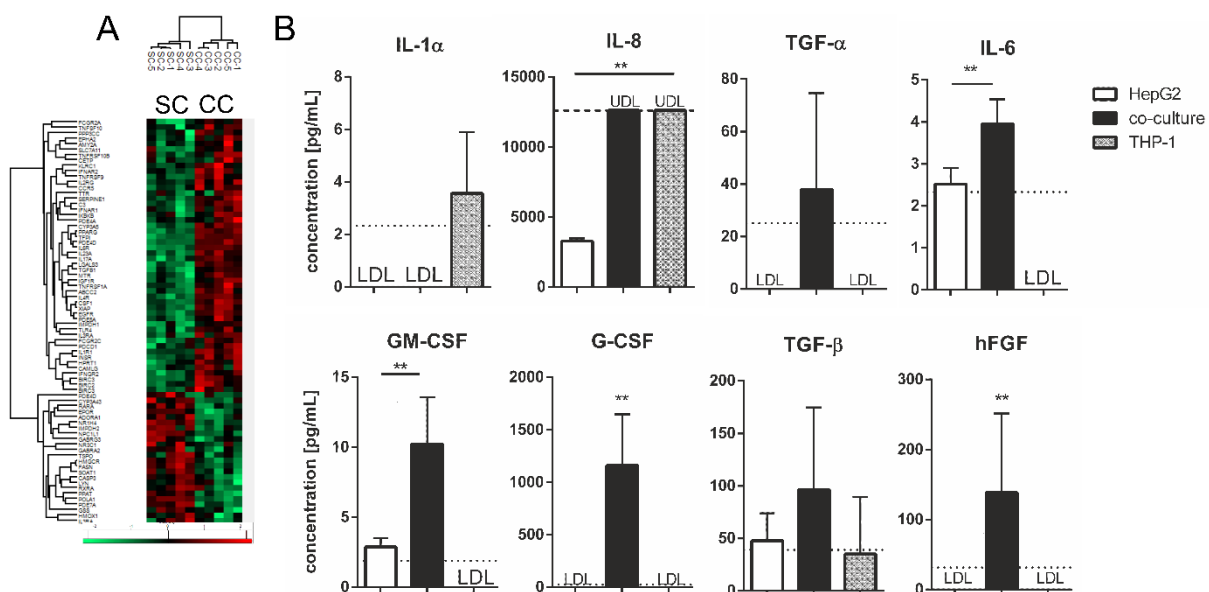


**Fig. 4.** Inflammation is induced in the co-culture of HepG2 and differentiated THP-1 cells. (A) Heat map of HepG2 cells in single culture (SC) or co-culture (CC) with PMA-differentiated THP-1 cells after 24 h ( $n = 5$ ). Gene symbols and the Z-score of significantly (exclusion  $p > 0.05$ ) up- or downregulated genes based on the IPA gene list are shown. An enlarged heat map is shown in the supplementary material (S2). (B) Secretion of TNF- $\alpha$ , IL-8, TGF- $\alpha$ , IL-6, GM-CSF, G-CSF, TGF- $\beta$  and hFGF in the supernatant of individually cultured and co-cultivated cells after 24 h ( $n = 6$ ). The means and standard deviations (SD) are shown with the upper (UDL) (---) and the lower detection limits (LDL) of the assay (···). \*\* $p < 0.01$ .

In conclusion, the secretion differed between individually cultivated cells and the co-cultivation of HepG2 with differentiated THP-1 cells (Fig. 4).

### **3.4. Pro-inflammatory conditions in co-culture activate the AHR signalling pathway**

Next, we were interested, whether xenobiotic metabolism might be affected under co-culture conditions. Therefore, genes representing phase I and phase II xenobiotic metabolism whose expression levels were found to be significantly elevated were selected from the microarray data (Fig. 5A). Using Ingenuity® Pathway Analysis (IPA®) software, we concluded that most (70.0%) of these

Indirect co-cultivation of HepG2 with differentiated THP-1 cells induces AHR signaling and release of pro-inflammatory cytokines.

genes were downregulated (Fig. 5A). In addition, the IPA® analysis indicated the activation of the AHR in co-culture. Immunoblot assays confirmed an increase in the amount of AHR protein in HepG2 cells after co-cultivation and a comparable amount of aryl hydrocarbon receptor nuclear translocator (ARNT) (Fig. 5B). As a result, known AHR target genes were transcriptionally upregulated in co-cultivated HepG2 cells compared to single-cultivated HepG2 cells (Fig. 5C): 74-fold for *CYP1A1*, 48-fold for *CYP1A2* and 4-fold for *CYP1B1*.

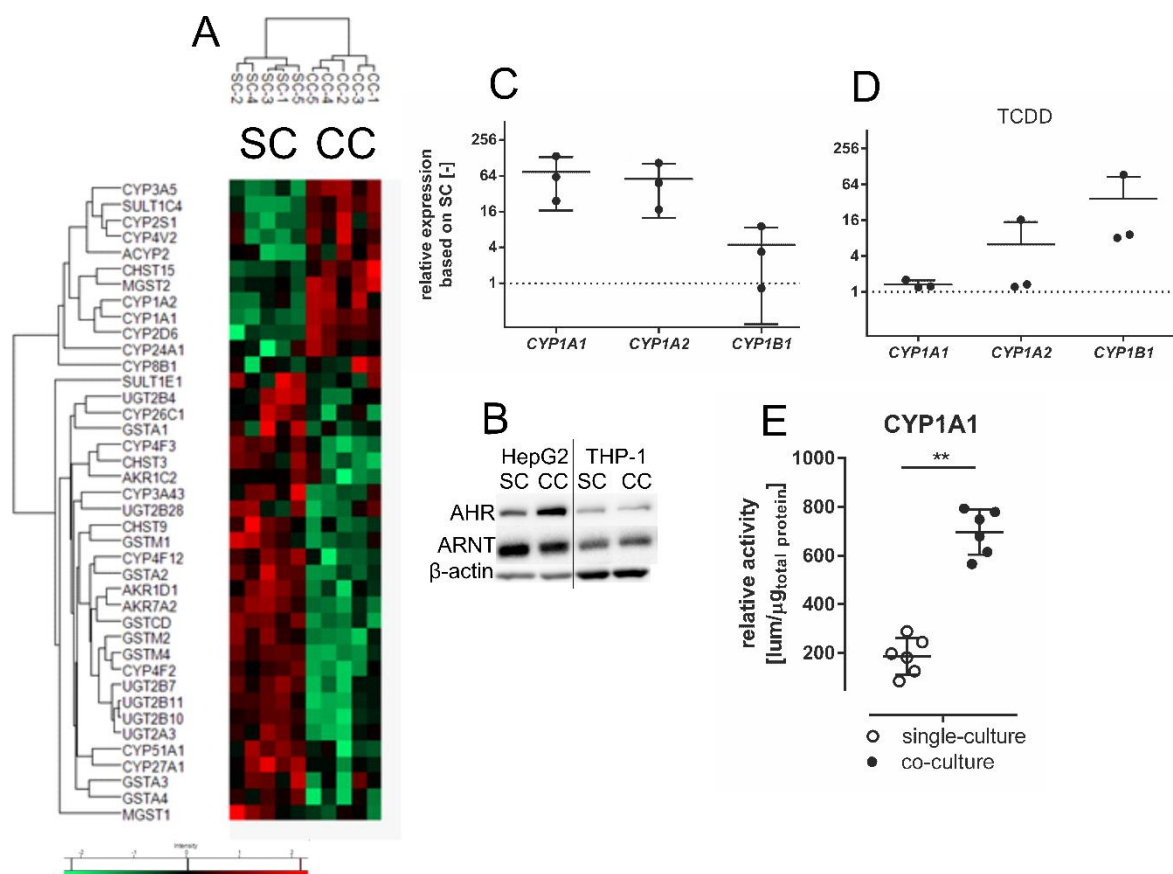


**Fig. 5.** Effects of co-cultivation on xenobiotic metabolism. (A) HepG2 cells were cultivated in single culture (SC) or co-culture (CC) for 24 h ( $n = 5$ ). The gene symbols and the Z-score of significantly and differentially expressed genes are shown. (B) Co-cultivation increased the amounts of AHR and ARNT. One representative blot of three biological replicates is shown. (C) Co-culture of HepG2 cells resulted in the increased expression of *CYP1A1* and *CYP1A2* genes, compared to single-cultivated cells. (D) Addition of 10 nM TCDD in CC systems resulted in no further induction of cytochrome P450 1A1 (*CYP1A1*), but an additional induction of cytochrome P450 1A2 (*CYP1A2*), and cytochrome P450 1B1 (*CYP1B1*) expression ( $n = 3$ ). (E) Compared to individually cultivated cells, HepG2 cells in co-culture showed increased cytochrome P450 1A1 (*CYP1A1*) enzyme activity ( $n = 6$ ). \*\* $p < 0.01$ .

Next, we studied, whether a classical inducer of AHR, 2,3,7,8-tetrachlorodibenzo-*p*-dioxin (TCDD), is able to further induce the expression of AHR target genes in co-culture. Therefore, we treated single-

### Indirect co-cultivation of HepG2 with differentiated THP-1 cells induces AHR signaling and release of pro-inflammatory cytokines.

and co-cultivated cells with the AHR activator TCDD. Compared to treated single-cultivated HepG2 cells, the co-cultivated HepG2 cells showed clearly upregulated *CYP1A2* and *CYP1B1* gene expression, only (Fig. 5D). The additional induction of *CYP1A1* by TCDD was only minor. Finally, we were interested, whether the increased gene and protein expression resulted in increased enzyme activity of the target gene. The enzyme activity of *CYP1A1* was significantly higher ( $p < 0.01$ ) in co-cultivated HepG2 cells than in individually cultivated HepG2 cells (Fig. 5E), indicating that the AHR receptor pathway was not only activated but also resulted in higher amounts of functional enzyme.

This result implies that compared to the individual cultivation of HepG2 cells, the co-cultivation of HepG2 cells with differentiated THP-1 cells results in the activation of AHR target genes and an increased *CYP1A1* enzyme activity.

### **3.5. Cholesterol biosynthesis is enhanced in co-culture**

The liver is the main organ of cholesterol synthesis. The microarray data revealed that all genes in the cholesterol biosynthesis pathway were significantly ( $p < 0.05$ ) downregulated under co-cultivation compared to individual cultivation (Fig. 6A). In contrast, the cellular cholesterol concentration was significantly increased in co-cultivated HepG2 cells after 24 h relative to the individually cultivated cells (Fig. 6B). Thus, we studied these contradictory results in more detail. HepG2 cells were treated with the HMG-CoA reductase inhibitor lovastatin, and the expression of a master regulator of cholesterol synthesis, sterol regulatory element binding transcription factor 1 (*SREBF1*) (Shimano et al., 1996), was determined (Fig. 6C). As expected, lovastatin treatment induced the significant upregulation (2-fold) of the transcription factor *SREBF1* in single culture. In co-culture, however, a 1.5-fold downregulation was detected (Fig. 6C). This treatment-dependent regulation indicated the presence of a negative feedback mechanism in co-culture. For clarification, we determined the cellular cholesterol concentration in single- and co-cultivated HepG2 cells after lovastatin treatment. In single-cultivated cells, the amount of cholesterol decreased relative to the level in co-cultivated cells (Fig. 6B). To further evaluate the effect of lovastatin, we compared individually cultivated and co-cultivated cells at different time points. In individually cultivated HepG2 cells, the effect of lovastatin occurred after 48 h (Fig. 6D). However, in co-cultivated cells, a significant ( $p < 0.05$ ) reduction in the cellular cholesterol concentration occurred after 24 h and remained constant for 48 h (Fig. 6D), indicating that lovastatin affected the lipid metabolism in co-cultivated cells responded faster than in individually cultivated cells.

Indirect co-cultivation of HepG2 with differentiated THP-1 cells induces AHR signaling and release of pro-inflammatory cytokines.

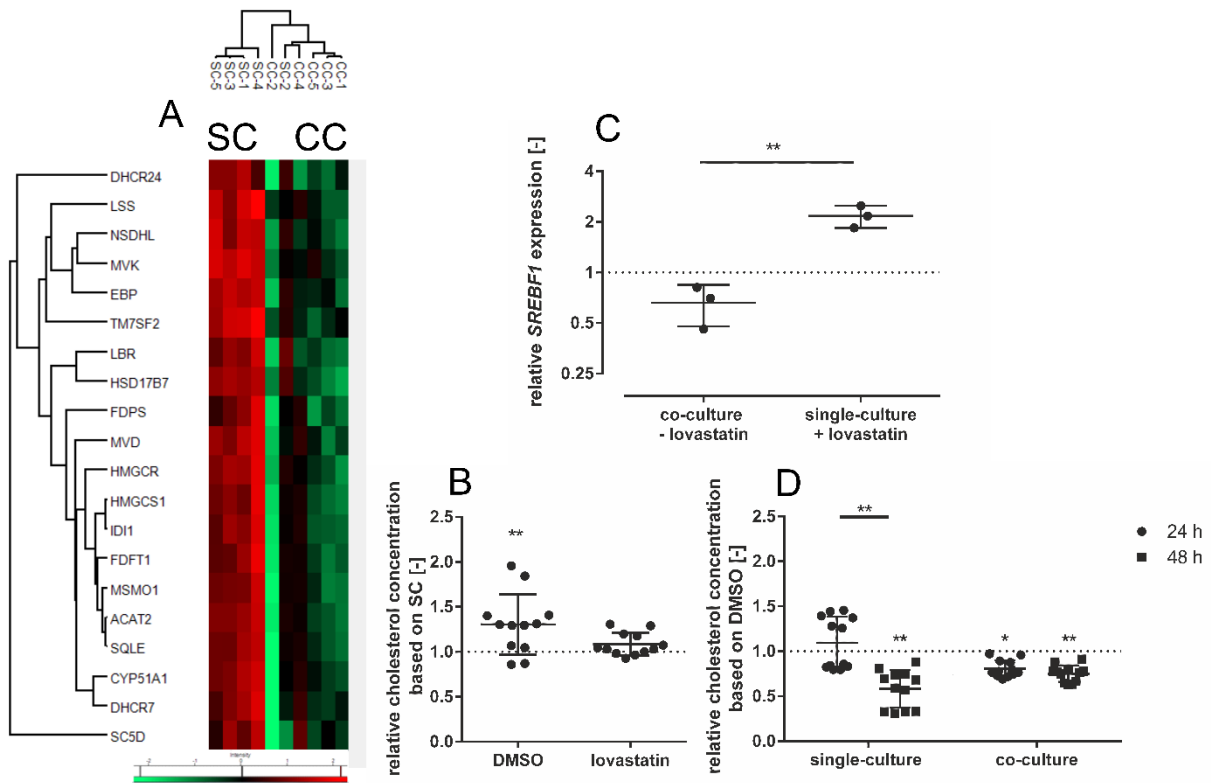


**Fig. 6.** Effects of co-culture on cholesterol biosynthesis. (A) Heat map of HepG2 cells in single culture (SC) or HepG2 cells co-cultured (CC) with PMA-differentiated THP-1 cells after 24 h ( $n = 5$ ). The gene symbols and the Z-score of significantly (exclusion  $p > 0.05$ ) expressed genes are shown. (B) Co-cultivation increased the relative cholesterol concentration in co-cultivated HepG2 cells. This increase was suppressed by 1  $\mu$ M lovastatin. (C) Lovastatin (1  $\mu$ M) increased the expression of sterol regulatory element binding transcription factor 1 (*SREBF1*) in individually cultivated HepG2 cells. During co-cultivation, the expression of *SREBF1* was decreased in HepG2 cells ( $n = 3$ ). (D) Cholesterol concentration in co-cultivated lovastatin-treated HepG2 cells decreased after 24 h and remained constant for 48 h. Cholesterol concentration in individually cultivated HepG2 cells decreased after 48 h relative to the corresponding DMSO control. Measurement data ( $\bullet, \blacksquare$ ), mean  $\pm$  SD and respective control ( $\cdots$ ) are shown. \* $p < 0.05$  and \*\* $p < 0.01$ .

In summary, we have shown that cholesterol biosynthesis is increased in co-cultivated HepG2 cells, despite reduced *SREBF1* expression. The cholesterol-lowering effect of lovastatin occurred earlier in co-culture than in individual culture.

### 3.6. Total lipid synthesis is decreased in co-culture

Next, we were interested, whether the total lipid amount and the related metabolism were affected during co-cultivation. Transcriptional analysis showed that 65% of the significantly ( $p < 0.05$ ) regulated genes related to lipid metabolism were upregulated in co-culture (Fig. 7A). However, these significantly upregulated genes could not be assigned to a distinct lipid metabolic pathway. Therefore, we

Indirect co-cultivation of HepG2 with differentiated THP-1 cells induces AHR signaling and release of pro-inflammatory cytokines.

quantified the amount of lipid droplets in HepG2 cells upon individual cultivation and co-cultivation. In general, the total area of lipid droplets in HepG2 cells was significantly ( $p < 0.01$ ) reduced in co-culture by 76% (Fig. 7B). To further elucidate this result, we studied the expression and concentration of fatty acid synthase (FAS), a key enzyme in lipid synthesis. The gene array data (Fig. 7A) and qPCR showed that the expression of *FASN* in HepG2 cells was significantly downregulated by 0.6-fold and that the protein concentration was reduced by 0.7-fold under co-culture conditions, supporting the reduction in the amount of lipid droplets (Fig. 7C+D).

Accordingly, total lipid synthesis seems to be lowered in co-cultivated HepG2 cells.

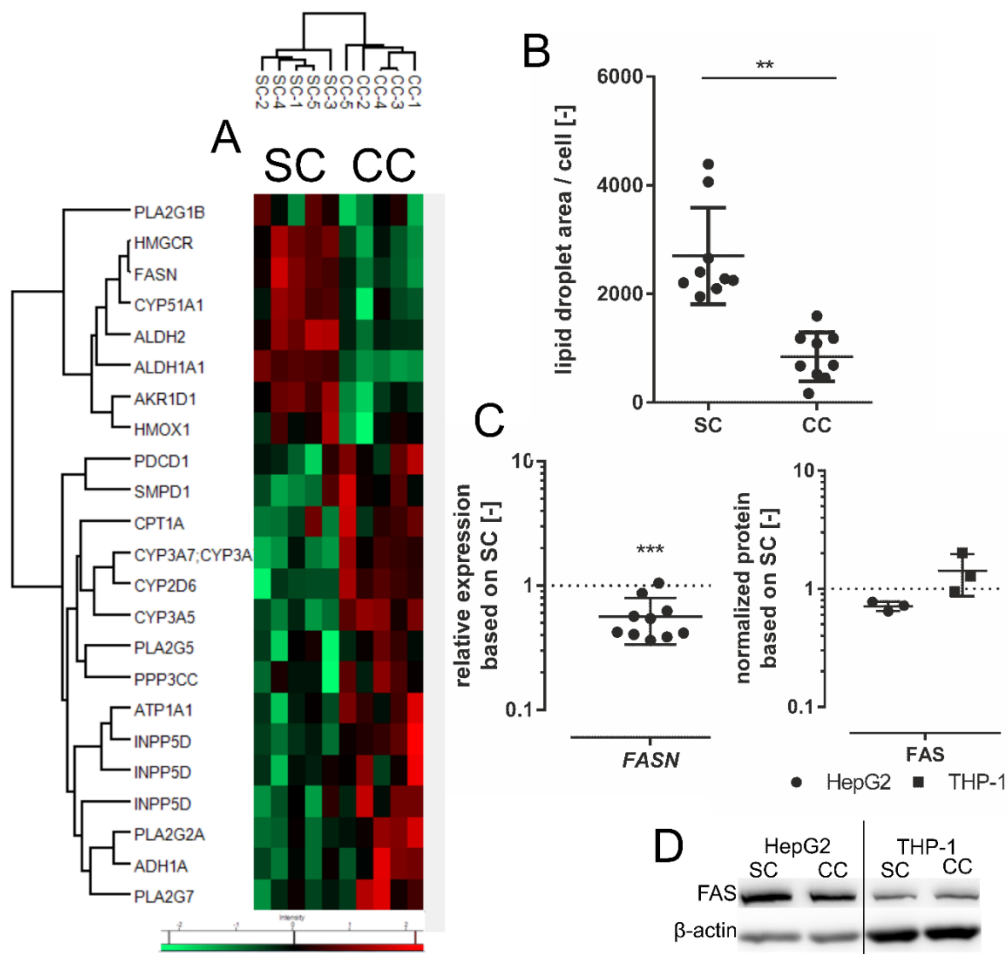


**Fig. 7.** Lipid metabolism. (A) Heat map of differentially expressed genes in HepG2 cells in single culture (SC) and co-culture (CC) with PMA-differentiated THP-1 cells. The gene symbols and the Z-score (exclusion  $p > 0.05$ ) after 24 h are shown ( $n = 5$ ). (B) Effect of SC and CC on the intracellular lipid droplet area (normalized to cell number) of HepG2 cells after 24 h ( $n = 3$ ). Each dot (●) represents a microscopic image. (C) HepG2 cells cultivated for 24 h in CC, showed reduced expression of fatty acid synthase (*FASN*) normalized to SC (···) and HPRT ( $n = 10$ ). The amount of fatty acid synthase (FAS) protein in CC was slightly reduced compared to in the SC (···) of HepG2 (●) or THP-1 (▪) cells ( $n = 3$ ). (D) Amount of FAS protein under SC and CC conditions. \*\* $p < 0.01$ , \*\*\* $p < 0.005$ .



Indirect co-cultivation of HepG2 with differentiated THP-1 cells induces AHR signaling and release of pro-inflammatory cytokines.

### **3.7. Co-culture activates key events of the AOP fibrosis**

The global transcriptome analysis of the co-culture indicated an increased expression of genes related to liver fibrosis. To validate this prediction, we studied key events (KE) of the adverse outcome pathway number 38 (Landesmann, 2016), visualized the presence of extracellular collagen and determined the upregulation of fibrosis-related genes (Fig. 8). The 'KE 1' requires hepatocyte injury. Hepatocyte injury is often related to the amount of intracellular ATP, which was significantly ( $p < 0.01$ ) reduced in co-cultivated HepG2 cells (Fig. 8B). 'KE 2' is the activation of Kupffer cells (KC). The transcriptome analysis of all associated genes (*e.g.*, cytokines and corresponding receptors) showed KC activation. In brief, 86% of all significantly ( $p < 0.05$ ) regulated genes examined for KE 2 were upregulated (Fig. 8C). Regarding 'KE 3', enhanced *TGFB1* expression was detected (up to 1.7-fold) in co-cultivated HepG2 cells compared to individually cultivated cells (Fig. 8D). The activation of these key events should result in an accumulation of collagen in the co-culture system. Staining and photometric quantification shows that a rather small but significant ( $p < 0.05$ ) accumulation (1.14-fold) of collagen occurred in co-cultivated HepG2 cells (Fig. 8E). In order to validate these unexpected finding further, the presence of extracellular collagen was analysed using Sirius Red (Fig. 8F). The images clearly proved, that staining occurred in cells and not, as expected for the extracellular matrix, outside of the cells. Finally, the expression of genes related to fibrosis was studied. In the co-culture the expression of pro-fibrotic genes for smooth muscle  $\alpha$  actin (*ACTA2*) and SMAD family member 7 (*SMAD7*) were down-regulated and only the expression of SMAD family member 3 (*SMAD3*) was upregulated, relative to the single cultured HepG2 cells (Fig. 8G).

Indirect co-cultivation of HepG2 with differentiated THP-1 cells induces AHR signaling and release of pro-inflammatory cytokines.

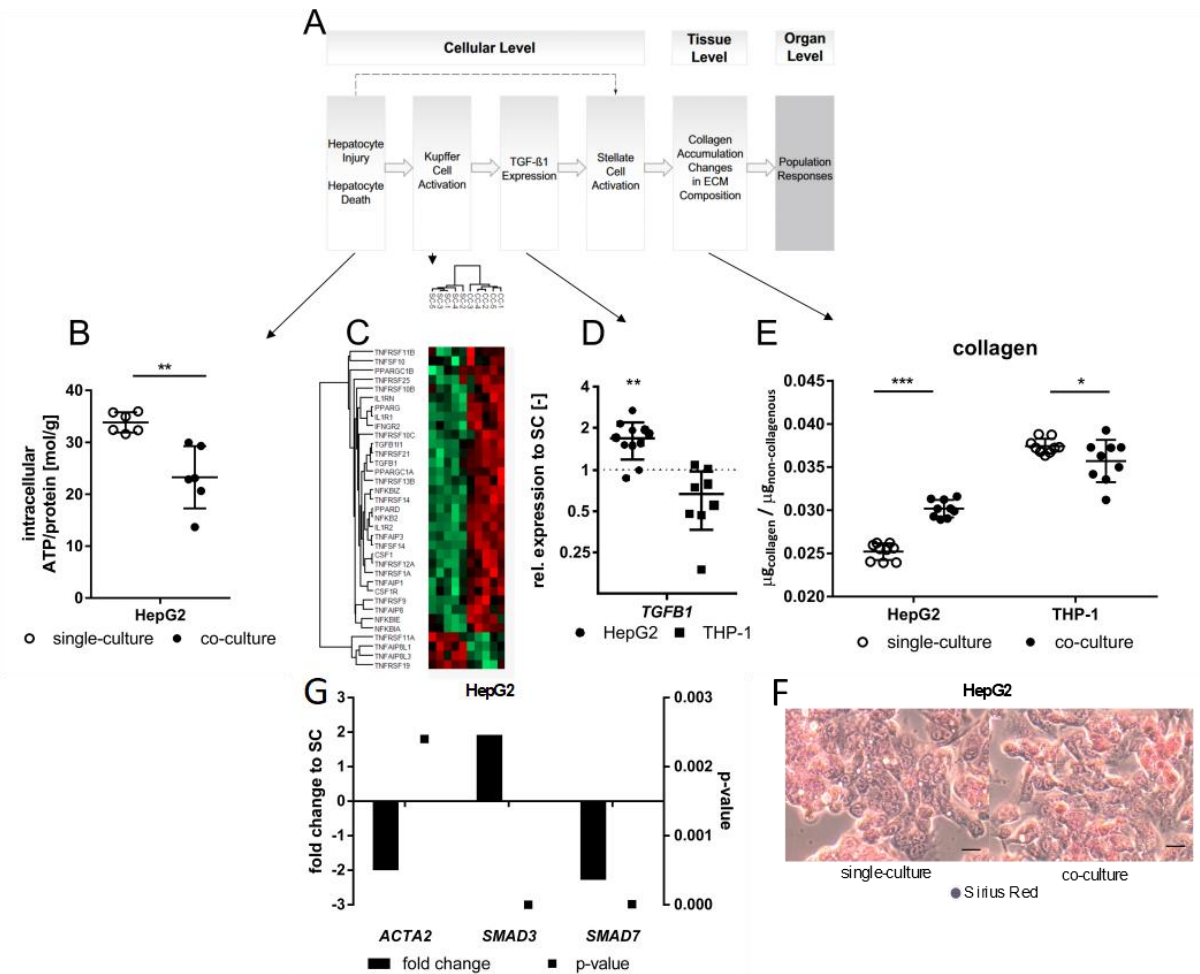


**Fig. 8.** Application of key events of the adverse outcome pathway (AOP) of ‘fibrosis’ (A) AOP analysis according to Horvat and co-workers (Horvat et al., 2017), including the gene symbol of transforming growth factor  $\beta$  1 (*TGFB1*) and the extracellular matrix (ECM). (B) ATP concentration per g total protein of HepG2 cells cultivated for 24 h under single culture (SC) or co-culture conditions (CC) with PMA-differentiated THP-1 cells. Individual measurement data (○, ●), mean  $\pm$  SD are given ( $n = 3$ ). (C) HepG2 cells were cultivated under SC or CC for 24 h ( $n = 5$ ). The gene symbols and the Z-score of significantly (exclusion  $p > 0.05$ ) and differentially expressed relevant genes for Kupffer cell activation are shown (Horvat et al., 2017). An enlarged heat map is shown in supplementary fig. S3. (D) Expression of *TGFB1* normalized to SC (···) HepG2 cells or PMA-differentiated THP-1 cells (■) and HPRT are shown ( $n = 11$ ). (E) The concentration of collagen significantly increased under the CC with HepG2 cells and PMA-differentiated THP-1 within 24 h. Data were normalized to the total amount of non-collagenous protein ( $n = 3$ ). (F) Representative microscopic image of HepG2 cells after cultivation under SC or CC for 24 h. The collagen staining (Sirius Red) was exclusively detectable in the intracellular compartments. (G) Fold change (CC relative to SC,  $n = 5$ ) of fibrosis associated gene expression assessed from the transcriptomic analysis, including the respective  $p$ -value. The gene for smooth muscle  $\alpha$  actin (*ACTA2*) and SMAD family member 7 (*SMAD7*) were downregulated in CC compared to SC, while SMAD family member 3 (*SMAD3*) was upregulated. \* $p < 0.05$ , \*\* $p < 0.01$ , and \*\*\* $p < 0.005$ . (For interpretation of the references to colour in this figure legend, the reader is referred to the web version of this article.)

## Indirect co-cultivation of HepG2 with differentiated THP-1 cells induces AHR signaling and release of pro-inflammatory cytokines.

In summary, while several of the KEs of the AOP fibrosis are met, the co-culture does not represent a fibrotic state and is in its present form not useful for studying fibrosis.

### **4. Discussion**

In this study, we characterized changes at the cellular level that were induced by the co-cultivation of HepG2 and PMA-differentiated THP-1 cells. The main focus was on the hepatic cell line. Transcriptome analyses of co-cultivated and individually cultivated HepG2 cells were taken as the basis for all further investigations. The previously reported pro-inflammatory properties of this co-culture (Wewering et al., 2017a; Granitzny et al., 2017; Wewering et al., 2017b) were studied in close detail in order to characterize the system further. Except for IL-1 $\alpha$ , the concentrations of all detected cytokines were found increased in the supernatant of co-cultivated cells (Fig. 4B).

Next, we compared the cytokine concentration measured under co-cultivation conditions with reported serum concentrations of healthy humans. The IL-6 concentration in our *in vitro* model was in a similar range as found in healthy human serum (Table 1), and GM-CSF is the only cytokine that showed a lower concentration than the reported values (Table 1). All other detected cytokines (IL-8, TGF- $\alpha$ , G-CSF, TGF- $\beta$ , hFGF) had higher concentrations in the supernatant of the co-culture than in healthy human serum (Table 1). Even though that the absolute numbers of the *in vitro* concentrations are not directly comparable with the *in vivo* data, the concentrations are in the same range. Surprisingly, IL-1 $\alpha$  was only detected in the supernatant of THP-1 cells under single culture conditions (Fig. 4B). Under co-cultivation conditions, no secretion was detectable, hence indicating that indirect cell-cell interactions (HepG2-THP-1) occurred. Therefore, co-cultivation is associated with the release of the inflammatory cytokines IL-8, TGF- $\alpha$  and G-CSF in the supernatant, most likely due to complex cell-cell interactions.

Indirect co-cultivation of HepG2 with differentiated THP-1 cells induces AHR signaling and release of pro-inflammatory cytokines.

**Table 1.** Comparison of cytokine concentration in the supernatant of co-cultivated HepG2 cells with THP-1 cells and healthy human serum. The following cytokines were quantified: interleukin 8 (IL-8), transforming growth factor  $\alpha$  (TGF- $\alpha$ ), interleukin 6 (IL-6), granulocyte macrophage colony-stimulating factor (GM-CSF), granulocyte colony stimulating factor (G-CSF), transforming growth factor  $\beta$  (TGF- $\beta$ ), human fibroblast growth factor (hFGF) and interleukin 1  $\alpha$  (IL-1 $\alpha$ ). The mean concentration ( $\pm$  SD) in the co-culture supernatant and the mean concentration and concentration range in human serum are shown.

Cytokine	Concentration in co-culture [pg/ml] (SD)	Mean concentration (range) in healthy human serum [pg/ml]	Reference for serum concentrations
IL-8	>12603.06 (-)	29.3 (24.4-35.9)	(Kleiner et al., 2013)
TGF- $\alpha$	56.87 (27.47)	3.2 (0.93-26.8)	(Kim et al., 2011)
IL-6	3.95 (0.58)	2.91 (0.16-37.7)	(Kim et al., 2011)
GM-CSF	10.22 (3.33)	38.3 (26.3-63.8)	(Kleiner et al., 2013)
G-CSF	1162.29 (485.3)	45.5 (34-53.6)	(Kleiner et al., 2013)
TGF- $\beta$	96.37 (90.08)	49.1 (not given)	(Wu et al., 2002)
hFGF	138.48 (110.09)	41.7 (33.2-49.5)	(Kleiner et al., 2013)
IL-1 $\alpha$	<1.89	<1.4	(Kleiner et al., 2013)

Xenobiotic metabolism is also affected in a pro-inflammatory environment. An increase in the IL-6 serum levels of patients undergoing allogeneic bone marrow transplantation was associated with a decrease in cyclosporine metabolism (Chen et al., 1994). The liver is important for phase I and phase II metabolism of xenobiotic substances (Anzenbacher and Zanger, 2012), and it has been shown that cytokines can affect biotransformation (Prescott et al., 1975). Xenobiotic metabolism (membrane transport, phase I and phase II) is reduced by 10 ng/ml IL-6 in primary human hepatocytes and HepaRG cells (Klein et al., 2015). In addition, the phase I enzyme CYP1A1 is repressed by IL-6 and TNF- $\alpha$  in primary human hepatocytes (Muntane-Relat et al., 1995). Previously, we have shown that the secretion of TNF- $\alpha$  increases under co-cultivation conditions up to 63.5 pg/ml (Padberg et al., 2019), and here we report that the IL-6 concentration was 3.9 pg/ml (Table 1). In contrast to the reported data (Muntane-Relat et al., 1995), CYP1A1 enzyme activity also increased (Fig. 5E), indicating that the interaction of cytokines and xenobiotic metabolism might be more complex and different in the HepG2 and THP-1 co-culture system than in individually cultivated primary hepatocytes. The upregulation of CYP1A1 in the co-cultivated HepG2 cells could also be induced by other non-investigated pathways/receptors, such as the constitutive androstane receptor (CAR) and the liver X receptor  $\alpha$  signalling (LXR $\alpha$ ) pathways (Santes-Palacios et al., 2016). Indeed, the AHR pathway was

Indirect co-cultivation of HepG2 with differentiated THP-1 cells induces AHR signaling and release of pro-inflammatory cytokines.

activated in co-cultivated HepG2 cells. An assessment based on the higher concentration of AHR (Fig. 5B) and upregulated expression of the target genes *CYP1A1*, *CYP1A2* and *CYP1B1* (Fig. 5C). Interestingly, Nguyen and co-workers showed that humans exposed to dioxin (a potent activator of the AHR pathway) showed significantly increased gene expression of *TNF* and *IL-6* in whole blood cells (Nguyen et al., 2017). In addition to ligand-dependent activation, AHR overexpression can also result from the expression of IL-6 (Chen et al., 2011). Therefore, we concluded that the expression and activation of AHR in the co-culture resulted from increased cytokine signalling, which finally results in an increased enzyme activity (Fig. 5E).

In addition to the biotransformation of xenobiotics, the liver is crucial for lipid metabolism, including cholesterol biosynthesis (Repa and Mangelsdorf, 2000). The biosynthesis of cholesterol increases in the co-culture system (Fig. 6), while the amount of total lipids, determined as lipid droplets, is reduced (Fig. 7B).

An increase in the sensitivity of co-cultured HepG2 cells towards lovastatin, a classical sterol biosynthesis inhibitor, occurred under co-cultivation (Fig. 6D). Lovastatin (HMG-CoA reductase inhibitor) reduced the cholesterol concentration in the co-culture after 24 h. In contrast, the reduction occurred in single-cultivated HepG2 only after 48 h. This result demonstrates that the co-culture system has an improved sensitivity towards a classical sterol biosynthesis inhibitor. Previously, enhanced sensitivity to the DILI-inducing substance ketoconazole was demonstrated due to increases in oxidative stress-related proteins and pro-inflammatory cytokine secretion (Wewering et al., 2017a). This finding was supported by a mechanistic approach, testing a larger set of drugs (Granitzny et al., 2017). Therefore, it is concluded that the co-culture exhibits not only a higher sensitivity to DILI-inducing substances but might also respond more rapidly to drug exposure. This has to be studied in more detail in future. Whether this enhanced sensitivity is based on the reduced lipid droplets in the co-cultivated HepG2 (Fig. 7B) remains also to be proven. It is known that lipid droplets maintain organelle homeostasis and prevent reactive oxygen species (ROS), lipid overload, hypoxia and apoptotic cell death (Baenke et al., 2013).

Surprisingly, the increased cholesterol biosynthesis (Fig. 6) does not lead to an increase in total lipids (Fig. 7B), but rather to a decrease in the number of lipid droplets. Since acetyl-CoA is the common precursor of cholesterol and fatty acids, it can be concluded that acetyl-CoA is not limited and that the regulation of the two pathways must occur at later stages. We identified a decrease in the lipid droplet area per cell (Fig. 7B) and validated the hypothesis that *de novo* fatty acid (FA) synthesis was reduced in co-culture, since the gene expression of FAS and the amount of FAS protein was decreased in the

Indirect co-cultivation of HepG2 with differentiated THP-1 cells induces AHR signaling and release of pro-inflammatory cytokines.

co-culture compared to the individual cultures (Fig. 7C+D). The reduction of FAS and the lipids indicates, that the  $\beta$ -oxidation of FA is increased in co-cultivation compared to HepG2 cells alone, thereby providing ATP. The decreased intracellular ATP amount in co-cultivated HepG2 cells supports this (Fig. 8B). An increased CYP expression (Fig. 5C) and protein biosynthesis (Fig. 5E) supports the need for energy further, because protein biosynthesis is one of the most energy consuming cellular processes (Lindqvist et al., 2018). Also the enhanced cholesterol biosynthesis in co-cultivation (Fig. 6) is an ATP demanding anabolic pathway (Korman et al., 2014). Taken together the co-cultivated HepG2 cells have an higher ATP demand compared to the HepG2 cells alone and this is most likely covered by the oxidation of FA.

The aforementioned changes in lipid metabolism can be closely linked to the inflammatory environment during co-cultivation. The hormone leptin promotes FA oxidation, resulting in a reduction of hepatic triglycerides and cytokine secretion (GM-CSF, IL-1 $\alpha$ , IL-1 $\beta$ , IL-6, IL-10 and IL-18) in murine KC *in vitro* (Metlakunta et al., 2017). However, the authors showed that typical leptin-induced FA oxidation was not a consequence of the cytokine release (Metlakunta et al., 2017). This result provides evidence that the interplay of the cytokines with each other and with cells and tissues is complex. IL-6 is a pleiotropic cytokine and has multiple effects on hepatic lipid metabolism (Hassan et al., 2014). In general, lipid metabolism is disturbed during inflammatory processes (Tall and Yvan-Charvet, 2015).

The inflammatory pattern of the co-culture does not indicate a pathophysiological pattern like non-alcoholic fatty liver disease (NAFLD) or steatohepatitis, even though the typical pro-inflammatory cytokines (*e.g.*, IL-6, IL-8 and TNF- $\alpha$ ) are increased (Braunersreuther et al., 2012; Niederreiter and Tilg, 2018). Since the lipid droplet area in the presented co-culture was reduced (Fig. 7B), the system did not represent a true model of fatty liver disease.

A pro-inflammatory co-culture system might also enable the investigation of liver fibrosis *in vitro*. Liver fibrosis is associated with abundant extracellular matrix (ECM) proteins, like collagen. Hepatic stellate cells are the main mediators of ECM production (Bataller and Brenner, 2005). Recently, Prestigiacomo and co-workers (Prestigiacomo et al., 2017) developed a co-culture system, composed of three cell lines: HepaRG, differentiated THP-1 and hTERT-HSC for studying fibrosis. ECM production and fibrosis become clinically relevant when dysregulated, eventually leading to chronic liver diseases (Pellicoro et al., 2014). This liver injury can be induced *in vitro* using the indirect co-cultivation of rat hepatic stellate cells and rat KC (Nieto, 2006). In the presented co-cultivation system, the main key events of the AOP for fibrosis (Horvat et al., 2017) were observable (Fig. 8). Due to the absence of stellate cells, however, we were unable to prove key event 4, that is, the activation of the latter cell type. Stellate cells are an

## Indirect co-cultivation of HepG2 with differentiated THP-1 cells induces AHR signaling and release of pro-inflammatory cytokines.

essential contributor to hepatic fibrosis (Horvat et al., 2017). A small but significant collagen accumulation, could be confirmed (Fig. 8E) in HepG2 cells. The synthesis of collagen 1 by HepG2 cells has been reported (Zhang et al., 2020), and that collagen production can be induced by 10  $\mu$ M all-*trans* retinoic acid (Wang et al., 2013). This finding shows that stellate cell-independent collagen accumulation can occur *in vitro*. While several KE of the AOP fibrosis were detected in our co-culture system, it does not represent a fibrotic state, because there was no extracellular accumulation of collagen (Fig. 8F). In addition, *ACTA2* and *SMAD7* (Rockey et al., 2019), important during the development of fibrosis were downregulated (Fig. 8G) and only *SMAD3* was upregulated, relative to the single culture. Therefore, this example demonstrates, that AOPs should be used with care. The presence of KE are important parameters in an AOP, but in the case of complex pathological processes like fibrosis the presence of KE might be misleading. Especially, if *in vitro* systems do not consist of the cell types relevant for the pathological process. Stellate cells in the case of fibrosis. This is clearly demonstrated by an *in vitro* co-culture system of HepRG, THP-1 and a stellate cell line, that is able to mimic the fibrotic pathology (Prestigiacomo et al., 2017).

### **5. Conclusion**

Biochemical changes that were induced by the co-cultivation of HepG2 and PMA-differentiated THP-1 cells were characterized. In general, indirect co-cultivation was associated with an inflammatory cytokine composition in the supernatant. Enzymes involved in xenobiotic metabolism (CYP1A1, CYP1A2 and CYP1B1) increased, as determined by mRNA expression. Besides differential gene expression the enzymatic activity also increased. These observations were due to activation of the AHR signalling pathway. In addition, the lipid metabolism was disturbed, indicated by an increased cholesterol biosynthesis, a shortened reaction time upon lovastatin treatment, and a reduced *de novo* fatty acid synthesis.

In summary, the co-culture of HepG2 and PMA-differentiated THP-1 is a simple *in vitro* method with increased release of inflammatory cytokines (IL-8, TGF- $\beta$ , IL-6, GM-CSF, G-CSF, TGF- $\beta$  and hFGF) and an activated AHR pathway with differential expression of genes related to biotransformation and an increased CYP1A1 enzymatic activity. Finally, we consider that this co-cultivation is a method for a fast and uncomplicated screening of substances that affect the release of pro-inflammatory cytokines or AHR signalling and related enzyme activities.

Indirect co-cultivation of HepG2 with differentiated THP-1 cells induces AHR signaling and release of pro-inflammatory cytokines.

## References

- Albrecht et al., 2019 W. Albrecht, F. Kappenberg, T. Brecklinghaus, R. Stoeber, R. Marchan, M. Zhang, K. Ebbert, H. Kirschner, M. Grinberg, M. Leist, W. Moritz, C. Cadenas, A. Ghallab, J. Reinders, N. Vartak, C. van Thriel, K. Golka, L. Tolosa, J.V. Castell, G. Damm, D. Seehofer, A. Lampen, A. Braeuning, T. Buhrke, A.-C. Behr, A. Oberemm, X. Gu, N. Kittana, B. van de Water, R. Kreiling, S. Fayyaz, L. van Aerts, B. Smedsrød, H. Ellinger-Ziegelbauer, T. Steger-Hartmann, U. Gundert-Remy, A. Zeigerer, A. Ullrich, D. Runge, S.M.L. Lee, T.S. Schiergens, L. Kuepfer, A. Aguayo-Orozco, A. Sachinidis, K. Edlund, I. Gardner, J. Rahnenführer, J.G. Hengstler Prediction of human drug-induced liver injury (DILI) in relation to oral doses and blood concentrations Arch. Toxicol., 93 (6) (2019), pp. 1609-1637
- Anzenbacher and Zanger, 2012 P. Anzenbacher, U.M. Zanger Metabolism of Drugs and Other Xenobiotics Wiley-VCH, Weinheim (2012)
- Baenke et al., 2013 F. Baenke, B. Peck, H. Miess, A. Schulze Hooked on fat: the role of lipid synthesis in cancer metabolism and tumour development Dis. Model. Mech., 6 (6) (2013), pp. 1353-1363
- Bataller and Brenner, 2005 R. Bataller, D.A. Brenner Liver fibrosis J. Clin. Invest., 115 (2) (2005), pp. 209-218
- Braunersreuther et al., 2012 V. Braunersreuther, G.L. Viviani, F. Mach, F. Montecucco Role of cytokines and chemokines in non-alcoholic fatty liver disease World J. Gastroenterol., 18 (8) (2012), pp. 727-735
- Bro and Smilde, 2014 R. Bro, A.K. Smilde Principal component analysis Anal. Methods, 6 (9) (2014), pp. 2812-2831
- Carpenter et al., 2006 A.E. Carpenter, T.R. Jones, M.R. Lamprecht, C. Clarke, I.H. Kang, O. Friman, D.A. Guertin, J.H. Chang, R.A. Lindquist, J. Moffat, P. Golland, D.M. Sabatini CellProfiler: image analysis software for identifying and quantifying cell phenotypes Genome Biol., 7 (10) (2006), p. R100
- Chen et al., 1994 Y.L. Chen, V. Le Vraux, A. Leneuve, F. Dreyfus, A. Stheneur, I. Florentin, M. De Sousa, J.P. Giroud, B. Flouvat, L. Chauvelot-Moachon Acute-phase response, interleukin-6, and alteration of cyclosporine pharmacokinetics Clin. Pharmacol. Ther., 55 (6) (1994), pp. 649-660
- Chen et al., 2011 P.H. Chen, H. Chang, J.T. Chang, P. Lin Aryl hydrocarbon receptor in association with RelA modulates IL-6 expression in non-smoking lung cancer Oncogene, 31 (2011), p. 2555
- Granitzny et al., 2017 A. Granitzny, J. Knebel, M. Muller, A. Braun, P. Steinberg, C. Dasenbrock, T. Hansen Evaluation of a human in vitro hepatocyte-NPC co-culture model for the prediction of idiosyncratic drug-induced liver injury: a pilot study Toxicol. Rep., 4 (2017), pp. 89-103
- Hassan et al., 2014 W. Hassan, L. Ding, R.Y. Gao, J. Liu, J. Shang Interleukin-6 signal transduction and its role in hepatic lipid metabolic disorders Cytokine, 66 (2) (2014), pp. 133-142
- Hewitt and Hewitt, 2004 N.J. Hewitt, P. Hewitt Phase I and II enzyme characterization of two sources of HepG2 cell lines Xenobiotica, 34 (3) (2004), pp. 243-256
- Horvat et al., 2017 T. Horvat, B. Landesmann, A. Lostia, M. Vinken, S. Munn, M. Whelan Adverse outcome pathway development from protein alkylation to liver fibrosis Arch. Toxicol., 91 (4) (2017), pp. 1523-1543



Indirect co-cultivation of HepG2 with differentiated THP-1 cells induces AHR signaling and release of pro-inflammatory cytokines.

- Kim et al., 2011 H.O. Kim, H.S. Kim, J.C. Youn, E.C. Shin, S. Park Serum cytokine profiles in healthy young and elderly population assessed using multiplexed bead-based immunoassays *J. Transl. Med.*, 9 (2011), p. 113
- Klein et al., 2015 M. Klein, M. Thomas, U. Hofmann, D. Seehofer, G. Damm, U.M. Zanger A systematic comparison of the impact of inflammatory Signaling on absorption, distribution, metabolism, and excretion gene expression and activity in primary human hepatocytes and HepaRG cells *Drug Metab. Dispos.*, 43 (2) (2015), p. 273
- Kleiner et al., 2013 G. Kleiner, A. Marcuzzi, V. Zanin, L. Monasta, G. Zauli Cytokine levels in the serum of healthy subjects *Mediat. Inflamm.*, 2013 (2013), Article 434010
- Korman et al., 2014 T.P. Korman, B. Sahachartsiri, D. Li, J.M. Vinokur, D. Eisenberg, J.U. Bowie A synthetic biochemistry system for the in vitro production of isoprene from glycolysis intermediates *Protein Sci.*, 23 (5) (2014), pp. 576-585
- Kurycina et al., 2018 A.V. Kurycina, M.V. Erokhina, O.A. Makarevich, V.Y. Sysoeva, L.N. Lepekha, S.A. Kuznetsov, G.E. Onishchenko Plasticity of human THP-1 cell phagocytic activity during Macrophagic differentiation *Biochem. Mosc.*, 83 (3) (2018), pp. 200-214
- Landesmann, 2016 B. Landesmann Adverse Outcome Pathway on Protein Alkylation Leading to Liver Fibrosis OECD Publishing OECD Series on Adverse Outcome Pathways, No. 2 (2016)
- Lin et al., 2012 J. Lin, L. Schyschka, R. Muhl-Benninghaus, J. Neumann, L. Hao, N. Nussler, S. Dooley, L. Liu, U. Stockle, A.K. Nussler, S. Ehnert Comparative analysis of phase I and II enzyme activities in 5 hepatic cell lines identifies Huh-7 and HCC-T cells with the highest potential to study drug metabolism *Arch. Toxicol.*, 86 (1) (2012), pp. 87-95
- Lindqvist et al., 2018 L.M. Lindqvist, K. Tandoc, I. Topisirovic, L. Furic Cross-talk between protein synthesis, energy metabolism and autophagy in cancer *Curr. Opin. Genet. Dev.*, 48 (2018), pp. 104-111
- Livak and Schmittgen, 2001 K.J. Livak, T.D. Schmittgen Analysis of relative gene expression data using real-time quantitative PCR and the 2(T)(-Delta Delta C) method *Methods*, 25 (4) (2001), pp. 402-408
- Lund et al., 2016 M.E. Lund, J. To, B.A. O'Brien, S. Donnelly The choice of phorbol 12-myristate 13-acetate differentiation protocol influences the response of THP-1 macrophages to a pro-inflammatory stimulus *J. Immunol. Methods*, 430 (2016), pp. 64-70
- Metlakunta et al., 2017 A. Metlakunta, W. Huang, M. Stefanovic-Racic, N. Dedousis, I. Sipula, R.M. O'Doherty Kupffer cells facilitate the acute effects of leptin on hepatic lipid metabolism *Am. J. Physiol. Endocrinol. Metab.*, 312 (1) (2017), pp. E11-E18
- Mosmann, 1983 T. Mosmann Rapid colorimetric assay for cellular growth and survival: application to proliferation and cytotoxicity assays *J. Immunol. Methods*, 65 (1-2) (1983), pp. 55-63
- Muntane-Relat et al., 1995 J. Muntane-Relat, J.C. Ourlin, J. Domergue, P. Maurel Differential effects of cytokines on the inducible expression of CYP1A1, CYP1A2, and CYP3A4 in human hepatocytes in primary culture *Hepatology*, 22 (4) (1995), pp. 1143-1153 Pt 1
- Nguyen et al., 2017 C.H. Nguyen, T. Nakahama, T.T. Dang, H.H. Chu, L. Van Hoang, T. Kishimoto, N.T. Nguyen Expression of aryl hydrocarbon receptor, inflammatory cytokines, and incidence of

Indirect co-cultivation of HepG2 with differentiated THP-1 cells induces AHR signaling and release of pro-inflammatory cytokines.

- rheumatoid arthritis in Vietnamese dioxin-exposed people *J. Immunotoxicol.*, 14 (1) (2017), pp. 196-203
- Niederreiter and Tilg, 2018 L. Niederreiter, H. Tilg Cytokines and fatty liver diseases *Liver Research*, 2 (1) (2018), pp. 14-20
- Nieto, 2006 N. Nieto Oxidative-stress and IL-6 mediate the fibrogenic effects of [corrected] Kupffer cells on stellate cells *Hepatology*, 44 (6) (2006), pp. 1487-1501
- Padberg et al., 2019 F. Padberg, P. Tarnow, A. Luch, S. Zellmer Minor structural modifications of bisphenol a strongly affect physiological responses of HepG2 cells *Arch. Toxicol.*, 93 (6) (2019), pp. 1529-1541
- Pellicoro et al., 2014 A. Pellicoro, P. Ramachandran, J.P. Iredale, J.A. Fallowfield Liver fibrosis and repair: immune regulation of wound healing in a solid organ *Nat. Rev. Immunol.*, 14 (2014), p. 181
- Plotly Technologies Inc, 2015 Plotly Technologies Inc Collaborative Data Science, Plotly Technologies Inc., Montréal <https://plot.ly/create/> (2015)
- Prescott et al., 1975 L.F. Prescott, J.A. Forrest, K.K. Adjepon-Yamoah, N.D. Finlayson Drug metabolism in liver disease *J. Clin. Pathol. Suppl. (R. Coll. Pathol.)*, 9 (1975), pp. 62-65
- Prestigiacomo et al., 2017 V. Prestigiacomo, A. Weston, S. Messner, F. Lampart, L. Suter-Dick Pro-fibrotic compounds induce stellate cell activation, ECM-remodelling and Nrf2 activation in a human 3D-multicellular model of liver fibrosis *PLoS One*, 12 (6) (2017), Article e0179995
- Repa and Mangelsdorf, 2000 J.J. Repa, D.J. Mangelsdorf The role of orphan nuclear receptors in the regulation of cholesterol homeostasis *Annu. Rev. Cell Dev. Biol.*, 16 (2000), pp. 459-481
- Rockey et al., 2019 D.C. Rockey, Q. Du, Z. Shi Smooth muscle  $\alpha$ -actin deficiency leads to decreased liver fibrosis via impaired cytoskeletal signaling in hepatic stellate cells *Am. J. Pathol.*, 189 (11) (2019), pp. 2209-2220
- Roth et al., 2003 R.A. Roth, J.P. Luyendyk, J.F. Maddox, P.E. Ganey Inflammation and drug idiosyncrasy - is there a connection? *J. Pharmacol. Exp. Ther.*, 307 (1) (2003), pp. 1-8
- Santes-Palacios et al., 2016 R. Santes-Palacios, D. Ornelas-Ayala, N. Cabanas, A. Marroquin-Perez, A. Hernandez-Magana, S. Del Rosario Olguin-Reyes, R. Camacho-Carranza, J.J. Espinosa-Aguirre Regulation of human cytochrome P4501A1 (hCYP1A1): a plausible target for chemoprevention? *Biomed. Res. Int.*, 2016 (2016), Article 5341081
- Schwende et al., 1996 H. Schwende, E. Fitzke, P. Ambs, P. Dieter Differences in the state of differentiation of THP-1 cells induced by phorbol ester and 1,25-dihydroxyvitamin D3 *J. Leukoc. Biol.*, 59 (4) (1996), pp. 555-561
- Shimano et al., 1996 H. Shimano, J.D. Horton, R.E. Hammer, I. Shimomura, M.S. Brown, J.L. Goldstein Overproduction of cholesterol and fatty acids causes massive liver enlargement in transgenic mice expressing truncated SREBP-1a *J. Clin. Invest.*, 98 (7) (1996), pp. 1575-1584
- Soldatow et al., 2013 V.Y. Soldatow, E.L. Lecluyse, L.G. Griffith, I. Rusyn In vitro models for liver toxicity testing *Toxicol Res (Camb)*, 2 (1) (2013), pp. 23-39

Indirect co-cultivation of HepG2 with differentiated THP-1 cells induces AHR signaling and release of pro-inflammatory cytokines.

- Tall and Yvan-Charvet, 2015 A.R. Tall, L. Yvan-Charvet Cholesterol, inflammation and innate immunity Nat. Rev. Immunol., 15 (2015), p. 104
- Toyoda et al., 2017 Y. Toyoda, K. Kashikura, T. Soga, Y.I. Tagawa Metabolomics of an in vitro liver model containing primary hepatocytes assembling around an endothelial cell network: comparative study on the metabolic stability and the effect of acetaminophen treatment J. Toxicol. Sci., 42 (4) (2017), pp. 445-454
- Tyanova et al., 2016 S. Tyanova, T. Temu, P. Sinitcyn, A. Carlson, M.Y. Hein, T. Geiger, M. Mann, J. Cox The Perseus computational platform for comprehensive analysis of (prote)omics data Nat. Methods, 13 (2016), p. 731
- Wang et al., 2013 W. Wang, G. Xu, C.L. Ding, L.J. Zhao, P. Zhao, H. Ren, Z.T. Qi All-trans retinoic acid protects hepatocellular carcinoma cells against serum-starvation-induced cell death by upregulating collagen 8A2 FEBS J., 280 (5) (2013), pp. 1308-1319
- Wewering et al., 2017a F. Wewering, F. Jouy, D.K. Wissenbach, S. Gebauer, M. Blüher, R. Gebhardt, R. Pirow, M. von Bergen, S. Kalkhof, A. Luch, S. Zellmer Characterization of chemical-induced sterile inflammation in vitro: application of the model compound ketoconazole in a human hepatic co-culture system Arch. Toxicol., 91 (2) (2017), pp. 799-810
- Wewering et al., 2017b F. Wewering, F. Jouy, S. Caliskan, S. Kalkhof, M. von Bergen, A. Luch, S. Zellmer Hepatic co-cultures in vitro reveal suitable to detect Nrf2-mediated oxidative stress responses on the bladder carcinoma o-anisidine Toxicol. in Vitro, 40 (2017), pp. 153-160
- Wu et al., 2002 H.S. Wu, Y.F. Li, C.I. Chou, C.C. Yuan, M.W. Hung, L.C. Tsai The concentration of serum transforming growth factor beta-1 (TGF-beta1) is decreased in cervical carcinoma patients Cancer Investig., 20 (1) (2002), pp. 55-59
- Zeilinger et al., 2016 K. Zeilinger, N. Freyer, G. Damm, D. Seehofer, F. Knospel Cell sources for in vitro human liver cell culture models Exp. Biol. Med. (Maywood), 241 (15) (2016), pp. 1684-1698
- Zhang et al., 2020 Q. Zhang, X. Chang, H. Wang, Y. Liu, X. Wang, M. Wu, H. Zhan, S. Li, Y. Sun TGF- $\beta$ 1 mediated Smad signaling pathway and EMT in hepatic fibrosis induced by Nano NiO in vivo and in vitro Environ. Toxicol., 35 (4) (2020), pp. 419-429
- Zhou et al., 2019 Y. Zhou, J.X. Shen, V.M. Lauschke Comprehensive evaluation of Organotypic and microphysiological liver models for prediction of drug-induced liver injury Front. Pharmacol., 10 (2019), p. 1093

Novel indirect co-culture of immortalised hepatocytes with monocyte derived macrophages is characterised by pro-inflammatory cytokine networks

### **3.3 Novel indirect co-culture of immortalised hepatocytes with monocyte derived macrophages is characterised by pro-inflammatory cytokine networks**

Florian Padberg, Tessa Höper, Sebastian Henkel, Dominik Driesch, Andreas Luch, and Sebastian Zellmer

*Toxicology in Vitro* volume 73, 105134 (2021)

Published online: 2 March 2021

DOI: 10.1016/j.tiv.2021.105134

Link: <https://doi.org/10.1016/j.tiv.2021.105134>

Involvement of the author within this publication: project planning: 90 %, project execution: 80 %, data analysis: 70 %, writing the manuscript: 70 %

The supplementary material to the publication embedded on the following pages is contained in Annex III.

Novel indirect co-culture of immortalised hepatocytes with monocyte derived macrophages is characterised by pro-inflammatory cytokine networks

**Abstract**

The liver is composed of different cell populations. Interactions of different cell populations can be investigated by a newly established indirect co-culture system consisting of immortalised primary human hepatocytes and human monocyte derived macrophages (MDMs). Using the time-dependent cytokine secretion of the co-cultures and single cultures, correlation networks (including the cytokines G-CSF, CCL3, MCP-1, CCL20, FGF, TGF- $\beta$ 1, GM-CSF, IL-8, IL-6, IL-1 $\beta$ , and IL-18) were generated and the correlations were validated by application of IL-8 and TNF- $\alpha$ -neutralising antibodies. The data reveal that IL-8 is crucial for the interaction between hepatocytes and macrophages *in vitro*. In addition, transcriptome analyses showed that a change in the ratio between macrophages and hepatocytes may trigger pro-inflammatory signalling pathways of the acute phase response and the complement system (release of, *e.g.*, certain cyto- and chemokines). Using diclofenac and LPS showed that the release of cytokines is increasing with higher ratios of MDMs. Altogether, we could demonstrate that the current co-culture system is better suited to mirror the *in vivo* situation when compared to previously established co-culture systems composed of HepG2 and differentiated THP-1 cells. Further, our data reveal that the cytokine IL-8 is crucial for the interaction between hepatocytes and macrophages *in vitro*.

Keywords: co-culture, Fa2N-4, monocyte derived macrophages, cytokine correlation network, acute phase

**Introduction**

The liver is one of the largest organs in the human body (Abdel-Misih and Bloomston, 2010). It consists of parenchymal cells (hepatocytes) and a variety of non-parenchymal cell populations such as Kupffer cells, stellate cells and endothelial cells (Kmiec, 2001).

Primary hepatocytes are well suited for the investigation of substance-specific metabolic effects. However, liver cell physiology and metabolism are characterised by large inter-individual variations and during *in vitro* cultivation cellular de-differentiation and changes of metabolic capacities occur within days (Soldatow et al., 2013). Such inter-individual differences can be excluded by using hepatic cell lines. However, these cell lines usually originate from an intravital tumour environment and thus may have altered metabolic activities (Wilkening et al., 2003).

The hepatic Fa2N-4 cell line represents an SV-40 immortalised, non-tumorigenic primary human cell line (Mills et al., 2004). Fa2N-4 cells are able to metabolise drugs like diclofenac (DCN), due to the

Novel indirect co-culture of immortalised hepatocytes with monocyte derived macrophages is characterised by pro-inflammatory cytokine networks

expression and activity of cytochrome P450-dependent monooxygenases (CYP) 2C9 (Mills et al., 2004; Ripp et al., 2006) and CYP3A4, or UDP-glucuronosyltransferases (UGT) 2B7 and UGT1A9 (Hariparsad et al., 2008). In this context, the expression, inducibility, and activity of CYP1A2, CYP2C9, and CYP3A4 were shown to be comparable between Fa2N-4 and primary hepatocytes (Hariparsad et al., 2008; Mills et al., 2004). In contrast to HepaRG cells, Fa2N-4 cells can be used immediately and no differentiation time of 2–4 weeks is required (Aninat et al., 2006; Gripon et al., 2002). Furthermore, while HepaRG cells originate from a female hepatocarcinoma (Aninat et al., 2006), Fa2N4 cells have a non-tumorigenic origin (Mills et al., 2004).

Kupffer cells are the largest population of tissue macrophages in the liver (Dixon et al., 2013) and play an important role during drug induced liver injury (DILI) (Ju and Reilly, 2012), liver regeneration (Michalopoulos, 2017) and drug metabolism (Ding et al., 2004) to name a few physiological processes. The interaction between hepatocytes, Kupffer cells and infiltrating macrophages is relevant for substance specific hepatotoxicity. In general, liver macrophages, such as Kupffer cells, appear to express markers of different macrophage lineages simultaneously (Guillot and Tacke, 2019). In the physiological human liver, a large inter-individual variability in the ratio of Kupffer cells to hepatocytes (average =  $14.5 \pm 9.1\%$ ) has been reported (Brouwer et al., 1988). Similarly, a range of 8–12% has been described by Gebhardt (1992). Kupffer cells can bind and incorporate proteins, foreign particles, bacteria, yeasts and viruses *via* endocytosis (Wardle, 1987). However, for the operability of *in vitro* models, it should be considered that the availability of primary Kupffer cells is limited and subject to a large inter-individual variability (Wu et al., 2020). Following a metabolic or toxic damage of liver tissue, a massive infiltration of blood mononuclear cells (PBMC), which differentiate into macrophages, occurs (Tacke and Zimmermann, 2014).

Many studies have shown that the *in vitro* co-cultivation of hepatocytes and Kupffer cells (or Kupffer cell-like models) can be used to characterise tissue responses upon exposure to hepatotoxic substances (Granitzny et al., 2017; Rose et al., 2016; Wewering et al., 2017b). Melino et al. (2012) were able to show that hepatocytes responded to secreted factors from differentiated THP-1 cells.

Thus, HepG2 cells are converted into an “inflammatory phenotype” (based on transcriptomic data) while growing in THP-1 conditioned medium (Melino et al., 2012). Indirect co-cultivation of HepG2 and differentiated THP-1 cells (HepG2/THP-1) is a useful *in vitro* approach to identify substances responsible for drug induced liver injury and to discriminate DILI from non-DILI substances (Granitzny et al., 2017; Padberg et al., 2020). Furthermore, HepG2/THP-1 co-culture can help to characterise the causative mechanisms of hepatotoxicity. An important effect of ketoconazole is the induction of an NRF2-mediated oxidative stress response that could be identified in HepG2/THP-1 co-culture (Wewering et al., 2017b). Other data also showed that primary co-cultures consisting of hepatocytes

## Novel indirect co-culture of immortalised hepatocytes with monocyte derived macrophages is characterised by pro-inflammatory cytokine networks

and Kupffer cells in direct contact show specific DILI-trovaflaxacin dependent hepatotoxic effect. The hepatotoxic effect is indicated by the alteration of interleukin (IL)-6 and tumour necrosis factor  $\alpha$  (TNF- $\alpha$ ) levels and CYP3A metabolic capacity (Rose et al., 2016). A recently described *in vitro* co-culture model composed of non-differentiated PBMCs in combination with HepG2 allows an identification of DILI-inducing drugs (Oda et al., 2021). Results from pro-inflammatory *in vitro* models are also known from animal models. It has been shown that moderate inflammation *in vivo* is induced by low doses of lipopolysaccharides (LPS). This lowers the threshold for adverse effects and allows the identification of DILI substances (Buchweitz et al., 2002; Deng et al., 2006; Zou et al., 2009). Since LPS is modified by Kupffer cells, which affects its toxicity, and subsequently degraded by hepatocytes (Treon et al., 1993), it is important to consider not only hepatocytes in the elucidation of compound-specific effects.

In this study we investigated a novel indirect co-culture system, based on Fa2N-4 cells in combination with blood monocyte derived macrophages (MDMs), without a LPS induced inflammation. To simulate the differences between physiological and inflammatory conditions, different Fa2N-4 to MDM ratios of 15% (Brouwer et al., 1988) and 50% were used. The ratio of 50% represent a more than three-fold increase in MDM cell numbers, which has been detected in inflammatory processes of the portal region of human liver (Karakucuk et al., 1989). With these two co-culture systems, time dependent cytokine secretion and alterations of the transcriptome were investigated. The release of cytokines, as well as the phosphorylation status of acute phase associated transcription factor p38 mitogen-activated protein kinase (p38) were determined. Based on the cytokine data, correlation networks were generated using statistical methods. The robustness was studied by using interleukin 8 neutralising antibodies ( $\alpha$ IL-8) and the TNF- $\alpha$  neutralising drug Adalimumab (AMB, EMEA/H/C/004475). Furthermore, the effects of DCN and LPS on the cytokine secretion was studied using single and co-cultures with 15% and 50% MDMs.

### **Materials and Methods**

All methods were carried out according to the manufacturer's protocol. Only modifications are described below.

#### Chemicals and antibodies

All chemicals were purchased from Sigma-Aldrich (Taufkirchen, Germany) unless stated otherwise. Dulbecco's phosphate-buffered saline (DPBS) was a product of PAN-Biotech (Aidenbach, Germany). AMB was purchased from Selleck chemicals (BIOZOL, Eching, Germany) and  $\alpha$ IL-8 was a

Novel indirect co-culture of immortalised hepatocytes with monocyte derived macrophages is characterised by pro-inflammatory cytokine networks

product of R&D Systems (Bio-Techne GmbH, Wiesbaden-Nordenstadt, Germany). The complete list of antibodies is given in table S1.

Cell culture

All following cell cultivations were conducted under treatment with 0.1% dimethyl sulfoxide (DMSO), including solvent controls. All consumables were purchased from TPP (Trasadingen, Switzerland). Microscopic images were taken with an Observer.A1 microscope (LD Plan Neoflua 40×/0.60) from Zeiss (Jena, Germany). Cell cultivation and incubation was performed at 37 °C and 5% CO<sub>2</sub>. Penicillin (100 U/ml), 100 µg/ml streptomycin, and 2 mM L-glutamine were added to all cell culture media. Further additives are listed in the cultivation conditions of the individual cells below.

Hepatocyte cultures

The SV-40 immortalised hepatocytes (Fa2N-4) were purchased from SEKISUI-XenoTech (tebu-bio, Offenbach, Germany). After thawing, Fa2N-4 cells were seeded at a density of  $2 \times 10^5$  cells per cm<sup>2</sup> and cultivated in Williams E (PAN-Biotech, Aidenbach, Germany) containing 10% (v/v) FCS, 100 nM dexamethasone, and 10 µg/ml recombinant human insulin. After 4 h the culture medium was replaced by Williams E containing 100 nM dexamethasone and 10 µg/ml recombinant human insulin for 24 h.

Monocyte isolation and differentiation into macrophages (MDMs)

Human buffy coats were obtained from anonymised donors, with their consent (votum of the ethics committee: EA4/071/13), from the blood bank (Deutsches Rotes Kreuz, Berlin, Germany). PBMCs were isolated from buffy coats based on the Ficoll® Plaque Plus density gradient centrifugation (450 xg, 35 min, 20 °C). Then, PBMCs were collected at the interphase, followed by three washing steps and a centrifugation at 200 xg with autoMACS Running Buffer (Miltenyi Biotec, Bergisch Gladbach, Germany) at 4 °C to carefully remove the thrombocytes. Monocytes were separated due to the adhesion-properties of the cells. Therefore, the PBMCs were resuspended in RPMI (PAN-Biotech, Aidenbach, Germany) containing 10% (v/v) FCS and incubated for 1 h at a density of  $0.8 \times 10^6$  cells per cm<sup>2</sup>. After careful removal of all non-adhered cells, differentiation to MDMs was started using RPMI containing 10% (v/v) FCS and 25 ng/ml macrophage-colony-stimulating factor (M-CSF) over six days with a medium change every two days. After the differentiation, all non-adherent cells were removed by washing with DPBS. The MDMs were detached using 10 mM EDTA in DPBS for 30 min at 4 °C.



## Novel indirect co-culture of immortalised hepatocytes with monocyte derived macrophages is characterised by pro-inflammatory cytokine networks

### Co-cultivation

MDMs were seeded either into the well directly (for the single-cultivation) or into the Falcon® cell culture inserts (VWR, Darmstadt, Germany) for the co-cultivation using Williams E medium, supplemented with 100 nM dexamethasone and 10 µg/ml recombinant human insulin. The 50% and 15% MDMs corresponded to a density of  $1 \times 10^5$  and  $0.3 \times 10^5$  cells per  $\text{cm}^2$ , respectively. After 24 h, the media of MDMs and Fa2N-4 was replaced with Williams E supplemented with 10 µg/ml recombinant human insulin and the MDMs containing cell culture inserts were inserted into the Fa2N-4 culture well. This represents the time point 0. Culture medium with 0.1% DMSO was used as control and cultivated alike to the samples.

### HepG2/THP-1 co-cultivation

HepG2 and THP-1 cells were grown in RPMI supplemented with 10% (v/v) FCS. Single culture THP-1 cells were supplemented additionally with 1 mM sodium pyruvate and 10 mM HEPES. The co-culture was established using Falcon® cell culture inserts (VWR, Darmstadt, Germany) according to Wewering et al. (2017a). HepG2 cells were seeded at a density of  $1.3 \times 10^5$  cells per  $\text{cm}^2$ . THP-1 cells were differentiated by 100 nM phorbol 12-myristate 13-acetate (PMA) for 24 h and were seeded at a density of  $0.65 \times 10^5$  cells (corresponding to a density of 50%) or  $0.2 \times 10^5$  (representing a density of 15%) per  $\text{cm}^2$ .

### Cytotoxicity testing

Cytotoxicity was assessed by measuring the activity of the adenylate kinase (AK) in the supernatant using the ToxiLight™ assay (Lonza, Basel, Switzerland). LDH activity in the supernatant was measured using the Cytotoxicity Detection Kit (Roche, Basel, Switzerland). In addition, the MTT Assay was performed according to Mosmann (1983) followed by cell lysis with DMSO. All values were corrected for the DMSO (0.1%) solvent controls.

### RNA isolation procedure

RNA was isolated using the NucleoSpin® RNA Kit (Machery-Nagel, Düren, Germany) according to the manufacturer's protocol.

### Microarray analyses

All samples (RNA integrity number (RIN) >8.5) were analysed using a Human Clariom™ S Assay (Applied Biosystems, Foster City, CA, USA). Further information is provided in the supplementary section.

Novel indirect co-culture of immortalised hepatocytes with monocyte derived macrophages is characterised by pro-inflammatory cytokine networks

Microarray data have been deposited in the Gene Expression Omnibus (GEO) database, [www.ncbi.nlm.nih.gov/geo](http://www.ncbi.nlm.nih.gov/geo) (accession no. GSE156627).

Flow-cytometry analyses

FACS-buffer (1% FCS, 0.2 mM EDTA in DPBS) was used for all washing and incubation steps at 4 °C. After staining with LIVE/DEAD™ Fixable Near-IR Dead Cell Stain Kit (Thermo Scientific, Waltham, MA, USA) the cells were fixed with Roti®-Histofix 4% (Roth, Karlsruhe, Germany) for 10 min. The functional antibody or the corresponding isotype controls were diluted in FACS-buffer, applied to the cells and incubated at 4 °C for 15 min. Fluorescence intensities were measured with the FACS Aria III (BD Biosciences, Heidelberg, Germany) with the following settings: PE channel: 585/42 nm, FITC channel: 530/30, APC channel: 660/20, BV421 channel: 450/40, Alexa Fluor 700 channel: 730/45, PerCP channel: 695/23, live/dead channel: 780/60 and generated data were analysed with the FlowJo v 10 software (FlowJo LLC, Ashland, OR, USA).

Cytokine measurements

Cytokines in the supernatant were quantified using the Cytokine LEGENDplex™ system (Biolegend, San Diego, CA, USA), including the Inflammation Panel 1 (IL-1 $\beta$ , TNF- $\alpha$ , MCP-1, IL-6, IL-8, IL-10, IL-12, IL-18) and the Custom Human Assay (TGF- $\beta$ 1, GM-CSF, G-CSF, FGF, CCL3, CCL20, HGF, TGF- $\alpha$ ). The results were analysed using LEGENDplex™ 8.0 software (Biolegend, San Diego, CA, USA).

Western blot analysis

Cells were lysed at 4 °C in RIPA buffer (50 mM Tris/HCl (pH 7.4), 159 mM NaCl, 1 mM EDTA, 1% Igepal®, 0.25% sodium deoxycholate) supplemented with a protease inhibitor cocktail (Merck, Darmstadt, Germany), composed of 200  $\mu$ M phenylmethylsulfonyl fluoride and 1 mM sodium orthovanadate. Protein concentrations were determined with the Pierce™ BCA Protein Assay Kit (Thermo Scientific, Waltham, MA, USA), and equal amounts of protein were applied to SDS-PAGE and, after separation, transferred to nitrocellulose membranes. After binding of primary antibodies (16 h at 4 °C), the secondary antibody (horseradish peroxidase labelled) was added for 1 h, and the staining was visualised with Pierce ECL Substrate (Thermo Fisher Scientific, Waltham, MA, USA) using a ChemiDoc XRS (Bio-Rad, Munich, Germany). The signal intensity was normalised to the loading control  $\beta$ -actin and then the ratio of phosphorylated (P) to total p38 protein was calculated.

Novel indirect co-culture of immortalised hepatocytes with monocyte derived macrophages is characterised by pro-inflammatory cytokine networks

Data pre-processing and analysis

All time-resolved data of cytokine concentrations in the supernatant were used for the correlation network analysis. The correlation uses individual replicates and not mean values since the data are paired over both time points and replicates, *i.e.* for a given time point the values of all cytokines originate from the same sample. Data compilation and network generation were performed using the statistical language and environment R (version 3.6.3) (R Core Team, 2018). In detail, in a first step all values below their lower detection limit were set to the half value of that detection limit. Subsequently, all values were log-transformed. Individual samples were grouped (time point 0 h belonging to all groups) with respect to their conditions *i.e.* to either single or one of the co-cultures later becoming individual networks. In particular, for the MDM culture as well as the co-culture the data of the different macrophage ratios (15% and 50%) were combined. Within these data groups for each pair of cytokines, their correlation coefficients and respective p-values were determined by Spearman rank correlation. The p-values were adjusted according to Benjamini-Hochberg.

Subsequently, a filter was applied to all pairwise connections with respect to the p-value (significant for  $p \leq 0.05$ ) as well as the correlation coefficient (threshold of  $\rho \leq -0.2$  and  $\rho \geq 0.6$  according to coefficients' distribution and confidence intervals). The remaining connections after filtering were employed to visualise the respective non-directed correlation networks.

Data shown are based on at least three independent biological replicates. Means, standard deviations and ANOVA p-values followed by Bonferroni correction were calculated with GraphPad Prism 6 (Statcon, Witzenhausen, Germany). The Z-scores were calculated and visualised with Perseus Software (Tyanova et al., 2016). The Z-score was based on the mean values of the individual cytokine concentrations (values below their lower detection limit were set to the half value of that detection limit) in the corresponding cultivations. Venn diagrams were created using jvenn (Bardou et al., 2014). Volcano-plots were created using Transcriptome Analysis Console (TAC), version 4.0.1.36 (Applied Biosystems, Foster City, CA, USA). Significant ( $p < 0.05$ ) gene expressions were analysed using Ingenuity® Pathway Analysis (IPA) software (Qiagen, Aarhus, Denmark). Furthermore, only those pathways embedded in the IPA software, that were assigned to liver and immune cell associated pathways, were included in the analysis.

Novel indirect co-culture of immortalised hepatocytes with monocyte derived macrophages is characterised by pro-inflammatory cytokine networks

**Results**

Macrophage derived monocytes express specific markers

During differentiation, characteristic morphological changes of the round shaped PBMCs to elongated fibroblast-like MDMs became obvious (Fig. 1 A). We determined typical macrophage markers and compared those with markers of T-, B- and dendritic cells. About 26% of the PBMCs were CD14<sup>+</sup> monocytes and therefore potential macrophage precursors. Almost all (>90%) MDMs were positive for typical macrophage markers (CD83, CD14, CD86, toll-like receptor 4 (TLR4), human leukocyte antigen-DR isotype (HLA-DR) and CD163). Only 28% of the MDMs were also CD209<sup>+</sup>, being a marker for dendritic cells and M2 macrophages. Furthermore, CD3<sup>+</sup> cells, characteristic for T-cells, were only present before the differentiation of PBMCs (Fig. 1 C). Altogether, these surface markers indicated a successful differentiation of the PBMCs to MDMs. A co-culture system composed of these MDMs and the hepatic cell line Fa2N-4 was then developed. The viability of the two cell populations was found to be unaffected by the co-culture condition, since no increased release of the cytoplasmic marker adenylate kinase (AK) was measurable in the supernatant of the cell culture. Even an increase in the ratio of MDMs from 15% to 50% resulted in no changes of the AK level in the supernatant (Fig. 1 B).

Novel indirect co-culture of immortalised hepatocytes with monocyte derived macrophages is characterised by pro-inflammatory cytokine networks

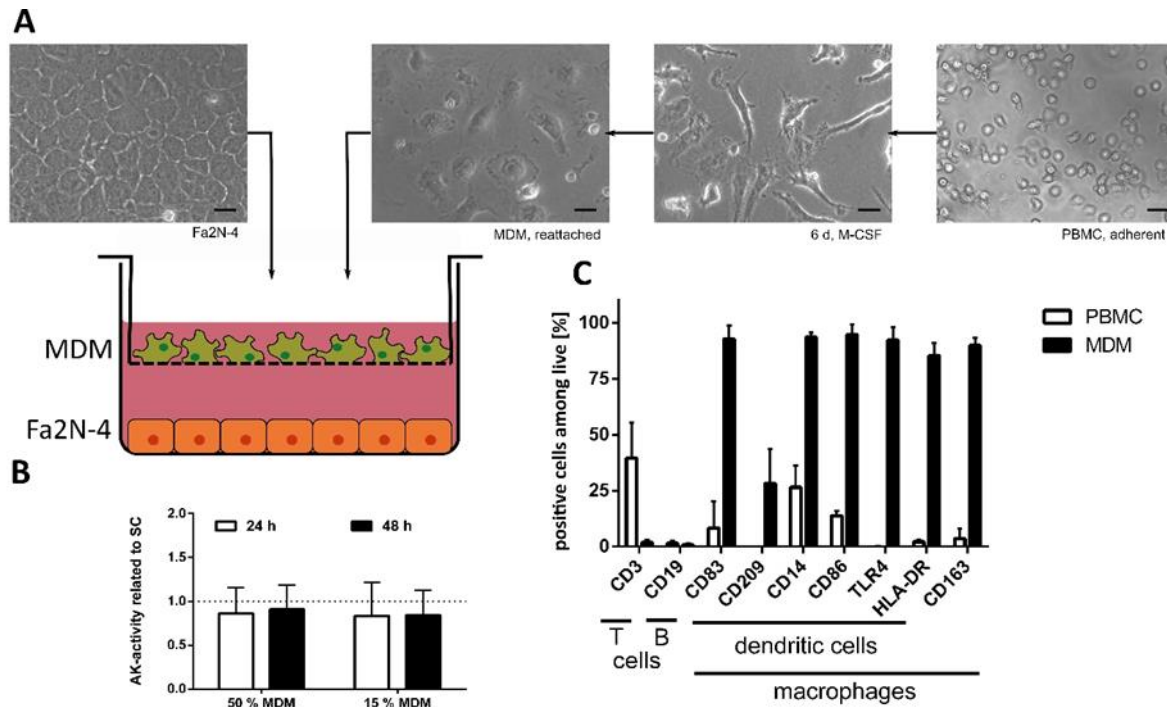


**Figure 1:** Set-up of the co-culture, cytotoxicity and expression of cell specific surface markers. **(A)** Images of the Fa2N-4 cells and of the differentiation process from peripheral blood mononuclear cells (PBMC) after 6 d of differentiation with 25 ng/ml of macrophage colony stimulating factor (M-CSF) to monocyte derived macrophages (MDMs). The scale bar denotes 20  $\mu$ m. **(B)** Toxicity of physiological (15 %) and pro-inflammatory (50 %) ratios of MDM-to-Fa2N-4 cells were tested. The dotted line represents the reference (single culture, SC) of the adenylate kinase (AK) in the supernatant. **(C)** The presence of CD163, toll-like receptor 4 (TLR4) and human leukocyte antigen - DR isotype (HLA-DR) indicated a successful differentiation of the PBMCs into MDMs. n=3, bars represent mean  $\pm$  SD

Culture conditions affect Fa2N-4 gene expression

Next, changes of the Fa2N-4 gene expression in the co-culture (relative to the individual culture) were determined at two different time points (24 h and 48 h) and two different ratios of MDMs (15% and 50%). The physiological conditions were simulated with a co-culture consisting of 15% MDMs (CC 15%) and for inflammatory conditions a co-culture with 50% MDMs (CC 50%) was used.

In general, the total number of differential expressed genes was independent of the number of macrophages (Fig. 2 A). Microarray data indicated that 357 genes were significantly ( $p < 0.05$ ) differentially regulated during physiological co-cultivation (CC 15%) and 419 genes during inflammatory co-cultivation (CC 50%) after 24 h (Fig. 2 B). A prolongation of the cultivation time to 48 h resulted in about 30% more significantly expressed genes in both co-cultures, compared to single cultivated Fa2N-4 cells (Fig. 2 B). Among all genes pro-inflammatory signalling pathways took a

Novel indirect co-culture of immortalised hepatocytes with monocyte derived macrophages is characterised by pro-inflammatory cytokine networks

central role, especially in the CC 50% after 24 h. Under these conditions, we were able to identify the signalling pathways of the “complement system” and the “acute phase response signalling” (Fig. 2 C) as top two of all regulated pathways. A total of 16 signalling pathways are marked as significantly regulated ( $p < 0.05$ ). The gene lists of exclusively significant genes of the CC 50% (567 genes) after 24 h were used for the pathway analyses. In the CC 50% after 24 h, 18% of significantly regulated genes could be attributed to “complement system signalling” and showed a high probability of regulation ( $p < 0.01$ ). The “acute phase response signalling” was also identified, with lower ratios (up to 9%) but with partially higher probabilities of  $p < 0.001$  (Fig. 2 C) and 21% of the expected associated target gene expression. After an incubation time of 48 h we were able to identify other signalling pathways like neuroinflammation and T-helper cell associated pathways. We did not consider these pathways in further analysis, since they were not related to hepatic pathophysiology and contain no or only 9% of the expected associated target gene expressions.

Novel indirect co-culture of immortalised hepatocytes with monocyte derived macrophages is characterised by pro-inflammatory cytokine networks

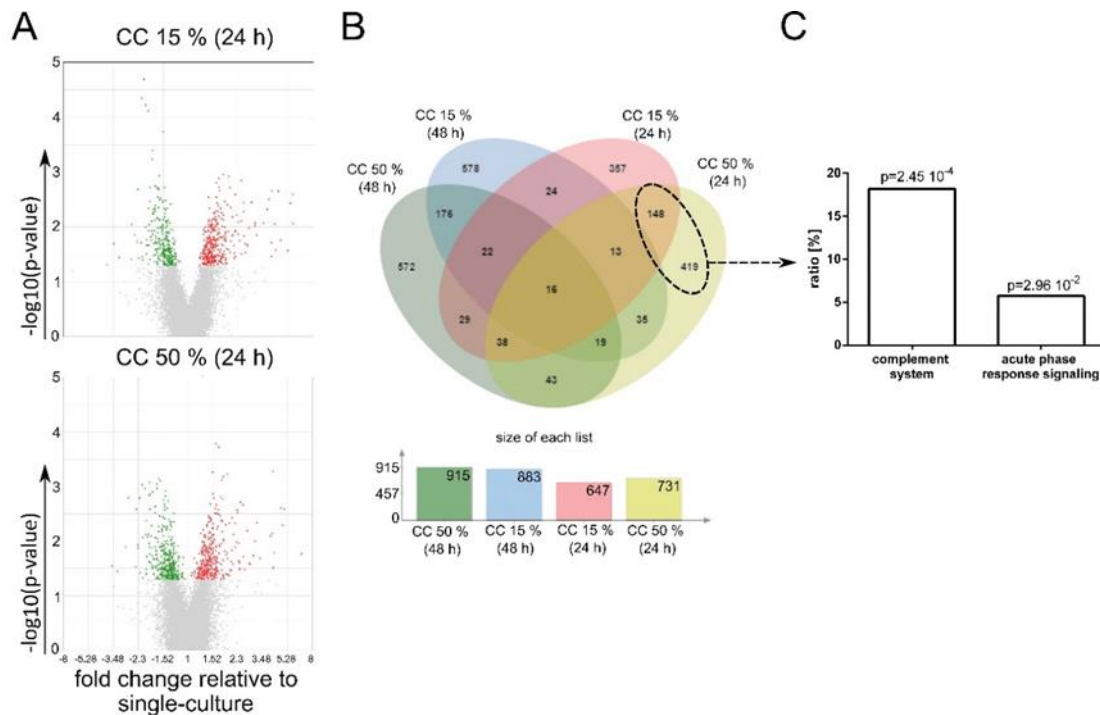


**Figure 2:** Microarray analysis reveals time- and MDM-dependent differences in the gene expression of Fa2N-4 cells. Fa2N-4 cells were co-cultivated with monocyte derived macrophages (MDMs). Physiological (CC 15 %) and pro-inflammatory (CC 50 %) conditions were studied and related to the corresponding single cell culture of Fa2N-4 cells (n=3). **(A)** Volcano-plots included all significantly upregulated (red) and downregulated (green) genes of the CC 15 % and CC 50 % after 24 h. The significance was set to  $p < 0.05$  ( $\log_{10}(p) > 1.3$ ). **(B)** Venn diagram and the size of each gene list of significantly ( $p < 0.05$ ) expressed genes based on microarray analysis. Different MDM ratios and cultivation times (24 h or 48 h) resulted in specific expression patterns. **(C)** Significantly regulated genes of the pro-inflammatory signalling pathways "complement system" and "acute phase response" in relation to all genes involved (ratio) and their respective p-value (after 24 h) of expressed genes of the CC 50 %.

In summary, inflammatory signalling pathways are activated within 24 h during co-cultivation.

An acute phase transcription factor is phosphorylated

Especially in the CC 50 %, our transcriptome analysis indicated a major role for the acute phase response signalling.

Therefore, the phosphorylation of the transcription factor p38 was studied. The relative phosphorylation (P-p38/p38) was  $0.8 \pm 0.1$  in Fa2N-4 cells,  $2.0 \pm 0.4$  in the CC 15% and  $1.5 \pm 0.3$  CC 50% after 4 h of co-cultivation (Fig. 3).

Novel indirect co-culture of immortalised hepatocytes with monocyte derived macrophages is characterised by pro-inflammatory cytokine networks

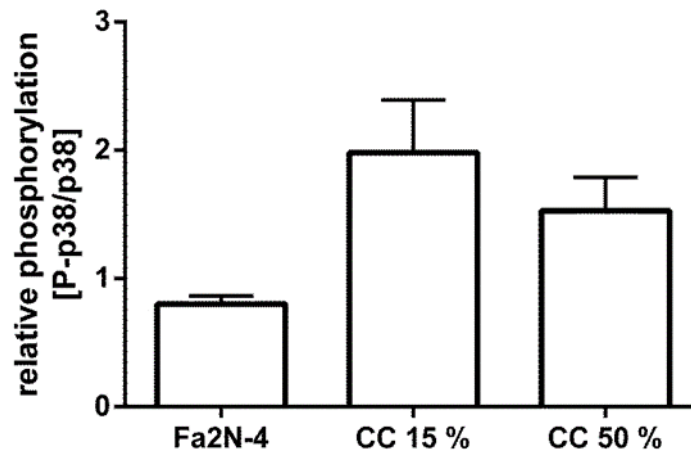


**Figure 3:** Semi-quantitative western blot analysis of phosphorylation of the transcription factor p38. Western blot analysis Fa2N-4 cells with (“CC”) and without MDMs after 4 h. Physiological (15 %, n= 3) and pro-inflammatory (50 %, n=3) MDM numbers were used. (n=2). Shown are the mean and the SD of the culture dependent phosphorylation of p38 mitogen-activated protein kinase (p38) in Fa2N-4 cells. Figure S2 shows a representative blot.

In summary, the indirect co-cultivation of Fa2N-4 and MDM (Fa2N-4/MDM) cells results in the phosphorylation of the transcription factor p38.

Cytokine secretion depends on the culture conditions

Next, we analysed the time-dependent release of cytokines in the co-cultures (Fig. 4). In contrast to MDMs, secreted cytokines of Fa2N-4 cells accumulated after 48 h of cultivation (Fig. 4 A). The majority of cytokines showed a steep increase in single cell cultivated Fa2N-4 cells and during co-cultivation after 48 h. However, hepatocyte growth factor (HGF), transforming growth factor (TGF)- $\alpha$ , TNF- $\alpha$ , IL-10, and IL-12 showed no clear time-dependent accumulation (Fig. 4 A, g, h, j, n, o). In general, co-cultures showed increased absolute levels of cytokine secretion. Among others, the concentration of fibroblast growth factor (FGF) in co-culture reached up to 7532.5 pg/ml in CC 15% after 48 h and IL-8 reached up to 892.3 pg/ml in CC 50% after 48 h. The absolute concentration of IL-6 in the co-culture was 200-fold higher compared to the single cultures with a maximum concentration of 892.3 pg/ml (Fig. 4 A).



Novel indirect co-culture of immortalised hepatocytes with monocyte derived macrophages is characterised by pro-inflammatory cytokine networks

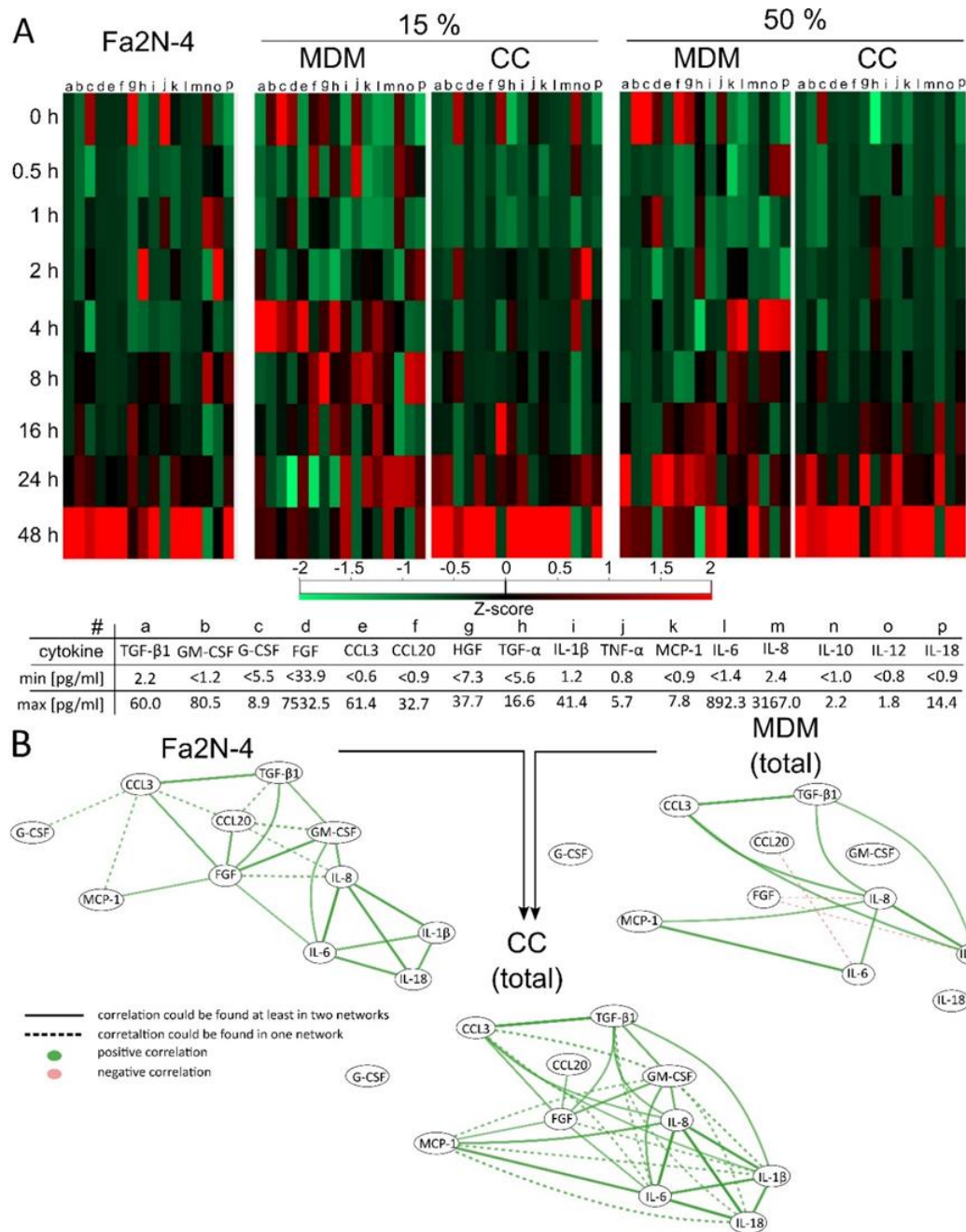


**Figure 4:** Effect of co-culture on cytokine secretion and its temporal progression. Fa2N-4 cells were co-cultivated with monocyte derived macrophages (MDMs) for 48 h. Physiological (15 %) and pro-inflammatory (50 %) MDM numbers were used. **(A)** Heatmaps of the time-dependent cytokine concentration in the supernatant included the Z-score of the means within one row of the heatmap. Letters (a-p) indicate the individual cytokines. Only the lowest (min) and highest (max) cytokine concentrations are shown (complete data are given in table S2). **(B)** The time-dependent concentrations were used for the generation of correlation networks. Solid lines (—) indicate that these correlations occur in the co-culture network and in at least one of the single cultivation networks. Dotted lines (---) identify additional correlations occurring in the respective network. A positive correlation is labelled green and a negative correlation is labelled red. The data were generated from three independent experiments.

Novel indirect co-culture of immortalised hepatocytes with monocyte derived macrophages is characterised by pro-inflammatory cytokine networks

In summary, most of the investigated cytokines accumulated in cultures consisting of Fa2N-4 cells only and in the co-cultures of Fa2N-4/MDMs after 48 h (Figure 4 A).

Correlation networks visualise the relationship between secreted cytokines

Next, a statistical approach was used to identify significant Spearman correlations (indicated by respective correlation coefficients and p-values) between cytokine concentration values (Fig. 4 B). The co-cultures CC 15% and CC 50% were combined, because it is assumed that the behaviour of each of the single cultures and the co-culture is structurally the same but that the two ratios lead to different inflammatory states represented by respective cytokine concentrations. The correlation network indicated that the chemokine (C-C motif) ligand (CCL) 20 played a central role in the individual cultivation of Fa2N-4 cells, since correlations exist to five other cytokines: CCL3, FGF, TGF- $\beta$ 1, granulocyte-macrophage colony-stimulating factor (GM-CSF), and IL-8. The secretion of FGF seemed to be also important in the Fa2N-4 associated correlation network. Six FGF-dependent correlations were identified in the Fa2N-4 single cell cultivations and in the co-cultivations with MDMs. While CCL20-FGF showed significant correlation in co-culture, the central cytokine in this network was IL-8, which was correlated to seven other cytokines. Interestingly, IL-8 differed in terms of correlation between the individual cultures and co-cultivations. However, all of the IL-8 connections in the co-cultivation network could be found in at least one of the single cultivation networks. Among the correlations of IL-8 in the co-cultivation network, the one to IL-6 was the strongest based on its correlation coefficient (table S3). Strikingly, the connection between IL-8 and FGF showed opposing correlation in the individual networks: positive for Fa2N-4 and negative for MDM cells (Fig. 4 B). Further, there were some other connections that showed differences between the MDMs and the co-cultivation network: another change in its direction occurred between FGF and IL-1 $\beta$ . Finally, there were FGF correlations that cannot be found in the MDM network but occur in co-cultivation (FGF-TGF- $\beta$ 1, FGF-CCL3, and FGF-MCP-1).

In summary, cytokine secretion in co-culture was more complex and correlations between the cytokines changed when compared to single cultures. Therefore, the correlation network of the co-culture did not represent a simple merge of the Fa2N-4 and MDM networks but showed additional cytokine interactions between the two cell types.

Since inflammatory processes seemed to dominate after 48 h (Fig. 4), all further investigations were performed at the time point of 24 h of cultivation. To investigate the central role of IL-8 in the co-culture, further studies were conducted in the presence of  $\alpha$ IL-8.

Novel indirect co-culture of immortalised hepatocytes with monocyte derived macrophages is characterised by pro-inflammatory cytokine networks

$\alpha$ IL-8 affects the cytokine release

The neutralising antibody  $\alpha$ IL-8 was used to investigate the role of IL-8 in the correlation network and to study how its reduction/elimination affects the outcome. For this purpose we added  $\alpha$ IL-8 (100 ng/ml) to all samples. An acute toxic effect of  $\alpha$ IL-8 was excluded by analysing the LDH activity in the cell culture supernatant (*cf.* figure S1).

To investigate the effects of  $\alpha$ IL-8 treatment on the secreted cytokines, we determined the total cytokine concentration in the supernatant (table S2) after 24 h, which was normalized to the control (Fig. 5A). The  $\alpha$ IL-8 treatment led not only to a reduction of the average concentration of IL-8, but also diminished the monocyte chemoattractant protein 1 (MCP-1) in all cultivations (Fig. 5 A). FGF was reduced in the supernatant of Fa2N-4 cells, however the MDM cells secreted more FGF under the influence of  $\alpha$ IL-8. Additionally, HGF was secreted only in the single cultures (Fa2N-4 and MDM cells, respectively). In contrast, treatment with  $\alpha$ IL-8 induced GM-CSF secretion only in the co-cultivation system. CCL20 secretion due to  $\alpha$ IL-8 treatment was detected in the Fa2N-4 cells.

Novel indirect co-culture of immortalised hepatocytes with monocyte derived macrophages is characterised by pro-inflammatory cytokine networks

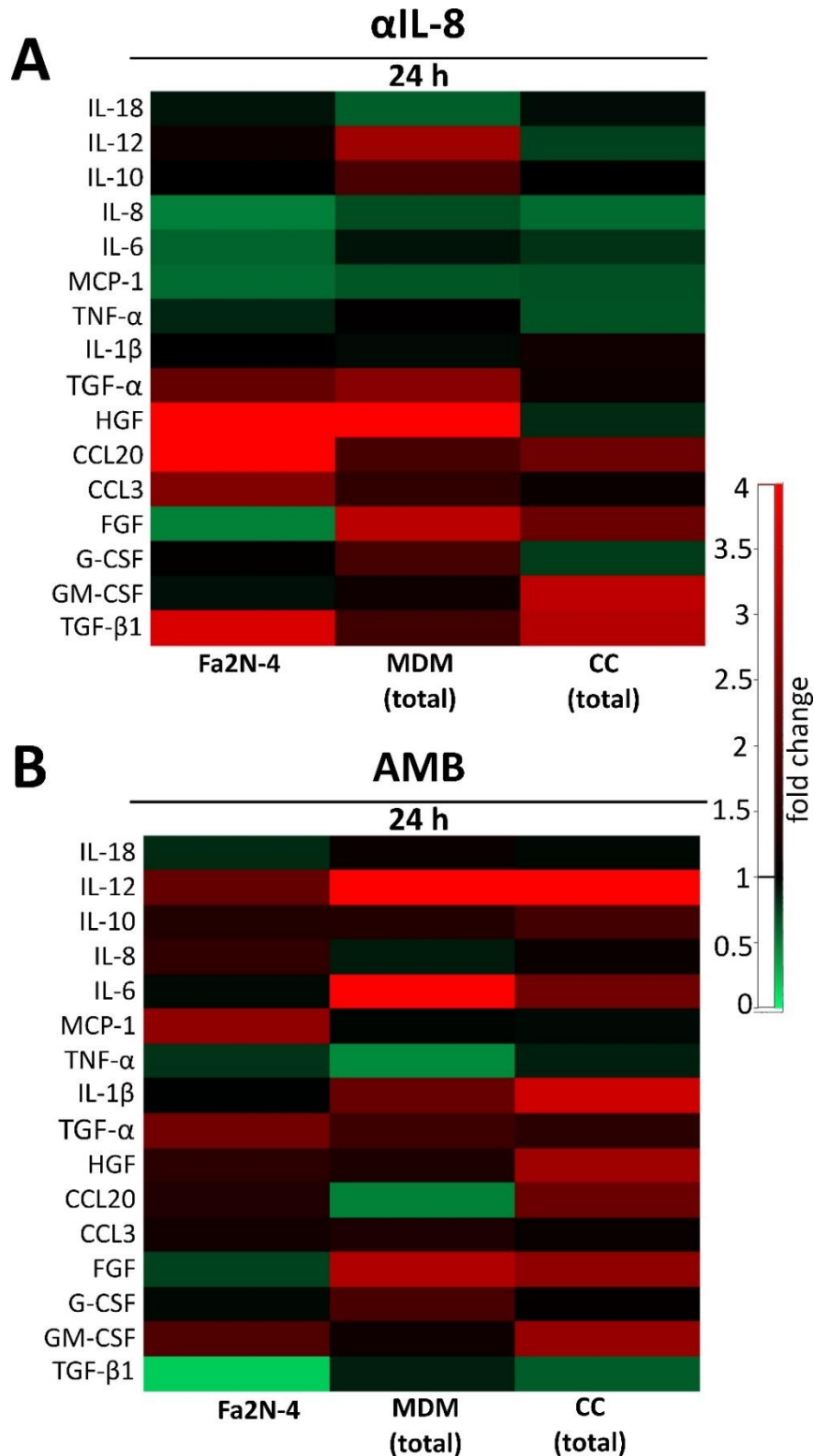


**Figure 5:** Analysis of  $\alpha$ IL-8- and TNF- $\alpha$ -specific alterations of the cytokine secretion pattern. Fa2N-4 cells were co-cultivated (CC) with monocyte derived macrophages (MDMs) for 24 h. Physiological (15 %) and pro-inflammatory (50 %) MDM-to-Fa2N-4 ratios were used. All measured cytokine concentrations were related to the corresponding control (fold change) to analyse **(A)** the IL-8 neutralising antibody ( $\alpha$ IL-8, 100 ng/ml) specific effect and **(B)** the TNF- $\alpha$  neutralising effect of Adalimumab (AMB, 500 ng/ml).

Novel indirect co-culture of immortalised hepatocytes with monocyte derived macrophages is characterised by pro-inflammatory cytokine networks

In summary,  $\alpha$ IL-8 treatment provoked specific changes in the cytokine secretion pattern, thus supporting the certain role of IL 8 in inflammatory cytokine networks of hepatic cells.

Adalimumab treatment alters the secretion of cytokines

Adalimumab (AMB) was used to study the effect of a decreased tumour necrosis factor  $\alpha$  (TNF- $\alpha$ ) concentration on the correlation network.

The concentration of TNF- $\alpha$  after treatment with AMB was in the range of 1.7 pg/ml  $\pm$  0.2 to 5.5 pg/ml  $\pm$  3.2 after 4 h (data not shown) and in the range of 1.6 pg/ml  $\pm$  0.7 to 4.0 pg/ml  $\pm$  1.1 after 24 h, respectively. In the untreated cell culture, TNF- $\alpha$  showed no significant correlation to changes of the levels of other cytokines (Fig. 4 B). Upon treatment of the cultures with AMB, a role of TNF- $\alpha$  in the co-culture system could be identified (Fig. 5 B). Twenty-four hours after addition of AMB to the co-culture, an increased secretion of cytokines, present in the afore depicted correlation network (*e.g.* GM-CSF, CCL20, FGF, IL-1 $\beta$ ) was determined (up to 3.4-fold) compared to the corresponding controls. In addition, treatment resulted in a reduced IL-6 secretion (0.7-fold) similar to TGF- $\beta$ 1 (0.6-fold) (Fig. 5 B). In the single culture of Fa2N-4 cells, a reduction of TGF- $\beta$ 1 and FGF (0.2-fold and 0.7-fold) occurred, while MCP-1 secretion increased 2.7-fold after 24 h (Fig. 5 B). In the single cultivated MDMs, the cytokine CCL20 decreased (0.5-fold), while the concentration of IL-6 increased (8.6-fold) after 24 h of AMB treatment (Fig. 5 B).

In summary, treatment with the TNF- $\alpha$  neutralising AMB leads to major changes in the cytokine secretion.

Treatment with diclofenac and lipopolysaccharide leads to changes in cytokine secretion depending on the inflammatory status.

The Fa2N-4/MDM were treated with the non-steroidal drug DCN and with LPS. In order to exclude acute toxic effects, 5 % of the effective concentration (EC<sub>5</sub>) was calculated for DCN, using the MTT assay (figure S3) and LPS, using the LDH assay (figure S4). Concentrations of 157  $\mu$ M for DCN and 100 ng/ml for LPS were used in further experiments. Figure 6 gives an overview of the treatment dependent cytokine secretion at different cultivations. In contrast to the untreated co-cultures (*cf.* figure 4) the drug treatment resulted in a higher release of cytokines.

Novel indirect co-culture of immortalised hepatocytes with monocyte derived macrophages is characterised by pro-inflammatory cytokine networks

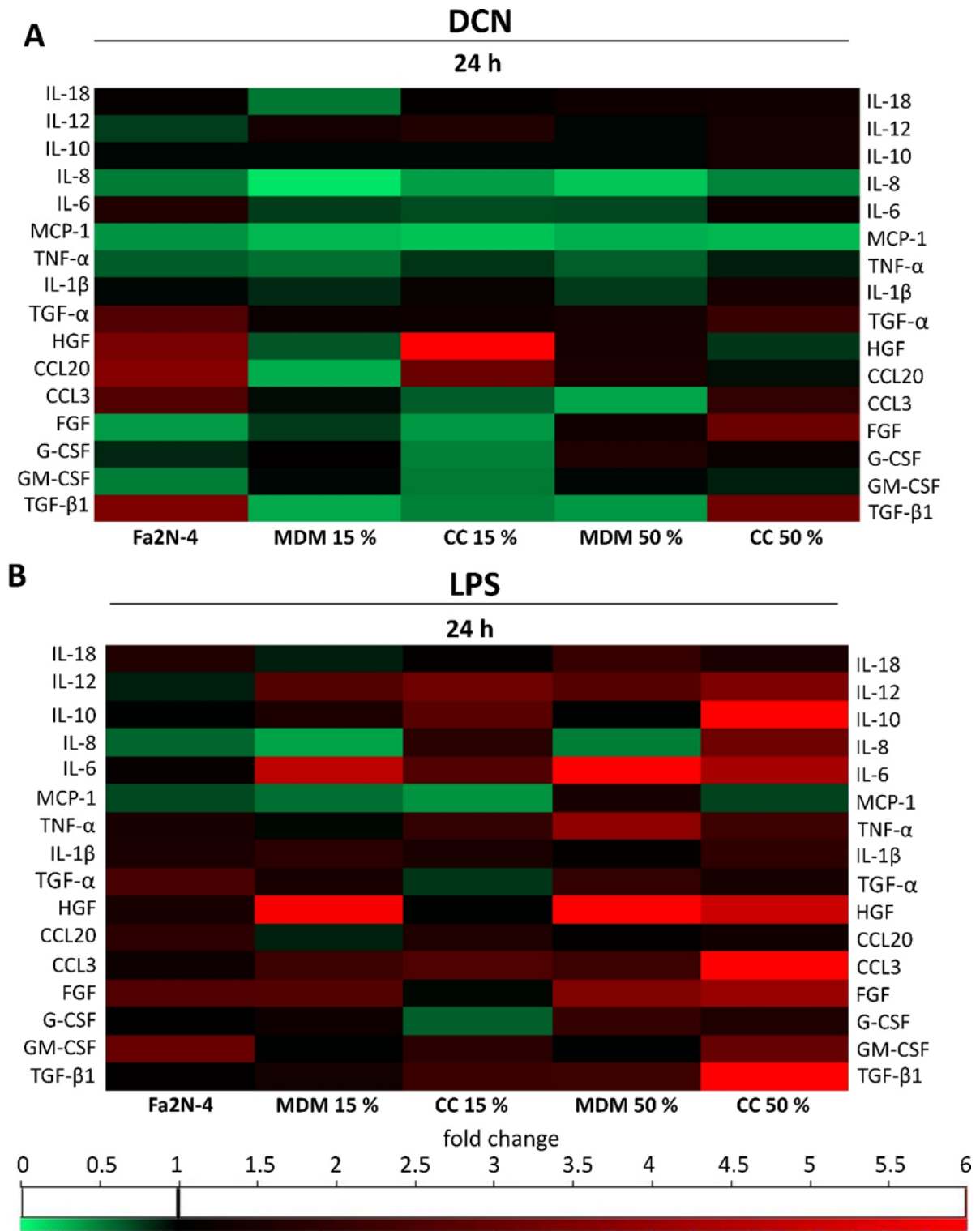


**Figure 6** Analysis of DCN and LPS specific alterations of the cytokine secretion pattern. Fa2N-4 cells were co-cultivated (CC) with monocyte derived macrophages (MDM) for 24 h. Physiological (15 %) and pro-inflammatory (50 %) MDM to Fa2N-4 ratios were used. All measured cytokine concentrations were related to the corresponding control (fold change) to analyse (A) the diclofenac (DCN, 157  $\mu$ M) and (B) lipopolysaccharides (LPS, 100 ng/ml). Data are based on three biological replicates. For visualisation a cut-of value of 6-fold was chosen. The particular fold changes are given in table S4.

### Novel indirect co-culture of immortalised hepatocytes with monocyte derived macrophages is characterised by pro-inflammatory cytokine networks

Fig. 6 summarizes the different co-cultivation conditions in order to compare the treatment-related effects in relation to the inflammatory status (*e.g.* 15% MDMs and 50% MDMs). In general, treatment with 157  $\mu$ M DCN lead to a reduction in cytokine secretion in the CC 15% compared to the control (Fig. 6 A). Only selected cytokines such as HGF and CCL20 in the single culture of Fa2N-4 as well as TGF- $\beta$ 1 and FGF in the pro-inflammatory co-culture (CC 50%) showed an increase in secretion compared to the control. The pattern is different in LPS treated cultures (Fig. 6 B). After 24 h, a clear increase in secretion of nine cytokine can be detected; most prominently in the pro-inflammatory (CC 50%) co-culture culture. The concentration of the cytokines IL-10, IL-8, IL-6, HGF, CCL3, FGF, and TGF- $\beta$ 1 are higher compared to the control and, except for IL-6 and HGF, also in the corresponding single cultivation of MDMs (MDM 50%).

It can be concluded that the co-culture (CC 15%) under the influence of DCN leads to reduced cytokine secretion, whereas individual cytokines are increasingly secreted in the pro-inflammatory co-cultivation with 50% MDMs. A similar increased cytokine secretion can be observed after LPS treatment of the pro-inflammatory CC 50%.

### Comparison of cytokine profiles in FA2N-4/MDM and HepG2/THP-1 co-cultures

The newly established indirect co-cultivation of Fa2N-4 and MDM (Fa2N-4/MDM) cells was compared with already established similar systems. For this purpose we selected the co-culture model consisting of HepG2 and PMA-differentiated THP-1 (Padberg et al., 2020; Padberg et al., 2019). For better comparability, the HepG2/THP-1 cells were cultivated in similar numbers as the Fa2N-4/MDM cells. Subsequently, the same cytokines were measured in the supernatant at the same time intervals and a correlation network was calculated. In general, HepG2 cells formed a much less complex correlation network of cytokines than Fa2N-4 cells and THP-1 cells form a more complex network compared to MDMs.

Networks for Fa2N-4/MDM and HepG2/THP-1 co-cultivation were based on similar cytokines (Fig. 7 and Fig. 4 B). However, the cytokines TGF- $\beta$ 1, FGF and IL-6 played a minor role in HepG2/THP-1 co-cultivation compared to Fa2N-4/MDM co-cultivation. Yet, correlations of TNF- $\alpha$  and TGF- $\alpha$  were detectable in HepG2/THP-1 co-cultivation (Fig. 7). In addition, HepG2/THP-1 co-cultivation revealed a correlation between interleukin 1 $\beta$  (IL-1 $\beta$ ) and interleukin 18 (IL-18). All other correlations were also present in either the THP-1 or the HepG2 single culture networks. In the co-culture the results obtained looked like some sort of addition of the THP-1 and HepG2 networks (Fig. 7). Altogether, the cytokine network found in the Fa2N-4/MDM co-culture (Fig. 4 B) was more complex, compared to the network detected in HepG2/THP-1 co-culture (Fig. 7).

Novel indirect co-culture of immortalised hepatocytes with monocyte derived macrophages is characterised by pro-inflammatory cytokine networks

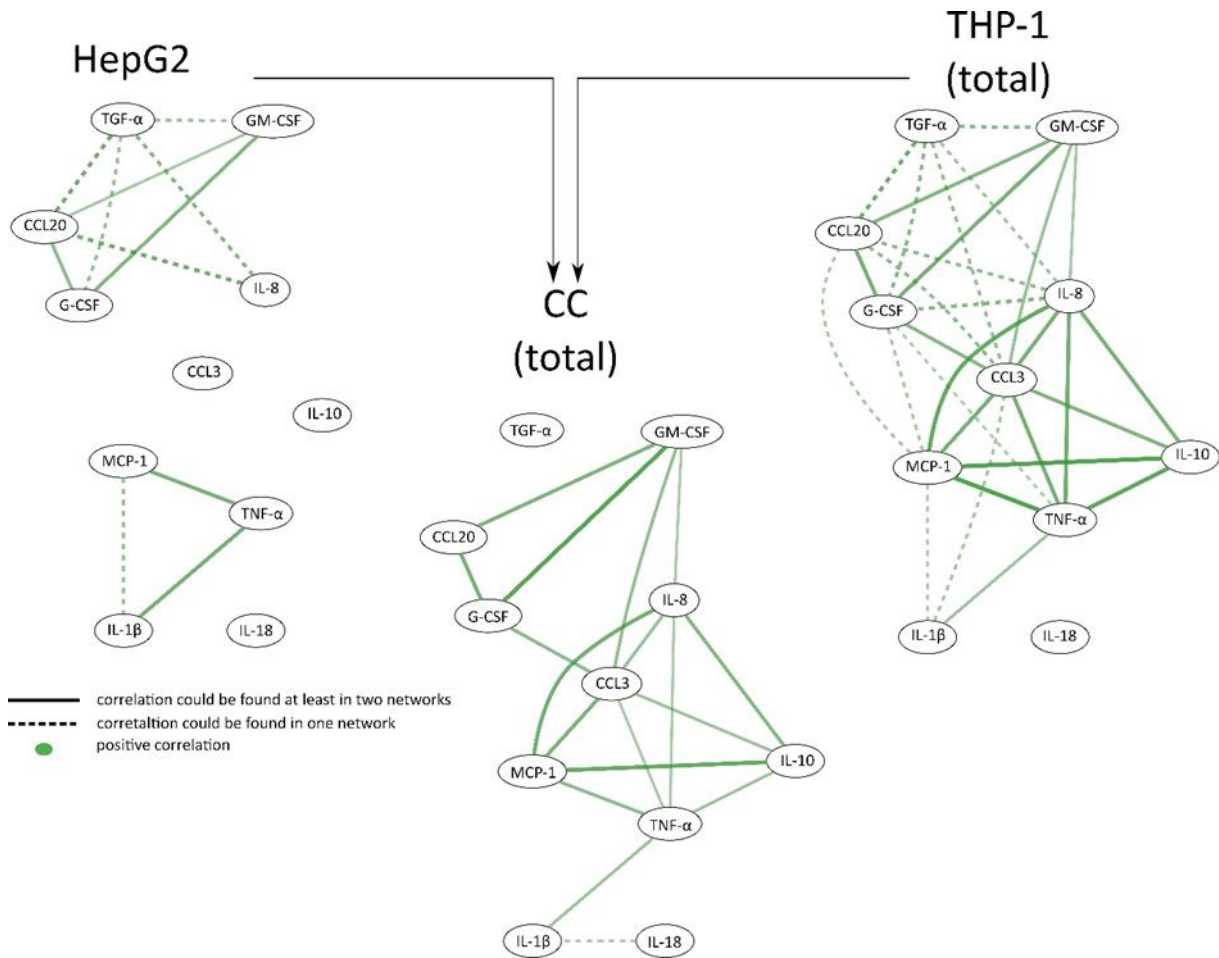


**Figure 7** Correlation network analysis of the HepG2/THP-1 co-cultivation reveals additive effects. HepG2 cells were co-cultivated (CC) with PMA-differentiated THP-1 cells. Physiological (15 %) and pro-inflammatory (50 %) THP-1 numbers were used. Overall 16 cytokines were measured (given in table S5) at the same time points (0, 0.5, 1, 2, 4, 8, 16, 24 and 48 h) like the Fa2N-4/MDM co- and single cell cultivation (*cf.* figure 4). Solid lines (—) indicate that these correlations occur in the co-cultivation network and in at least one of the single cultivation networks. Dotted lines (---) identify additional correlations occurring in the respective network. n=3



Novel indirect co-culture of immortalised hepatocytes with monocyte derived macrophages is characterised by pro-inflammatory cytokine networks

## **Discussion**

A novel co-culture system, consisting of immortalised hepatocytes (Fa2N-4) and MDM cells, has been established. In a first step, the differentiation of MDMs was characterised. Differentiated MDM cells expressed typical surface markers (Bertani et al., 2017; Cao et al., 2005; Lai et al., 2006; Taylor et al., 2004): CD83, CD209, CD14, CD86, TLR4, HLA-DR and CD163 (Fig. 1). However, only 28% of the MDMs were CD209 positive (CD209<sup>+</sup>, Fig. 1). Among liver cells, Kupffer cells were also reported to be positive for CD209 (Lai et al., 2006). In addition to Kupffer cells, also human anti-inflammatory M2 macrophages (but no pro-inflammatory M1 macrophages) were CD209<sup>+</sup> (Buchacher et al., 2015). This indicates that CD209 negative (CD209<sup>-</sup>) MDMs in this co-culture system might represent the heterogeneity of macrophages migrating into the liver due to an inflammatory response. Thus, this Fa2N-4/MDM system is independent of the limited availability of primary Kupffer cells and primary human hepatocytes. In contrast to the model of Oda et al. (2021) which relies on PBMCs this study consists of differentiated PBMCs (MDMs).

An inflammatory status of cellular systems can improve the detection of adverse chemicals. It is known that modest inflammation during drug therapy lowers the hepatotoxic threshold and leads to adverse effects (Roth and Ganey, 2011). These adverse effect can be reproduced in an animal model by performing co-treatment with low doses of lipopolysaccharides (LPS) (Buchweitz et al., 2002; Deng et al., 2006; Zou et al., 2009). In contrast to several studies, we did not use LPS to simulate an inflammatory environment, but increased the number of MDM cells in the co-culture (CC 50%) and compared these with the “physiological” number of MDMs present (CC 15%). The “physiological” concentration was calculated from data published by (Brouwer et al., 1988), who reported an average of  $14.5 \pm 9.1\%$  Kupffer cells from seven human liver preparations. To our knowledge, our paper is the first work in which the extent of the pro-inflammatory status depends on the hepatocyte-to-MDM ratio and not on prior substance-specific induction of pro-inflammation. Hence this novel co-culture system allows to study adverse substance effects depending on its inflammatory status.

The number of MDM cells and the total incubation time (24 h or 48 h) affected the gene expression pattern of Fa2N-4 cells (Fig. 2). Independent transcriptome-based pathway analysis of the two different co-cultures (CC 15% and CC 50%, respectively) after 24 h revealed the activation of an acute phase response mainly in the CC 50% culture (Fig. 2 C) which could be confirmed by the phosphorylation of p38 (Fig. 3). Coulouarn et al. (2004) have shown that the gene expression in primary human liver cells correlated with the severity of the acute phase response and supporting our data of the transcriptome-based pathway analysis in connection with the phosphorylation of p38.

Novel indirect co-culture of immortalised hepatocytes with monocyte derived macrophages is characterised by pro-inflammatory cytokine networks

It is well known that the secretion of various pro-inflammatory cytokines (*e.g.* IL-6, TNF- $\alpha$ , IL-1 $\beta$ ) is part of an acute phase reaction (Ramadori and Christ, 1999). Therefore, we investigated the time course of secreted cytokines (Fig. 4 A) and established a correlation network of these cytokines (Fig. 4 B). Similar to the *in vivo* situation, cytokine secretion in co-culture was more complex compared to single cultivated cells and did not represent the sum of the Fa2N-4 and MDM dependent networks (Fig. 4 B). IL-8 played a central role under co-cultivation conditions, as indicated by seven correlations to other cytokines and an elevated absolute concentration (Fig. 4). In contrast, the previously studied HepG2/THP-1 co-culture systems (Granitzny et al., 2017; Padberg et al., 2020; Wewering et al., 2017b) showed only five correlations of IL-8 to other cytokines (Fig. 7).

*In vivo* correlations between IL-8, IL-6 and IL-1 $\beta$ , that have been described in the literature (Table 1), occurred only in the Fa2N-4/MDM network and were absent in the HepG2/THP-1 co-culture (using a cut-off value of  $p < 0.05$ ). To validate the *in vitro* cytokine correlations in HepG2/THP-1 and Fa2N-4/MDM networks further, information from literature was retrieved. Table 1 compares the two correlation networks in focus (Fig. 4 B + Fig. 7) with the data found in the literature. The single- and co-cultivation of Fa2N-4 and MDM cells showed more similarities between *in vivo* reported correlation networks (*c.f.* Fig. 4 B) than the co-cultivation of HepG2 and THP-1 cells (Fig. 7). However, Fa2N-4/MDM co-cultivation did not mirror all cytokine profiles reported in the literature. This might be related to the absence of other hepatic cells such as endothelial cells and Ito cells (Brouwer et al., 1988; Gebhardt, 1992) that are present in healthy liver. Furthermore, the concentrations of some cytokines, like TNF- $\alpha$  in Fa2N-4/MDM co-cultures (Table 1 + Fig. 4 B) and IL-6 in HepG2/THP-1 co-cultivations (Table 1 + Fig. 7), were at the lowest level of possible quantification, which also caused the absence of respective nodes and edges in the correlation networks. In addition, the (statistically) absence of correlations between cytokines in the correlation network did not necessarily indicate that there was no biological dependence. The absence might be based on the predefined cut-off value of  $p < 0.05$ , set in the statistical analysis (*c.f.* Fig. 4 B). This in particular includes cytokines that are present at high concentrations, but have no correlation to any other cytokine. As already mentioned, IL-8 is of particular importance in the Fa2N-4/MDM co-culture and potential correlations can be confirmed by the literature (Table 1).

Novel indirect co-culture of immortalised hepatocytes with monocyte derived macrophages is characterised by pro-inflammatory cytokine networks

**Table 1.** Comparison of the established correlation network analyses of the co-cultures with literature data. Correlation network analyses of co-cultivations (CC) of Fa2N-4 cells with monocyte derived macrophages (MDMs) and HepG2 cells with PMA-differentiated THP-1 cells (*cf.* figure 4 B + 7) were compared with inflammatory cytokine profiles from the literature. The literature data shown here were based on liver-associated cell types in an inflammatory state (e.g. virus infections, exposure to lipopolysaccharide, thioacetamide, carbon tetrachloride or ethanol). Shown were either complete agreement (✓) or at least one agreement (✓) of the direct correlations with the cytokine profiles found in the literature.

Fa2N-4/MDMs			HepG2/THP-1			literature		
Fa2N-4	MDM	CC	HepG2	THP-1	CC	Cytokines	species	reference
✓		✓	✓	✓	✓	IL-1 $\beta$ , IL-6, TNF- $\alpha$ , TGF- $\beta$ 1	mouse	(Meng et al., 2012)
✓		✓	✓	✓	✓	IL-1 $\beta$ , IL-6, TNF- $\alpha$	mouse	(Dong et al., 2019)
✓		✓	✓	✓	✓	IL-1 $\beta$ , IL-6, IL-10, TNF- $\alpha$	mouse	(Yang et al., 2010)
✓		✓				IL-1 $\beta$ , IL-6	mouse	(Qin et al., 2012)
✓	✓	✓	✓	✓	✓	IL-1 $\beta$ , IL-8, TGF- $\beta$ 1, MCP-1	mouse	(Dou et al., 2019)
✓	✓	✓	✓	✓	✓	IL-1 $\beta$ , IL-6, TNF- $\alpha$ , MCP-1	mouse	(Mandrekar et al., 2011)
✓		✓	✓	✓	✓	IL-1 $\beta$ , IL-6, TNF- $\alpha$ , CCL3	mouse	(Denaes et al., 2016) [108]
✓	✓	✓				IL-1 $\beta$ , IL-6, IL-8	human	(Hosel et al., 2009)
✓		✓			✓	IL-1 $\beta$ , IL-18	human	(Shrivastava et al., 2013)
✓		✓			✓	IL-1 $\beta$ , IL-12, IL-18	mouse	[109]

Novel indirect co-culture of immortalised hepatocytes with monocyte derived macrophages is characterised by pro-inflammatory cytokine networks

In general, IL-8 and the corresponding receptor C-X-C motif chemokine receptor 1 (CXCR1) are responsible for the recruitment of macrophages and neutrophils (Ishida et al., 2006). We investigated the role of IL-8 in our co-culture system by using the neutralising antibody  $\alpha$ IL-8 (Fig. 5 A). The heatmap (Fig. 5 A) showed that the concentration of IL-8 decreased in the presence of  $\alpha$ IL-8, as expected. Some correlations predicted by the correlation network were confirmed. A decrease in IL-8 resulted in a reduced secretion of FGF in single cultured Fa2N-4 cells, supporting the prediction that both are positive correlated (Fig. 4 B). In MDM cells, the decrease of IL-8 resulted in an increased secretion of FGF, supporting the predicted negative correlation. Furthermore, the correlation network (Fig. 4 B) indicated that MCP-1 correlates positively with IL-8 in co-cultures and in single cultivated MDMs. Reduction of IL-8 by the treatment with  $\alpha$ IL-8 resulted in a decrease of MCP-1 in co-cultures and single-cultivated MDM cells (Fig. 5 A). This positive correlation could be supported by expression data from the literature. An increase in the gene expression of MCP-1 and IL-8 has been previously shown in co-cultures of HepaRG cells with PBMCs (Beringer et al., 2019).

The depletion of IL-8 also resulted in some unexpected findings, which did not match the predictions of the correlation network. A positive correlation existed between IL-8 and CCL20 in FA2N-4 single cultures (Fig. 4 B). Despite this positive correlation, the CCL20 concentration increased after lowering the level of IL-8 (Fig. 5 A).

Besides the influence of IL-8 we investigated the effect of TNF- $\alpha$  on cytokine secretion using AMB. AMB is a monoclonal TNF- $\alpha$  neutralising IgG1 antibody used for the treatment of patients with rheumatoid arthritis (French et al., 2016). It is capable of inducing DILI (Ghabril et al., 2013) and thus has been listed in the DILIrank dataset (Chen et al., 2016).

Treatment with AMB resulted in several changes of the cytokine concentrations. Obviously, IL-6 was reduced in co-culture after treatment with AMB (Fig. 5 B). The connection between IL-6 and TNF- $\alpha$  has been described before: In a mouse model, TNF- $\alpha$  in the serum peaked at 1.5 h and IL-6 after 4 h after LPS injection (Hong et al., 2009). This temporal relationship of TNF- $\alpha$  and IL-6 after LPS treatment was also shown in cultured rat hepatocytes (Saad et al., 1995). Furthermore, a positive correlation between IL-6 and TGF- $\beta$ 1 is likely, since murine fibroblasts showed an IL-6 induced expression of TGF- $\beta$ 1 (Luckett-Chastain and Gallucci (2009)). Therefore, the predictions of the correlation network are supported by literature. The negative correlation of CCL20 and IL-6 in the single culture of MDM cells was confirmed, since an increase of IL-6 increased resulted in a decrease of TGF-  $\beta$ 1 (Fig. 4 B). In addition, the positive correlation of TGF- $\beta$ 1 and FGF in single cultured Fa2N-4 cells (Fig. 4 B) was confirmed, since both decreased after the AMB induced reduction of TNF- $\alpha$  (Fig. 5 B). Similar to the  $\alpha$ IL-8 treatments, not all correlations of the cytokine network could be validated *via* an AMB induced decrease of TNF- $\alpha$ . A reduction of the FGF concentration in single culture of Fa2N-4 cells should lead

Novel indirect co-culture of immortalised hepatocytes with monocyte derived macrophages is characterised by pro-inflammatory cytokine networks

to a reduction of MCP-1 concentration according to the correlation network (Fig. 4 B). However, this MCP-1 reduction did not occur after AMB treatment (Fig. 5 B).

After 24 h of AMB treatment (Fig. 5 B) three additional positive correlations could be verified in co-culture with regard to FGF levels (with CCL20, IL-1 $\beta$  and GM-CSF, *c.f.* Fig. 4 B). In summary, we could confirm several correlation predictions. With regard to the effect of AMB, the secretion of FGF and IL-6 led to changes in other associated cytokine secretions exclusively under co-cultivation condition.

Besides the general neutralisation of TNF- $\alpha$ , AMB is known as a potential DILI inducing substance (Frider et al., 2013). Another DILI inducing substance is DCN (Boelsterli, 2003), although the structure and mode of action are completely different. Fig. 6 A gives an overview of the changed cytokine secretion as a result of DCN treatment depending on the cultivation set-up. The simulation of a healthy cell ratio (CC 15%) leads to a reduction of most cytokine secretion after DCN treatment when compared to control. This confirms the known anti-inflammatory effect of DCN (Skoutakis et al., 1988). Another more differentiated cytokine secretion pattern was present in the pro-inflammatory CC 50%. The down-regulated cytokine secretion of IL-8, MCP-1 and GM-CSF in particular follows the postulated positive correlation based upon network analyses (Fig. 4 B). The detectable upregulation of TGF- $\beta$ 1 and FGF secretion in the CC 50% after DCN treatment compared to the control was also predicted by the network analyses. However, DCN treatment can also show that other measured cytokines such as HGF and TGF- $\alpha$  play a role in co-cultivation although they do not show dependencies in the correlation networks. The reason for this is the generally low secretion of these cytokines in the absence of stimulating drugs or xenobiotics.

To investigate the induction of the cytokine secretion in more detail, cultures were treated with LPS (Fig. 6 B). Especially the pro-inflammatory CC 50% responded to LPS treatment with an increased secretion of IL-12, IL-10, IL-8, IL-6, HGF, CCL3, FGF, GM-CSF and TGF- $\beta$ 1 compared to the untreated control (Fig. 6 B). Most of these cytokines are mapped in the correlation network. In general, secretion of cytokines in the LPS-treated pro-inflammatory CC 50% system is known from the early and late response of monocytes and macrophages. IL-6, IL-8 and IL-12 can be attributed to the early response (up to 6 h after treatment) and IL-10, TGF- $\beta$ 1 and GM-CSF (up to 24 h after treatment) are known from the late response (Rossol et al., 2011). Furthermore, an increase in the HGF concentration in the supernatant of the CC 50% is detectable after the LPS treatment. In a rat model, HGF is known to prevent LPS-induced liver failure (Kaido et al., 1997). This indicates that our co-culture system shows a response to LPS and, in addition, supports the reported protective effect of HGF.

In summary, reduction of TNF- $\alpha$  by AMB treatment and the reduction of IL-8 by  $\alpha$ IL-8 treatment (Fig. 5) resulted in decreases of several correlated cytokines, indicating the validity of the network (Fig. 4 B). The treatment with DCN or LPS shows, that the ratio of MDMs affects the amount of cytokines

Novel indirect co-culture of immortalised hepatocytes with monocyte derived macrophages is characterised by pro-inflammatory cytokine networks

released. The data demonstrate that co-cultivation of Fa2N-4 and MDMs creates a complex cytokine correlation network. This novel Fa2N-4/MDM co-culture shows a high similarity to published *in vivo* data.

## Conclusion

A successful co-cultivation of an immortalised hepatic cell line (Fa2N-4) with monocyte derived macrophages (MDMs) was established. This resulted in the release of pro-inflammatory cytokines. It triggers pathways such as an acute phase response and the complement system. The concentrations of the cytokines released differed between co- and individually cultured cells as well as between a corresponding model consisting of HepG2 and differentiated THP-1 cells. A network of cytokine interactions showed that IL-8 plays a central role in the network. Changes in the IL-8 level affected numerous other cytokines, which allowed to validate the central role of IL-8. In addition, treatment with the TNF- $\alpha$  neutralising antibody (AMB), DCN and LPS showed that the resulting changes in cytokine secretion could be partially predicted by the correlation network. Especially the treatment of DCN and LPS proved that the CC 50% simulates a pro-inflammatory status with an further increase of cytokine secretion. During the AMB exposure FGF, likewise to IL-6, was an important soluble factor.

## References

- Abdel-Misih, S.R., Bloomston, M., 2010. Liver anatomy. *Surgical Clinics of North America* 90, 643-653.
- Aninat, C., Piton, A., Glaise, D., Le Charpentier, T., Languouët, S., Morel, F., Guguen-Guillouzo, C., Guillouzo, A., 2006. Expression of cytochromes P450, conjugating enzymes and nuclear receptors in human hepatoma HepaRG cells. *Drug Metabolism and Disposition: The Biological Fate of Chemicals* 34, 75-83.
- Bardou, P., Mariette, J., Escudié, F., Djemiel, C., Klopp, C., 2014. jvenn: an interactive Venn diagram viewer. *BMC Bioinformatics* 15, 293.
- Beringer, A., Molle, J., Bartosch, B., Miossec, P., 2019. Two phase kinetics of the inflammatory response from hepatocyte-peripheral blood mononuclear cell interactions. *Scientific Reports* 9, 8378.
- Bertani, F.R., Mozetic, P., Fioramonti, M., Iuliani, M., Ribelli, G., Pantano, F., Santini, D., Tonini, G., Trombetta, M., Businaro, L., Selci, S., Rainer, A., 2017. Classification of M1/M2-polarized human macrophages by label-free hyperspectral reflectance confocal microscopy and multivariate analysis. *Scientific Reports* 7, 8965-8965.
- Boelsterli, U.A., 2003. Diclofenac-induced liver injury: a paradigm of idiosyncratic drug toxicity. *Toxicology and Applied Pharmacology* 192, 307-322.

Novel indirect co-culture of immortalised hepatocytes with monocyte derived macrophages is characterised by pro-inflammatory cytokine networks

- Brouwer, A., Barelds, R.J., de Leeuw, A.M., Blauw, E., Plas, A., Yap, S.H., van den Broek, A.M., Knook, D.L., 1988. Isolation and culture of Kupffer cells from human liver. Ultrastructure, endocytosis and prostaglandin synthesis. *Journal of Hepatology* 6, 36-49.
- Buchacher, T., Ohradanova-Repic, A., Stockinger, H., Fischer, M.B., Weber, V., 2015. M2 Polarization of Human Macrophages Favors Survival of the Intracellular Pathogen *Chlamydia pneumoniae*. *PLoS One* 10, e0143593.
- Buchweitz, J.P., Ganey, P.E., Bursian, S.J., Roth, R.A., 2002. Underlying endotoxemia augments toxic responses to chlorpromazine: is there a relationship to drug idiosyncrasy? *Journal of Pharmacology and Experimental Therapeutics* 300, 460-467.
- Cao, W., Lee, S.H., Lu, J., 2005. CD83 is preformed inside monocytes, macrophages and dendritic cells, but it is only stably expressed on activated dendritic cells. *The Biochemical journal* 385, 85-93.
- Chen, M., Suzuki, A., Thakkar, S., Yu, K., Hu, C., Tong, W., 2016. DILLrank: the largest reference drug list ranked by the risk for developing drug-induced liver injury in humans. *Drug Discov Today* 21, 648-653.
- Coulouarn, C., Lefebvre, G., Derambure, C., Lequerre, T., Scotte, M., Francois, A., Cellier, D., Daveau, M., Salier, J.-P., 2004. Altered gene expression in acute systemic inflammation detected by complete coverage of the human liver transcriptome. *Hepatology* 39, 353-364.
- Denaes, T., Lodder, J., Chobert, M.N., Ruiz, I., Pawlotsky, J.M., Lotersztajn, S., Teixeira-Clerc, F., 2016. The Cannabinoid Receptor 2 Protects Against Alcoholic Liver Disease Via a Macrophage Autophagy-Dependent Pathway. *Scientific Reports* 6, 28806.
- Deng, X., Stachlewitz, R.F., Liguori, M.J., Blomme, E.A.G., Waring, J.F., Luyendyk, J.P., Maddox, J.F., Ganey, P.E., Roth, R.A., 2006. Modest Inflammation Enhances Diclofenac Hepatotoxicity in Rats: Role of Neutrophils and Bacterial Translocation. *Journal of Pharmacology and Experimental Therapeutics* 319, 1191.
- Ding, H., Tong, J., Wu, S.C., Yin, D.K., Yuan, X.F., Wu, J.Y., Chen, J., Shi, G.G., 2004. Modulation of Kupffer cells on hepatic drug metabolism. *World Journal of Gastroenterology* 10, 1325-1328.
- Dixon, L.J., Barnes, M., Tang, H., Pritchard, M.T., Nagy, L.E., 2013. Kupffer cells in the liver. *Compr Physiol* 3, 785-797.
- Dong, X., Liu, J., Xu, Y., Cao, H., 2019. Role of macrophages in experimental liver injury and repair in mice. *Experimental and Therapeutic Medicine* 17, 3835-3847.
- Dou, L., Shi, X., He, X., Gao, Y., 2019. Macrophage Phenotype and Function in Liver Disorder. *Front Immunol* 10, 3112.
- French, J.B., Bonacini, M., Ghabril, M., Foureau, D., Bonkovsky, H.L., 2016. Hepatotoxicity Associated with the Use of Anti-TNF- $\alpha$  Agents. *Drug Safety* 39, 199-208.
- Frider, B., Bruno, A., Ponte, M., Amante, M., 2013. Drug-induced liver injury caused by adalimumab: a case report and review of the bibliography. *Case Reports Hepatol* 2013, 406901.
- Gebhardt, R., 1992. Metabolic zonation of the liver: Regulation and implications for liver function. *Pharmacology and Therapeutics* 53, 275-354.

Novel indirect co-culture of immortalised hepatocytes with monocyte derived macrophages is characterised by pro-inflammatory cytokine networks

- Ghabril, M., Bonkovsky, H.L., Kum, C., Davern, T., Hayashi, P.H., Kleiner, D.E., Serrano, J., Rochon, J., Fontana, R.J., Bonacini, M., 2013. Liver Injury From Tumor Necrosis Factor- $\alpha$  Antagonists: Analysis of Thirty-four Cases. *Clinical Gastroenterology and Hepatology* 11, 558-564.e553.
- Granitzny, A., Knebel, J., Muller, M., Braun, A., Steinberg, P., Dasenbrock, C., Hansen, T., 2017. Evaluation of a human *in vitro* hepatocyte-NPC co-culture model for the prediction of idiosyncratic drug-induced liver injury: A pilot study. *Toxicol Rep* 4, 89-103.
- Gripon, P., Rumin, S., Urban, S., Le Seyec, J., Glaise, D., Cannie, I., Guyomard, C., Lucas, J., Trepo, C., Guguen-Guillouzo, C., 2002. Infection of a human hepatoma cell line by hepatitis B virus. *Proceedings of the National Academy of Sciences of the United States of America* 99, 15655-15660.
- Guillot, A., Tacke, F., 2019. Liver Macrophages: Old Dogmas and New Insights. *Hepatology Commun* 3, 730-743.
- Hariparsad, N., Carr, B.A., Evers, R., Chu, X., 2008. Comparison of immortalized Fa2N-4 cells and human hepatocytes as *in vitro* models for cytochrome P450 induction. *Drug Metabolism and Disposition: The Biological Fate of Chemicals* 36, 1046-1055.
- Hong, Y.-H., Chao, W.-W., Chen, M.-L., Lin, B.-F., 2009. Ethyl acetate extracts of alfalfa (*Medicago sativa* L.) sprouts inhibit lipopolysaccharide-induced inflammation *in vitro* and *in vivo*. *Journal of Biomedical Science* 16, 64.
- Hosel, M., Quasdorff, M., Wiegmann, K., Webb, D., Zedler, U., Broxtermann, M., Tedjokusumo, R., Esser, K., Arzberger, S., Kirschning, C.J., Langenkamp, A., Falk, C., Buning, H., Rose-John, S., Protzer, U., 2009. Not interferon, but interleukin-6 controls early gene expression in hepatitis B virus infection. *Hepatology* 50, 1773-1782.
- Ishida, Y., Kondo, T., Kimura, A., Tsuneyama, K., Takayasu, T., Mukaida, N., 2006. Opposite roles of neutrophils and macrophages in the pathogenesis of acetaminophen-induced acute liver injury. *European Journal of Immunology* 36, 1028-1038.
- Ju, C., Reilly, T., 2012. Role of immune reactions in drug-induced liver injury (DILI). *Drug Metabolism Reviews* 44, 107-115.
- Kaido, T., Yamaoka, S., Seto, S.-i., Funaki, N., Kasamatsu, T., Tanaka, J., Nakamura, T., Imamura, M., 1997. Continuous hepatocyte growth factor supply prevents lipopolysaccharide-induced liver injury in rats. *FEBS Letters* 411, 378-382.
- Karakucuk, I., Dilly, S.A., Maxwell, J.D., 1989. Portal tract macrophages are increased in alcoholic liver disease. *Histopathology* 14, 245-253.
- Kmieciak, Z., 2001. Cooperation of liver cells in health and disease, *Advances in Anatomy, Embryology and Cell Biology* 161, pp. 1-151.
- Lai, W.K., Sun, P.J., Zhang, J., Jennings, A., Lalor, P.F., Hubscher, S., McKeating, J.A., Adams, D.H., 2006. Expression of DC-SIGN and DC-SIGNR on human sinusoidal endothelium: a role for capturing hepatitis C virus particles. *American Journal of Pathology* 169, 200-208.
- Lockett-Chastain, L.R., Gallucci, R.M., 2009. Interleukin (IL)-6 modulates transforming growth factor-beta expression in skin and dermal fibroblasts from IL-6-deficient mice. *The British journal of dermatology* 161, 237-248.



Novel indirect co-culture of immortalised hepatocytes with monocyte derived macrophages is characterised by pro-inflammatory cytokine networks

- Mandrekar, P., Ambade, A., Lim, A., Szabo, G., Catalano, D., 2011. An essential role for monocyte chemoattractant protein-1 in alcoholic liver injury: regulation of proinflammatory cytokines and hepatic steatosis in mice. *Hepatology* 54, 2185-2197.
- Melino, M., Gadd, V.L., Walker, G.V., Skoien, R., Barrie, H.D., Jothimani, D., Horsfall, L., Jones, A., Sweet, M.J., Thomas, G.P., Clouston, A.D., Jonsson, J.R., Powell, E.E., 2012. Macrophage secretory products induce an inflammatory phenotype in hepatocytes. *World Journal of Gastroenterology* 18, 1732-1744.
- Meng, F., Wang, K., Aoyama, T., Grivennikov, S.I., Paik, Y., Scholten, D., Cong, M., Iwaisako, K., Liu, X., Zhang, M., Osterreicher, C.H., Stickel, F., Ley, K., Brenner, D.A., Kisseleva, T., 2012. Interleukin-17 signaling in inflammatory, Kupffer cells, and hepatic stellate cells exacerbates liver fibrosis in mice. *Gastroenterology* 143, 765-776 e763.
- Michalopoulos, G.K., 2017. Hepatostat: Liver regeneration and normal liver tissue maintenance. *Hepatology* 65, 1384-1392.
- Mills, J.B., Rose, K.A., Sadagopan, N., Sahi, J., de Morais, S.M., 2004. Induction of drug metabolism enzymes and MDR1 using a novel human hepatocyte cell line. *J Pharmacol Exp Ther* 309, 303-309.
- Mosmann, T., 1983. Rapid colorimetric assay for cellular growth and survival: application to proliferation and cytotoxicity assays. *J Immunol Methods* 65, 55-63.
- Oda, S., Uchida, Y., Aleo, M.D., Koza-Taylor, P.H., Matsui, Y., Hizue, M., Marroquin, L.D., Whritenour, J., Uchida, E., Yokoi, T., 2021. An *in vitro* coculture system of human peripheral blood mononuclear cells with hepatocellular carcinoma-derived cells for predicting drug-induced liver injury. *Archives of Toxicology* 95, 149-168.
- Padberg, F., Hering, H., Luch, A., Zellmer, S., 2020. Indirect co-cultivation of HepG2 with differentiated THP-1 cells induces AHR signalling and release of pro-inflammatory cytokines. *Toxicology in Vitro* 68, 104957.
- Padberg, F., Tarnow, P., Luch, A., Zellmer, S., 2019. Minor structural modifications of bisphenol A strongly affect physiological responses of HepG2 cells. *Archives of Toxicology* 93, 1529-1541.
- Qin, H., Holdbrooks, A.T., Liu, Y., Reynolds, S.L., Yanagisawa, L.L., Benveniste, E.N., 2012. SOCS3 deficiency promotes M1 macrophage polarization and inflammation. *J Immunol* 189, 3439-3448.
- R Core Team, 2018. R: A language and environment for statistical computing. URL <https://www.R-project.org/>, Vienna, Austria. R Foundation for Statistical Computing.
- Ramadori, G., Christ, B., 1999. Cytokines and the hepatic acute-phase response. *Seminars in Liver Disease* 19, 141-155.
- Ripp, S.L., Mills, J.B., Fahmi, O.A., Trevena, K.A., Liras, J.L., Maurer, T.S., de Morais, S.M., 2006. Use of immortalized human hepatocytes to predict the magnitude of clinical drug-drug interactions caused by CYP3A4 induction. *Drug Metabolism and Disposition: The Biological Fate of Chemicals* 34, 1742-1748.
- Rose, K.A., Holman, N.S., Green, A.M., Andersen, M.E., LeCluyse, E.L., 2016. Co-culture of Hepatocytes and Kupffer Cells as an *In Vitro* Model of Inflammation and Drug-Induced Hepatotoxicity. *Journal of Pharmaceutical Sciences* 105, 950-964.

Novel indirect co-culture of immortalised hepatocytes with monocyte derived macrophages is characterised by pro-inflammatory cytokine networks

- Rossol, M., Heine, H., Meusch, U., Quandt, D., Klein, C., Sweet, M.J., Hauschildt, S., 2011. LPS-induced cytokine production in human monocytes and macrophages. *Critical Reviews in Immunology* 31, 379-446.
- Roth, R.A., Ganey, P.E., 2011. Animal models of idiosyncratic drug-induced liver injury—Current status. *Critical Reviews in Toxicology* 41, 723-739.
- Saad, B., Frei, K., Scholl, F.A., Fontana, A., Maier, P., 1995. Hepatocyte-derived interleukin-6 and tumor-necrosis factor alpha mediate the lipopolysaccharide-induced acute-phase response and nitric oxide release by cultured rat hepatocytes. *European Journal of Biochemistry* 229, 349-355.
- Seki, E., Tsutsui, H., Nakano, H., Tsuji, N., Hoshino, K., Adachi, O., Adachi, K., Futatsugi, S., Kuida, K., Takeuchi, O., Okamura, H., Fujimoto, J., Akira, S., Nakanishi, K., 2001. Lipopolysaccharide-induced IL-18 secretion from murine Kupffer cells independently of myeloid differentiation factor 88 that is critically involved in induction of production of IL-12 and IL-1beta. *Journal of Immunology* 166, 2651-2657.
- Shrivastava, S., Mukherjee, A., Ray, R., Ray, R.B., 2013. Hepatitis C virus induces interleukin-1beta (IL-1beta)/IL-18 in circulatory and resident liver macrophages. *Journal of Virology* 87, 12284-12290.
- Skoutakis, V.A., Carter, C.A., Mickle, T.R., Smith, V.H., Arkin, C.R., Alissandratos, J., Petty, D.E., 1988. Review of Diclofenac and Evaluation of its Place in Therapy as a Nonsteroidal Antiinflammatory Agent. *Drug Intelligence and Clinical Pharmacy* 22, 850-859.
- Soldatow, V.Y., Lecluyse, E.L., Griffith, L.G., Rusyn, I., 2013. *In vitro* models for liver toxicity testing. *Toxicol Res (Camb)* 2, 23-39.
- Tacke, F., Zimmermann, H.W., 2014. Macrophage heterogeneity in liver injury and fibrosis. *J Hepatol* 60, 1090-1096.
- Taylor, P.R., Martinez-Pomares, L., Stacey, M., Lin, H.H., Brown, G.D., Gordon, S., 2004. Macrophage receptors and immune recognition. *Annual Review of Immunology* 23, 901-944.
- Treon, S.P., Thomas, P., Broitman, S.A., 1993. Lipopolysaccharide (LPS) processing by Kupffer cells releases a modified LPS with increased hepatocyte binding and decreased tumor necrosis factor-alpha stimulatory capacity. *Proceedings of the Society for Experimental Biology and Medicine* 202, 153-158.
- Tyanova, S., Temu, T., Sinitcyn, P., Carlson, A., Hein, M.Y., Geiger, T., Mann, M., Cox, J., 2016. The Perseus computational platform for comprehensive analysis of (prote)omics data. *Nature Methods* 13, 731.
- Wardle, E.N., 1987. Kupffer cells and their function. *Liver* 7, 63-75.
- Wewering, F., Jouy, F., Caliskan, S., Kalkhof, S., von Bergen, M., Luch, A., Zellmer, S., 2017a. Hepatic co-cultures *in vitro* reveal suitable to detect Nrf2-mediated oxidative stress responses on the bladder carcinogen o-anisidine. *Toxicol In Vitro* 40, 153-160.
- Wewering, F., Jouy, F., Wissenbach, D.K., Gebauer, S., Blüher, M., Gebhardt, R., Pirow, R., von Bergen, M., Kalkhof, S., Luch, A., Zellmer, S., 2017b. Characterization of chemical-induced sterile inflammation *in vitro*: application of the model compound ketoconazole in a human hepatic co-culture system. *Archives of Toxicology* 91, 799-810.

Novel indirect co-culture of immortalised hepatocytes with monocyte derived macrophages is characterised by pro-inflammatory cytokine networks

- Wilkening, S., Stahl, F., Bader, A., 2003. Comparison of primary human hepatocytes and hepatoma cell line Hepg2 with regard to their biotransformation properties. *Drug Metabolism and Disposition: The Biological Fate of Chemicals* 31, 1035-1042.
- Wu, X., Hollingshead, N., Roberto, J., Knupp, A., Kenerson, H., Chen, A., Strickland, I., Horton, H., Yeung, R., Soysa, R., Crispe, I.N., 2020. Human Liver Macrophage Subsets Defined by CD32. *Frontiers in Immunology* 11, 2108.
- Yang, H., Hreggvidsdottir, H.S., Palmblad, K., Wang, H., Ochani, M., Li, J., Lu, B., Chavan, S., Rosas-Ballina, M., Al-Abed, Y., Akira, S., Bierhaus, A., Erlandsson-Harris, H., Andersson, U., Tracey, K.J., 2010. A critical cysteine is required for HMGB1 binding to Toll-like receptor 4 and activation of macrophage cytokine release. *Proceedings of the National Academy of Sciences of the United States of America* 107, 11942-11947.
- Zou, W., Devi, S.S., Sparkenbaugh, E., Younis, H.S., Roth, R.A., Ganey, P.E., 2009. Hepatotoxic interaction of sulindac with lipopolysaccharide: role of the hemostatic system. *Toxicological sciences : an official journal of the Society of Toxicology* 108, 184-193.

## 4. Discussion

Substances may be inadvertently ingested (e.g., via migration of bisphenols from food contact materials into foodstuff). However, substances can also be intentionally ingested (e.g., nutrients or pharmaceuticals). After oral intake, the liver is exposed to these nutrients, noxious and/or pharmacologically active compounds. In the case that there are no data for potential hepatotoxic effects available, the read across approach might be applied. A basic requirement for the application are existing data on structurally similar compounds.

As already described (*cf.* chapter 1.2.2), the read across approach can be used to fill data gaps of target substances with data of structurally analogous substances [92]. Here, BPA and BPC are ideal candidates for read across. The difference rely on two additional methyl groups of BPC compared to BPA (*cf.* chapter 1.2, figure 2). To evaluate the applicability of the read across approach better, synthesized bisphenol A/C (BPA/C) was used. BPA/C is a structural intermediate between BPA and BPC, as it does carry only one additional methyl group (*cf.* chapter 3.1, table 1) when compared to BPA. The ECHA defined the grouping criteria of substances for a read across approach. Following the definition, the grouping is based on common functional groups, precursors, physicochemical, and/or biological properties [110]. Two of these defined grouping principles of the physicochemical and biological properties were clearly confirmed in this work (*cf.* chapter 3.1, table 1): The metabolic activity in the 3-(4,5-dimethylthiazol-2-yl)-2,5-diphenyltetrazolium bromide (MTT) assay in HepG2 cells (with regard to the  $EC_{50}$ ) and the oil water distribution coefficients ( $\log P_{ow}$ ) were comparable (*cf.* chapter 3.1, figure 1). In the beginning, these studies indicated that a read across approach is a reliable prediction method of the adverse effects of BPC to the source substance BPA.

By comparing the cellular effects of BPC to those of BPA and BPA/C it becomes obvious that these particular compounds are not in favor with the use of a read across approach. Table Table 1 provides a summary of the physiological effects of these compounds detected.

## Discussion

**Table 1.** Comparison of bisphenol A (BPA)-, bisphenol A/C (BPA/C)-, and bisphenol C (BPC)-induced effects in HepG2 cells. As indicated in chapter 3.1, treatment of HepG2 cells with BPC leads to certain cellular responses. This is exemplified in terms of an agreement (=), an increase (>) or a decrease (<) of the effects when compared to BPA or BPA/C treatment. Shown are the cell division ratio under influence of 1/3 of 10 % of the effective concentration (EC<sub>10</sub>) and the EC<sub>10</sub>.

		BPA/C compared to BPA	BPC compared to BPA	BPC compared to BPA/C
cell division ratio	EC <sub>10</sub>	>	=	=
	1/3 EC <sub>10</sub>	=	<	<
mitochondrial membrane potential		=	<	<
intracellular ATP/protein		=	<	<
<i>TGFB1</i> expression		<	=	>
<i>TNF</i> expression		=	>	>
estrogenic activity		>	<	<

According to this summary BPC does not trigger comparable cellular effects when compared to BPA and/or BPA/C. It is also impossible to correlate the effects based to the increasing number of methyl groups (BPA<BPA/C<BPC). The alleviating effect of BPC on the intracellular ATP level and the mitochondrial membrane potential ( $\Delta\Psi_m$ ) in HepG2 cells is particularly noticeable (*cf.* chapter 3.1, figure 3 + 4). The concentration of intracellular ATP is a sensitive endpoint for mitotoxicity in the absence of cell death [111] for which both methyl groups of BPC seems to be required. Further analyses showed that among the bisphenols studied (*cf.* chapter 3.1, figure 7), only BPC leads to a reduction in mitochondrial cytochrome c (CyC). It is known that the release of mitochondrial CyC into the cytoplasm leads to the activation of apoptosis-mediating enzymes (i.e. caspases), which trigger the intrinsic apoptosis pathway [112]. Obviously only BPC triggers intrinsic apoptosis in HepG2 cells. This raises the question if HepG2-based *in vitro* system could be instrumental and which cellular factors would be best to identify substance-specific adverse effects. One potential approach could be a HepG2/THP-1 co-culture. Yet this HepG2/THP-1 system has been already established by two independent groups, as published in Wewering *et al.* (2017) and Granitzny *et al.* (2017). Both groups could show that the HepG2/THP-1 system reacts more sensitive to substance treatment than the corresponding single cell culture of HepG2 cells [74, 75]. The group around Granitzny *et al.* could postulate TNF- $\alpha$  as a potential prognostic factor for the development of DILI *in vitro* [75]. When these HepG2/THP-1 co-cultures were now treated with the selected bisphenols, an increased concentration of TNF- $\alpha$  in the cell culture

## Discussion

supernatant could be observed in the case of BPC (*cf.* chapter 3.1, figure 6 B). This shows that TNF- $\alpha$  can be used as prognostic factor in HepG2/THP-1 co-cultures, but not in the corresponding single cultures.

In light of these results further questions arose: Why is the pro-inflammatory HepG2/THP-1 co-culture model more sensitive to substance treatment? This co-culture represents a pro-inflammatory system [74] and the pro-inflammatory cytokines have been quantified in the supernatant (*cf.* chapter 3.2, figure 4 B). Moderate tissue inflammation enhance cellular sensitivity and lowers the toxic threshold of a cellular system. This was demonstrated by the use of LPS in animal models [103-106]. According to these animal studies a moderate inflammation may lead to altered substance metabolism and thus to altered toxic effects. Therefore, the next step was to investigate the changes in physiological processes of HepG2 cells under the pro-inflammatory influence of PMA-differentiated THP-1 cells. In this co-culture we found an activation of the AHR signaling pathway. Co-cultivation not only increases the expression of typical target genes of this pathway, but also increases the corresponding CYP1A1 enzyme activity in HepG2 cells (*cf.* chapter 3.2, figure 5). This activation is associated with changes in the concentration of cytokines found in the supernatant. It is known that in primary hepatocytes CYP1A1 is repressed by cytokines such as IL-6 and TNF- $\alpha$  [113]. These data suggest that the concentration of an individual cytokine does not reflect a single cellular process, but rather the complex interaction of the latter. The pro-inflammatory CYP1A1 induction can also be caused by other signaling pathways. This includes CAR and the liver X receptor  $\alpha$  signaling (LXR $\alpha$ ) pathways [114].

Besides the influence on *CYP1A1* expression, CAR is also involved in hepatocellular physiology. Studies in rats have shown that the activation of CAR (by phenobarbital) leads to an increase in total serum cholesterol and stimulated lipolysis [115]. These changes in cholesterol biosynthesis and *de novo* FA synthesis was also identified in co-cultured HepG2 cells. Yet, increased cholesterol biosynthesis (*cf.* chapter 3.2, figure 6) in the co-cultured HepG2 cells did not lead to an increase in total lipids compared to single-cultured HepG2 cells; even a reduction of the LD content was detectable (*cf.* chapter 3.2, figure 7). The common precursor of these two biochemical reactions, acetyl coenzyme A, is most likely not the limiting factor here, as otherwise the increase in cholesterol amount could not be explained. The reduced expression of fatty acid synthase (FAS) based on RNA and protein levels, together with the reduced content of total lipids leads to the conclusion that the *de novo* FA synthesis is reduced, whereas the  $\beta$ -oxidation of FAs is increased. The  $\beta$ -oxidation seems to be more pronounced in co-cultured HepG2 cells than in individual-cultured HepG2 cells. Through this  $\beta$ -oxidation additional ATP is generated, covering the energy demand of the cell [116]. In general, the ATP content in co-cultured HepG2 cells is significantly lower than in individually cultivated HepG2 cells (*cf.* chapter 3.2, figure 8 B).

## Discussion

This indicates an increased protein biosynthesis, the highest energy consuming cellular process [117]. Cholesterol biosynthesis is also an ATP-consuming biochemical process [118]. Both processes together could be the cause for the lower intracellular ATP concentration. In summary, the co-cultured HepG2 cells have a higher ATP consumption than HepG2 cells alone, apparently covered by FA  $\beta$ -oxidation.

The putatively increased  $\beta$ -oxidation of co-cultured HepG2 cells reduce the amount of LDs in this co-culture compared to HepG2 cells alone (*cf.* chapter 3.2, figure 7). This may explain why HepG2/THP-1 co-culture shows the aforementioned increased chemical sensitivity in comparison to single cell cultivation. As it is already known, a characteristic of LDs is the maintenance of organelle homeostasis, preventing the formation of reactive oxygen species, hypoxia, and apoptotic cell death [119].

These changes in cellular biochemical processes are exclusively recognized in the HepG2/THP-1 co-culture. It is very likely that the above mentioned changes are related to the pro-inflammatory properties and the secretion of soluble factors. As an example, the pleiotropic cytokine IL-6 has multiple effects on hepatic lipid metabolism [120]. Correlation networks were investigated to get an overview of possible interactions and correlations between the secreted cytokines. It becomes obvious that HepG2 cells alone show only few possible correlations between different cytokines. THP-1 cells, on the other hand, are characterized by a large number of potential correlations that seem to determine the correlations of the cytokines in the HepG2/THP-1 co-culture as well (*cf.* chapter 3.3, figure 7). However, cytokine IL-6 did not show any association with the cytokines in the correlation network determined. Overall, an additive effect of the correlation networks of HepG2/THP-1 co-culture with respect to the corresponding single cultivations was observed (*cf.* 3.3 figure 7).

It has long been known that transformed hepatocyte cell lines (such as HepG2 cells) secrete lower levels of cytokines than primary hepatocytes [121]. Accordingly, an IL-8 concentration was detected in the supernatant of primary hepatocytes of  $1159 \pm 94$  pg/ml, whereas in the supernatant of HepG2 cells a concentration of  $87 \pm 6$  pg/ml was quantified [121]. In HepG2/THP-1 co-culture, IL-8 signaling seems to play a prominent role in the correlation network compared to the individual HepG2-cultivation. This is also shown by the increased IL-8 secretion of  $>12603$  pg/ml vs. 29 pg/ml as measured in co- and single culture, respectively. This increased secretion of IL-8 was already noted in an earlier publication and linked to the pro-inflammatory status of HepG2/THP-1 [74]. When the primary co-culture system consisting of Fa2N-4 and MDM was used, it can be seen that IL-8 also plays a prominent role here, demonstrated by an increased secretion (up to 3167 pg/ml) in the co-culture. Thus, a correlation of IL-8 with seven other cytokines in the corresponding network exists (*cf.* chapter 3.3, figure 4), indicating a pro-inflammatory environment. Moreover, the Fa2N-4/MDM co-culture has the

## Discussion

advantage that no tumor cell lines are employed and that the inflammatory status can be changed simply by changing the hepatocyte-MDM cell ratio, with no necessity for LPS.

We found that adjustments in the hepatocyte-MDM cell ratio leads to changes in the signaling pathways based on alterations in gene expression. It has been shown that higher MDM numbers result in an acute-phase response signaling (*cf.* chapter 3.3, figure 2). In connection with the phosphorylation of the transcription factor of p38 mitogen-activated protein kinase (*cf.* chapter 3.3, figure 3), these analyses indicate that the acute response signaling pathway is being activated. In general, the liver is the major producer of acute-phase proteins and it is therefore an essential part of the innate immune system's response to infection [122]. These correlations, along with its pro-inflammatory status, indicate that the Fa2N-4/MDM system might be able to simulate the subsequent modulation of the innate immune system *in vitro*.

As mentioned before, IL-8 is a central cytokine in the Fa2N-4/MDM culture. For this reason, the IL-8-neutralizing antibody ( $\alpha$ IL-8) was used to evaluate the correlation network (*cf.* chapter 3.3, figure 5 A). The positive correlations of IL-8 with FGF (in Fa2N-4 cells only) and MCP-1 (in Fa2N-4/MDM and MDM cells only) were confirmed, whereas the correlation with CCL20 (in Fa2N-4 cells only) could not be confirmed, potentially due to the complex interference with other cytokines.

Next, the newly developed cell culture system, combining Fa2N-4 and MDM cells, was treated with known DILI substances and cytokine secretion was measured.

Treatment with DILI substance AMB (*cf.* chapter 3.3, figure 5 B) can answer two questions. Firstly, because of its property as a TNF- $\alpha$ -neutralizing antibody, AMB is able to validate the correlation network with reference to the literature. Secondly, AMB is known as a potential DILI-inducing substance. By treating the Fa2N-4/MDM culture with AMB, it is possible to confirm the postulated nodes of the correlation network, even though TNF- $\alpha$  itself shows no correlation to the cytokines studied. In the mouse model, a time dependence in serum concentration of TNF- $\alpha$  (peaked at 1.5 h) and IL-6 (peaked at 4 h) could be measured after LPS injection [123]. According to a study of murine fibroblasts, a positive correlation of IL-6 and TGF- $\beta$ 1 can be detected [124]. Based on these two studies, a temporal correlation (TNF- $\alpha$  – IL-6 – TGF- $\beta$ ) of cytokine secretion can be postulated. In the cytokine secretion data of the Fa2N-4/MDM system after 24 h, an AMB-dependent reduction of TGF- $\beta$  can be seen (*cf.* chapter 3.3, figure 5 B). These analyses therefore support the assumption of the existence of a correlation network (IL-6 – TGF- $\beta$ ) expressed in the Fa2N-4/MDM culture. The second objective of this treatment was to consider AMB as a potential DILI-inducing substance. Comparison of the U.S. DILI Network database between 2003 and 2011 and a detailed literature review show that AMB is a



## Discussion

potentially DILI-inducing substance [125]. These cases are documented with patients suffering from Crohn's disease, psoriatic arthritis, or rheumatoid arthritis [125]. For these inflammatory diseases, associated with AMB-DILI, the pro-inflammatory Fa2N-4/MDM system may provide evidence for the adverse effects of AMB. The increase of IL-12 secretion is particularly noticeable when Fa2N-4/MDM co-cultures are treated with AMB. It is long been known that TNF- $\alpha$  KO mice show significantly higher inducible IL-12 serum concentrations [126]. IL-12 is an early pro-inflammatory cytokine with immunomodulating effects, like the differentiation of Type 1 helper T cells and cytotoxic T cells [127]. Besides the up-regulation of pro-inflammatory IL-12 in AMB-treated Fa2N-4/MDM co-cultures compared to the control, some growth factors (HGF, FGF) also appear to be upregulated. Altered secretion of these measured growth factors can also be detected in Fa2N-4/MDM cultures upon DCN treatment (*cf.* chapter 3.3, figure 6 A). However, the fundamental differences of the substances AMB and DCN in the mode of action and structure make a further comparison as potential DILI substance difficult. Nevertheless, the common aspect of increased HGF secretion in the different treatments should be considered in more detail. A recent transcriptome study shows that HGF is among the top activated upstream regulators ( $p < 0.0001$ ) in a mouse model with acetaminophen-dependent DILI [128]. This could be an indication that the DILI substance induced HGF dependent signaling could be comparable between the Fa2N-4/MDM system and the *in vivo* situation. Furthermore, HGF might be a potential biomarker in the Fa2N-4/MDM system.

As described above, DCN is known as a potential DILI-triggering substance [54]. In the Fa2N-4/MDM system adverse effects of DCN can now be investigated with regard to physiological and pro-inflammatory conditions (*cf.* chapter 3.3, figure 6 A). The cytokine secretion is mainly reduced after DCN treatment under healthy conditions (CC 15 %) compared to the corresponding control. This clearly indicates the anti-inflammatory effect of DCN [129]. However, an increased secretion of HGF under healthy conditions (CC 15 %) can be detected. This indicates that HGF might be a novel biomarker for the DILI identification of DCN under healthy conditions (CC 15 %). In general, it has been shown that HGF protects from anti-tuberculosis drug-induced (isoniazid/rifampicin) hepatotoxicity in a mouse model [130]. It is therefore possible that this protective effect also occurs under healthy (CC 15 %) conditions and is therefore a DCN specific effect. This assumption is reinforced by the effect of DCN in the pro-inflammatory Fa2N-4/MDM co-culture (CC 50 %), since under these conditions the secretion of HGF is downregulated. Also, the reduction of cytokines from CC 15 % is no longer detectable (except for MCP-1 and IL-8). This indicates a shift in the effect of DCN depending on the inflammatory status of the Fa2N-4/MDM system. A slightly increased secretion of FGF and TGF- $\beta$ 1 in the CC 50 % is visible when compared to the corresponding control. It is known that FGF is activated in an autocrine loop by

## Discussion

TGF- $\beta$ 1 and leads to a growth stimulation of human myofibroblastic liver cells [131]. This could be an indication of altered physiological cellular processes. Based on these data, it can be concluded that the effect of DCN is clearly dependent on the inflammatory status of the Fa2N-4/MDM system, i.e. the ratio of MDM herein.

LPS treatment, like DCN treatment, also shows differences in cytokine secretion depending on the inflammatory status of the Fa2N-4/MDM system (*cf.* chapter 3.3, figure 6 B). Thus, the secretion of nine cytokines is increased exclusively in pro-inflammatory Fa2N-4/MDM co-culture, except for IL-6 and HGF, which are also upregulated in healthy Fa2N-4/MDM co-culture. This increased secretion after LPS treatment was to be expected, as LPS is a strong pro-inflammatory stimulus [132]. However, the composition of these individual cytokines is specific. Thus, many typical LPS-inducible cytokines of early response (4 h to 6 h post treatment) of monocytes and macrophages are found, such as IL-12, IL-8, and IL-6, and some cytokines of late response (16 h to 24 h post treatment), such as IL-10, TGF- $\beta$ 1, and GM-CSF [133] were identified in the Fa2N-4/MDM co-cultures. Even after treatment with LPS, an increased HGF secretion can be detected compared to control. In rat models, HGF has been shown to prevent acute liver failure induced by LPS [134]. This *in vivo* study suggests that HGF should also reduce cytokine production after LPS treatment in the Fa2N-4/MDM system. The reason why HGF does not reduce cytokine secretion in the pro-inflammatory Fa2N-4/MDM culture is probably due to the use of cells with HGF overexpression and secretion in the cited *in vivo* study [134]. This would mean that in the healthy Fa2N-4/MDM system (CC 15 %) the secretion of HGF might be sufficient to reduce the effect of LPS. In contrast, the protective effect of HGF is not sufficient to reduce cytokine secretion in the pro-inflammatory Fa2N-4/MDM system (CC 50 %). This indicates that the Fa2N-4/MDM co-culture system responds to LPS treatment with the supposed protective effect of HGF depended on the inflammatory status.

In summary, these analyses demonstrate that Fa2N-4/MDM system reacts specifically with the secretion of relevant cytokines to LPS treatment and that the pro-inflammatory status can be further induced.

## 5. Conclusion & Outlook

The liver as an important metabolic organ can be affected by adverse effects of xenobiotic substances.

BPA and its derivatives can be ingested unintentionally and trigger these adverse effects in the liver. In this work it could be shown that despite comparable physicochemical properties bisphenol derivatives have fundamentally different cellular effects. The methylation of both phenolic rings (as in BPC) is responsible for the decoupling effect of the mitochondrial membrane and the induction of intrinsic apoptosis. This adverse effect could not be identified in all the other BPA derivatives investigated. Therefore a read across between different bisphenols should be used carefully since the effects on cellular level may not fulfil the predictions. Especially with regard to the replacement of BPA in consumer products, a screening of further derivatives could be reasonable in the future. This screening could be done with the help of the prognostic factor TNF- $\alpha$  in the HepG2/THP-1 co-culture system.

The pro-inflammatory HepG2/THP-1 co-culture system is characterized by an altered physiology of HepG2 cells. The co-cultivation changes the xenobiotic metabolism by activating the AHR (followed by an increased expression of the target genes *CYP1A1*, *CYP1A2*, and *CYP1B1*) in HepG2 cells. The increased sensitivity described above is probably due to the altered *de novo* FA synthesis and reduced intracellular LDs. This alteration maybe based on the intercellular exchange of the soluble factors. Future studies can determine which factor is responsible for this in detail. This factor would then be a potential biomarker to predict an increased sensitivity of the liver to substances with potentially adverse effects.

For both cultivation systems (HepG2/THP-1 and Fa2N-4/MDM) correlation networks of the secreted cytokines were established. It became obvious that most cytokine correlations in the HepG2/THP-1 co-culture system originate from THP-1 cells and that the correlation network of the co-culture can be described by additive effects. The Fa2N-4/MDM co-culture system forms a much more complex correlation network. In general, it has been shown that the inflammatory status in the Fa2N-4/MDM system can be changed by altering the ratio of MDM to Fa2N-4 cells (simply by regulating the acute phase response pathway in terms of gene expression analysis). The Fa2N4/MDM system reacts specifically to treatments (AMB, DCN or LPS) by secretion of cytokines. TNF- $\alpha$  does not appear to be a prognostic factor, thus contrasting HepG2/THP-1 system. However, the analyses show that the secretion of HGF is a promising starting point for further analyses. Furthermore, the question arises to what extent physiological processes of Fa2N-4 cells are influenced in the Fa2N-4/MDM system and whether they are comparable to those in the HepG2/THP-1 system.

## Conclusion & Outlook

The limitations of both cell culture systems is the origin of the cells from an intravital tumour environment (HepG2) and the cellular differences to Kupffer cells (THP-1 and MDM). In future, detailed comparisons between the properties of MDM and Kupffer cells should be carried out. This comparison could at least decrease the limitation of using MDM instead of native Kupffer cells. Furthermore the influence of other cell types (e.g. endothelial and stellate cells) cannot be investigated in the systems considered here (HepG2/THP-1 or Fa2N-4/MDM). However, this would mean a significant increase in complexity and would thus be contrary to reproducible applicability.

In conclusion, HepG2/THP-1 provides a simple and rapid *in vitro* system that has an increased chemical sensitivity compared to the individual cultivation of HepG2 cells. The Fa2N-4/MDM system, on the other hand, offers a good opportunity to directly investigate the adverse effects *in vitro* and to draw conclusions about potential substance effects *in vivo*.

## 6. References

- [1] S.R. Abdel-Misih, M. Bloomston, Liver anatomy, *Surg. Clin. North Am.* 90(4) (2010) 643-53.
- [2] R.J. Schulze, M.B. Schott, C.A. Casey, P.L. Tuma, M.A. McNiven, The cell biology of the hepatocyte: A membrane trafficking machine, *J. Cell Biol.* 218(7) (2019) 2096-2112.
- [3] M.S. Roberts, B.M. Magnusson, F.J. Burczynski, M. Weiss, Enterohepatic Circulation, *Clin. Pharmacokinet.* 41(10) (2002) 751-790.
- [4] Z. Kmiec, Cooperation of liver cells in health and disease, *Advances in Anatomy, Embryology and Cell Biology* 161, 2001, pp. 1-151.
- [5] R. Gebhardt, Metabolic zonation of the liver: regulation and implications for liver function, *Pharmacol. Ther.* 53(3) (1992) 275-354.
- [6] D.K. Seviour, O. Pelkonen, J.T. Ahokas, Hepatocytes: the powerhouse of biotransformation, *Int. J. Biochem. Cell Biol.* 44(2) (2012) 257-61.
- [7] H. Wang, A.D. Quiroga, R. Lehner, Chapter 7 - Analysis of Lipid Droplets in Hepatocytes, in: H. Yang, P. Li (Eds.), *Methods Cell Biol.*, Academic Press 2013, pp. 107-127.
- [8] C.J. Fielding, P.E. Fielding, CHAPTER 19 - Dynamics of lipoprotein transport in the circulatory system, in: D.E. Vance, J.E. Vance (Eds.), *Biochemistry of Lipids, Lipoproteins and Membranes (Fifth Edition)*, Elsevier, San Diego, 2008, pp. 533-553.
- [9] L. Rui, Energy metabolism in the liver, *Comprehensive Physiology* 4(1) (2014) 177-197.
- [10] W. Huang, A. Metlakunta, N. Dedousis, P. Zhang, I. Sipula, J.J. Dube, D.K. Scott, R.M. Doherty, Depletion of Liver Kupffer Cells Prevents the Development of Diet-Induced Hepatic Steatosis and Insulin Resistance, *Diabetes* 59(2) (2010) 347.
- [11] C. Kupffer, Ueber Sternzellen der Leber, *Archiv für mikroskopische Anatomie* 12(1) (1876) 353-358.
- [12] L.J. Dixon, M. Barnes, H. Tang, M.T. Pritchard, L.E. Nagy, Kupffer cells in the liver, *Compr Physiol* 3(2) (2013) 785-97.
- [13] A. Brouwer, R.J. Barelids, A.M. de Leeuw, E. Blauw, A. Plas, S.H. Yap, A.M. van den Broek, D.L. Knook, Isolation and culture of Kupffer cells from human liver. Ultrastructure, endocytosis and prostaglandin synthesis, *J. Hepatol.* 6(1) (1988) 36-49.
- [14] A.T. Nguyen-Lefebvre, A. Horuzsko, Kupffer Cell Metabolism and Function, *Journal of enzymology and metabolism* 1(1) (2015) 101.
- [15] M.M. Diesselhoff-den Dulk, R.W. Crofton, R. van Furth, Origin and kinetics of Kupffer cells during an acute inflammatory response, *Immunology* 37(1) (1979) 7-14.
- [16] I. Klein, J.C. Cornejo, N.K. Polakos, B. John, S.A. Wuensch, D.J. Topham, R.H. Pierce, I.N. Crispe, Kupffer cell heterogeneity: functional properties of bone marrow derived and sessile hepatic macrophages, *Blood* 110(12) (2007) 4077-4085.
- [17] F. Tacke, H.W. Zimmermann, Macrophage heterogeneity in liver injury and fibrosis, *J. Hepatol.* 60(5) (2014) 1090-6.
- [18] P.J. Murray, Macrophage Polarization, *Annu. Rev. Physiol.* 79(1) (2017) 541-566.

## References

- [19] A. Guillot, F. Tacke, Liver Macrophages: Old Dogmas and New Insights, *Hepatol Commun* 3(6) (2019) 730-743.
- [20] N. Kawada, M. Parola, Chapter 12 - Interactions of Stellate Cells with Other Non-Parenchymal Cells, in: C.R. Gandhi, M. Pinzani (Eds.), *Stellate Cells in Health and Disease*, Academic Press, Boston, 2015, pp. 185-207.
- [21] E.N. Wardle, Kupffer cells and their function, *Liver* 7(2) (1987) 63-75.
- [22] J.I. Odegaard, R.R. Ricardo-Gonzalez, A. Red Eagle, D. Vats, C.R. Morel, M.H. Goforth, V. Subramanian, L. Mukundan, A.W. Ferrante, A. Chawla, Alternative M2 activation of Kupffer cells by PPARdelta ameliorates obesity-induced insulin resistance, *Cell Metab.* 7(6) (2008) 496-507.
- [23] A. Neyrinck, S.L. Eeckhoudt, C.J. Meunier, S. Pampfer, H.S. Taper, R.K. Verbeeck, N. Delzenne, Modulation of paracetamol metabolism by Kupffer cells: A study on rat liver slices, *Life Sci.* 65(26) (1999) 2851-2859.
- [24] C.J. Omiecinski, J.P. Vanden Heuvel, G.H. Perdew, J.M. Peters, Xenobiotic Metabolism, Disposition, and Regulation by Receptors: From Biochemical Phenomenon to Predictors of Major Toxicities, *Toxicol. Sci.* 120(suppl\_1) (2010) S49-S75.
- [25] U.M. Zanger, M. Schwab, Cytochrome P450 enzymes in drug metabolism: Regulation of gene expression, enzyme activities, and impact of genetic variation, *Pharmacol. Ther.* 138(1) (2013) 103-141.
- [26] T.J. Gan, Diclofenac: an update on its mechanism of action and safety profile, *Curr. Med. Res. Opin.* 26(7) (2010) 1715-31.
- [27] S. Shen, M.R. Marchick, M.R. Davis, G.A. Doss, L.R. Pohl, Metabolic activation of diclofenac by human cytochrome P450 3A4: role of 5-hydroxydiclofenac, *Chem. Res. Toxicol.* 12(2) (1999) 214-22.
- [28] C. King, W. Tang, J. Ngui, T. Tephly, M. Braun, Characterization of rat and human UDP-glucuronosyltransferases responsible for the in vitro glucuronidation of diclofenac, *Toxicol. Sci.* 61(1) (2001) 49-53.
- [29] H. Stierlin, J.W. Faigle, A. Sallmann, W. Kung, W.J. Richter, H.P. Kriemler, K.O. Alt, T. Winkler, Biotransformation of diclofenac sodium (Voltaren®) in animals and in man, *Xenobiotica* 9(10) (1979) 601-610.
- [30] A. Tkachenko, M. Bermudez, S. Irmer-Stooff, D. Genkinger, F. Henkler-Stephani, G. Wolber, A. Luch, Nuclear transport of the human aryl hydrocarbon receptor and subsequent gene induction relies on its residue histidine 291, *Arch. Toxicol.* 92(3) (2018) 1151-1160.
- [31] P. Ramadoss, C. Marcus, G.H. Perdew, Role of the aryl hydrocarbon receptor in drug metabolism, *Expert Opin. Drug Metab. Toxicol.* 1(1) (2005) 9-21.
- [32] M. Granado, A.I. Martín, T. Priego, M.A. Villanúa, A. López-Calderón, Inactivation of Kupffer cells by gadolinium administration prevents lipopolysaccharide-induced decrease in liver insulin-like growth factor-I and IGF-binding protein-3 gene expression, *J. Endocrinol.* 188(3) (2006) 503-11.
- [33] H. Ding, J. Tong, S.C. Wu, D.K. Yin, X.F. Yuan, J.Y. Wu, J. Chen, G.G. Shi, Modulation of Kupffer cells on hepatic drug metabolism, *World J. Gastroenterol.* 10(9) (2004) 1325-8.

## References

- [34] O. Niemelä, S. Parkkila, B. Bradford, Y. Iimuro, M. Pasanen, R.G. Thurman, Effect of Kupffer cell inactivation on ethanol-induced protein adducts in the liver, *Free Radic. Biol. Med.* 33(3) (2002) 350-355.
- [35] J.B. French, M. Bonacini, M. Ghabril, D. Foureau, H.L. Bonkovsky, Hepatotoxicity Associated with the Use of Anti-TNF- $\alpha$  Agents, *Drug Saf.* 39(3) (2016) 199-208.
- [36] I. Ordás, D.R. Mould, B.G. Feagan, W.J. Sandborn, Anti-TNF monoclonal antibodies in inflammatory bowel disease: pharmacokinetics-based dosing paradigms, *Clin. Pharmacol. Ther.* 91(4) (2012) 635-46.
- [37] J.A. Del Campo, P. Gallego, L. Grande, Role of inflammatory response in liver diseases: Therapeutic strategies, *World J. Hepatol.* 10(1) (2018) 1-7.
- [38] Y. Koyama, D.A. Brenner, Liver inflammation and fibrosis, *The Journal of clinical investigation* 127(1) (2017) 55-64.
- [39] M.W. Robinson, C. Harmon, C. O'Farrelly, Liver immunology and its role in inflammation and homeostasis, *Cell. Mol. Immunol.* 13(3) (2016) 267-276.
- [40] E. Liaskou, D.V. Wilson, Y.H. Oo, Innate immune cells in liver inflammation, *Mediators Inflamm.* 2012 (2012) 949157-949157.
- [41] P. Knolle, J. Schlaak, A. Uhrig, P. Kempf, K.H. Meyer zum Büschenfelde, G. Gerken, Human Kupffer cells secrete IL-10 in response to lipopolysaccharide (LPS) challenge, *J. Hepatol.* 22(2) (1995) 226-9.
- [42] I.N. Crispe, Hepatocytes as Immunological Agents, *Journal of immunology (Baltimore, Md. : 1950)* 196(1) (2016) 17-21.
- [43] J.V. Castell, M.J. Gómez-Lechón, M. David, T. Hirano, T. Kishimoto, P.C. Heinrich, Recombinant human interleukin-6 (IL-6/BSF-2/HSF) regulates the synthesis of acute phase proteins in human hepatocytes, *FEBS Lett.* 232(2) (1988) 347-50.
- [44] C.A. Norris, M. He, L.-I. Kang, M.Q. Ding, J.E. Radder, M.M. Haynes, Y. Yang, S. Paranjpe, W.C. Bowen, A. Orr, G.K. Michalopoulos, D.B. Stolz, W.M. Mars, Synthesis of IL-6 by hepatocytes is a normal response to common hepatic stimuli, *PLoS One* 9(4) (2014) e96053-e96053.
- [45] R. Bataller, D.A. Brenner, Liver fibrosis, *The Journal of clinical investigation* 115(2) (2005) 209-218.
- [46] R. Bataller, D.A. Brenner, Liver fibrosis, *J. Clin. Invest.* 115(2) (2005) 209-18.
- [47] S. David, J.P. Hamilton, Drug-induced Liver Injury, *US Gastroenterol. Hepatol. Rev.* 6 (2010) 73-80.
- [48] R.A. Roth, P.E. Ganey, Intrinsic versus idiosyncratic drug-induced hepatotoxicity--two villains or one?, *J. Pharmacol. Exp. Ther.* 332(3) (2010) 692-7.
- [49] J. Uetrecht, Mechanistic Studies of Idiosyncratic DILI: Clinical Implications, *Front. Pharmacol.* 10 (2019) 837.
- [50] R.J. Andrade, M.I. Lucena, A. Alonso, M. García-Cortes, E. García-Ruiz, R. Benitez, M.C. Fernández, G. Pelaez, M. Romero, R. Corpas, J.A. Durán, M. Jiménez, L. Rodrigo, F. Nogueras, R. Martín-Vivaldi, J.M. Navarro, J. Salmerón, F.S. de la Cuesta, R. Hidalgo, HLA class II

## References

- genotype influences the type of liver injury in drug-induced idiosyncratic liver disease, *Hepatology* 39(6) (2004) 1603-12.
- [51] A.K. Daly, P.T. Donaldson, P. Bhatnagar, Y. Shen, I. Pe'er, A. Floratos, M.J. Daly, D.B. Goldstein, S. John, M.R. Nelson, J. Graham, B.K. Park, J.F. Dillon, W. Bernal, H.J. Cordell, M. Pirmohamed, G.P. Aithal, C.P. Day, D. Study, I.S. Consortium, HLA-B\*5701 genotype is a major determinant of drug-induced liver injury due to flucloxacillin, *Nat. Genet.* 41(7) (2009) 816-9.
- [52] N. Chalasani, H.L. Bonkovsky, R. Fontana, W. Lee, A. Stolz, J. Talwalkar, K.R. Reddy, P.B. Watkins, V. Navarro, H. Barnhart, J. Gu, J. Serrano, Features and Outcomes of 899 Patients With Drug-Induced Liver Injury: The DILIN Prospective Study, *Gastroenterology* 148(7) (2015) 1340-52.e7.
- [53] Mechanisms of Drug-induced Liver Injury, *Schiff's Diseases of the Liver*, pp. 774-798.
- [54] U.A. Boelsterli, Diclofenac-induced liver injury: a paradigm of idiosyncratic drug toxicity, *Toxicol. Appl. Pharmacol.* 192(3) (2003) 307-22.
- [55] R. Teschke, Top-ranking drugs out of 3312 drug-induced liver injury cases evaluated by the Roussel Uclaf Causality Assessment Method, *Expert Opin. Drug Metab. Toxicol.* 14(11) (2018) 1169-1187.
- [56] E.H. Lee, J.H. Oh, S. Selvaraj, S.M. Park, M.S. Choi, R. Spanel, S. Yoon, J. Borlak, Immunogenomics reveal molecular circuits of diclofenac induced liver injury in mice, *Oncotarget* 7(12) (2016) 14983-5017.
- [57] K. Zeilinger, N. Freyer, G. Damm, D. Seehofer, F. Knospel, Cell sources for in vitro human liver cell culture models, *Exp. Biol. Med. (Maywood)* 241(15) (2016) 1684-98.
- [58] V.Y. Soldatow, E.L. Lecluyse, L.G. Griffith, I. Rusyn, In vitro models for liver toxicity testing, *Toxicol Res (Camb)* 2(1) (2013) 23-39.
- [59] Y. Toyoda, K. Kashikura, T. Soga, Y.I. Tagawa, Metabolomics of an in vitro liver model containing primary hepatocytes assembling around an endothelial cell network: comparative study on the metabolic stability and the effect of acetaminophen treatment, *J. Toxicol. Sci.* 42(4) (2017) 445-454.
- [60] J.V. Castell, R. Jover, C.P. Martinez-Jimenez, M.J. Gmez-Lechn, Hepatocyte cell lines: their use, scope and limitations in drug metabolism studies, *Expert Opin. Drug Metab. Toxicol.* 2(2) (2006) 183-212.
- [61] N.J. Hewitt, P. Hewitt, Phase I and II enzyme characterization of two sources of HepG2 cell lines, *Xenobiotica* 34(3) (2004) 243-56.
- [62] J. Lin, L. Schyschka, R. Muhl-Benninghaus, J. Neumann, L. Hao, N. Nussler, S. Dooley, L. Liu, U. Stockle, A.K. Nussler, S. Ehnert, Comparative analysis of phase I and II enzyme activities in 5 hepatic cell lines identifies Huh-7 and HCC-T cells with the highest potential to study drug metabolism, *Arch. Toxicol.* 86(1) (2012) 87-95.
- [63] D.P. Aden, A. Fogel, S. Plotkin, I. Damjanov, B.B. Knowles, Controlled synthesis of HBsAg in a differentiated human liver carcinoma-derived cell line, *Nature* 282(5739) (1979) 615-6.
- [64] N.B. Javitt, Hep G2 cells as a resource for metabolic studies: lipoprotein, cholesterol, and bile acids, *The FASEB Journal* 4(2) (1990) 161-168.



## References

- [65] S. Wilkening, F. Stahl, A. Bader, Comparison of primary human hepatocytes and heptoma cell line HepG2 with regard to their biotransformation properties, *Drug Metabolism and Disposition* 31(8) (2003) 1035.
- [66] L. Tolosa, M.T. Donato, G. Pérez-Cataldo, J.V. Castell, M.J. Gómez-Lechón, Upgrading cytochrome P450 activity in HepG2 cells co-transfected with adenoviral vectors for drug hepatotoxicity assessment, *Toxicol. In Vitro* 26(8) (2012) 1272-7.
- [67] J. Barretina, G. Caponigro, N. Stransky, K. Venkatesan, A.A. Margolin, S. Kim, C.J. Wilson, J. Lehár, G.V. Kryukov, D. Sonkin, A. Reddy, M. Liu, L. Murray, M.F. Berger, J.E. Monahan, P. Morais, J. Meltzer, A. Korejwa, J. Jané-Valbuena, F.A. Mapa, J. Thibault, E. Bric-Furlong, P. Raman, A. Shipway, I.H. Engels, J. Cheng, G.K. Yu, J. Yu, P. Aspesi, Jr., M. de Silva, K. Jagtap, M.D. Jones, L. Wang, C. Hatton, E. Palessandolo, S. Gupta, S. Mahan, C. Sougnez, R.C. Onofrio, T. Liefeld, L. MacConaill, W. Winckler, M. Reich, N. Li, J.P. Mesirov, S.B. Gabriel, G. Getz, K. Ardlie, V. Chan, V.E. Myer, B.L. Weber, J. Porter, M. Warmuth, P. Finan, J.L. Harris, M. Meyerson, T.R. Golub, M.P. Morrissey, W.R. Sellers, R. Schlegel, L.A. Garraway, The Cancer Cell Line Encyclopedia enables predictive modelling of anticancer drug sensitivity, *Nature* 483(7391) (2012) 603-607.
- [68] J.B. Mills, K.A. Rose, N. Sadagopan, J. Sahi, S.M. de Moraes, Induction of drug metabolism enzymes and MDR1 using a novel human hepatocyte cell line, *J. Pharmacol. Exp. Ther.* 309(1) (2004) 303-9.
- [69] N. Hariparsad, B.A. Carr, R. Evers, X. Chu, Comparison of immortalized Fa2N-4 cells and human hepatocytes as in vitro models for cytochrome P450 induction, *Drug Metab. Dispos.* 36(6) (2008) 1046-55.
- [70] S.R. Khetani, S.N. Bhatia, Microscale culture of human liver cells for drug development, *Nat. Biotechnol.* 26 (2007) 120.
- [71] S. March, V. Ramanan, K. Trehan, S. Ng, A. Galstian, N. Gural, M.A. Scull, A. Shlomai, M.M. Mota, H.E. Fleming, S.R. Khetani, C.M. Rice, S.N. Bhatia, Micropatterned coculture of primary human hepatocytes and supportive cells for the study of hepatotropic pathogens, *Nat. Protoc.* 10(12) (2015) 2027-53.
- [72] Y. Edling, L.K. Sivertsson, A. Butura, M. Ingelman-Sundberg, M. Ek, Increased sensitivity for troglitazone-induced cytotoxicity using a human in vitro co-culture model, *Toxicol. In Vitro* 23(7) (2009) 1387-95.
- [73] H. Schwende, E. Fitzke, P. Ambs, P. Dieter, Differences in the state of differentiation of THP-1 cells induced by phorbol ester and 1,25-dihydroxyvitamin D3, *J. Leukoc. Biol.* 59(4) (1996) 555-61.
- [74] F. Wewering, F. Jouy, D.K. Wissenbach, S. Gebauer, M. Blüher, R. Gebhardt, R. Pirow, M. von Bergen, S. Kalkhof, A. Luch, S. Zellmer, Characterization of chemical-induced sterile inflammation in vitro: application of the model compound ketoconazole in a human hepatic co-culture system, *Arch. Toxicol.* 91(2) (2017) 799-810.
- [75] A. Granitzny, J. Knebel, M. Muller, A. Braun, P. Steinberg, C. Dasenbrock, T. Hansen, Evaluation of a human in vitro hepatocyte-NPC co-culture model for the prediction of idiosyncratic drug-induced liver injury: A pilot study, *Toxicol Rep* 4 (2017) 89-103.
- [76] Phenol, Ullmann's Encyclopedia of Industrial Chemistry, pp. 1-20.

## References

- [77] H. Fiege, H.-W. Voges, T. Hamamoto, S. Umemura, T. Iwata, H. Miki, Y. Fujita, H.-J. Buysch, D. Garbe, W. Paulus, Phenol Derivatives, Ullmann's Encyclopedia of Industrial Chemistry (2000).
- [78] L. Carwile Jenny, T. Luu Henry, S. Bassett Laura, A. Driscoll Daniel, C. Yuan, Y. Chang Jennifer, X. Ye, M. Calafat Antonia, B. Michels Karin, Polycarbonate Bottle Use and Urinary Bisphenol A Concentrations, *Environ. Health Perspect.* 117(9) (2009) 1368-1372.
- [79] C. Brede, P. Fjeldal, I. Skjevraak, H. Herikstad, Increased migration levels of bisphenol A from polycarbonate baby bottles after dishwashing, boiling and brushing, *Food Addit. Contam.* 20(7) (2003) 684-9.
- [80] K.A. Thayer, K.W. Taylor, S. Garantziotis, S.H. Schurman, G.E. Kissling, D. Hunt, B. Herbert, R. Church, R. Jankowich, M.I. Churchwell, R.C. Scheri, L.S. Birnbaum, J.R. Bucher, Bisphenol A, Bisphenol S, and 4-Hydroxyphenyl 4-Isopropoxyphenylsulfone (BPSIP) in Urine and Blood of Cashiers, *Environ. Health Perspect.* 124(4) (2016) 437-44.
- [81] J.R. Rochester, A.L. Bolden, Bisphenol S and F: A Systematic Review and Comparison of the Hormonal Activity of Bisphenol A Substitutes, *Environ. Health Perspect.* 123(7) (2015) 643-650.
- [82] J.R. Rochester, Bisphenol A and human health: A review of the literature, *Reprod. Toxicol.* 42 (2013) 132-155.
- [83] K. Mandrah, G.N.V. Satyanarayana, S.K. Roy, A dispersive liquid-liquid microextraction based on solidification of floating organic droplet followed by injector port silylation coupled with gas chromatography-tandem mass spectrometry for the determination of nine bisphenols in bottled carbonated beverages, *J Chromatogr A* 1528 (2017) 10-17.
- [84] C. Liao, K. Kannan, A survey of alkylphenols, bisphenols, and triclosan in personal care products from China and the United States, *Arch. Environ. Contam. Toxicol.* 67(1) (2014) 50-9.
- [85] C. Liao, F. Liu, K. Kannan, Bisphenol s, a new bisphenol analogue, in paper products and currency bills and its association with bisphenol a residues, *Environ. Sci. Technol.* 46(12) (2012) 6515-22.
- [86] S. Kitamura, T. Suzuki, S. Sanoh, R. Kohta, N. Jinno, K. Sugihara, S. Yoshihara, N. Fujimoto, H. Watanabe, S. Ohta, Comparative study of the endocrine-disrupting activity of bisphenol A and 19 related compounds, *Toxicol. Sci.* 84(2) (2005) 249-59.
- [87] EFSA, Scientific Opinion on the risks to public health related to the presence of bisphenol A (BPA) in foodstuffs, *EFSA Journal* 13(1) (2015) 3978.
- [88] N. Kuroda, Y. Kinoshita, Y. Sun, M. Wada, N. Kishikawa, K. Nakashima, T. Makino, H. Nakazawa, Measurement of bisphenol A levels in human blood serum and ascitic fluid by HPLC using a fluorescent labeling reagent, *Journal of Pharmaceutical and Biomedical Analysis* 30(6) (2003) 1743-1749.
- [89] ECHA, Inclusion of substances of very high concern in the Candidate List for eventual inclusion in Annex XIV, 2018.
- [90] ECHA, SUBSTANCE EVALUATION CONCLUSION as required by REACH Article 48 and EVALUATION REPORT for 4,4'-Isopropylidenediphenol EC No 201-245-8 CAS No 80-05-7, 2017.

## References

- [91] ECHA, International Chemical Identification: 4,4'-sulphonyldiphenol; bisphenol S, Proposal for Harmonised Classification and Labelling, <https://echa.europa.eu/documents/10162/13f73092-10b5-78f7-8d31-b83671948b81> (2019).
- [92] ECHA, Read-Across Assessment Framework (RAAF) - considerations on multi-constituent substances and UVCBs, (2017).
- [93] W. Völkel, T. Colnot, G.A. Csanády, J.G. Filser, W. Dekant, Metabolism and Kinetics of Bisphenol A in Humans at Low Doses Following Oral Administration, *Chem. Res. Toxicol.* 15(10) (2002) 1281-1287.
- [94] J.J. Pritchett, R.K. Kuester, I.G. Sipes, Metabolism of Bisphenol A in Primary Cultured Hepatocytes from Mice, Rats, and Humans, *Drug Metabolism and Disposition* 30(11) (2002) 1180.
- [95] H. Yokota, H. Iwano, M. Endo, T. Kobayashi, H. Inoue, S. Ikushiro, A. Yuasa, Glucuronidation of the environmental oestrogen bisphenol A by an isoform of UDP-glucuronosyltransferase, UGT2B1, in the rat liver, *The Biochemical journal* 340 ( Pt 2)(Pt 2) (1999) 405-409.
- [96] N. Hanioka, T. Naito, S. Narimatsu, Human UDP-glucuronosyltransferase isoforms involved in bisphenol A glucuronidation, *Chemosphere* 74(1) (2008) 33-6.
- [97] J.B. Matthews, K. Twomey, T.R. Zacharewski, In Vitro and in Vivo Interactions of Bisphenol A and Its Metabolite, Bisphenol A Glucuronide, with Estrogen Receptors  $\alpha$  and  $\beta$ , *Chem. Res. Toxicol.* 14(2) (2001) 149-157.
- [98] K.A. Thayer, D.R. Doerge, D. Hunt, S.H. Schurman, N.C. Twaddle, M.I. Churchwell, S. Garantziotis, G.E. Kissling, M.R. Easterling, J.R. Bucher, L.S. Birnbaum, Pharmacokinetics of bisphenol A in humans following a single oral administration, *Environ. Int.* 83 (2015) 107-115.
- [99] S. Waidyanatha, S.R. Black, R.W. Snyder, Y.L. Yueh, V. Sutherland, P.R. Patel, S.L. Watson, T.R. Fennell, Disposition and metabolism of the bisphenol analogue, bisphenol S, in Harlan Sprague Dawley rats and B6C3F1/N mice and in vitro in hepatocytes from rats, mice, and humans, *Toxicol. Appl. Pharmacol.* 351 (2018) 32-45.
- [100] N. Cabaton, D. Zalko, E. Rathahao, C. Canlet, G. Delous, M.C. Chagnon, J.P. Cravedi, E. Perdu, Biotransformation of bisphenol F by human and rat liver subcellular fractions, *Toxicol. In Vitro* 22(7) (2008) 1697-704.
- [101] J. Schmidt, P. Kotnik, J. Trontelj, Ž. Knez, L.P. Mašič, Bioactivation of bisphenol A and its analogs (BPF, BPAF, BPZ and DMBPA) in human liver microsomes, *Toxicol. In Vitro* 27(4) (2013) 1267-1276.
- [102] E.F. Efsa Panel on Food Contact Materials, A. Processing, Scientific Opinion on the risks to public health related to the presence of bisphenol A (BPA) in foodstuffs, *EFSA Journal* 13(1) (2015) 3978.
- [103] R.A. Roth, P.E. Ganey, Animal models of idiosyncratic drug-induced liver injury—Current status, *Crit. Rev. Toxicol.* 41(9) (2011) 723-739.
- [104] X. Deng, R.F. Stachlewitz, M.J. Liguori, E.A.G. Blomme, J.F. Waring, J.P. Luyendyk, J.F. Maddox, P.E. Ganey, R.A. Roth, Modest Inflammation Enhances Diclofenac Hepatotoxicity

## References

- in Rats: Role of Neutrophils and Bacterial Translocation, *J. Pharmacol. Exp. Ther.* 319(3) (2006) 1191.
- [105] W. Zou, S.S. Devi, E. Sparkenbaugh, H.S. Younis, R.A. Roth, P.E. Ganey, Hepatotoxic interaction of sulindac with lipopolysaccharide: role of the hemostatic system, *Toxicological sciences : an official journal of the Society of Toxicology* 108(1) (2009) 184-193.
- [106] J.P. Buchweitz, P.E. Ganey, S.J. Bursian, R.A. Roth, Underlying endotoxemia augments toxic responses to chlorpromazine: is there a relationship to drug idiosyncrasy?, *J. Pharmacol. Exp. Ther.* 300(2) (2002) 460-7.
- [107] S.P. Treon, P. Thomas, S.A. Broitman, Lipopolysaccharide (LPS) processing by Kupffer cells releases a modified LPS with increased hepatocyte binding and decreased tumor necrosis factor-alpha stimulatory capacity, *Proc. Soc. Exp. Biol. Med.* 202(2) (1993) 153-8.
- [108] T. Denaes, J. Lodder, M.N. Chobert, I. Ruiz, J.M. Pawlotsky, S. Lotersztajn, F. Teixeira-Clerc, The Cannabinoid Receptor 2 Protects Against Alcoholic Liver Disease Via a Macrophage Autophagy-Dependent Pathway, *Sci. Rep.* 6 (2016) 28806.
- [109] E. Seki, H. Tsutsui, H. Nakano, N. Tsuji, K. Hoshino, O. Adachi, K. Adachi, S. Futatsugi, K. Kuida, O. Takeuchi, H. Okamura, J. Fujimoto, S. Akira, K. Nakanishi, Lipopolysaccharide-induced IL-18 secretion from murine Kupffer cells independently of myeloid differentiation factor 88 that is critically involved in induction of production of IL-12 and IL-1beta, *J. Immunol.* 166(4) (2001) 2651-7.
- [110] ECHA, Read-Across Assessment Framework (RAAF), (2017).
- [111] L. Kamalian, A.E. Chadwick, M. Bayliss, N.S. French, M. Monshouwer, J. Snoeys, B.K. Park, The utility of HepG2 cells to identify direct mitochondrial dysfunction in the absence of cell death, *Toxicol. In Vitro* 29(4) (2015) 732-40.
- [112] S.W. Tait, D.R. Green, Mitochondria and cell death: outer membrane permeabilization and beyond, *Nat. Rev. Mol. Cell Biol.* 11(9) (2010) 621-32.
- [113] J. Muntane-Relat, J.C. Ourlin, J. Domergue, P. Maurel, Differential effects of cytokines on the inducible expression of CYP1A1, CYP1A2, and CYP3A4 in human hepatocytes in primary culture, *Hepatology* 22(4 Pt 1) (1995) 1143-53.
- [114] R. Santes-Palacios, D. Ornelas-Ayala, N. Cabanas, A. Marroquin-Perez, A. Hernandez-Magana, S. Del Rosario Olguin-Reyes, R. Camacho-Carranza, J.J. Espinosa-Aguirre, Regulation of Human Cytochrome P4501A1 (hCYP1A1): A Plausible Target for Chemoprevention?, *Biomed Res Int* 2016 (2016) 5341081.
- [115] N. Kiyosawa, K. Tanaka, J. Hirao, K. Ito, N. Niino, K. Sakuma, M. Kanbori, T. Yamoto, S. Manabe, N. Matsunuma, Molecular mechanism investigation of phenobarbital-induced serum cholesterol elevation in rat livers by microarray analysis, *Arch. Toxicol.* 78(8) (2004) 435-442.
- [116] S.M. Houten, R.J.A. Wanders, A general introduction to the biochemistry of mitochondrial fatty acid  $\beta$ -oxidation, *J. Inher. Metab. Dis.* 33(5) (2010) 469-477.
- [117] L.M. Lindqvist, K. Tandoc, I. Topisirovic, L. Furic, Cross-talk between protein synthesis, energy metabolism and autophagy in cancer, *Curr. Opin. Genet. Dev.* 48 (2018) 104-111.

## References

- [118] T.P. Korman, B. Sahachartsiri, D. Li, J.M. Vinokur, D. Eisenberg, J.U. Bowie, A synthetic biochemistry system for the in vitro production of isoprene from glycolysis intermediates, *Protein Sci.* 23(5) (2014) 576-85.
- [119] F. Baenke, B. Peck, H. Miess, A. Schulze, Hooked on fat: the role of lipid synthesis in cancer metabolism and tumour development, *Dis. Model. Mech.* 6(6) (2013) 1353-63.
- [120] W. Hassan, L. Ding, R.Y. Gao, J. Liu, J. Shang, Interleukin-6 signal transduction and its role in hepatic lipid metabolic disorders, *Cytokine* 66(2) (2014) 133-42.
- [121] D.L. Rowell, L. Eckmann, M.B. Dwinell, S.P. Carpenter, J.L. Raucy, S.K. Yang, M.F. Kagnoff, Human hepatocytes express an array of proinflammatory cytokines after agonist stimulation or bacterial invasion, *American Journal of Physiology-Gastrointestinal and Liver Physiology* 273(2) (1997) G322-G332.
- [122] L.E. Sander, S.D. Sackett, U. Dierssen, N. Beraza, R.P. Linke, M. Müller, J.M. Blander, F. Tacke, C. Trautwein, Hepatic acute-phase proteins control innate immune responses during infection by promoting myeloid-derived suppressor cell function, *The Journal of experimental medicine* 207(7) (2010) 1453-1464.
- [123] Y.-H. Hong, W.-W. Chao, M.-L. Chen, B.-F. Lin, Ethyl acetate extracts of alfalfa (*Medicago sativa* L.) sprouts inhibit lipopolysaccharide-induced inflammation in vitro and in vivo, *J. Biomed. Sci.* 16(1) (2009) 64.
- [124] L.R. Luckett-Chastain, R.M. Gallucci, Interleukin (IL)-6 modulates transforming growth factor-beta expression in skin and dermal fibroblasts from IL-6-deficient mice, *The British journal of dermatology* 161(2) (2009) 237-248.
- [125] M. Ghabril, H.L. Bonkovsky, C. Kum, T. Davern, P.H. Hayashi, D.E. Kleiner, J. Serrano, J. Rochon, R.J. Fontana, M. Bonacini, Liver injury from tumor necrosis factor- $\alpha$  antagonists: analysis of thirty-four cases, *Clin. Gastroenterol. Hepatol.* 11(5) (2013) 558-564.e3.
- [126] J. Hodge-Dufour, M.W. Marino, M.R. Horton, A. Jungbluth, M.D. Burdick, R.M. Strieter, P.W. Noble, C.A. Hunter, E. Puré, Inhibition of interferon gamma induced interleukin 12 production: a potential mechanism for the anti-inflammatory activities of tumor necrosis factor, *Proc. Natl. Acad. Sci. U. S. A.* 95(23) (1998) 13806-13811.
- [127] X. Ma, TNF-alpha and IL-12: a balancing act in macrophage functioning, *Microbes Infect* 3(2) (2001) 121-9.
- [128] B. Bhushan, S. Gunewardena, G. Edwards, U. Apte, Comparison of liver regeneration after partial hepatectomy and acetaminophen-induced acute liver failure: A global picture based on transcriptome analysis, *Food Chem. Toxicol.* 139 (2020) 111186.
- [129] V.A. Skoutakis, C.A. Carter, T.R. Mickle, V.H. Smith, C.R. Arkin, J. Alissandratos, D.E. Petty, Review of Diclofenac and Evaluation of its Place in Therapy as a Nonsteroidal Antiinflammatory Agent, *Drug Intell. Clin. Pharm.* 22(11) (1988) 850-859.
- [130] C. Enriquez-Cortina, M. Almonte-Becerril, D. Clavijo-Cornejo, M. Palestino-Domínguez, O. Bello-Monroy, N. Nuño, A. López, L. Bucio, V. Souza, R. Hernández-Pando, L. Muñoz, M.C. Gutiérrez-Ruiz, L.E. Gómez-Quiroz, Hepatocyte growth factor protects against isoniazid/rifampicin-induced oxidative liver damage, *Toxicol. Sci.* 135(1) (2013) 26-36.
- [131] J. Rosenbaum, S. Blazejewski, A.M. Préaux, A. Mallat, D. Dhumeaux, P. Mavier, Fibroblast growth factor 2 and transforming growth factor beta 1 interactions in human liver myofibroblasts, *Gastroenterology* 109(6) (1995) 1986-96.

## References

- [132] E. Jirillo, D. Caccavo, T. Magrone, E. Piccigallo, L. Amati, A. Lembo, C. Kalis, M. Gumenscheimer, The role of the liver in the response to LPS: experimental and clinical findings, *J. Endotoxin Res.* 8(5) (2002) 319-27.
- [133] M. Rossol, H. Heine, U. Meusch, D. Quandt, C. Klein, M.J. Sweet, S. Hauschildt, LPS-induced cytokine production in human monocytes and macrophages, *Crit. Rev. Immunol.* 31(5) (2011) 379-446.
- [134] T. Kaido, S. Yamaoka, S.-i. Seto, N. Funaki, T. Kasamatsu, J. Tanaka, T. Nakamura, M. Imamura, Continuous hepatocyte growth factor supply prevents lipopolysaccharide-induced liver injury in rats, *FEBS Lett.* 411(2) (1997) 378-382.

## 7. List of publications

### 7.1 Articles

- 1 Padberg, F., Tarnow, P., Luch, A., and Zellmer, S.: Minor structural modifications of bisphenol A strongly affect physiological responses of HepG2 cells. *Archives of Toxicology* volume 93, pages 1529–1541(2019)
- 2 Padberg, F., Hering, H., Luch, A., and Zellmer, S.: Indirect co-cultivation of HepG2 with differentiated THP-1 cells induces AHR signalling and release of pro-inflammatory cytokines. *Toxicology in Vitro* volume 68, 104957 (2020)
- 3 Padberg, F., Höper, T., Henkel S., Driesch, D., Luch, A., and Zellmer, S.: Novel indirect co-culture of immortalised hepatocytes with monocyte derived macrophages is characterised by pro-inflammatory cytokine networks, *Toxicology in Vitro* volume 73, 105134 (2021)

### 7.2 Poster and Talks

- 1 Poster: Annual Meeting of the German Society for Experimental Pharmacology and Toxicology (DGPT), Heidelberg, 06 – 09 March 2017, Padberg, F., Tarnow, P., Luch, A. , Zellmer, S.: The effects of different bisphenols on hepatic cell lines in single- and co-cultures
- 2 Poster: Signal Transduction – Receptors, Mediators and Genes (STS), Weimar, 08 – 10 November 2017, Padberg, F., Tarnow, P., Luch, A. , Zellmer, S.: Signaling pathways in hepatic cell cultures
- 3 Poster: 20<sup>th</sup> International Congress on In Vitro Toxicology (ESTIV2018), Berlin, 15 – 18 October 2018, Padberg, F., Tarnow, P., Luch, A. , Zellmer, S.: Co-culture systems may enable to detect the effects of bisphenols on certain signaling pathways
- 4 Poster: Annual Meeting of the German Society for Experimental Pharmacology and Toxicology (DGPT), Stuttgart, 25 – 28 February 2019, Padberg, F., P., Luch, A. , Zellmer, S.: Comparison of hepatoblastoma cells (HepG2) and immortalized primary human hepatocytes (Fa2N-4) after bisphenol A exposure
- 5 Talk: Leibniz Research Centre for Working Environment and Human Factors, department of Liver Toxicology, 01.October 2019, Dortmund, Padberg, F.: Bisphenol derivatives in hepatic co-cultivation

## **Annex I**

Supplementary information

### **Title:**

Minor structural modifications of bisphenol A strongly affect physiological responses of HepG2 cells

### **Authors**

Padberg F., Tarnow P., Luch A., and Zellmer S.

German Federal Institute for Risk Assessment (BfR), Department of Chemical and Product Safety,  
Max-Dohrn Strasse 8-10, 10589 Berlin, Germany

### **Journal**

*Archives of Toxicology* volume 93, pages1529–1541(2019)

Link: <https://doi.org/10.1007/s00204-019-02457-y>

### **Keywords**

2,2-bis(4-hydroxyphenyl) propane, 2,2-bis(4-hydroxy-3-methylphenyl) propane, 4,4'-sulfonyl-diphenol, mitochondria, intrinsic apoptosis, HepG2 cells



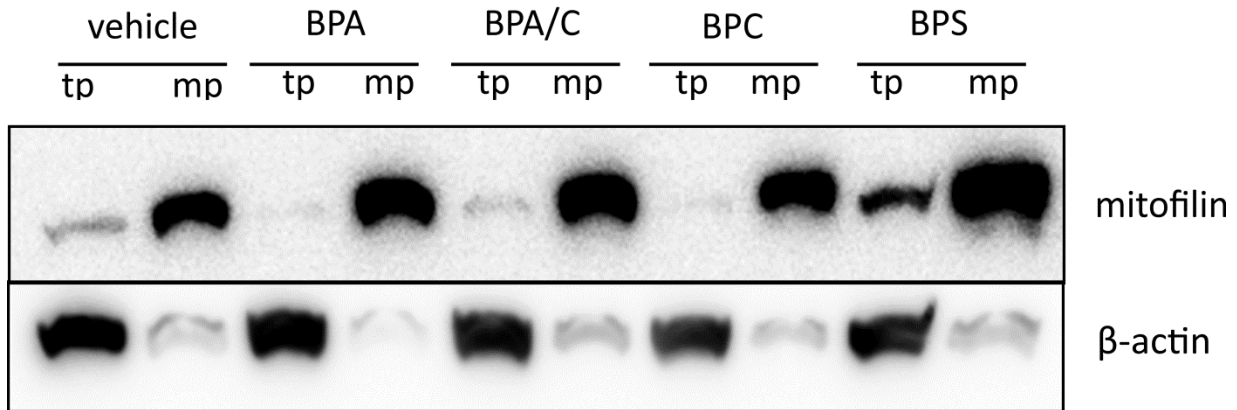


**Figure S1: Validation of mitochondrial purification.** HepG2 cells were treated with  $EC_{10}$  concentrations of bisphenol A (BPA), bisphenol A/C (BPA/C), bisphenol C (BPC) and bisphenol S (BPS) for 24 h. The total protein (tp) and the mitochondrial protein fraction (mp) were analyzed for the mitochondrial marker (mitofilin) content, with  $\beta$ -actin as loading control.

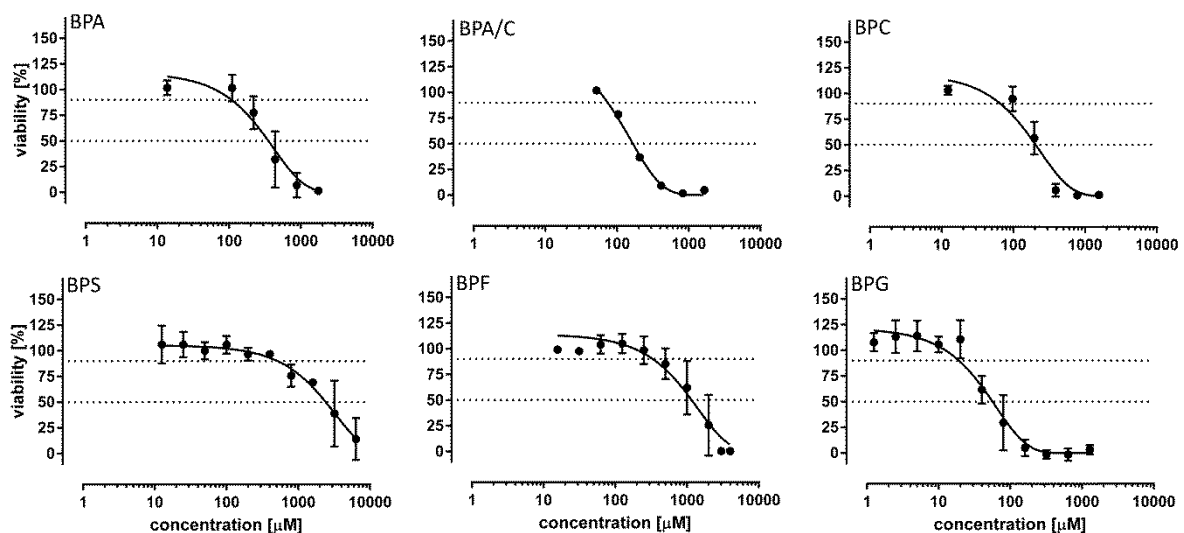


**Figure S2: Correlation between the viability and bisphenol concentration.** HepG2 cells were treated with different concentrations of bisphenol A (BPA), bisphenol A/C (BPA/C), bisphenol C (BPC), bisphenol S (BPS), bisphenol F (BPF) and bisphenol G (BPG) for 24 h ( $n=3$ ). The viability was derived via MTT-assay. Shown are 10 % and 50 % of the effective concentration (''), mean and SD (-).

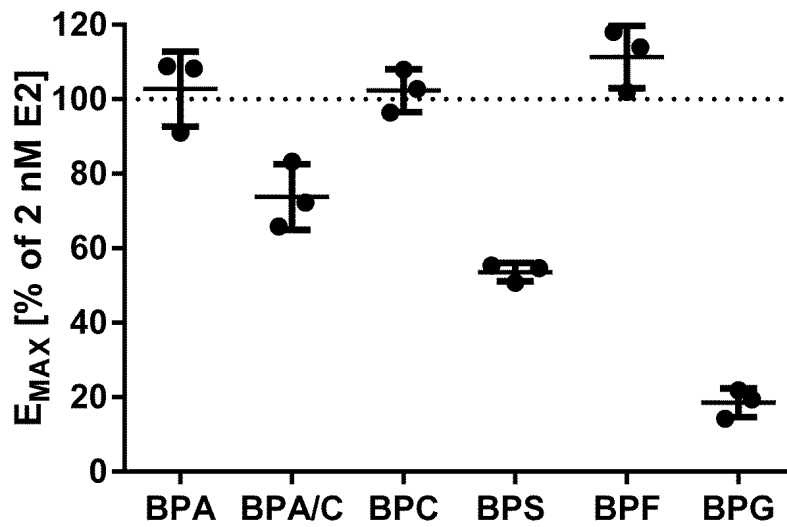


**Figure S3: Activation of estrogen receptor in relation to 2 nM estrogen (E<sub>MAX</sub>).** HeLa9902 cells were treated with different concentrations of bisphenol A (BPA), bisphenol A/C (BPA/C), bisphenol C (BPC), bisphenol S (BPS), bisphenol F (BPF) and bisphenol G (BPG) for 24 h (n=3). The activation was related to the positive control of 2 nM estrogen (•••). Shown are measurements (•), mean (—) and SD (—).

## **Annex II**

Supplementary material

### **Title:**

Indirect co-cultivation of HepG2 with differentiated THP-1 cells induces AHR signalling and release of pro-inflammatory cytokines

### **Authors**

Florian Padberg<sup>1,2</sup>, Henrik Hering<sup>1</sup>, Andreas Luch<sup>1,2</sup>, and Sebastian Zellmer<sup>1</sup>

<sup>1</sup>German Federal Institute for Risk Assessment (BfR), Department of Chemical and Product Safety, Max-Dohrn Strasse 8-10, 10589 Berlin, Germany

<sup>2</sup> Department of Biology, Chemistry, Pharmacy, Institute of Pharmacy, Freie Universität Berlin, Berlin, Germany

### **Journal**

*Toxicology in Vitro* volume 68, 104957 (2020)

Link: <https://doi.org/10.1016/j.tiv.2020.104957>

### **Keywords**

HepG2; THP-1; Co-culture; Lipids; Cholesterol; Cytokines; Inflammation; Metabolism; Adverse outcome pathway

Table S1: Antibodies

antigen	clone	host	Supplier
$\beta$ -actin	AC-15	mouse	abcam, Cambridge, UK
AHR	H-211	rabbit	Santa Cruz Biotechnology, Heidelberg, Germany
ARNT	H-172	rabbit	Santa Cruz Biotechnology, Heidelberg, Germany
FAS	EPR7465	rabbit	abcam, Cambridge, UK

Table S2: Primer

gene	forward primer	reverse primer	product
CYP1A1	TCCAAGAGTCCACCCTTCC	AAGCATGATCAGTGTAGGGATCT	72 bp
CPY1A2	ACAACCCTGCCAATCTCAAG	GGGAACAGACTGGGACAATG	68 bp
CYP1B1	TGGATTTGGAGAACGTACCG	CCACGACCTGATCCAATTCT	150 bp
SREBF1	GCTTTCTGCAACACAGCAAC	GGTCAGTGTGTCCTCCACCT	167 bp
FASN	CTTCCGAGATTCCATCCTACGC	TGGCAGTCAGGCTCACAAACG	131 bp
TGFB1	GTGGAAACCCACAACGAAAT	CACGTGCTGCTCCACTTTTA	165 bp

Microarray analysis

The RNA-integrity (RIN) was analyzed by an Agilent 2100 Bioanalyzer System (Agilent Technologies, Waldbronn, Germany) using an Agilent RNA 6000 Nano Kit (Agilent Technologies, Waldbronn, Germany) according to the manufacturer's protocol. Human Clariom™ S Assay (Applied Biosystems, Foster City, CA, USA) was performed with all samples (RIN >8.5) at ATLAS Biolabs (ATLAS Biolabs, Berlin, Germany). The sample signals were analyzed with the Transcriptome Analysis Console 4.0.1.36 (TAC) (Applied Biosystems, Foster City, CA, USA) and compared with Ingenuity pathway analysis® (IPA®) (QIAGEN Inc., <https://www.qiagenbioinformatics.com/products/ingenuity-pathway-analysis>, Qiagen, Hilden, Germany).

Exploratory grouping analysis

The Exploratory Grouping Analysis was performed with Transcriptome Analysis Console 4.0.1.36 (TAC) (Applied Biosystems, Foster City, CA, USA) with an AUC Threshold of 0.7, a distributed stochastic neighbor embedding (tSNE) Perplexity of 3 and a variance filter number of 20000.

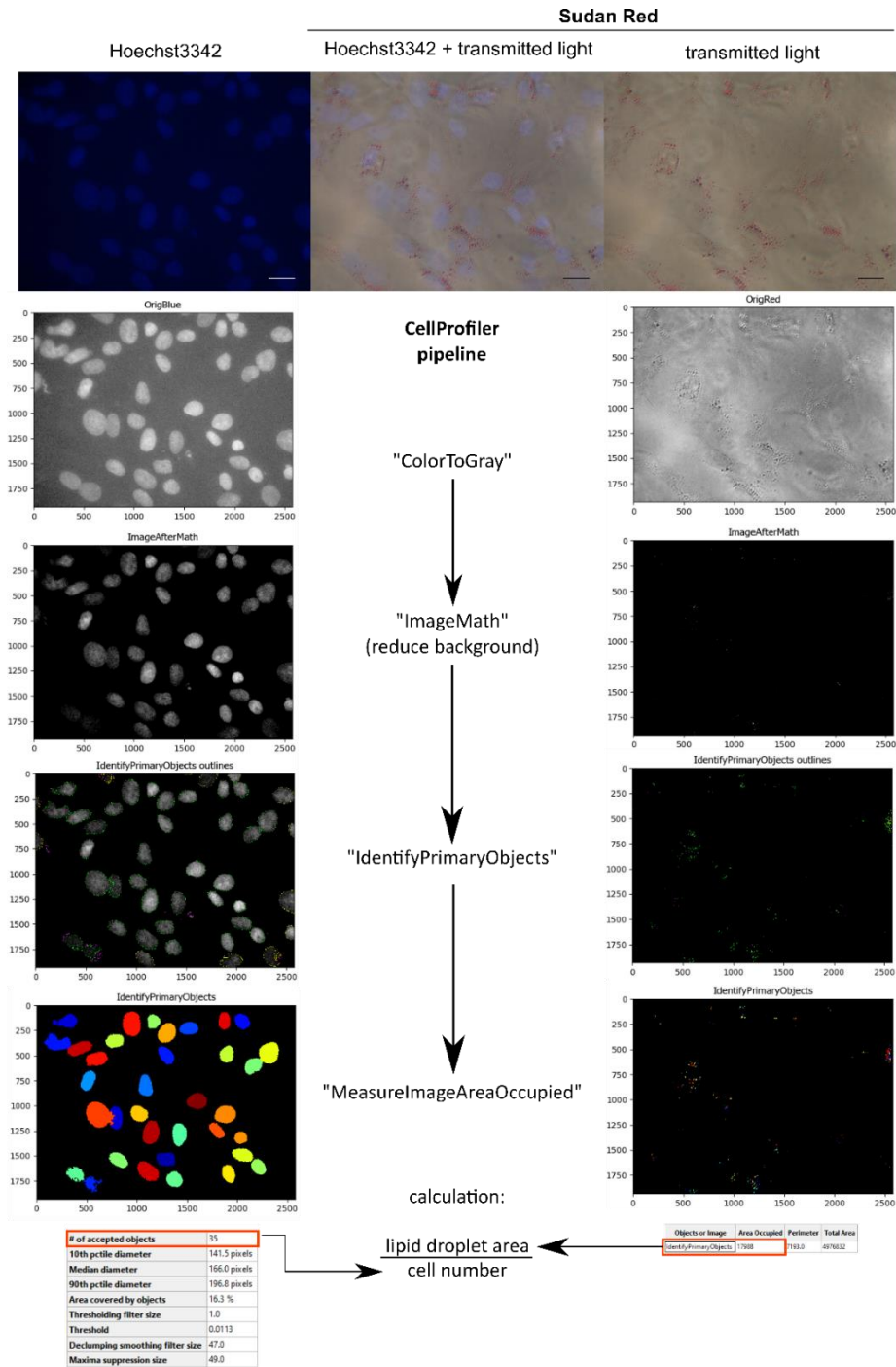


**Figure S1** Example of the evaluation and calculation of the lipid droplet area. The microscopic images were taken after a Sudan Red staining in the different channels for the Hoechst3342 and transmitted light. Subsequently, a grayscale image was created and the background of the respective measurement was minimized. Then the respective objects (based on their shape and expected size) were determined. The Hoechst3342 staining was then used to determine the cell count of each image and the area occupied by the Sudan Red staining was measured. The ratio of these ratios then formed the measurements of figure 7B.

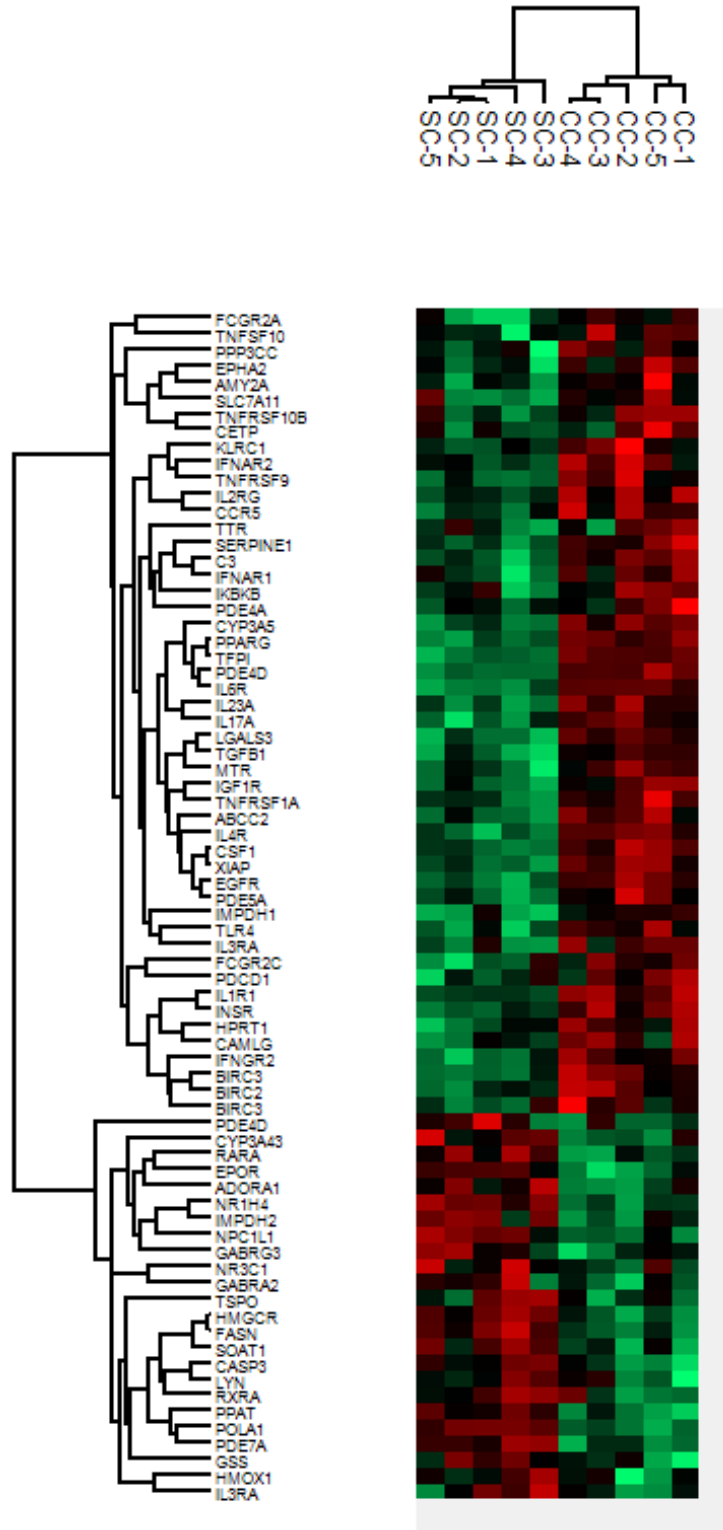


**Figure S2: Effects of co-cultivation on the xenobiotic metabolism.** HepG2 cells were cultivated in single- (SC) or co-culture (CC) for 24 h (n=5). Shown are the gene symbols and the Z-score of significantly (exclusion  $p > 0.05$ ) different expressed genes of the transcriptome analysis console (TAC)-gene list.

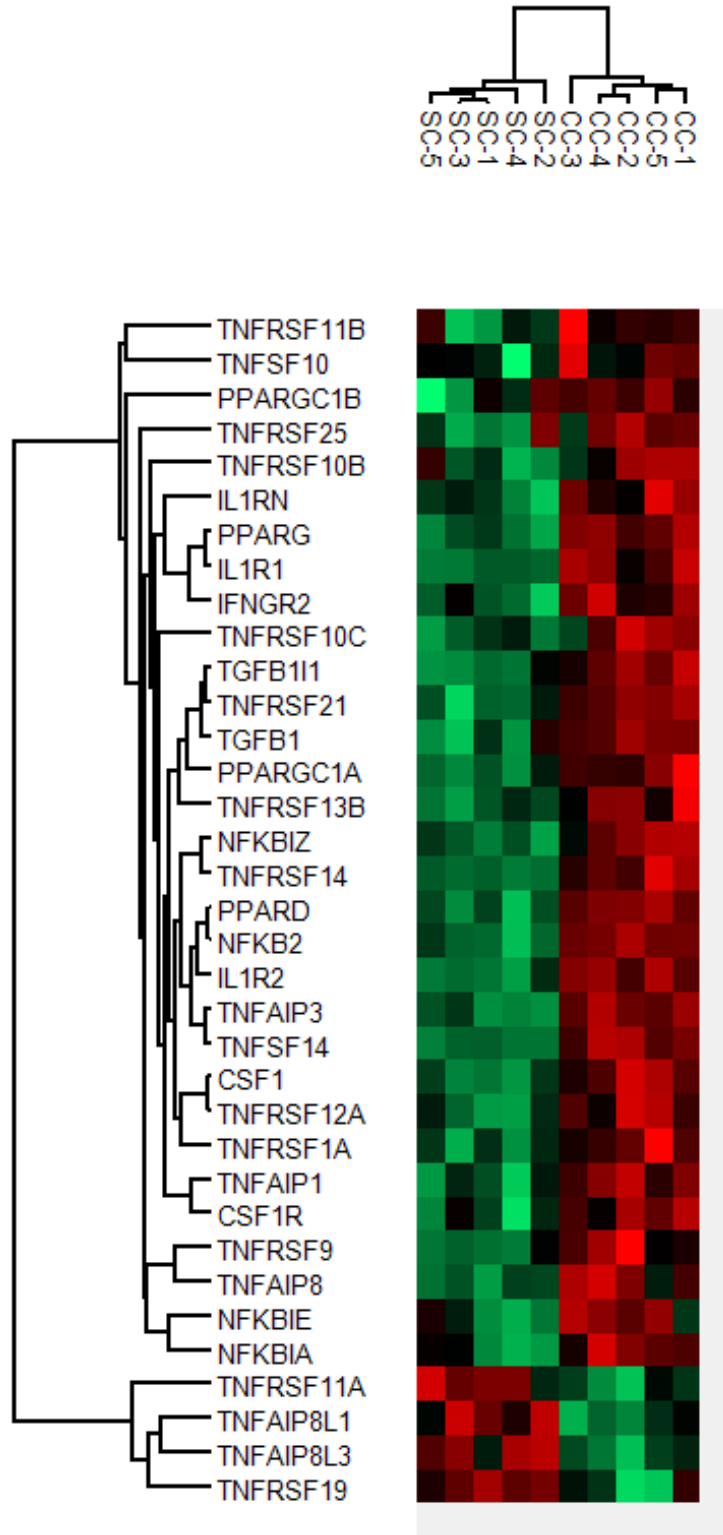


**Figure S3: Differential and significantly expressed genes related to Kupffer cell activation.** Shown are the gene symbols and the Z-score of significant (exclusion  $p > 0.05$ ) expressed genes in HepG2 after 24 h of single- (SC) or co-cultivation (CC).

## **Annex III**

Supplementary material

### **Title:**

Novel indirect co-culture of immortalised hepatocytes with monocyte derived macrophages is characterised by pro-inflammatory cytokine networks

### **Authors:**

Florian Padberg<sup>1,2</sup>, Tessa Höper<sup>1</sup>, Sebastian Henkel<sup>3</sup>, Dominik Driesch<sup>3</sup>, Andreas Luch<sup>1,2</sup>, and Sebastian Zellmer<sup>1</sup>

<sup>1</sup>German Federal Institute for Risk Assessment (BfR), Department of Chemical and Product Safety, Max-Dohrn Strasse 8-10, 10589 Berlin, Germany

<sup>2</sup>Department of Biology, Chemistry, Pharmacy, Institute of Pharmacy, Freie Universität Berlin, Arnimallee 22, 14195 Berlin, Germany

<sup>3</sup>BioControl Jena GmbH, Hans-Knöll-Straße 6, 07745 Jena, Germany

### **Journal**

*Toxicology in Vitro* volume 73, 105134 (2021)

Link: <https://doi.org/10.1016/j.tiv.2021.105134>

### **Keywords**

co-culture, Fa2N-4, monocyte derived macrophages, cytokine correlation network, acute phase

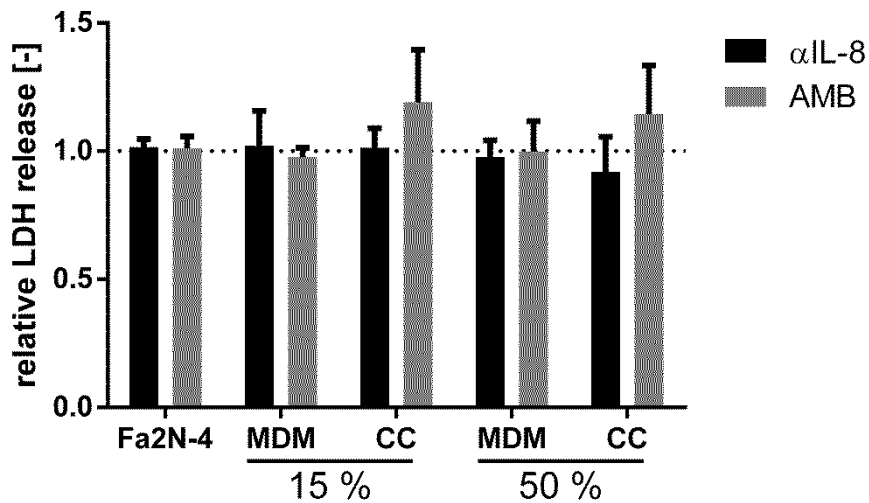


Table S1: Antibodies

antigen	clone	host	Supplier	fluorophore
$\beta$ -actin	AC-15	mouse	abcam, Cambridge, UK	
CD3	UCHT1	mouse	BD Pharmingen™, Heidelberg, Germany	Alexa Fluor® 700
CD14	M5E2	mouse	BD Pharmingen™, Heidelberg, Germany	PE
CD19	HIB19	mouse	BD Pharmingen™, Heidelberg, Germany	APC
CD83	HB15e	mouse	BD Pharmingen™, Heidelberg, Germany	FITC
CD86	IT2.2	mouse	BioLegend, Koblenz, Germany	Brilliant Violet 421™
CD163	REA812	human	Miltenyi Biotec, Bergisch Gladbach, Germany	FITC
CD209	DCN47.5	mouse	Miltenyi Biotec, Bergisch Gladbach, Germany	APC
TLR4	HTA125	mouse	Thermo Scientific, Waltham, MA, USA	PE
HLA-DR	AC122	mouse	Miltenyi Biotec, Bergisch Gladbach, Germany	PerCP
p38	polyclonal	rabbit	Cell Signaling, Frankfurt a. M., Germany	
P-p38	28B10	mouse	Cell Signaling, Frankfurt a. M., Germany	

Microarray analysis

The RNA-integrity (RIN) was analysed by an Agilent 2100 Bioanalyzer System (Agilent Technologies, Waldbronn, Germany) using an Agilent RNA 6000 Nano Kit (Agilent Technologies, Waldbronn, Germany) according to the manufacturer's protocol. Human Clariom™ S Assay (Applied Biosystems, Foster City, CA, USA) was performed with all samples (RIN >8.5) at ATLAS Biolabs (ATLAS Biolabs, Berlin, Germany). The sample signals were analysed with the Transcriptome Analysis Console 4.0.1.36 (TAC) (Applied Biosystems, Foster City, CA, USA) and compared with Ingenuity pathway analysis® (IPA®) (QIAGEN Inc., <https://www.qiagenbioinformatics.com/products/ingenuity-pathway-analysis>, Qiagen, Hilden, Germany).



**Figure S1. Analysis of the  $\alpha$ IL-8-dependent toxicity.** Fa2N-4 cells were co-cultivated (CC) with monocyte derived macrophages (MDMs) for 24 h. Physiological (15 %) and pro-inflammatory (50 %) MDM numbers were used. These cultivations were treated with DMSO (control), neutralising antibody ( $\alpha$ IL-8, 100 ng/ml) or adalimumab (AMB, 500 ng/ml). For each experiment (n=3) the activity of LDH was determined to exclude an acute toxic effect.

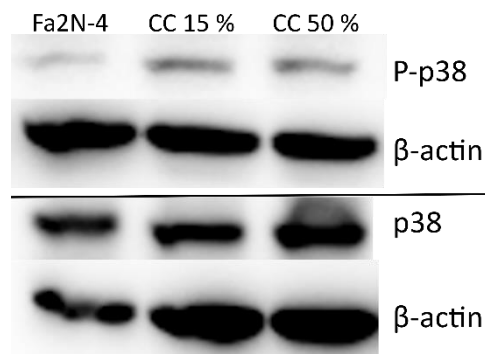


**Figure S2 western blot analysis of phosphorylation of the transcription factor p38.** Western blot analysis Fa2N-4 cells with (CC) and without the presence of monocyte derived macrophages (MDMs) after 4 h. Physiological (15 %) and pro-inflammatory (50 %) MDM numbers were used. These cultivations were treated with DMSO (control). Shown is the culture dependent phosphorylation of p38 mitogen-activated protein kinase (p38) in Fa2N-4 cells. One of three representative blots is depicted.  $\beta$  actin was used as loading control.

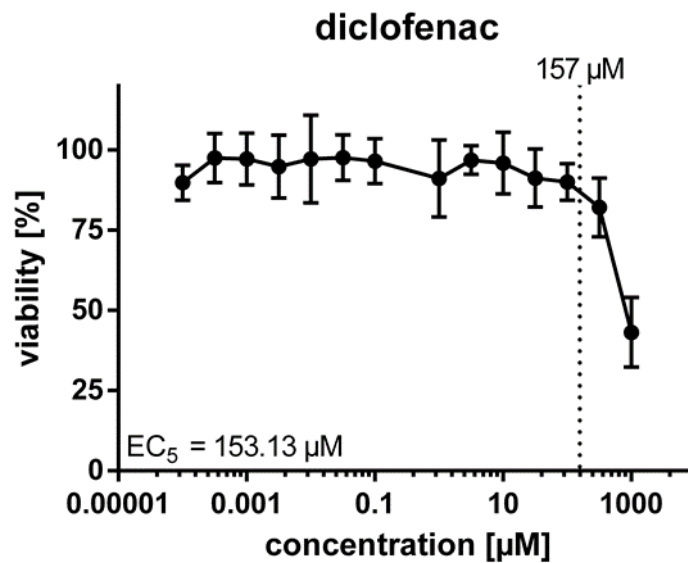


**Figure S3 analysis of the diclofenac toxicity.** Fa2N-4 cells were incubated with various concentrations of diclofenac (DCN) for 24 h (n=3). The viability was calculated related to the solvent (DMSO) control. Given are 5 % of the effective concentration ( $EC_5$ ) (calculated under the program environment R) and the toxic human serum concentration (157  $\mu\text{M}$ ).

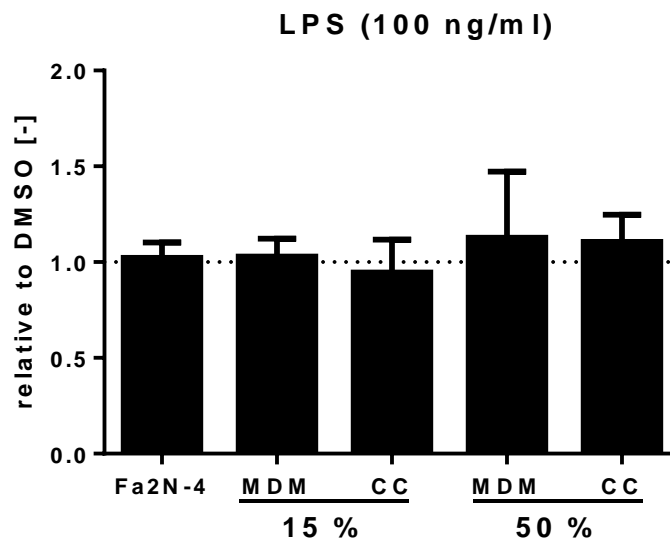


**Figure S4 analysis of the LPS toxicity.** Fa2N-4 cells were co-cultivated (CC) with monocyte derived macrophages (MDM) for 24 h. Healthy (15 %) and pro-inflammatory (50 %) MDM numbers were used. These cultivations were treated with DMSO (0.1 %) or lipopolysaccharides (LPS) (100 ng/ml). For every experiment (n=3) the activity of the LDH was determined to exclude an acute toxic effect.

Supplementary material

Padberg et al. (2021), *Toxicology in Vitro*

**Table S2 measured time dependent cytokine concentration.** Fa2N-4 cells were co-cultivated (CC) with monocyte derived macrophages (MDM). Single- (SC) and co- cultivation under physiological (15 %) and pro-inflammatory (50 %) MDM-to-Fa2N-4 ratios were used. At the indicated time, samples of the supernatant were taken and the cytokine concentration was determined. n=3

		timepoint [h]	TGF-β1 [pg/ml]			GM-CSF [pg/ml]			G-CSF [pg/ml]			FGF [pg/ml]		
			0	2.24	2.24	2.24	1.84	<1.23	1.43	5.81	6.39	7.61	83.56	<33.89
CC 15 %	0.5	2.24	2.24	2.24	<1.23	<1.23	<1.23	<5.50	<5.50	<5.50	44.56	37.71	92.23	
	1	2.24	2.24	2.24	<1.23	<1.23	1.63	<5.50	<5.50	<5.50	48.12	37.71	44.56	
	2	2.24	7.45	3.36	<1.23	11.03	2.18	<5.50	8.26	6.39	<33.89	105.76	63.12	
	4	2.24	10.79	2.24	<1.23	19.6	5.26	<5.50	<5.50	<5.50	<33.89	115.11	48.12	
	8	2.24	6.07	3.03	<1.23	28.74	16.05	6.39	6.39	<5.50	48.12	105.76	48.12	
	16	13.74	2.39	2.71	6.76	5.09	15.74	<5.50	<5.50	<5.50	55.46	63.12	48.12	
	24	17.35	9.89	27.98	10.05	19.95	58.55	<5.50	<5.50	<5.50	71.08	115.11	96.67	
	48	59.97	19.41	24.92	43.63	64.64	32.23	9.63	6.99	<5.50	1041.75	7532.51	587.05	
	0	2.24	2.24	2.24	1.84	<1.23	1.43	5.81	6.39	7.61	83.56	<33.89	55.46	
CC 50 %	0.5	2.24	2.24	2.24	<1.23	<1.23	<1.23	<5.50	<5.50	<5.50	48.12	55.46	37.71	
	1	2.24	2.24	2.24	<1.23	<1.23	<1.23	<5.50	<5.50	<5.50	63.12	37.71	63.12	
	2	3.96	2.24	2.24	<1.23	6.37	4.75	<5.50	5.81	<5.50	<33.89	92.23	71.08	
	4	2.24	2.24	2.24	<1.23	20.29	4.42	<5.50	<5.50	<5.50	37.71	75.17	<33.89	
	8	2.24	2.24	2.24	<1.23	28.32	6.37	<5.50	6.99	6.39	44.56	115.11	71.08	
	16	10.56	2.39	2.24	9.11	<1.23	20.64	<5.50	<5.50	5.81	92.23	129.62	55.46	
	24	28.98	7.66	20.41	11.54	24.31	59.87	5.81	<5.50	6.99	63.12	171.11	96.67	
	48	49.92	10.79	51.55	33.14	33.6	26.67	10.71	8.93	<5.50	938.22	1991.66	915.97	
	0	2.24	2.24	2.24	1.84	<1.23	1.43	5.81	6.39	7.61	83.56	<33.89	55.46	
Fa2N-4	SC 0.5	2.24	2.24	2.24	<1.23	<1.23	1.43	<5.50	<5.50	<5.50	44.56	44.56	48.12	
	SC 1	2.24	2.24	2.24	<1.23	<1.23	<1.23	7.61	<5.50	<5.50	<33.89	55.46	<33.89	
	SC 2	2.24	2.24	2.24	<1.23	<1.23	3.21	<5.50	5.81	5.81	37.71	37.71	71.08	
	SC 4	2.24	2.71	2.71	<1.23	26.27	4.42	<5.50	<5.50	<5.50	37.71	83.56	63.12	
	SC 8	2.24	2.24	2.24	<1.23	28.32	13.42	5.81	5.81	<5.50	55.46	55.46	63.12	
	SC 16	2.24	2.24	2.24	16.36	17.3	24.31	5.81	<5.50	<5.50	129.62	199.06	55.46	
	SC 24	2.24	3.36	7.45	5.8	22.07	40.98	<5.50	6.39	6.99	55.46	210.66	253.16	
	SC 48	15	26.19	17.35	13.98	80.48	43.09	6.39	8.93	6.39	2574.37	3619.51	1680.92	
	0	2.24	2.24	2.24	1.84	<1.23	1.43	5.81	6.39	7.61	83.56	<33.89	55.46	
MDM	SC 15 % 0.5	5.5	2.24	2.71	<1.23	<1.23	<1.23	<5.50	<5.50	<5.50	<33.89	48.12	44.56	
	SC 15 % 1	2.39	2.24	3.7	<1.23	<1.23	<1.23	<5.50	5.81	<5.50	48.12	<33.89	71.08	
	SC 15 % 2	3.96	16.68	7.96	<1.23	<1.23	<1.23	<5.50	<5.50	<5.50	44.56	48.12	<33.89	
	SC 15 % 4	2.24	38.84	7.96	<1.23	<1.23	5.8	<5.50	7.61	6.99	48.12	<33.89	83.56	
	SC 15 % 8	2.39	7.66	2.24	<1.23	<1.23	<1.23	<5.50	5.81	<5.50	37.71	44.56	<33.89	
	SC 15 % 16	7.96	2.24	10.11	<1.23	<1.23	<1.23	5.81	<5.50	<5.50	63.12	48.12	<33.89	
	SC 15 % 24	18.58	2.24	9.23	<1.23	<1.23	<1.23	<5.50	<5.50	<5.50	<33.89	<33.89	<33.89	
	SC 15 % 48	23.52	2.24	2.24	1.24	1.43	1.24	<5.50	6.39	<5.50	48.12	48.12	44.56	
	0	2.24	2.24	2.24	1.84	<1.23	1.43	5.81	6.39	7.61	83.56	<33.89	55.46	
MDM	SC 50 % 0.5	2.24	2.24	2.24	<1.23	<1.23	<1.23	<5.50	<5.50	<5.50	48.12	44.56	<33.89	
	SC 50 % 1	4.58	2.24	2.24	<1.23	<1.23	<1.23	5.81	<5.50	<5.50	55.46	55.46	63.12	
	SC 50 % 2	2.24	2.24	2.24	<1.23	<1.23	<1.23	<5.50	<5.50	<5.50	<33.89	44.56	<33.89	
	SC 50 % 4	4.94	3.03	2.24	<1.23	<1.23	<1.23	<5.50	<5.50	<5.50	37.71	55.46	<33.89	
	SC 50 % 8	2.71	2.24	4.31	<1.23	<1.23	<1.23	<5.50	<5.50	<5.50	<33.89	63.12	55.46	
	SC 50 % 16	5.5	2.24	2.24	<1.23	<1.23	<1.23	<5.50	<5.50	<5.50	<33.89	71.08	37.71	
	SC 50 % 24	37.28	6.36	9.23	<1.23	<1.23	<1.23	<5.50	<5.50	<5.50	55.46	83.56	<33.89	
	SC 50 % 48	23.52	2.24	2.71	<1.23	<1.23	<1.23	<5.50	<5.50	<5.50	<33.89	<33.89	55.46	

Supplementary material

Padberg et al. (2021), Toxicology in Vitro

Continued table S2

	timepoint [h]	CCL3 [pg/ml]			CCL20 [pg/ml]			HGF [pg/ml]			TGF-α [pg/ml]				
		0	0.98	<0.62	<0.62	1.23	<0.91	1.42	37.73	<7.29	<7.29	10.81	<5.62	<5.62	
CC 15 %	0.5	<0.62	<0.62	<0.62		1.02	<0.91	<0.91	<7.29	<7.29	<7.29	9.67	<5.62	9.12	
CC 15 %	1	<0.62	<0.62	<0.62		1.23	0.93	1.23	<7.29	<7.29	<7.29	6.56	6.09	6.56	
CC 15 %	2	<0.62		9.96	2.11	<0.91	1.62	1.82	<7.29	<7.29	14.33	10.23	7.05	7.54	
CC 15 %	4	<0.62		10.42	2.4		1.13	1.34	1.54	<7.29	<7.29	8.05	11.4	8.05	
CC 15 %	8	<0.62		9.74	2.4		1.13	<0.91	0.93	<7.29		9.67	8.05	6.09	
CC 15 %	16		14.99	4.68	<0.62	<0.91	2.36	<0.91	9.47	34.43	14.33	8.05	12.62	7.54	
CC 15 %	24		19.15	13.62	30.1		0.93	2.75	0.93	<7.29	26.82	<7.29	9.67	9.67	
CC 15 %	48		61.42	18.89	27.72		8.66	24.31	2.46	<7.29	9.47	<7.29	13.25	13.89	
	0		0.98	<0.62	<0.62		1.23	<0.91	1.42	37.73	<7.29	<7.29	10.81	<5.62	
CC 50 %	0.5	<0.62	<0.62	<0.62	<0.91		1.23	<0.91	<7.29	<7.29	<7.29	8.05	<5.62	6.09	
CC 50 %	1	<0.62	<0.62	<0.62	<0.91	<0.91		<0.91		12.27	<7.29	8.58	7.54	6.56	
CC 50 %	2	<0.62	<0.62	<0.62	<0.91		1.23	<0.91	<7.29		9.47	<7.29	9.12	8.05	
CC 50 %	4	<0.62	<0.62	<0.62	<0.91		1.74	<0.91	<7.29	<7.29		9.67	6.56	6.09	
CC 50 %	8	<0.62	<0.62	<0.62		1.13	1.54		1.13	<7.29		9.47	<7.29	<5.62	
CC 50 %	16		11	<0.62	<0.62		1.02	1.54	1.42	12.27	20.11	<7.29	<5.62	9.67	
CC 50 %	24		30.92	7.41	22.49	<0.91	2.85	<0.91		<7.29	54.37	14.33	5.63	6.09	
CC 50 %	48		51.82	12.77	52.26		12.48	14.71	5.97	<7.29	9.47	<7.29	15.89	12.62	
	0		0.98	<0.62	<0.62		1.23	<0.91	1.42	37.73	<7.29	<7.29	10.81	<5.62	
Fa2N-4	SC	0.5	<0.62	<0.62	<0.62	<0.91	<0.91	<0.91	<7.29	<7.29	<7.29	7.54	<5.62	6.09	
	SC	1	<0.62	<0.62	<0.62	<0.91	<0.91		1.62	<7.29	<7.29	<5.62	8.05	10.23	
	SC	2	<0.62	<0.62	<0.62	<0.91	<0.91		1.23	<7.29	<7.29	7.54	10.23	16.58	
	SC	4	<0.62	<0.62	<0.62		1.42	1.62	1.02	<7.29	<7.29	<5.62	12	<5.62	
	SC	8	<0.62	<0.62	<0.62		1.02	1.34	1.13	<7.29		12.27	7.05	9.12	
	SC	16	<0.62	<0.62	<0.62		2.04	1.95	1.23	9.47	20.11	<7.29	10.23	9.12	
	SC	24	<0.62		2.79	5.82		1.42	4.79	3.06	9.47	17.69	<7.29	8.05	6.09
	SC	48		18.22	25.88	18.62		22.94	32.72	15.59	12.27	9.47	<7.29	11.4	12
	0		0.98	<0.62	<0.62		1.23	<0.91	1.42	37.73	<7.29	<7.29	10.81	<5.62	
MDM	SC 15 %	0.5		0.98	<0.62	<0.62		1.13	<0.91	2.04	<7.29	<7.29	7.05	6.09	
	SC 15 %	1	<0.62	<0.62	<0.62		2.79	1.23	1.02	<0.91	<7.29	12.27	<5.62	7.05	
	SC 15 %	2	<0.62		18.75	0.98		1.02	<0.91	<0.91	<7.29	<7.29	<5.62	5.63	
	SC 15 %	4	<0.62		38.73	7.95	<0.91	1.13		0.93	<7.29	20.11	14.33	8.05	
	SC 15 %	8	<0.62		16.26	4.07		1.13	1.95	<0.91	17.69	50.42	<7.29	8.05	
	SC 15 %	16		7.41	<0.62	7.95		1.34	1.82	<0.91	<7.29	9.47	<7.29	7.54	
	SC 15 %	24		20.25	<0.62	9.28	<0.91	<0.91	<0.91	<7.29	12.27	<7.29	<5.62	6.09	
	SC 15 %	48		25.28	<0.62	<0.62		0.93	1.23	<0.91	12.27	<7.29	<7.29	9.67	
	0		0.98	<0.62	<0.62		1.23	<0.91	1.42	37.73	<7.29	<7.29	10.81	<5.62	
MDM	SC 50 %	0.5	<0.62	<0.62	<0.62	<0.91	<0.91	<0.91	<7.29	<7.29	<7.29	6.09	<5.62	7.54	
	SC 50 %	1		2.4	<0.62	<0.62	<0.91	<0.91	<0.91	<7.29	<7.29	12	<5.62	<5.62	
	SC 50 %	2	<0.62	<0.62	<0.62		0.93	<0.91	0.93		9.47	<7.29	6.56	6.09	
	SC 50 %	4		4.68	<0.62	<0.62	<0.91	<0.91	<0.91	<7.29	9.47	<7.29	6.56	<5.62	
	SC 50 %	8		1.73	<0.62	<0.62	<0.91	<0.91	<0.91	<7.29	<7.29	7.54	5.63	<5.62	
	SC 50 %	16		7.95	<0.62	1.36	<0.91	1.13	<0.91	<7.29	26.82	<7.29	7.05	9.12	
	SC 50 %	24		39.85	6.87	9.74	<0.91	1.74	<0.91		9.47	37.73	<7.29	8.58	
	SC 50 %	48		24.68	<0.62	<0.62	<0.91	<0.91	<0.91	17.69	12.27	<7.29	<5.62	<5.62	

Supplementary material

Padberg et al. (2021), Toxicology in Vitro

Continued table S2

	timepoint [h]	IL-1β [pg/ml]			TNF-α [pg/ml]			MCP-1 [pg/ml]			IL-6 [pg/ml]			
		0	1.17	1.17	1.17	0.81	0.81	2.12	2.04	<0.87	1.48	2.47	<1.43	<1.43
CC 15 %	0.5	1.4	1.17	3.52	1.18	0.81	0.81	<0.87	<0.87	<0.87	<1.43	<1.43	<1.43	
CC 15 %	1	1.17	1.17	4.37	1	0.81	0.81	<0.87	<0.87	1.61	<1.43	<1.43	2.47	
CC 15 %	2	1.17	11.48	3.3	0.92	0.81	0.81	<0.87	3.15	1.23	<1.43	19.86	<1.43	
CC 15 %	4	1.17	14.42	1.17	0.81	0.81	0.92	0.94	1.23	1.75	2.47	28.52	7.14	
CC 15 %	8	1.17	15.18	9.26	0.81	0.81	0.81	1.23	2.52	2.2	4.05	30.17	18.1	
CC 15 %	16	7.12	1.17	3.3	0.81	0.81	1.25	3.44	0.94	2.04	28.25	<1.43	16.42	
CC 15 %	24	20.41	1.17	24.28	0.81	0.81	0.81	2.78	1.11	1.11	100.78	<1.43	75.92	
CC 15 %	48	30.62	24.56	28.07	1.25	5.66	0.85	5.56	7.76	3.64	388.84	392.22	141.22	
	0	1.17	1.17	1.17	0.81	0.81	2.12	2.04	<0.87	1.48	2.47	<1.43	<1.43	
CC 50 %	0.5	3.74	1.17	3.3	0.92	0.81	1.18	<0.87	1.48	<0.87	<1.43	2.03	<1.43	
CC 50 %	1	1.17	2.91	5.93	0.81	0.81	0.81	<0.87	1.61	1.11	<1.43	<1.43	2.03	
CC 50 %	2	1.24	8.85	2.72	0.81	0.81	0.81	<0.87	4.16	1.48	<1.43	21.47	4.57	
CC 50 %	4	1.17	12.46	3.3	0.81	0.81	0.81	1.11	1.11	1.23	5.82	13.83	9.7	
CC 50 %	8	2.48	16.39	4.37	0.81	0.81	0.81	2.2	1.61	2.78	15.6	20.54	18.76	
CC 50 %	16	19.46	9.53	5.54	0.85	0.81	0.85	1.48	5.19	2.96	92.62	30.17	16.83	
CC 50 %	24	19.93	1.17	26.86	1.54	0.81	1.63	3.34	1.11	3.95	213.47	<1.43	204.14	
CC 50 %	48	41.43	34.78	31.62	2.23	0.81	0.81	7.31	7.61	4.72	892.29	372.49	443.77	
	0	1.17	1.17	1.17	0.81	0.81	2.12	2.04	<0.87	1.48	2.47	<1.43	<1.43	
Fa2N-4	SC	0.5	1.57	1.17	1.17	0.81	0.81	0.81	<0.87	<0.87	<1.43	<1.43	<1.43	
	SC	1	1.57	1.17	1.17	0.81	0.81	0.81	<0.87	<0.87	<1.43	<1.43	2.03	
	SC	2	1.17	1.17	3.52	0.85	0.85	0.81	1.48	2.36	1.48	<1.43	1.71	<1.43
	SC	4	1.17	1.17	1.17	0.81	0.81	0.81	<0.87	<0.87	0.94	<1.43	2.36	3.42
	SC	8	1.57	5.54	9.96	0.81	0.81	1.25	<0.87	<0.87	1.23	2.36	2.7	15.2
	SC	16	8.59	1.17	1.4	0.81	0.81	1.18	1.48	1.48	1.11	20.09	<1.43	6.54
	SC	24	13.51	1.17	9.96	0.81	0.81	0.81	3.95	1.23	2.04	36.71	<1.43	50.05
	SC	48	24.28	19.46	24.56	0.81	0.81	0.81	6.61	5.68	2.7	145.28	195.28	176.29
	0	1.17	1.17	1.17	0.81	0.81	2.12	2.04	<0.87	1.48	2.47	<1.43	<1.43	
MDM	SC 15 %	0.5	6.46	1.17	1.94	1.91	1.63	0.81	<0.87	1.11	1.35	1.71	4.44	2.94
	SC 15 %	1	1.17	1.17	1.17	0.81	0.81	0.81	<0.87	<0.87	2.36	<1.43	1.92	4.18
	SC 15 %	2	1.17	6.46	1.94	0.92	0.81	1.18	<0.87	4.38	2.2	2.82	12.7	14.41
	SC 15 %	4	1.17	19.22	1.17	0.81	0.81	0.81	<0.87	4.38	3.15	1.61	41.99	9.2
	SC 15 %	8	1.17	10.25	9.82	0.81	2.42	0.81	<0.87	6.07	4.72	2.82	18.32	23.38
	SC 15 %	16	7.83	1.17	14.42	0.81	0.81	0.81	1.11	1.23	3.84	2.7	<1.43	52.03
	SC 15 %	24	18.31	1.17	14.23	0.81	0.81	0.81	3.84	2.2	4.38	10.38	5.12	31.3
	SC 15 %	48	29.01	3.3	1.17	0.81	0.81	0.81	3.64	1.61	1.61	15.6	<1.43	4.84
	0	1.17	1.17	1.17	0.81	0.81	2.12	2.04	<0.87	1.48	2.47	<1.43	<1.43	
MDM	SC 50 %	0.5	4.37	2.48	1.17	0.81	0.81	1.43	<0.87	<0.87	<0.87	3.18	<1.43	5.39
	SC 50 %	1	1.4	1.17	1.17	0.81	0.81	0.81	1.11	0.94	1.89	2.14	1.92	6.69
	SC 50 %	2	1.17	1.17	3.52	0.81	0.81	1	<0.87	2.52	5.19	2.47	16.42	24.86
	SC 50 %	4	3.52	1.17	1.17	0.81	0.81	0.81	2.52	4.16	4.83	4.57	16.01	11.07
	SC 50 %	8	6.89	1.17	7.59	0.81	0.81	0.92	2.04	4.72	4.83	4.57	17.68	29.61
	SC 50 %	16	9.26	1.17	11.8	0.81	0.81	0.81	4.72	1.35	4.38	16.21	<1.43	16.63
	SC 50 %	24	26.57	1.17	21.39	1.09	0.81	1.43	5.56	0.94	5.68	16.21	<1.43	19.64
	SC 50 %	48	27.16	10.7	1.4	2.3	0.85	0.81	2.96	3.64	2.78	12.7	13.83	15.2

Supplementary material

Padberg et al. (2021), Toxicology in Vitro

Continued table S2

	timepoint [h]	IL-8 [pg/ml]			IL-10 [pg/ml]			IL-12 [pg/ml]			IL-18 [pg/ml]				
	0	3.93	2.42	2.42	<0.96	<0.96	1.69	<0.76	<0.76	<0.76	<0.88	<0.88	<0.88		
	0	3.93	2.42	2.42	<0.96	<0.96	1.69	<0.76	<0.76	<0.76	<0.88	<0.88	<0.88		
CC 15 %	0.5	4.83	2.42	5.06	1.32	<0.96	<0.96	<0.76	<0.76	<0.76	1.8	0.9	2.21		
CC 15 %	1	3.93	6.4	8.55	<0.96	<0.96	<0.96	<0.76	<0.76	<0.76	<0.88	1.38	2.4		
CC 15 %	2	7.37	52.39	15.18	1.4	<0.96	<0.96	1.46	<0.76	<0.76	1.64	3.41	1.74		
CC 15 %	4	6.4	97.93	24.79	1.69	<0.96	<0.96	<0.76	<0.76	<0.76	2.09	5.51	2.4		
CC 15 %	8	7.57	117.52	41.63	<0.96	<0.96	<0.96	<0.76	<0.76	<0.76	1.38	5	2.4		
CC 15 %	16	81.34	2.42	24.27	<0.96	<0.96	<0.96	<0.76	<0.76	<0.76	3.41	<0.88	3.82		
CC 15 %	24	119.56	2.42	320.24	1.32	<0.96	<0.96	<0.76	<0.76	0.97	6.15	0.9	5.4		
CC 15 %	48	1107.28	627.42	244.15	<0.96	<0.96	<0.96	<0.76	<0.76	<0.76	7.19	14.37	3.18		
	0	3.93	2.42	2.42	<0.96	<0.96	1.69	<0.76	<0.76	<0.76	<0.88	<0.88	<0.88		
CC 50 %	0.5	2.42	3.33	9.26	<0.96	<0.96	<0.96	<0.76	<0.76	<0.76	0.9	1.19	1.06		
CC 50 %	1	4.61	4.61	11.5	1.23	<0.96	<0.96	<0.76	<0.76	<0.76	1.06	1.64	1.06		
CC 50 %	2	3.74	58.62	12.39	<0.96	<0.96	<0.96	<0.76	<0.76	<0.76	<0.88	3.26	2.28		
CC 50 %	4	10.27	60.27	15.91	<0.96	<0.96	<0.96	<0.76	<0.76	<0.76	2.21	3.65	1.8		
CC 50 %	8	21.55	73.03	24.27	<0.96	<0.96	<0.96	<0.76	<0.76	<0.76	3.99	2.6	3.26		
CC 50 %	16	111.59	35.2	27.83	<0.96	<0.96	1.23	<0.76	<0.76	<0.76	6.48	4.71	2.6		
CC 50 %	24	386.62	2.42	455.42	<0.96	<0.96	1.5	<0.76	<0.76	<0.76	4.62	<0.88	6.04		
CC 50 %	48	3166.98	322.88	1237.06	<0.96	<0.96	<0.96	<0.76	0.97	<0.76	7.81	10.93	7.31		
	0	3.93	2.42	2.42	<0.96	<0.96	1.69	<0.76	<0.76	<0.76	<0.88	<0.88	<0.88		
Fa2N-4	SC	0.5	2.42	2.42	2.42	1.15	<0.96	<0.96	<0.76	0.81	<0.76	<0.88	<0.88	1.38	
	SC	1	2.42	2.42	2.42	1.06	<0.96	1.58	0.81	<0.76	0.81	0.98	1.38	2.09	
	SC	2	2.42	2.42	8.11	<0.96	<0.96	<0.96	<0.76	1.01	1.46	1.48	1.15	2.4	
	SC	4	2.42	13	4.4	<0.96	<0.96	1.23	<0.76	<0.76	<0.76	<0.88	1.53	2.09	
	SC	8	4.61	14.83	29.31	2.16	<0.96	<0.96	<0.76	<0.76	0.77	2.6	1.8	5.2	
	SC	16	47.65	2.42	7.17	<0.96	<0.96	<0.96	<0.76	<0.76	<0.76	3.99	0.98	1.91	
	SC	24	63.12	2.42	67.3	1.32	<0.96	<0.96	<0.76	<0.76	<0.76	4.25	<0.88	3.49	
	SC	48	265.12	221.09	105.01	<0.96	<0.96	<0.96	0.81	<0.76	<0.76	6.83	4.25	4.08	
		0	3.93	2.42	2.42	<0.96	<0.96	1.69	<0.76	<0.76	<0.76	<0.88	<0.88	<0.88	
MDM	SC 15 %	0.5	24.53	2.42	8.33	1.15	<0.96	1.15	<0.96	0.81	0.77	<0.76	<0.88	<0.88	2.03
	SC 15 %	1	8.55	2.42	10.27	<0.96	<0.96	1.58	<0.76	<0.76	<0.76	<0.88	<0.88	1.06	
	SC 15 %	2	4.83	31.82	14.14	<0.96	<0.96	<0.96	<0.76	0.77	0.81	<0.88	2.03	1.8	
	SC 15 %	4	7.17	104.1	10.67	<0.96	<0.96	1.23	<0.76	<0.76	<0.76	<0.88	1.38	<0.88	
	SC 15 %	8	12.69	64.88	35.2	<0.96	<0.96	<0.96	0.81	0.97	0.97	<0.88	2.74	1.74	
	SC 15 %	16	26.14	2.42	73.69	<0.96	<0.96	<0.96	<0.76	<0.76	<0.76	<0.88	<0.88	1.53	
	SC 15 %	24	92.9	18.87	87.33	<0.96	2.16	<0.96	<0.76	1.8	<0.76	<0.88	0.98	2.4	
	SC 15 %	48	187.23	6.4	6.22	<0.96	1.15	<0.96	<0.76	<0.76	<0.76	1.48	1.29	1.48	
		0	3.93	2.42	2.42	<0.96	<0.96	1.69	<0.76	<0.76	<0.76	<0.88	<0.88	<0.88	
MDM	SC 50 %	0.5	13.16	2.42	11.5	<0.96	<0.96	1.69	0.92	<0.76	<0.76	<0.88	1.53	2.28	
	SC 50 %	1	20.17	3.11	3.74	<0.96	<0.96	<0.96	<0.76	<0.76	<0.76	0.98	<0.88	1.06	
	SC 50 %	2	17.44	5.06	16.09	1.23	<0.96	1.78	<0.76	<0.76	1.19	<0.88	<0.88	1.48	
	SC 50 %	4	26.41	19.95	9.5	<0.96	<0.96	<0.96	<0.76	<0.76	<0.76	<0.88	1.91	<0.88	
	SC 50 %	8	30.54	18.45	42.45	0.98	<0.96	2.85	0.77	<0.76	<0.76	<0.88	2.03	1.74	
	SC 50 %	16	56.48	2.42	49.97	<0.96	<0.96	1.96	<0.76	<0.76	<0.76	0.9	<0.88	<0.88	
	SC 50 %	24	423.06	4.4	178.07	1.06	<0.96	1.78	<0.76	<0.76	<0.76	1.19	<0.88	1.38	
	SC 50 %	48	607.07	25.32	11.5	<0.96	1.4	<0.96	<0.76	<0.76	0.81	0.9	2.28	1.48	













Supplementary material

Padberg et al. (2021), *Toxicology in Vitro*

**Table S4 particular fold changes of DCN and LPS specific alterations of the cytokine secretion pattern.**

Fa2N-4 cells were co-cultivated (CC) with monocyte derived macrophages (MDM) for 24 h. Single- (SC) and co- cultivation under physiological (15 %) and pro-inflammatory (50 %) MDM-to-Fa2N-4 ratios were used. All measured cytokine concentrations were related to the corresponding control (fold change) to analyse the effect of diclofenac (DCN, 157 µM) and lipopolysaccharides (LPS, 100 ng/ml).

				TGF-β1			GM-CSF			G-CSF			FGF			CCL3			CCL20		
	cultivation	celltype	time [h]																		
157 µM DCN	SC 15 %	MDM	24	0.25	0.73	0.06	1	1	1	2.304	0.555	0.362	1	0.825	0.559	0.309	0.282	2.34	0.193	0.699	0.103
	SC 50 %	MDM		0.13	0.46	0.64	1	1	1	2.304	0.479	2.088	3.48	0.094	0.406	0.309	0.381	0.404	3.027	0.588	1
	SC	Fa2N4		4.11	0.16	6.26	0.066	1	0.491	1.103	0.434	1.092	0.559	0.287	0.362	1.086	2.035	4.627	1	1	8.874
	CC 15 %	Fa2N4/MDM		0.53	0.43	0.54	0.304	0.304	1	0.659	0.308	0.573	0.371	0.149	0.701	0.493	0.874	0.614	4.407	0.348	4.552
	CC 50%	Fa2N4/MDM		1.32	0.54	7.75	1	1	0.712	1.556	1.103	1	3.793	4.905	0.653	3.694	0.562	1.668	1.431	1	0.469
100 ng/ml LPS	SC 15 %	MDM	24	3.86	0.02	0.24	1	1	1	2.528	0.555	0.757	6.703	1	0.2	3.931	0.107	2.507	1.154	0.193	1.31
	SC 50 %	MDM		1.93	3.07	1.53	1	1	1	2.528	1.322	2.304	9.565	0.472	0.583	2.215	3.512	0.777	2.445	0.276	0.411
	SC	Fa2N4		0.26	1.37	1.53	0.956	1	7.156	1.103	1	0.911	2.781	3.045	1.957	0.517	1	2.292	0.276	1	4.407
	CC 15 %	Fa2N4/MDM		0.65	2.56	3.2	1.881	0.304	3.29	0.659	1	0.249	1.817	0.417	0.701	0.554	2.941	4.176	3.63	0.742	0.469
	CC 50%	Fa2N4/MDM		0.03	32.2	242	1	5.159	2.922	1	2.617	1.177	2.087	8.708	1.192	0.277	41.36	30.13	0.588	2.874	0.469
				HGF			TGF-α			IL-1β			TNF-α			MCP-1					
	cultivation	celltype	time [h]																		
157 µM DCN	SC 15 %	MDM	24	1	1	0.07	2.478	0.234	1	1.042	1.091	0.466	0.613	0.61	0.519	0.385	0.368	0.128			
	SC 50 %	MDM		2.51	1	1	1	0.404	2.92	1.099	0.865	0.41	0.644	0.504	0.803	0.566	0.288	0.109			
	SC	Fa2N4		1	1	8.1	3.404	1	3.404	1	1	1	0.571	0.5	0.893	0.397	0.456	0.444			
	CC 15 %	Fa2N4/MDM		6.34	15	10.9	1.601	1.48	0.886	2.146	0.427	1	0.487	1	0.968	0.311	0.215	0.2			
	CC 50%	Fa2N4/MDM		1	1	0.44	3.569	1.633	1.179	2.439	1	0.983	1.034	1.149	0.548	0.327	0.307	0.238			
100 ng/ml LPS	SC 15 %	MDM	24	16.1	1	0.39	1	0.234	3.239	2.281	1.489	1.739	1.411	0.596	0.929	1.461	0.191	0.072			
	SC 50 %	MDM		17.2	1	1	2.478	0.404	3.08	1.248	1.595	0.41	1.131	7.093	3.141	0.255	0.209	4.008			
	SC	Fa2N4		1	2.51	1	3.74	0.746	2.767	1	2.537	1	0.571	2.38	1.471	0.265	0.835	1.062			
	CC 15 %	Fa2N4/MDM		1	1	1	1.25	0.746	0.404	2.439	1.156	1	0.487	2.791	2.722	0.208	0.132	0.944			
	CC 50%	Fa2N4/MDM		14	1	0.11	2.065	1.236	1	2.341	2.756	0.712	2	3.397	1.117	0.178	1.078	0.986			
				IL-6			IL-8			IL-10			IL-12			IL-18					
	cultivation	celltype	time [h]																		
157 µM DCN	SC 15 %	MDM	24	0.35	1	1	0.1	0.132	0.097	1	1	1	2.889	0.429	1	0.955	0.328	0.358			
	SC 50 %	MDM		0.88	1	0.33	0.343	0.264	0.066	1	1	1	1	1	1	1.444	0.358	2.128			
	SC	Fa2N4		2.66	1.75	0.69	0.892	0.673	0.019	1	1	1	1	1	0.321	1.277	1.193	0.957			
	CC 15 %	Fa2N4/MDM		0.8	0.89	0.47	0.658	0.422	0.078	1	1	1	1	3.667	0.346	1.509	1.412	0.4			
	CC 50%	Fa2N4/MDM		0.98	1.32	1.53	0.598	0.631	0.272	1	2.231	1	1	2.2	1	1.217	1.631	1.133			
100 ng/ml LPS	SC 15 %	MDM	24	0.55	12.6	1	0.849	0.161	0.078	1	1	2.678	1	2.714	4.111	0.73	1	0.954			
	SC 50 %	MDM		4.12	210	6.97	0.418	0.468	0.655	1	1	1	2.889	4.111	1	1.233	1.514	3.487			
	SC	Fa2N4		2.09	0.58	0.76	0.965	0.269	0.588	1	1	1	1	1	0.679	1.79	2.514	0.676			
	CC 15 %	Fa2N4/MDM		1.67	1.53	4.52	0.639	0.904	3.811	1	4.893	2.298	2.444	6.333	0.731	1.096	1.588	0.558			
	CC 50%	Fa2N4/MDM		1.25	4.12	7.37	0.249	3.033	6.214	1	14.25	4.992	3.889	1.517	5	1.149	2.565	0.88			

Supplementary material

Padberg et al. (2021), *Toxicology in Vitro*

**Table S5 measured time dependent cytokine concentration.** HepG2 cells were co-cultivated (CC) with PMA differentiated THP-1 cells. Single- (SC) and co- cultivation under physiological (15 %) and pro-inflammatory (50 %) THP-1-to-HepG2 ratios were used. At the indicated time, samples of the supernatant were taken and the cytokine concentration was determined. n=3

		timepoint [h]	TGF-β1 pg/ml			GM-CSF pg/ml			G-CSF pg/ml			FGF pg/ml		
		0	1.02	<0.97	3.05	<0.54	<0.54	0.65	<1.31	<1.31	<1.31	<69.38	234.54	<69.38
CC 15 %	HepG2/THP-1	0.5	5.17	<0.97	3.96	<0.54	<0.54	<0.54	4.39	4.39	6.05	<69.38	<69.38	<69.38
CC 15 %	HepG2/THP-1	1	1.94	<0.97	1.52	<0.54	<0.54	0.65	2.79	<1.31	2.03	234.54	<69.38	<69.38
CC 15 %	HepG2/THP-1	2	4.15	<0.97	1.8	0.86	1.35	0.94	13.16	8.63	7.76	651.09	<69.38	<69.38
CC 15 %	HepG2/THP-1	4	5.17	1.52	3.41	2.47	9.33	2.85	34.33	51.26	35.42	234.54	318.92	318.92
CC 15 %	HepG2/THP-1	8	15.02	<0.97	6.98	4.34	10.28	7.15	40.93	70.85	92.05	485.76	<69.38	568.56
CC 15 %	HepG2/THP-1	16	21.24	2.24	4.15	4.02	9.86	4.43	30.06	31.12	34.33	651.09	<69.38	318.92
CC 15 %	HepG2/THP-1	24	1.52	1.8	1.26	0.79	13.01	8.44	7.76	57.21	116.37	<69.38	318.92	318.92
CC 15 %	HepG2/THP-1	48	<0.97	9	13.71	0.65	24.5	5.13	5.21	154.07	52.44	<69.38	568.56	318.92
		0	1.02	<0.97	3.05	<0.54	<0.54	0.65	<1.31	<1.31	<1.31	<69.38	234.54	<69.38
CC 50 %	HepG2/THP-1	0.5	6.05	<0.97	1.26	<0.54	<0.54	0.59	7.76	5.21	5.21	402.59	234.54	<69.38
CC 50 %	HepG2/THP-1	1	3.41	1.26	1.02	0.65	<0.54	0.65	5.21	<1.31	2.79	318.92	<69.38	402.59
CC 50 %	HepG2/THP-1	2	6.05	1.52	<0.97	1.22	1.35	1.09	15.98	9.52	9.52	402.59	<69.38	234.54
CC 50 %	HepG2/THP-1	4	5.38	<0.97	2.24	4.51	3.78	1.54	85.25	39.82	15.98	<69.38	<69.38	<69.38
CC 50 %	HepG2/THP-1	8	13.07	<0.97	4.15	13.01	29.88	4.02	213.02	374.6	37.6	568.56	<69.38	402.59
CC 50 %	HepG2/THP-1	16	25.81	3.05	4.15	12.85	24.76	9.59	60.86	178.01	90.67	234.54	234.54	318.92
CC 50 %	HepG2/THP-1	24	75.23	1.94	1.94	16.78	1.13	5.22	137.86	8.63	47.76	234.54	<69.38	<69.38
CC 50 %	HepG2/THP-1	48	26.69	1.8	20.84	17.99	1.01	10.28	90.67	4.39	120.86	149.07	<69.38	<69.38
		0	1.02	<0.97	3.05	<0.54	<0.54	0.65	<1.31	<1.31	<1.31	<69.38	234.54	<69.38
SC	HepG2	0.5	<0.97	1.26	2.72	<0.54	<0.54	<0.54	<1.31	<1.31	2.79	<69.38	<69.38	149.07
SC	HepG2	1	1.94	<0.97	2.55	0.59	<0.54	0.72	<1.31	<1.31	2.03	<69.38	<69.38	149.07
SC	HepG2	2	4.15	1.52	1.26	<0.54	1.22	0.59	2.79	9.52	2.79	<69.38	485.76	<69.38
SC	HepG2	4	4.15	<0.97	1.94	<0.54	<0.54	<0.54	<1.31	<1.31	2.03	<69.38	<69.38	234.54
SC	HepG2	8	13.39	1.02	1.8	0.59	<0.54	0.65	2.03	<1.31	5.21	402.59	<69.38	<69.38
SC	HepG2	16	19.68	3.05	3.96	0.59	0.79	0.79	5.21	2.79	5.21	<69.38	<69.38	318.92
SC	HepG2	24	1.8	3.05	<0.97	0.86	31.44	0.65	7.76	277.03	4.39	318.92	<69.38	<69.38
SC	HepG2	48	98.23	2.55	22.44	0.72	34.43	0.86	7.76	369.27	5.21	<69.38	815.57	149.07
		0	1.02	<0.97	3.05	<0.54	<0.54	0.65	<1.31	<1.31	<1.31	<69.38	234.54	<69.38
SC 15 %	THP-1	0.5	<0.97	<0.97	3.05	<0.54	0.65	0.59	<1.31	<1.31	<1.31	<69.38	<69.38	<69.38
SC 15 %	THP-1	1	2.24	<0.97	1.52	<0.54	<0.54	0.65	<1.31	<1.31	2.03	149.07	<69.38	<69.38
SC 15 %	THP-1	2	<0.97	1.02	<0.97	<0.54	<0.54	<0.54	<1.31	<1.31	<1.31	<69.38	<69.38	<69.38
SC 15 %	THP-1	4	1.26	<0.97	1.02	0.72	<0.54	0.59	2.79	<1.31	<1.31	<69.38	<69.38	234.54
SC 15 %	THP-1	8	<0.97	<0.97	<0.97	<0.54	<0.54	<0.54	2.79	<1.31	<1.31	<69.38	<69.38	149.07
SC 15 %	THP-1	16	66.67	1.52	1.26	6.71	1.84	0.79	65.81	19.86	4.39	149.07	149.07	149.07
SC 15 %	THP-1	24	25.38	1.52	<0.97	7.95	1.13	0.72	58.42	8.63	2.03	485.76	568.56	234.54
SC 15 %	THP-1	48	1.52	<0.97	1.52	1.31	1.09	1.44	16.94	15.03	6.05	318.92	149.07	318.92
		0	1.02	<0.97	3.05	<0.54	<0.54	0.65	<1.31	<1.31	<1.31	<69.38	234.54	<69.38
SC 50 %	THP-1	0.5	<0.97	1.26	2.72	<0.54	<0.54	<0.54	<1.31	<1.31	<1.31	<69.38	<69.38	149.07
SC 50 %	THP-1	1	1.52	<0.97	1.02	<0.54	<0.54	<0.54	<1.31	<1.31	<1.31	234.54	<69.38	149.07
SC 50 %	THP-1	2	1.8	<0.97	1.8	<0.54	0.79	0.59	2.79	5.21	<1.31	318.92	<69.38	<69.38
SC 50 %	THP-1	4	9.55	<0.97	<0.97	0.59	<0.54	<0.54	13.16	<1.31	<1.31	2046.19	<69.38	402.59
SC 50 %	THP-1	8	1.02	<0.97	1.26	0.59	0.65	0.59	7.76	4.39	5.21	<69.38	<69.38	402.59
SC 50 %	THP-1	16	1.8	2.24	1.02	1.31	1.74	1.13	7.76	15.98	2.79	651.09	<69.38	318.92
SC 50 %	THP-1	24	54.04	<0.97	1.52	0.65	0.94	0.79	7.76	6.05	5.21	<69.38	<69.38	402.59
SC 50 %	THP-1	48	3.59	<0.97	<0.97	1.59	1.09	1.74	11.32	11.32	6.05	318.92	402.59	<69.38







Supplementary material

Padberg et al. (2021), *Toxicology in Vitro*

Continued table S5

		timepoint	IL-8			IL-10			IL-12			IL-18		
		[h]	pg/ml			pg/ml			pg/ml			pg/ml		
		0	11.29	101.54	<0.47	0.78	0.98	1.17	<0.91	<0.91	<0.91	<0.17	0.89	0.89
CC 15 %	HepG2/THP-1	0.5	36.17	16.7	47.32	1.09	<0.44	0.94	<0.91	<0.91	<0.91	0.4	1.02	0.37
CC 15 %	HepG2/THP-1	1	32919	132	168.58	26.52	1.3	3.38	<0.91	<0.91	<0.91	0.5	1.27	1.37
CC 15 %	HepG2/THP-1	2	1200	1732.62	1254.45	0.98	1.3	3.07	<0.91	<0.91	<0.91	<0.17	1.48	1.95
CC 15 %	HepG2/THP-1	4	110.4	7858.48	4847.15	<0.44	1.09	6.06	<0.91	<0.91	<0.91	<0.17	0.4	0.89
CC 15 %	HepG2/THP-1	8	9863	18196.56	14200.04	1.3	6.55	5.38	<0.91	<0.91	<0.91	0.17	1.77	0.72
CC 15 %	HepG2/THP-1	16	8504	15697	8368.85	2.12	2.37	3.63	<0.91	<0.91	<0.91	<0.17	<0.17	<0.17
CC 15 %	HepG2/THP-1	24	25231	>33713.06	25231.2	19.04	4.95	10.23	<0.91	<0.91	<0.91	<0.17	0.24	0.57
CC 15 %	HepG2/THP-1	48	19015	32007.7	25875.78	8.93	5.38	8.62	<0.91	<0.91	<0.91	0.21	0.29	0.4
		0	11.29	101.54	<0.47	0.78	0.98	1.17	<0.91	<0.91	<0.91	<0.17	0.89	0.89
CC 50 %	HepG2/THP-1	0.5	68.42	176.61	61.16	<0.44	1.17	0.98	<0.91	<0.91	<0.91	<0.17	0.6	0.37
CC 50 %	HepG2/THP-1	1	31133	22871.2	<0.47	27.89	46.75	<0.44	<0.91	<0.91	<0.91	2.71	0.17	<0.17
CC 50 %	HepG2/THP-1	2	1436	1490.29	1836.05	0.87	1.22	3.38	<0.91	<0.91	<0.91	0.93	3.26	1.89
CC 50 %	HepG2/THP-1	4	1336	3960.9	2265.51	8.62	2.12	0.45	<0.91	<0.91	<0.91	<0.17	2.71	0.6
CC 50 %	HepG2/THP-1	8	580.5	26544.37	6856.66	5.38	9.56	1.89	<0.91	<0.91	<0.91	0.89	1.37	0.29
CC 50 %	HepG2/THP-1	16	17806	26544.37	14200.04	2.37	5.38	6.06	<0.91	<0.91	<0.91	<0.17	0.76	0.68
CC 50 %	HepG2/THP-1	24	22871	2174.58	13925.03	7.75	<0.44	5.83	<0.91	<0.91	<0.91	2.08	<0.17	0.47
CC 50 %	HepG2/THP-1	48	21304	767.22	24009.57	8.62	<0.44	9.08	<0.91	<0.91	<0.91	1.37	<0.17	1.12
		0	11.29	101.54	<0.47	0.78	0.98	1.17	<0.91	<0.91	<0.91	<0.17	0.89	0.89
SC	HepG2	0.5	6.3	52.35	18.29	0.87	<0.44	<0.44	<0.91	<0.91	<0.91	<0.17	0.32	0.21
SC	HepG2	1	24.2	25.17	35.76	<0.44	0.45	1.63	<0.91	<0.91	<0.91	<0.17	0.72	0.57
SC	HepG2	2	138.5	<0.47	60.01	<0.44	<0.44	0.98	<0.91	<0.91	<0.91	0.17	<0.17	0.68
SC	HepG2	4	4374	127.82	116.9	0.98	0.5	<0.44	<0.91	<0.91	<0.91	0.47	0.72	<0.17
SC	HepG2	8	456.6	355.21	404.09	1.06	<0.44	<0.44	<0.91	<0.91	<0.91	<0.17	0.5	0.32
SC	HepG2	16	329.4	493.07	481.8	0.57	1.06	1.09	<0.91	<0.91	<0.91	<0.17	<0.17	0.21
SC	HepG2	24	22871	27238.15	736.76	40.4	10.75	<0.44	<0.91	<0.91	<0.91	0.4	1.32	<0.17
SC	HepG2	48	1576	28706.52	1947.36	0.87	18.78	0.84	<0.91	<0.91	<0.91	0.57	1.27	0.47
		0	11.29	101.54	<0.47	0.78	0.98	1.17	<0.91	<0.91	<0.91	<0.17	0.89	0.89
SC 15 %	THP-1	0.5	58.3	0.83	<0.47	<0.44	1.48	<0.44	<0.91	<0.91	<0.91	<0.17	1.32	<0.17
SC 15 %	THP-1	1	196.7	115.94	117.86	2.44	0.57	0.5	<0.91	<0.91	<0.91	0.29	0.17	1.07
SC 15 %	THP-1	2	690.9	281.08	368.92	5.05	0.84	2.25	<0.91	<0.91	<0.91	<0.17	0.37	0.47
SC 15 %	THP-1	4	344.6	467.22	520.48	2.44	3.15	2.19	<0.91	<0.91	<0.91	0.47	<0.17	<0.17
SC 15 %	THP-1	8	1668	951.21	1168.9	6.18	5.16	7.2	<0.91	<0.91	<0.91	0.17	0.93	0.29
SC 15 %	THP-1	16	29484	13143.69	5391.44	4.07	8.62	11.65	<0.91	<0.91	<0.91	0.21	0.21	1.12
SC 15 %	THP-1	24	22871	28706.52	4429.83	4.85	30.42	23.93	<0.91	<0.91	<0.91	<0.17	0.47	1.32
SC 15 %	THP-1	48	18197	32918.71	164.69	23.31	11.47	2.07	<0.91	<0.91	<0.91	0.6	<0.17	1.71
		0	11.29	101.54	<0.47	0.78	0.98	1.17	<0.91	<0.91	<0.91	<0.17	0.89	0.89
SC 50 %	THP-1	0.5	1.61	96.52	79.77	<0.44	1.09	0.87	<0.91	<0.91	<0.91	<0.17	1.89	0.21
SC 50 %	THP-1	1	326.9	236.2	243.47	1.3	3.55	3.63	<0.91	<0.91	<0.91	0.37	0.24	0.5
SC 50 %	THP-1	2	15073	669.14	545.3	3.55	7.33	6.8	<0.91	<0.91	<0.91	0.32	2.02	0.5
SC 50 %	THP-1	4	7390	1423.3	897.03	3.98	13.63	7.75	<0.91	<0.91	<0.91	1.59	1.22	<0.17
SC 50 %	THP-1	8	6467	4722.73	2336.93	16.77	20.95	20.39	<0.91	<0.91	<0.91	<0.17	2.02	0.93
SC 50 %	THP-1	16	28707	32918.71	16358.7	10.06	34.73	23.93	<0.91	<0.91	<0.91	0.5	1.77	<0.17
SC 50 %	THP-1	24	536.9	14773.53	23430.46	<0.44	15.59	32.71	<0.91	<0.91	<0.91	<0.17	0.5	0.72
SC 50 %	THP-1	48	26544	29483.9	19443.28	24.88	18	100.38	<0.91	<0.91	<0.91	1.77	<0.17	1.32